PETROLOGY OF THE LATE JURASSIC TO EARLY CRETACEOUS COALS FROM THE YANG CAO GOU BASIN, NORTHEAST CHINA

TIE ZHAO, B.Sc.
Department of Geology and Geophysics
The University of Adelaide
South Australia 5005
Australia

November 1993

A thesis submitted to the University of Adelaide in the fulfilment of the requirements for the degree of Master of Science

Awarded 1994

Contents

Chapter 4. COAL MEASURES OF THE YANG CAO GOU BASIN

Chapter 5. PETROLOGY AND GEOCHEMISTRY OF COALS FROM THE YANG CAO GOU BASIN

CHAPTER 6. COAL ORGANIC GEOCHEMISTRY AND OIL SOURCE POTENTIAL

ABSTRACT

The Yang Cao Gou Basin, is situated in Jiutai county to the northeast of Changchun city, Jilin province, and is one of several sedimentary coal sub-basins that developed in the late Jurassic to early Cretaceous along the eastern edge of the Songliao Basin, northeast China. The basin contains Jurassic and Cretaceous coal-bearing strata totaling over 2355 m in thickness and lying unconformably above granitic basement rocks.

Petrographic, reflectance, chemical and organic geochemistry studies on coal and shale samples representative of the coal seams of the different sub-basin have been carried out. Vitrinite is the dominant maceral observed in most samples. The high amount of vitrinite and low amount of inertinite indicate a reducing environment. Interpretation of lithotype variations within the seams indicates that the formation of the Yang Cao Gou coals were formed in wet forest-type swamps. Reflectances measured on vitrinite range from 0.35 to 0.67% placing the Yang Cao Gou coals between brown coal and bituminous coal.

There are three groups of coals deposited in the basin: Group II coals formed in shallow lakes, Group I coals formed in fan deltas, and lower Group coals formed in inter-lobe depressions within alluvial fans.

The Yang Cao Gou coal deposits shows a close relationship with paleaoenvironments. The topographic lows in front of and between alluvial fans, in fan delta plains and lake shores are the most favourable areas for coal accumulation.

LIST OF FIGURES

FIGURE PAGE

FIGURE PAGE

FIGURE PAGE

LIST OF TABLES

Statement

To the best of the writer's knowledge, and except where due reference is made in the text of the thesis, this thesis contains no copy or paraphrase of previously published material nor any material that has been accepted for the award of any other degree or diploma in any university.

I give consent to this copy of my thesis, when deposited in the University Library, being available for loan and photocopying.

November 1993, Tie Zhao

ACKNOWLEDGEMENTS

The author wishes to acknowledge B.H.P. Ltd. for providing financial assistance (B.H.P. postgraduate scholarship).

I would like to especially thank Prof. L. A. Frakes and Dr. David McKirdy (Department of Geology, The University of Adelaide).for their friendly advice and supervision; they have ushered me into a new field.

I am sincerely grateful to Mrs. Esther Frakes for her great moral encouragement and friendship throughout the years. Without her help to me and to my family, this study could hardly have been completed.

I would like to express my sincere thanks to Prof. Dongpu Zhao of the Changchun Geology of College for his initial suggestion on my research proposal and for his thoughtful arrangements for my field investigations carried out in China in late 1987.

I would like to thank staff members of The Geological Survey of Jilin province, P. R. China, in particular, Mr. Chunzi Yang, for their kind support, and for supplying data and samples during my field work.

I am especially grateful to staff members of The Bureau of Mineral Resources, Geology and Geophysics (BMR), in particular, Dr. C. Boreham, for help with the organic geochemical analyses.

I also greatly thank the staff members of AMDEL Limited, in particular, Mr. Brian Watson, for his supervision of the vitrinite reflectance measurements.

I would like to thank to DR. A. C. Cook (University of Wollongong) for valuable and useful suggestions and constructive comments.

I would like to thank Mr. Bernd Michaelsen for his time and personal assistance.

Thank are also due to:
Staff members of the department (UA) for technical assistance; in particular: Dr. K. Turnbull and Mr. P. McDuie (TOC), Mr. J. Stanley and Mrs. C. Badcock (XRD), Mr. W. Mussared and Mr. G. Trevelyan (sectioning), and Mr. R. Barrett (photography).

Last but not least, thanks to my dear wife Bo for moral support and for tolerating a massive disruption of our daily life.

CHAPTER 1

1.1 INTRODUCTION

The Yang Cao Gou Basin is one of several coal-bearing sub-basins that developed in the late Jurassic to Early Cretaceous along the eastern edge of the Songliao Basin, northeast China. It is located about 15 km northeast of Changchun, the capital city of Jilin and covers about 180 km^2 (about 38 km^2 with borehole control)(Fig. 1.1). Coal was first discovered in this basin in 1980 by the Geological Survey of Jilin. Since then, about 37,972 m of diamond drilling, 3900 m of rotary drilling and 2000 m of bucket auger drilling have been completed in the Yang Cao Gou coal deposits. Coal reserves amount to about 71 million tonnes and, in addition to the coal, about 4 million tonnes of bentonite and 29 million tonnes of zeolite are also available (Geological Survey of Jilin, 1984).

This thesis concentrates on determining the type and rank of the organic matter in the Yang Cao Gou coals in order to investigate facies changes and the influence of thermal effects caused by burial depth, intrusive bodies, or by both. As well, the depositional environments of the coal-bearing sequence and its hydrocarbon source rock potential are investigated.

Coal petrology is the study of the organic and inorganic components of coal, its origin and geological history. Petrological properties, especially as they relate to coal composition and history, provide much of the data for this study. The key approach to coal petrology is microscopic, and thus the greater share of this work is devoted to information from this source. The petrographic composition of coal is dependent on its environment of deposition, prevailing palaeoclimate and associated floral assemblages, its burial history, and the tectono-sedimentary setting (Teichmüller,1982). Coal composition also can be used for facies interpretation. The presence and abundance of macerals occurring as dispersed organic matter can also be used to characterize the organic facies in a sedimentary sequence (Cook, 1982b).

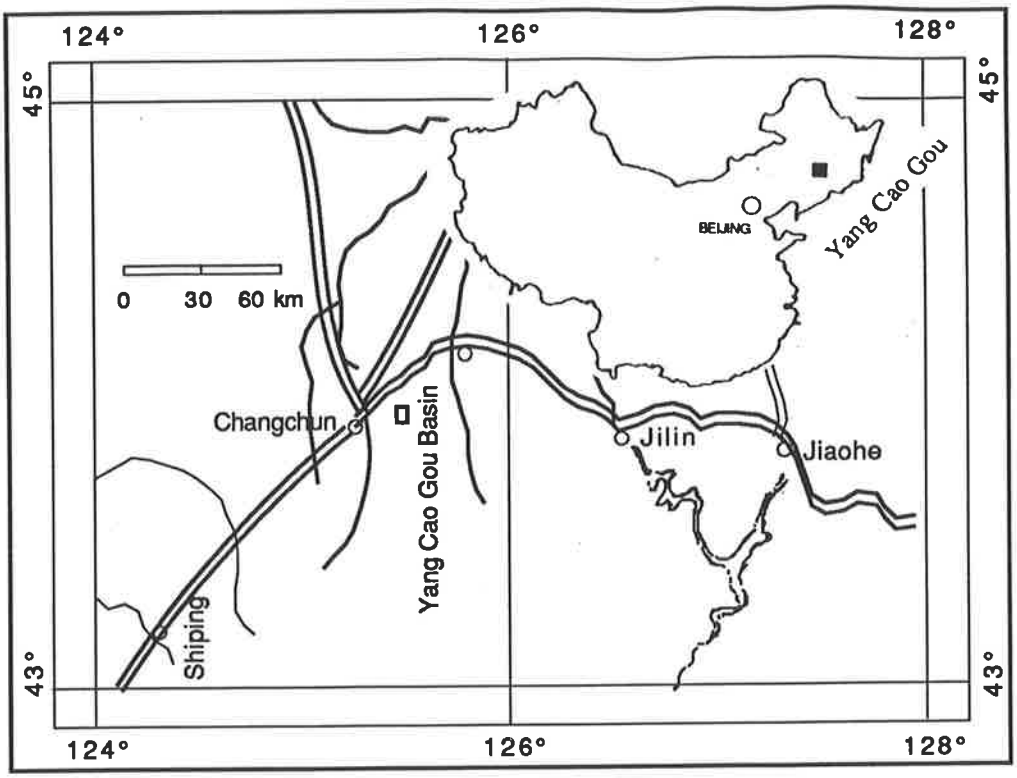

Fig. 1.1 Location map of Yang Cao Gou Basin

Source potential for petroleum relates to the abundance and composition of organic matter present in fine-grained sediments and possiblly, also to the organic matter in coal seam. Thus, the identification of organic facies, their temporal variation and their distribution within a sedimentary basin can help in locating areas of potential source rocks (Smith et al., 1981).

1.2 INTRODUCTION TO SONGLIAO BASIN

The Songliao Basin is a large basin located in northeast China where Mesozoic nonmarine sediments up to 7800 metres in thickness were deposited during the late Jurassic and Cretaceous (Wang, 1979; Zhai et al., 1984 ; Huang et al., 1984 and Yang et al., 1985). It trends in a NNE-SSW

direction and occupies an area of about 260,000 km^2. The basin is bordered by the Zhang Guancai Mountains and Mt Dahai in the east, the Great Xingan Mountains in the west, the Lesser Xingan Mountains in the north and the Liaxi hilly area and Inner Mongolia in the south (Fig. 1.2). Both late Jurassic deposits (3000 m) and Cretaceous deposits (4,800 m) are widespread throughout the basin.

The Songliao Basin is an intracratonic combination type basin. Its early growth was related to initial rifting of a continental block. There are indications of crustal extension in the area between the central constrained cratons and the continental margin (Fan, 1979). During the middle Cretaceous, the basin was depressed and a large lake covered 90,000-100,000 km^2. Fluvial-lacustrine clastic rocks, 4,300 m thick, were deposited in fresh to brackish water (Yang et al., 1985). The main source rocks and petroleum reservoirs discovered up to now are concentrated in the middle Cretaceous section. The Songliao basin is a major producer of oil from non-marine rocks (Yang et al., 1985). Most coals in the Songliao Basin are in the upper Jurassic and Early Cretaceous sequences. According to Fang (1979), the northeast-southwest oriented rift system began developing in the late Mesozoic, and led to the drifting of the Japanese islands and the opening of the Sea of Japan.

Many coal sub-basins (including the Yang Cao Gou) have been discovered in the Songliao Basin with more than 30 coal fields now delineated along its eastern edge. They are mainly represented by the late Jurassic Huoshiling and Shahezi Formations, as well as the early Cretaceous Yingcheng and Deng Lou Ku Formations. Most of the economic coals occur in the Shahezi and the Yingcheng Formations.

1.3 AIMS OF THE STUDY

The focus of the research in this thesis is to assess the petrographic characteristics of the Yang Cao Gou coal. The specific aims of the present study are:

(1) to document trends in coal type and rank in the Yang Cao Gou coal sub-basin;

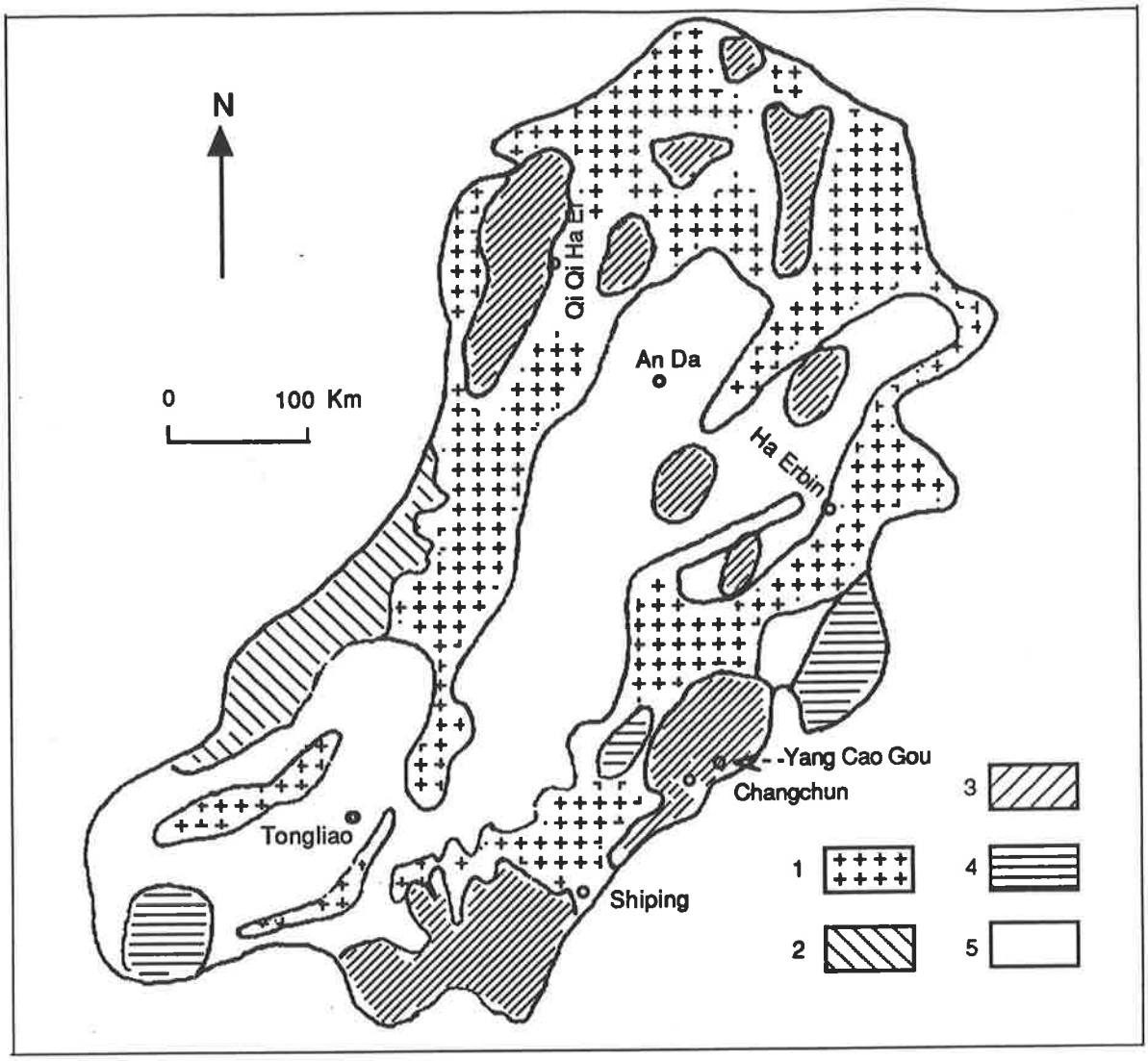

Fig. 1.2 Geological map of the Jurassic to early Cretaceous deposition in the Songliao Basin(modified from Yang, 1983)

1. upwarped district(Palaeozoic). 2. middle Jurassic. 3. Late Jurassic
4. early Cretaceous. 5. Cainozoic

(2) to assess the abundance and composition of the main lithotypes and to evaluate their lateral and vertical distribution within the basin;

(3) to determine the relationship between depositional environment and coal petrographic and geochemical composition;

(4) to relate variations in coal type and quality to coal seam geometry;

(5) to relate coal rank variations to coalification histories; and

(6) to assess the oil source potential of the various coal types identified.

1.4 PREVIOUS WORK

No prior petrographic work has been carried out on the coals in the study area. Previous geological investigations were mainly concerned with the stratigraphy and mineral prospectivity of the basin.

The major stratigraphic study of the Yang Coa Gou Basin was that by Yang (1986), and Zhao et al. (1987), who outlined the stratigraphy and correlation of Mesozoic coal measures near the eastern edge of the Songliao Basin. Studies of the sedimentary characteristics of the coal have been carried out by Liu (1988) and Zhao (1989).

CHAPTER 2 REGIONAL GEOLOGY

2.1 STRATIGRAPHY

Along the eastern margin of the Songliao Basin, sedimentary sequences of Mesozoic and Cenozoic age are developed that have a total thickness more than 2350 m (Fig. 2.1). They occur mainly in six separate structural sub-basins. The six basins appear to be remnant morphotectonic units of an original stratotectonic unit, as correlations can be made between the basins (Fig. 2.2). From south to north, they are: Shiping, Liufanzhi, Xinlicheng, Shibeiling, Yang Cao Gou, Yingcheng and Sanhewan sub-basins (Fig. 2.3). The sequence of which the Jurassic and Cretaceous coal measures are part, rests unconformably on Palaeozoic sediments and granitic basement rocks. It is subdivided into the following units:

(1) Lujiaton Formation - Lower Triassic
(2) Huoshiling (Anmin) - Upper Jurassic
(3) Shahezhi Formations - Upper Jurassic
(4) Yingcheng Formation - Lower Cretaceous
(5) Denglouku Formation - Lower Cretaceous
(6) Quantou Formations - Lower Cretaceous
(7) Qingshankou Formations - Lower Cretaceous
(8) Yaojia Formations - Lower Cretaceous
(9) Lanjiang Formations - Lower Cretaceous
(10) Fufengshan Formation - Tertiary
(11) Baishantu Formation - Quaternary
(12) Guxiangton Formation - Quaternary.

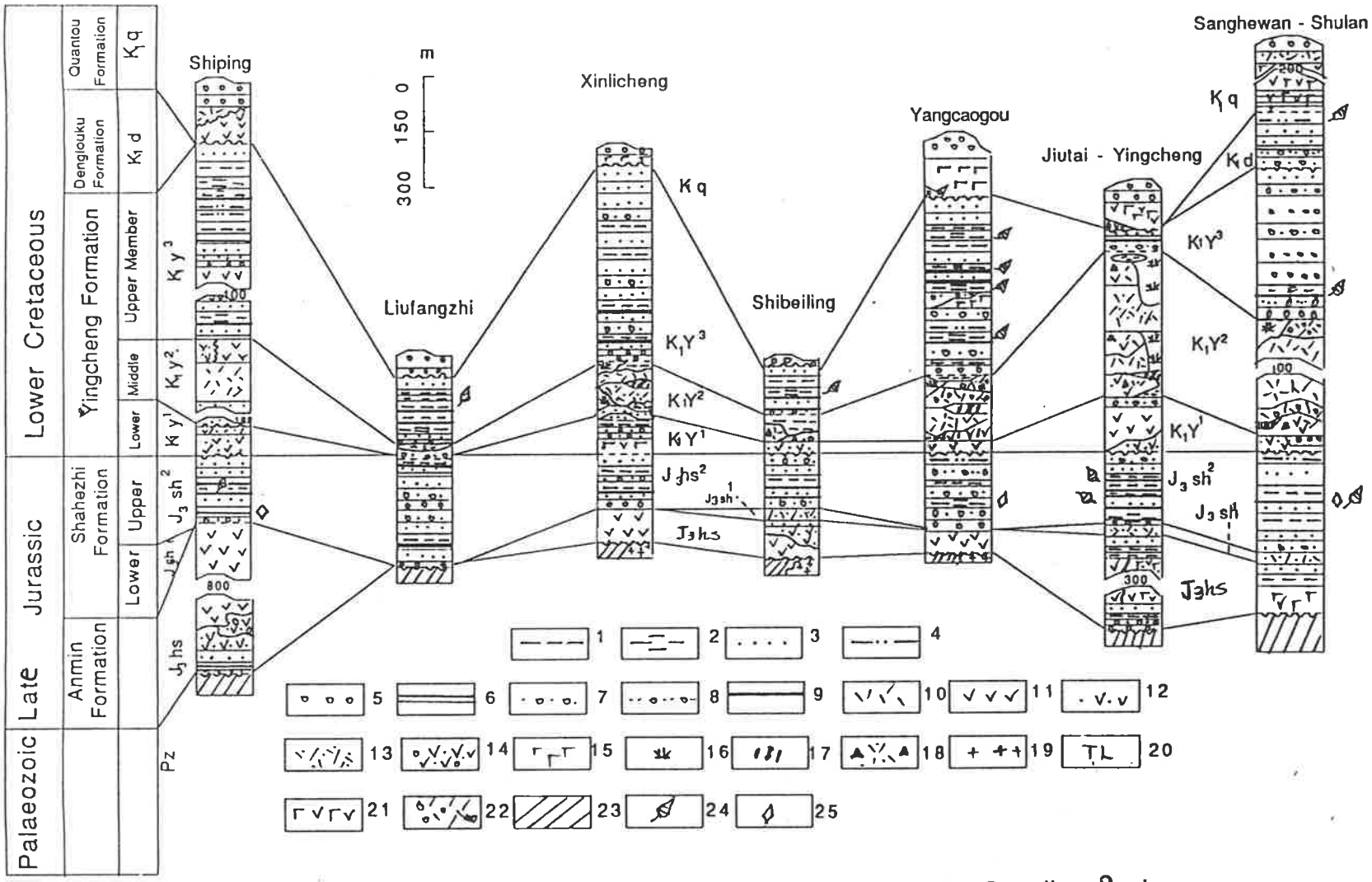

Fig. 2.1 Correlation of the coal measures, eastern margin of the Songliao Basin

1. Mudstone. 2. Carbonaceous mudstone. 3. Sandstone. 4. Muddy sandstone. 5. Conglomereate.6. Shale 7. Sandy conglomerate. 8. Conglomeratic sandstone. 9. Coal. 10. Rhyolite. 11. Andesite. 12. Andesite-tuff. 13. Rhyolitic tuff. 14. Andesitic agglomerate 15. Basalt. 16. Zeolite. 17. Pearlite. 18. Rhyolitic breccia lava. 19. Granite. 20. Luijaiton Formation, Tertiary. 21. Basaltic andesite 22. Spherulitic rhyolite. 23. Palaeozoic. 24. Plant fossil. 25. Animal fossil

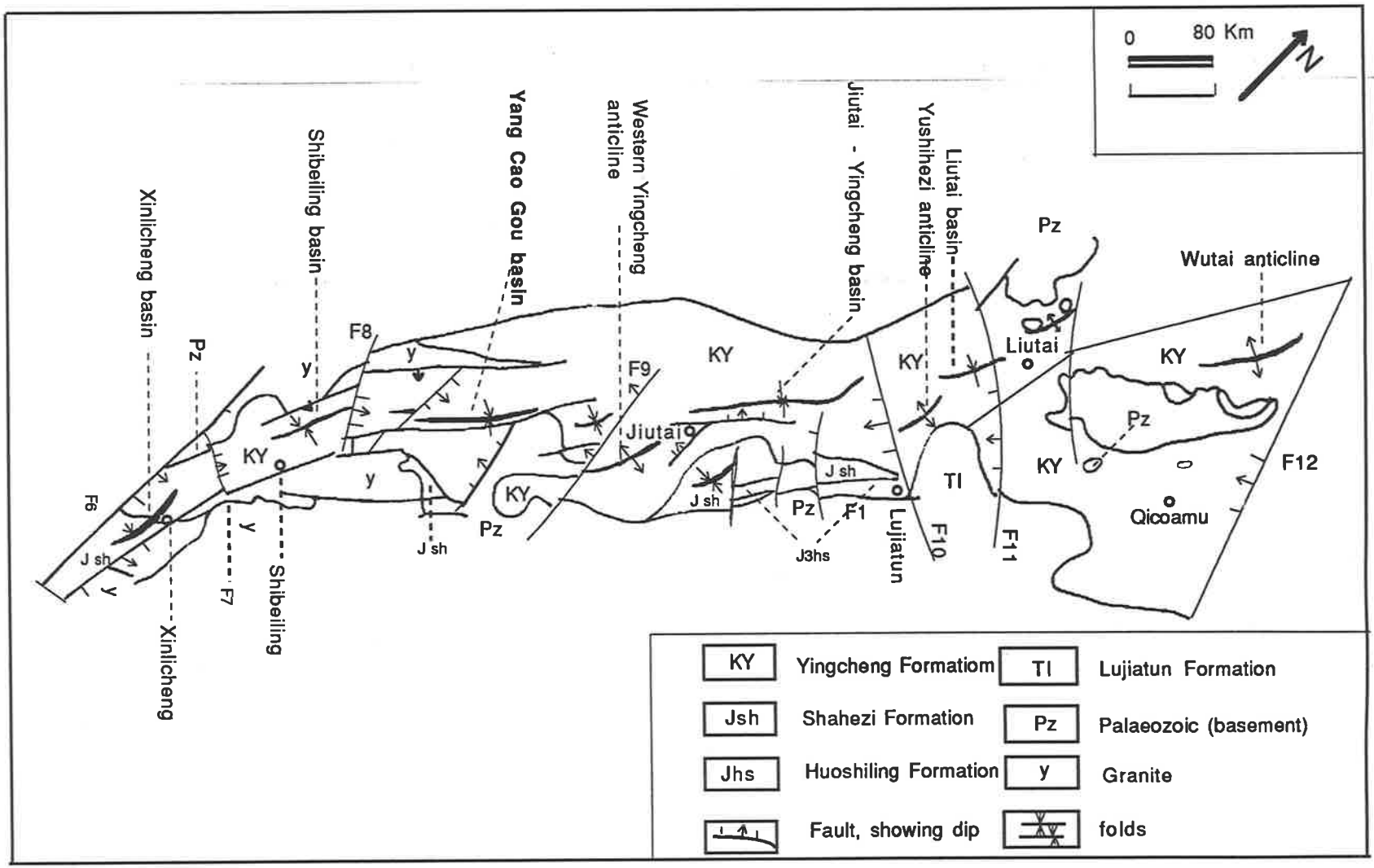

Fig. 2.2 Geology of the eastern edge of the Songliao Basin

2.1.1 LOWER TRIASSIC

Lujiaton Formation (Tl)

Ranging from 10 to 4745 m in thickness, the Lujiaton Formation has a limited occurrence and is mainly distributed in the Lu Jia Ton area of Jiutia County, covering an area of about 142 km². It is unconformably overlain by the Huoshiling Formation and rests unconformably on Late Permian sediments. This formation was subdivided into three members by the Geological Survey of Jilin (1986). The lower and middle members consist mainly of conglomerate, graywacke and calcareous sandstone. The upper member contains mainly carbonaceous sandstone and silty mudstone interbedded with four unworkable coal beds with high ash contents.

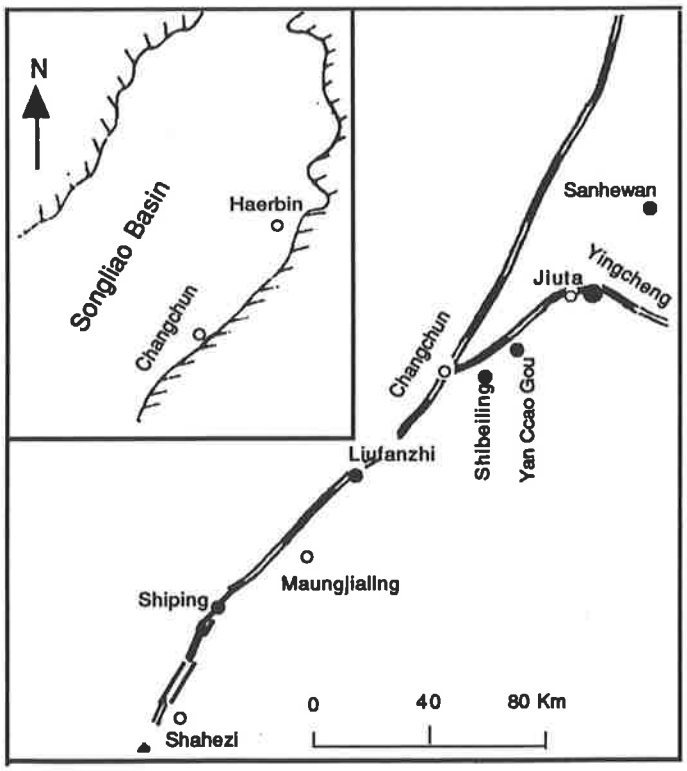

Fig. 2.3 Location map of the coal-bearing sub-basins, eastern margin of the Songliao Basin (modified from Yang, 1986)

● coal basin

2.1.2 UPPER JURASSIC

Huoshiling Formation (J_3hs)

The base of the upper Jurassic is represented by the Huoshiling Formation (or called An Min Formation locally), up to 200 m in thickness and consisting of dull purple andesite and minor interlayers of brown to purple sandstone and conglomerate with some lenses of coal. The rocks of the Huoshiling Formation unconformably overlie basement granite and are distributed in the southern central part of the basin. The Huoshiling Formation is preserved in the Yingcheng, Yang Cao Gou, Shibeiling and Si Ping areas (Fig. 2.1). The type section is in borehole Jiutai-7337, where the unit reaches a minimum thickness of 1153.71 m, as shown in Table 2.1.

Table 2.1 shows that the rocks of the Huoshiling Formation are dominantly intermediate to basic volcanic rocks interbedded with sediments and thin coal seams. The deposits represent volcanic eruptions (flows, tuffs and breccias) and coarse lake-swamp sediments.

Table 2.1 Type section of the Huoshinling (An Min) Formation, eastern margin of the Songliao basin (modified from Zhao et al., 1989)

Shahezi Formation	
Huoshiling Formation(J_3 hs)	Thickness (m)
(12) Grey and greyish purple sandy conglomerate, conglomerate	7
(11) Grey to greyish white, fine sandstone and coarse sandstone interbedded with carbonaceous thin layers of mudstone and coal	120
(10) Greyish green andesite, andesite basalt, tuff and tuffaceous breccia	140
(9) Greyish white, coarse to middle grain sandstone, brownish red sandy conglomerate and grey tuffaceous sandstone interbedded with coal	105
(8) Purple to greyish green andesite basalt	150
(7) Red andesite tuff and breccia	71
(6) Grey tuff	81
(5) Andesite tuff interbedded with andesite breccia	145
(4) Greyish green, dull green to black andesite interlayered with breccia	110
(3) Andesite breccia	23
(2) Sandstone, siltstone, conglomerate and carbonaceous mudstone	112
(1) Greyish andesite tuff, breccia and agglomerate	90
Borehole did not reach the base of the formation	

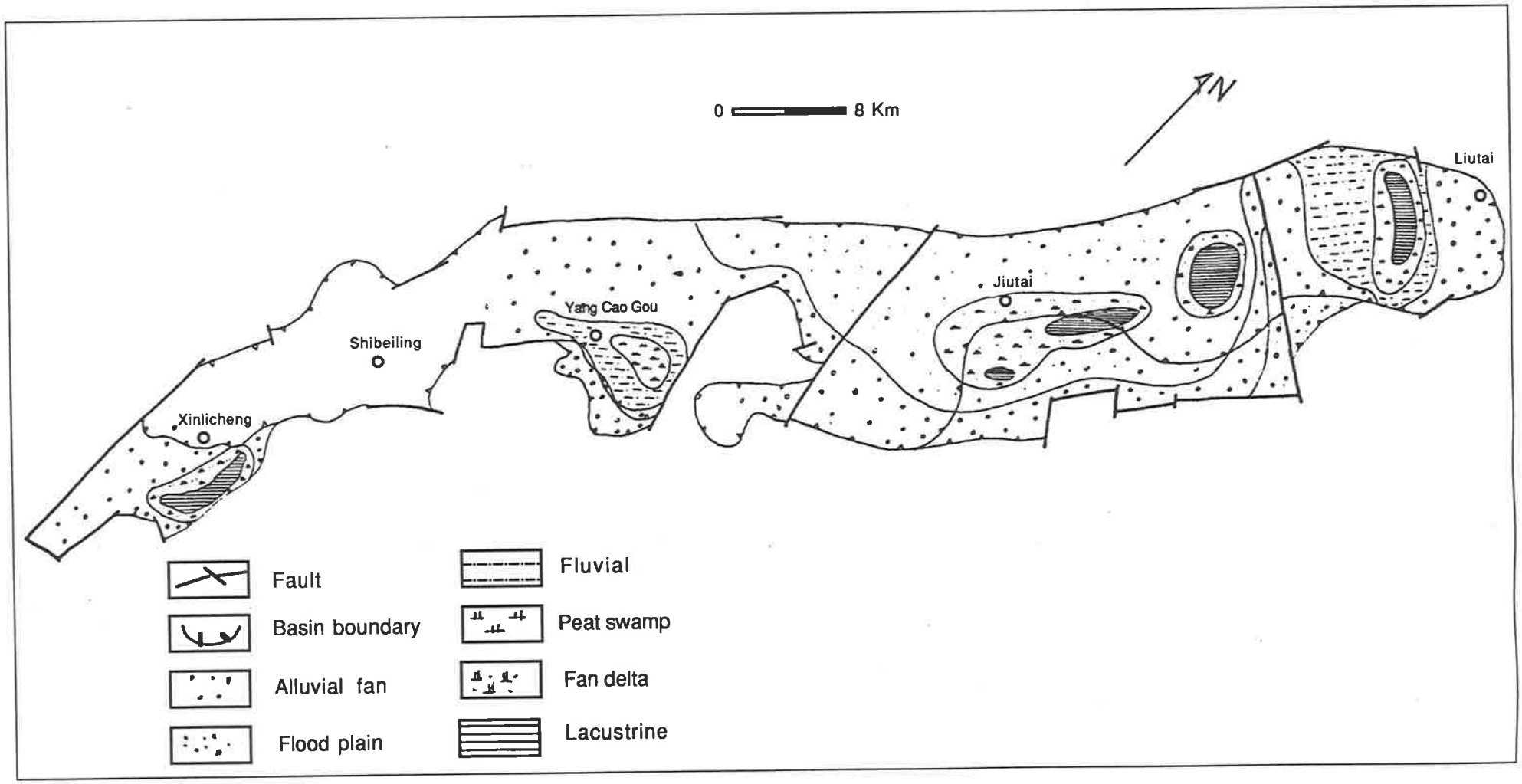

Fig. 2.4 Palaeogeographic map of the Sha He Zhi Formation (from Xinlicheng to Liutai), eastern edge of the Song Liao Basin (modified from Zhao et al., 1989).

Shahezi Formation (J_3sh)

The Huoshiling Formation is conformably onderlain by sediments of the Shahezi Formation which are widespread throughout the eastern margin of the Songliao Basin and are well developed in the Yingcheng, Yang Cao Gou, Shibeiling, Xinlicheng and Siping areas (Fig. 2.4). It is composed of up to 567 m of coarse sandstone, tuff, mudstone, and workable coal seams. On the basis of lithology, the Shahezi Formation can be subdivided into a lower acid volcanic member (J_3sh^1) and a upper clastic member containing coal (J_3sh^2). Based on palynological and megafloral evidence, the Shahezi Formation is of late Jurassic age (Yang, 1986).

The volcanic member, ranging from 0 to 89 m in thickness, consists mainly of greyish green and greyish white tuffs and tuffaceous breccias. This sequence is the typical key bed overlying the Huoshiling Formation, but is commonly not present in the area studied.

The clastic (coal) member (J_3sh^2), ranges up to 478 m in thickness and consists of, from bottom to top, greyish coarse and fine sandstones, conglomerate interlayered with mudstone and greyish black carbonaceous mudstone. Economic coal seams occur in the lower part, with mudstone, siltstone and sandy conglomerate in the upper part. Table 2.2 is the type section of the clastic member (from the same borehole as used in Table 2.1).

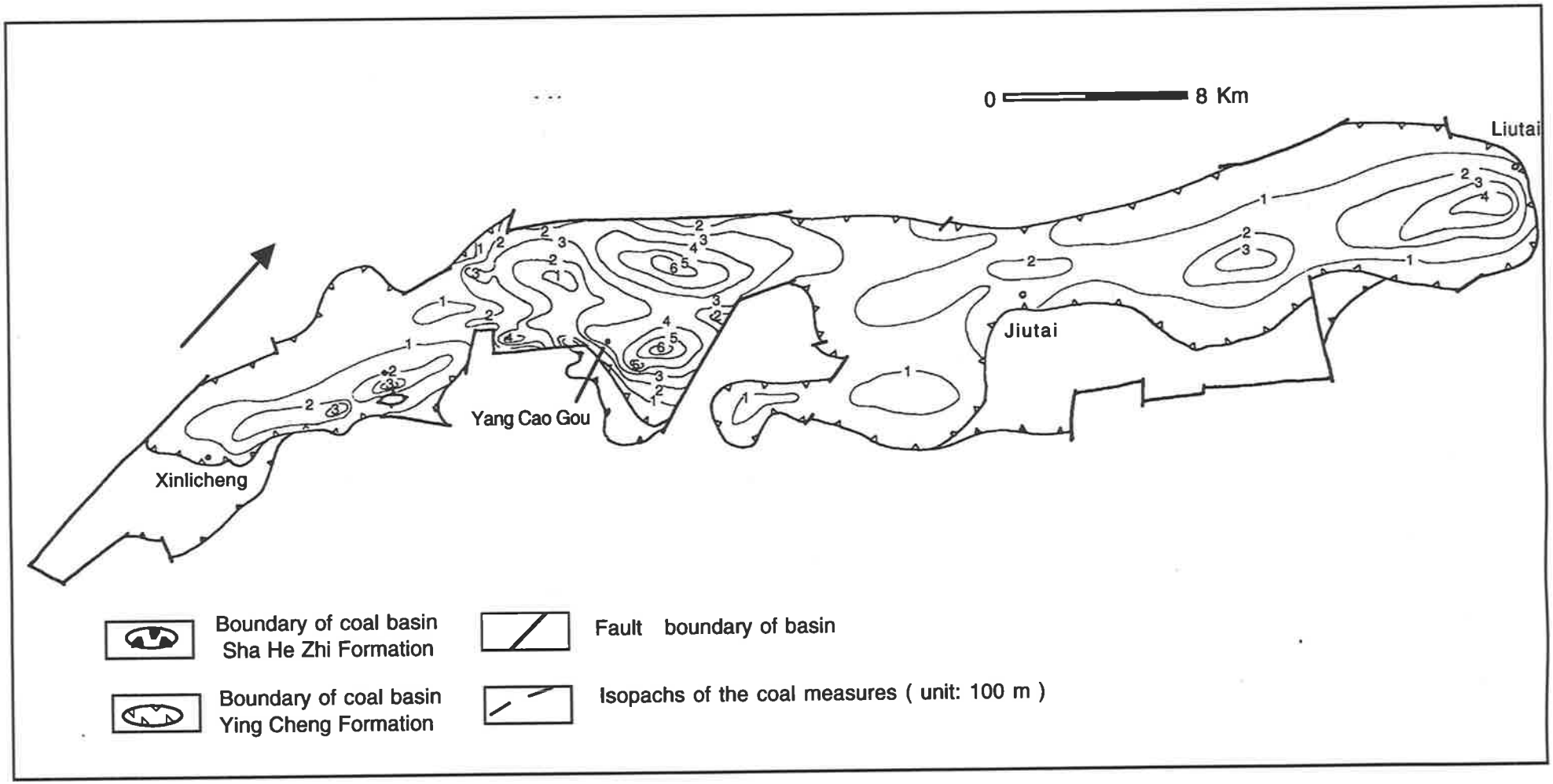

Fig. 2.5 Isopach map of the Yingcheng coal measures (from Xinlicheng to LiuTai), eastern edge of the Songliao Basin (modified from Zhao, 1989)

Table 2.2 Type section of clastic member (J_3sh^2) of Shahezi Formation (modified from Zhao et al., 1989).

Covered by Yingcheng Formation	
----------unconformity----------	
Clastic member(J_3sh^2)	Thickness(m)
(27) Dark grey to black carbonaceous mudstone and siltstone interlayered with thin coal	12
(26) Greyish white coarse sandstone	9
(25) Coal within carbonaceous mudstone	3
(24) Grey sandstone interbedded with siltstone and mudstone.	29
(23) Black mudstone interbedded with fine grained sandstone	4
(22) 1.7 m coal within sandstone and mudstone	3
(21) Grey sandstone, siltstone and mudstone	16
(20) Coal	0.3
(19) Grey coarse sandstone	10
(18) Thin coals within carbonaceous mudstone	5
(17) Thin coal and carbonaceous mudstone within grey coarse sandstone	10
(16) Black carbonaceous mudstone interlayered with siltstone and sandstone	48
(15) Coal	0.2
(14) Grey mudstone within greyish white coarse sandstone	4
Acid volcanic member (J_3sh^1) Green tuff	11

2.1.3 EARLY CRETACEOUS

Yingcheng Formation (K_1y)

The Yingcheng Formation rests unconfomably on the Shahezi Formation, and is distributed mainly around Shanghewan, Jiutai to Yingcheng, Yang Cao Gou, Shibeiling, Xinlicheng, Liufanzi and Siping areas (Figs. 2.1 and 2.5). It contains the most important coal seams on the eastern margin of the Songliao Basin. The Yingcheng Formation is composed dominantly of volcanic rocks, but includes clastic sediments and up to 5 economic coal seams, intercalated with andesite and basalt. Coal seams vary in thickness from about 1 m to 10 m. This formation is overlain unconformably by basalt of the Quan Tou Formation which is in turn unconformably overlain by the Qing Shan Kou Formation. The Yingcheng Formation varies in thickness from 210 to 983 m and can be subdivided into three members, of which the upper one is the thickest and contains the most important coal seams (Geological Survey of Jilin, 1986).

The lower member (K_1y^1) consists of intermediate to basic volcanic rocks and contains greyish green to dull grey andesitic breccia, tuff, agglomerate, andesite and basaltic andesite in the lower part and grey to greyish white tuffaceous sandstone, siltstone, sandy conglomerate, black carbonaceous mudstone and thin coal layers in the upper part of the sequence. The type section of this member is in bolehore Nongda-72-42 in the Xinlicheng area and is shown in Table 2.3.

Table 2.3 Type section of the lower member of the Yingcheng Formation, Early Cretaceous (modified from Zhao et al., 1989).

	Thickness (m)
Middle member of the Yingcheng Formation	
Lower member of the Yingcheng Formation (K_1y^1)	
Sandstone interlayered with conglomerate	12.6
Black mudstone and greyish white sandstone	15.3
Greyish white coarse sandstone	7.5
Greyish green sandstone	4.5
Green tuffaceous conglomerate	10.2
Dark grey to dull green basaltic andesite	16.2
----------unconformity----------	
Clastic member of the Shahezi Formation	

The middle member (K_1y^2), ranging from 15 to 720 m in thickness, consists mainly of acid lava and volcaniclastic rocks. It contains rhyolitic lava, breccia, zeolite and bentonite in the lower part, and rhyolite interlayered with obsidian and pearlite in the middle part, and bentonite, zeolite, tuff, and breccia lava in the upper part. Table 2.4 gives the stratigraphy of the middle member from borehole ZK901 in the Yang Cao Gou Basin.

Table 2.4. Stratigraphy of the middle member of Yingcheng Formation, eastern margin of the Songliao Basin (modified from Zhao et al., 1989)

covered by Upper member of Yingcheng Formation (K_1y_3)

----------unconformity----------

Middle member (K_1y_2)	Thickness (m)
Bentonite	2.4
Greyish green tuffaceous sandstone	21.0
Zeolite	23.7
Bentonite within zeolitic breccia tuff	8.8
Spherulitic rhyolite	4
Montmorillonitic tuffaceous breccia sandstone	1.9
Rhyolite and spherulitic rhyolite	145.0
Pearlite	4.0
Zeolite	13.3
Montmorillonitic breccia lava	19.1
Rhyolite and spherulitic rhyolite	21.3
Montmorillonitic spherulitic rhyolite	10.8
Rhyolite	20.0
Bentonite and pearlite within rhyolite	13.8
Zeolitic and montmorillonitic breccia	7.7
Pearlite	5.1
Zeolite	2.5

----------unconformity----------

Clastic member (J_3sh_2) of Shahezi Formation

Table 2.5 Stratigraphy of the upper member (K_1y^3) of the Yingcheng Formation, eastern margin of Songliao Basin (modified from Zhao et al., 1989).

Quantou Formation	
unconformity	
Upper member (K_1y^3) of Yingcheng Formation	Thickness (m)
Upper coal sub-member:	
Greyish white sandstone	49.2
Greyish white sandstone interbedded with carbonaceous mudstone	29.3
Tuffaceous sandstone	2.6
Shale and carbonaceous mudstone	11.0
Montmorillonitic tuff	1.5
Greyish black carbonaceous mudstone interbedded with greyish white sandstone	28.6
Four workable coals within carbonaceous mudstone and sandstone	12.8
Carbonaceous mudstone within tuffaceous sdandstone and breccia	18.3
Coal	10.0
Tuffaceous sandstone interbedded with carbonaceous mudstone	44.1
Bentonite within montmorillonitic tuffaceous sandstone	41.8
Andesite tuff and sandy conglomerate	13.9
Lower coal sub-member	
Basalt	36.7
Tuffaceous sandstone and conglomerate	12.7
Muddy sandstone within tuffaceous conglomerate	49.1
Conglomerate	15.5
Thin coal within carbonaceous mudstone and siltstone	4.9
Greyish white conglomerate	17.2
Greyish white sandstone and sandy conglomerate	16.6
Conglomerate	14.4
unconformity	
Middle member (K_1y^2) of Yingcheng Formation	

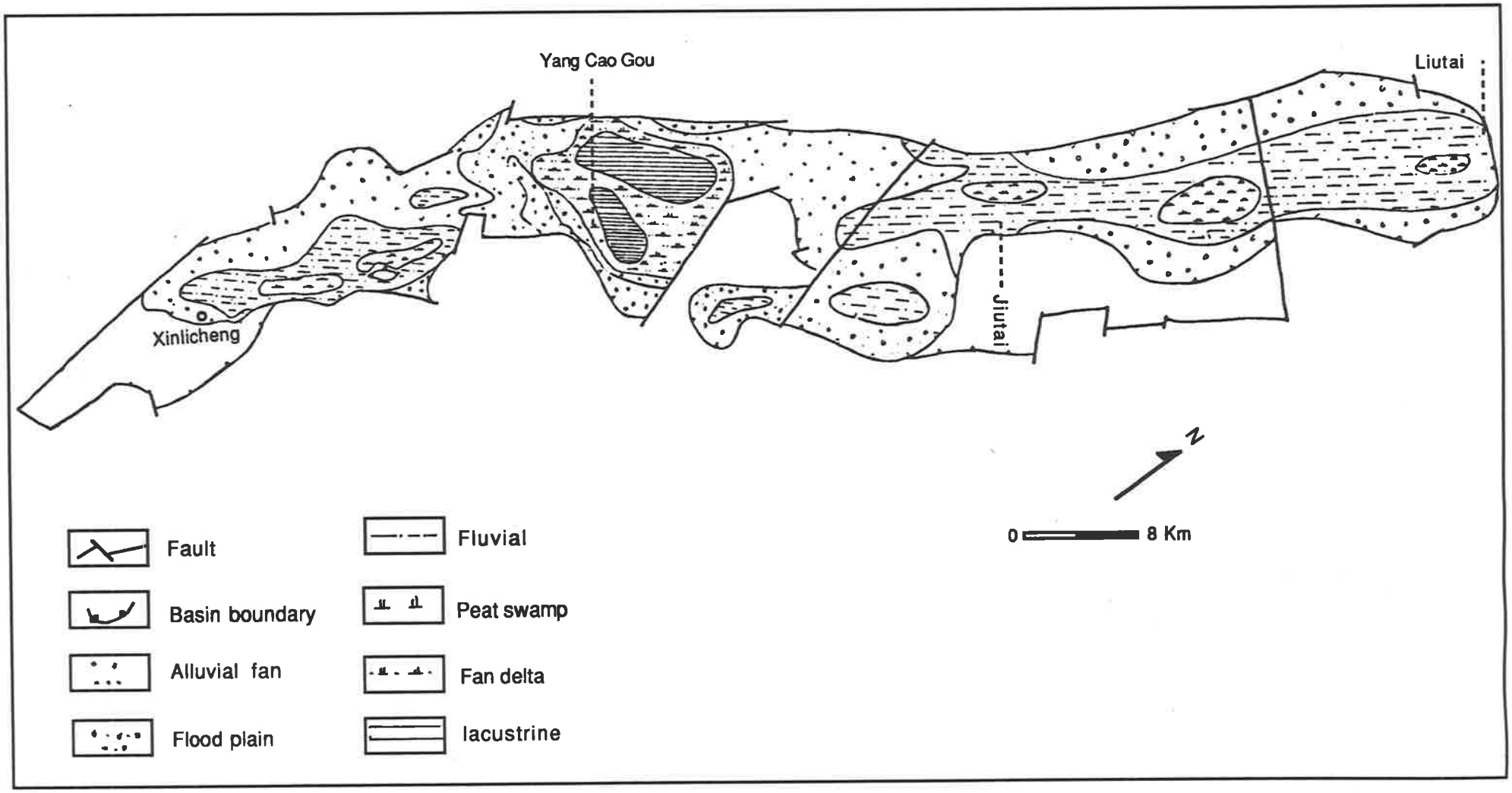

Fig. 2.6 Palaeogeographic map of the Ying Cheng Formation (from Xinlicheng to Liutai), eastern edge of Songliao Basin, modified from Zhao, 1989).

The upper member (K_1y^3) contains most of the coal seams in the Yang Cao Gou, Shibeiling, Xinlicheng and Liufangzi coal sub-basins (Fig. 2.6). This unit contains up to 10 economic seams ranging from 1 to 13 m in thickness, and can be subdivided into two sub-members: the upper coal sub-member and the lower coal sub-member, as illustrated in Table 2.5.

The lower coal sub-member, ranges up to 167m in thickness, consists of conglomerate, sandstone and mudstone interlayered with thin coal seams on the lower part, and sandstone, basalt and basaltic conglomerate on the upper part of the unit. The unit mainly occurs on the eastern part of the basin.

The upper coal sub-member, ranges up to 264m in thickness, consists of, from bottom to top, tuffaceous conglomerate, economical coal seams interlayered with mudstone.

Denglouku Formation (K_1d)

The Denglouku Formation covers about 15 km² in the Shu Lan area. It consists of up to 1540 m of conglomerate, greyish brown to carbonaceous sandstone, silty mudstone and unworkable coals. A representative stratigraphy of the Denglouku Formation is presented in bolehore 85-1 in Shalan county, as illustrated in Table 2.6:

Table 2.6 Stratigraphy of the Denglouku Formation, eastern margin of Songliao Basin (modified from Zhao et al., 1989)

Denglouku Formation (K_1d)	Thickness (m)
(9) Greyish white conglomeratic sandstone interbedded with coarse sandstone and siltstone	5.3
(8) Greyish black silty mudstone, fine sandstone, and muddy siltstone	4.3
(7) Carbonaceous fine sandstone within grey conglomeratic sandstone and coarse sandstone	19.6
(6) Muddy siltstone within grey to black sandstone and conglomeratic sandstone	11.1
(5) Siltstone interbedded with sandstone	33.8
(4) Greyish white conglomeratic coarse sandstone interbedded with siltstone	45.6
(3) Greyish white conglomerate interbedded with conglomeratic sandstone	82.5
(2) Black siltstone interbedded with silty mudstone and coal fragments	12.1
(1) Grey to carbonaceous conglomeratic sandstone, coarse sandstone and thin coal seams	7.6
---------- unconformity ----------	
Permian metamorphic sandstone	

Quantou Formation (K_1q)

This formation unconformably overlaps the Yingcheng Formation, Shahezi Formation, Palaeozoic sediments and crystalline rocks along the eastern margin of Songliao Basin and is over 1,000 m thick. In the lower part, it consists of up to 200 m of basalt and andesite. The upper part of the sequence (up to 1000 m thick) consists of conglomerate, greyish green muddy siltstone, conglomeratic sandstone, sandstone, and mudstone. Conchostraca and dinosaurian eggs have been found in this sequence.

CHAPTER 3 METHODOLOGY AND TERMINOLOGY

3.1 INTRODUCTION

Coal petrology is the study of the organic and inorganic components of coal, its origin and subsequent geological history, and its properties as they relate to its composition and history. The main research tool for coal petrology is the microscope. Coal petrology has proven its value in applications to many geological and technological problems, including interpretation of the depositional, structural and geothermal histories of coal basins, prediction of the utilization potential of coal and in petroleum exploration.

Petrographic variation of the coal can be assessed in terms of macerals (Stopes, 1935), microlithotypes (Seyler, 1943), or lithotypes (Stopes, 1935; Seyler, 1943). Macerals are entities which evolve from different organs or tissues of the original plant material during the course of primary accumulation and the early stages of biochemical degradation and early coalification (maturation). The main parameters used to distinguish the macerals in incident light are:

(1) reflectance and anisotropy;
(2) morphology, relief, and size; and
(3) fluorescence.

In low to intermediate rank coals (lignites to low-volatile bituminous), three maceral groups can be distinguished by different levels of reflectance, as follows:

Liptinites = dark grey, low reflectance;
Vitrinites = medium grey, medium reflectance;
Inertinites = light grey to white, high reflectance.

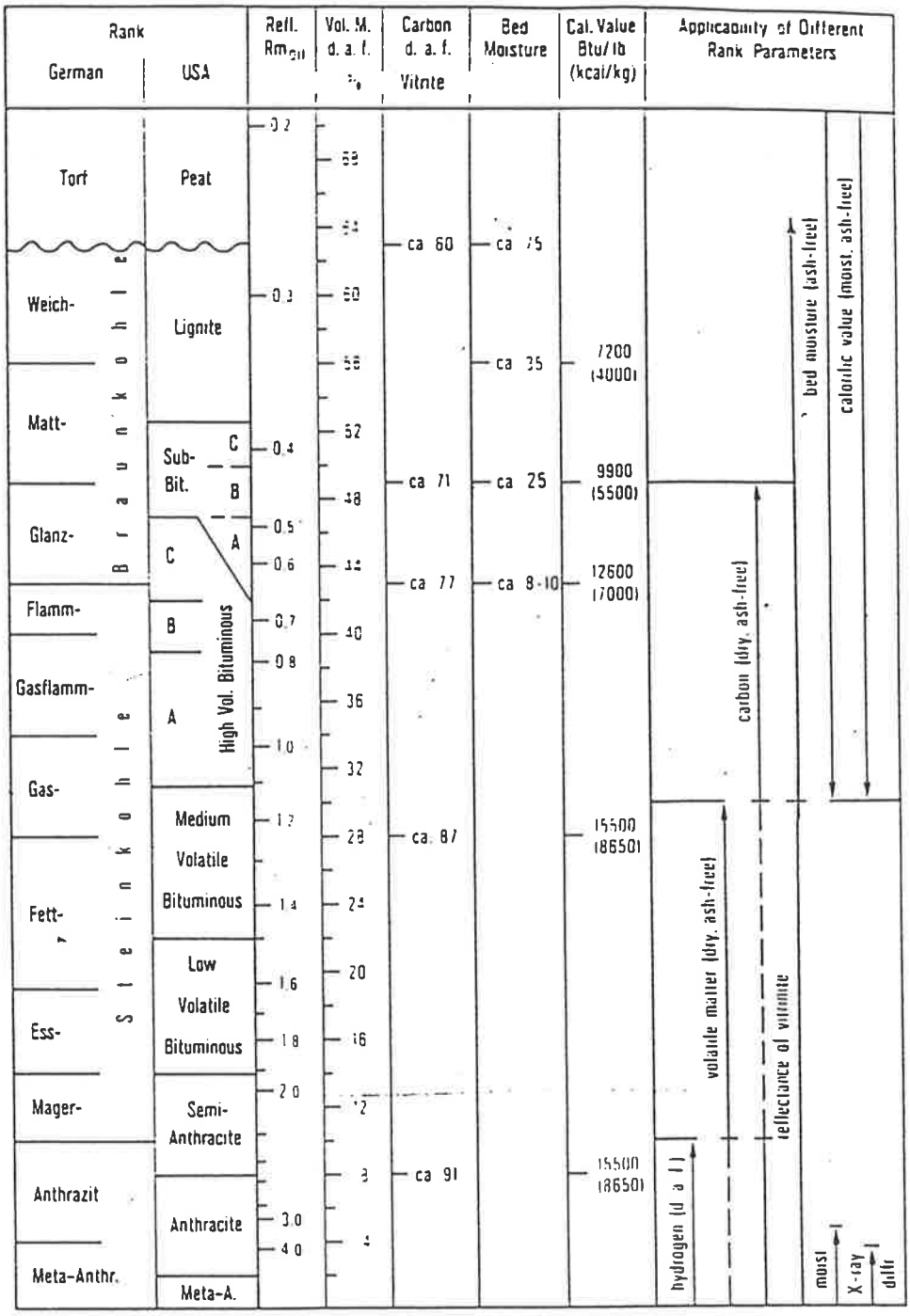

Fig. 3.1 Stages of coalification based on physical and chemical properties of the coal (from Teichmüller and Teichmüller, 1982).

With increasing rank the differences in reflectance between macerals diminish due to an overall convergence of chemical and physical properties (Fig 3.1).

The subdivision of these three groups are shown in Table 3.1. The maceral nomenclature used for this study follows the Australian Standard (Standards Association of Australia, 1986).

Microlithotypes are microscopic coal bands (>0.05 mm in band thickness) which contain specific associations of macerals.

The effect of floral composition and depositional environment on the petrographic composition of the coal is of primary importance but can be modified by overprinting during post-depositional coalification. Detailed petrographic studies can thus provide information about the coal facies at the time of deposition. Results from the work of Teichmüller (1962), Cohen and Spackman (1980), Casagrande et al., (1977), and Styan and Bustin (1983), show that coal macerals and microlithotypes can be associated with a coal facies. The environments of coal deposition are primarily related to the depth of water in peat swamps (Teichmüller et al., 1962). Diessel (1982) showed that particular maceral assemblages characterize certain palaeoenvironments. Diessel suggests that the presence of alginite is indicative of limnic or lacustrine conditions. It is also known that most alginite in coal has been derived from planktonic algae (Hutton et al., 1980) which, after death, accumulate on depositional interfaces. In their study of the petrography of Canadian coals, Hacquebard et al. (1967) demonstrated many of the interpretative techniques applicable to sedimentology from coal petrographic studies. Based on his study of the Sydney basin, Diessel (1982) concluded that forest moor facies are characterized by fine to medium- banded clarite and vitrite with little inertinite, and high concentrations of well preserved liptinite; open moor facies are composed of durite with abundant inertinite, liptinite and mineral matter; whereas the mixed reed moor and open moor facies are typified by high liptinite contents (with well-preserved spores), abundant inertinite and equal amounts of telovitrinite and detrovitrinite. The relative abundance of telovitrinite and detrovitrinite

Table 3.1 Coal maceral classification (AS 2856, 1986)

MACERAL GROUP	MACERAL SUBGROUP	MACERAL
VITRINITE	Telovitrinite	Textinite
		Texto-ulminite
		Eu-ulminite
		Telocollinite
	Detrovitrinite	Attrinite
		Densinite
		Desmocollinite
	Gelovitrinite	Corpogelinite
		Porigelinite
		Eugelinite
LIPTINITE		Sporinite
		Cutinite
		Resinite
		Liptodetrinite
		Alginite
		Suberinite
		Fluorinite
		Exsudatinite
		Bituminite
INERTINITE	Telo-Inertinite	Fusinite
		Semifusinite
		Sclerotinite
	Detro-Inertinite	Inertodetrinite
		Micrinite
	Gelo-Inertinite	Macrinite

are related to the degree of degradation of the humic material: the greater the degradation; the greater the proportion of structureless vitrinite.

In the Nanaimo Coalfield, British Columbia, Hacquebard et al. (1967) recognized seven petrographic intervals which they interpreted as telmatic forest moor facies and mixed open and reed moor facies. The telmatic forest moor facies is composed of bright, fine to medium-banded, clarite and thick bands of vitrite. Eu-ulminite and telocollinite are derived mainly from incompletely gelified xylem and cortex tissues. Therefore the high quantity of telocollinite and Eu-ulminite suggests that much of the seam was derived from woody material under moist conditions. The mixed open moor and reed moor facies is a semi-bright coal consisting of clarodurite and durite with much massive fusinite, dispersed micrinite, and liptinite. The variable petrographic composition of the coal with low telinite and high collinite, was interpreted to indicate repeated fluctuations in the groundwater level and deposition in a mixed open and reed moor environment.

Diessel (1982) designed a triangular diagram, with alginite + sporinite + inertodetrinite at the upper apex, vitrinite in the left apex and semifusinite + fusinite at the right apex of the triangle. In Yang Cao Gou coal, sporinite is relatively abundant, and alginite is rare. In the present work, sporinite and inertodetrinite therefore are represented at the upper apex of the triangle; the other two apices of the triangle remain the same as in the plot of Diessel (1982).

According to the facies triangle, if

$$\frac{(\text{Eu-ulminite} + \text{Telocollinite}) + (\text{Semifusinite} + \text{Fusinite})}{(\text{Sporinite} + \text{Inertodetrinite})} < 1$$

the coal was formed mainly under telmatic, reed moor or limnic conditions with little input from the forests. Diessel (1982) defined the gelification index as:

$$GI = \frac{\text{Vitrinite} + \text{Macrinite}}{\text{Semifusinite} + \text{Fusinite} + \text{Inertodetrinite}}$$

and the tissue preservation index as

$$TPI = \frac{\text{Eu-ulminite + Telocollinite + Semifusinte + Fusinite}}{\text{Desmocollinite + Macrinite + Inertodetrinite}}$$

The level of coalification (or organic maturation) is the result of the time/temperature history of the organic matter (Stach et al., 1982). A number of ways have been devised to determine the level of coalification of coal. Vitrinite reflectance is the most widely used, but other popular methods include volatile matter yield, carbon content, moisture content and calorific value. Volatile matter yield is unreliable for coals having yields in excess of 30% and moisture content is only suitable for low rank coals (Cook, 1975). The vitrinite reflectance method has a number of advantages over other methods: (1) it is sensitive to even minor changes in level of coalification; (2) as it is a microscopic method, determinations are always made on the same component; (3) vitrinite, with few exceptions, is the most common constituent; (4) vitrinite does not undergo retrograde coalification; (5) vitrinite does not readily react with fluids or other solids in the rocks; and (6) the method is applicable through the entire range of coalification (Bustin et al., 1983).

The vitrinite reflectance method for rank assessment is also very rapid and high degrees of accuracy and precision can be obtained. In the present study, coal rank is determined by measurement of vitrinite reflectance following the Australian Standard AS2418 (1982).

3.2 ANALYTICAL METHODS

3.2.1 SAMPLES

For this study, 205 samples were collected throughout the Yang Cao Gou Basin from 41 diamond drill cores (n=167) and five underground collieries (n=38). Five samples were also collected from each of the other six coal-bearing sub-basins along the eastern margin of the Songliao Basin. The

location and the sample types are shown in Appendix 1 and Figure 5.24. The samples from borehole cores and collieries were collected through the entire thickness of most coal seams.

3.2.2 SAMPLE PREPARATION

The most popular method for microscopic examination of coal involves the use of reflected light on polished surfaces under oil immersion.

In preparing samples for petrographic analysis, the raw coal was crushed to pass a 1 mm sieve and riffled to obtain about 8 g of sample. This was mixed with epoxy resin, allowed to set into a particulate mount and then ground and polished. Alternatively, coal block samples were cut perpendicular to bedding and then mounted and polished for petrographic analysis. These were cut and polished on a LOGITECH semi-automatic lapping machine to fit into plastic circular moulds (1" to 1 1/4" diameter). The cavity between the block and the mould was filled with "Araldite". When the resin had set, the section was removed from the mould and polished on a STRUERS DP-U4 diamond lap using 3 μm, I μm and then 0.25 μm polishing paste, and finally, by hand polishing on Selvyt cloth.

3.2.3 OPTICAL EQUIPMENT

In this study, instruments from the Coal Petrology Laboratory of the Department of Geology, University of Adelaide, were used. These included a Leitz ORTHOLUX II Pol microscope with three light sources white light for observation and photography, stabilized white light for reflectance measurements, and UV-blue light for fluorescence-mode microscopy. A Wild Photoautomat MPS 45 photometer, and a MPS 51S SPOT camera are attached to the microscope. This microscope is fitted with a Berek prism as the vertical illuminator. A X10 ocular and the X50 objective oil immersion lens were used for normal observation.

3.2.4 MACERAL ANALYSIS AND MICROLITHOTYPE ANALYSIS

The maceral analysis procedure and nomenclature of Australian Standard 2856 - 1986 is followed in this study. Maceral analyses were carried out under oil-immersion (DIN 5884) using 50x oil-immersion objectives and an automatic point counter at point spacings of 0.4 mm and with intervals between traverses of 0.8 mm. At least 500 points were counted, and visible minerals were counted individually. Each point was examined both in reflected light and in fluorescence mode. The number of the points counted for the macerals and mineral matter are expressed as percentages by volume of the total fields counted.

Microlithotype analysis was carried out in a similar manner to maceral analysis, under reflected light with oil immersion, but in this case the ocular of the microscope included a 20 point graticule. The distance between the outermost intersections of the graticule is 50 µm (Fig. 3.2). The nomenclature for microlithotype analysis is shown in Table 3.2.

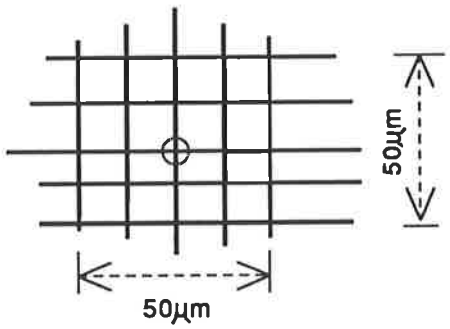

Fig. 3.2 Point graticule used for microlithotype analysis

Table 3.2 Microlithotype analysis using a 20 point graticule (modified from Mackowsky, 1982)

Microlithotype	Position of the graticule intersection with respect to macerals
Vitrite	All intersections on vitrinite
Liptite	All intersections on liptinite
Inertite	All intersections on inertinite
Clarite	All intersections on vitrinite and exinite with at least 1 intersection on each.
Durite	All intersections on inertinite and exinite, with at least 1 intersection on each.
Vitrinertite	All intersections on vitrinite and inertinite, with at least 1 intersection on each.
Trimacerite	At least one intersection on each of the three maceral groups
Minerals + V,E,I	At least one intersection on one of the three maceral groups and a mineral.
Minerals	All intersections on minerals

3.2.5 REFLECTANCE MEASUREMENTS

Vitrinite reflectance was measured for 40 samples from different locations and depths according to Australian Standard AS 2486 (Standards Association of Australia, 1981). Reflectance was measured in normally incident white light using oil immersion (DIN 58884) of refractive index 1.518, at a wavelength of 546 nm. The microphotometer was calibrated against synthetic yttrium aluminium garnet (YAG) synthetic gadolinium

gallium garnet (3G) standards of 0.917%, and 1.726% reflectance and a synthetic spinel standard of 0.413% reflectance. Maximum vitrinite reflectance was measured. The stage of the microscope was rotated to obtain the maximum reading and then rotated through 180 degrees for the second maximum reading. Each pair of readings was averaged and calculated as mean maximum vitrinite reflectance. Objective was used and the measurement area set on about 5 square microns.

For assessment of coal rank, maximum reflectances were taken from the vitrinite sub-maceral telocollinite, where identifiable. The number of measurements made depended upon the range of reflectance values encountered in the sample. The required number of measurements can be estimated from the following formulae (Australia Standard 2486, 1981):

$$N = \left[\frac{\text{Range}}{0.04}\right]^2 \qquad \text{or} \qquad N = \left[\frac{s}{0.01}\right]^2$$

where

N = number of individual reflectance readings

s = standard deviation.

3.2.6 ROCK-EVAL AND TOTAL ORGANIC CARBON ANALYSES

Rock-Eval analyses were carried out on 140 specimens collected from the Yang Cao Gou basin, in the Organic Geochemistry Laboratory, Bureau of Mineral Resources, Geology and Geophysics (BMR), Canberra and total organic carbon analyses were undertaken in the Department of Geology and Geophysics, Adelaide University.

The total organic carbon (TOC) was measured using the Leco Carbon Analyser. The samples were initially treated with HCl at 100 ^{0}C to remove inorganic carbonate and then combusted at 1250 ^{0}C in an oxygen stream to produce CO_2. The CO_2 was collected on ascarite absorbant in a sealed glass tube, the resultant weight change of which was measured.

Rock-Eval pyrolysis was combined with the recently developed procedure of quantitative pyrolysis-gas chromatography (PGC) in order to determine (1) the quantity, quality and thermal maturity of the organic matter; (2) the relationship between coal chemistry, organic petrography, and depositional environment and (3) the yield of paraffins, which is most important to the assessment of non-marine source rocks. The quantitative yields of C_7 to C_{27} normal hydrocarbons, low molecular weight aromatics (C_7 - C_9) and phenols (C_6 - C_8) were determined as described in Powell et al., (1991)

Sample size for Rock-Eval pyrolysis depends on the total organic carbon content: 10 mg and 100 mg of powdered sample for TOC values greater than 25% and less than 25%, respectively. Up to 22 samples including a standard were automatically run through the Rock-Eval II machine at one time.

Each sample was initially heated at 300 ^{0}C for 5 minutes; the amount of hydrocarbon released is expressed as S_1, in milligrams per gram of sample. Parameter S1 represents the volatile portion of the geologically generated bitumen (Espitalie et al., 1986). The sample was then heated further at 25 degrees C / min. up to 550 degrees C and maintained at that temperature for 1 minute. The amount of hydrocarbons generated during this cycle is derived from kerogen cracking and from the volatilisation and cracking of heavy extractable compounds such as resins and asphaltenes (Espitalie et al., 1986). This quantity is recorded as S_2 (mg/g). S_2 is the amount of hydrocarbons released during temperature-programmed pyrolysis (300 - 550 degrees C) and represents the bitumen that would be generated if burial and maturation continued to completion. S_3 is the quantity of CO_2 formed by pyrolysis of the organic matter, expressed in milligrams of CO_2 per gram (mg CO_2 / g) of rock. T_{max}, in degrees Celsius, is the temperature
of the maximum of the S_2 peak and represents an estimate of thermal maturity (Espitalie et al., 1985).

Based on the above parameters, several useful factors can be calculated. The hydrogen index (HI) is the normalized S_2 value (S_2/TOC), expressed as mg HC/g of TOC, which allows the types of OM (organic matter) to be

estimated (Table 3.3). The oxygen index (OI) is the normalized S_3 value (S_3/TOC), expressed in mg CO_2/g of TOC. Production index (PI) or transformation ratio (PI = S_1/S_{2+1} indicates the level of thermal maturation and also the presence of epigenetic hydrocarbons. S_2/S_3 indicates the type of the organic matter for low to moderately mature samples. T_{max} obtained from Rock-Eval pyrolysis indicates the level of thermal maturity.

Table 3.3 Rock-Eval interpretive guidelines (modified from Peters, 1986)

Source Rock Generation Potential			
Source Quality	TOC (wt%)	S_1	S_2
poor	0-0.5	0-0.5	0-0.25
fair	0.5-1.0	0.5-1.0	2.5-5.0
good	1-2	1-2	5-10
very good	>2	>2	10

Type of Hydrocarbons Generated		
Type	HI (mg HC/g TOC)	S_2/S_3
gas	0 - 150	0 -3
gas and oil	150 - 300	3 - 5
oil	> 300	> 5

CHAPTER 4. COAL MEASURES OF THE YANG CAO GOU BASIN

4.1 STRATIGRAPHY OF THE COAL MEASURES

The Yang Cao Gou Basin contains Jurassic and Cretaceous coal-bearing strata totalling over 2355 m in thickness and lying unconformably on granitic basement rocks. The stratigraphy of the more widespread upper member of Yingcheng Formation is summarised in Table 4.1. The geological map of the Yang Cao Gou basin is shown in Figure 4.1. The following discussion of the sequences is based largely on Yang (1986), Liu (1988) and Zhao (1989).

The basal An Min Formation (J_3am), ranging from 5 to 200 m in thickness, comprises a dull purple andesite, purple grey conglomerate containing tuffaceous sandstone, and dark greyish green andesitic conglomerate.

The Shahezi Formation (J_3sh) of late Jurassic age conformably overlies the An Min Formation. The unit is composed mainly of granitic and andesitic conglomerate, with coarse sandstones, tuff and mudstone. On the basis of lithology, the Shahezi Formation can be subdivided into three units. The lowest unit, 60 m thick, consists of granitic conglomerate intercalated with tuffaceous sandstone and mudstone. The second unit is approximately 70 m of carbonaceous mudstone intercalated with tuffaceous sandstone, sandy conglomerate, and containing abundant carbonized plant fragments. Above unit two is approximately 70 m of predominantly brown, fine to coarse grained, unsorted sandy conglomerate.

The Yingcheng Formation (K_1y) lies unconformably on Shahezi Formation, and contains the most important coal seams in this basin. It is composed dominantly of volcanic rocks, including clastic types and up to 5 economic coal seams, intercalated with andesitic basalt. Coal seams vary in thickness from about 1 to 10 m (Fig. 4.2). This formation is overlain by basalt of the Quan Tou Formation. The Yingcheng Formation varies in thickness from 78 to 300 m and can be subdivided into three members, of

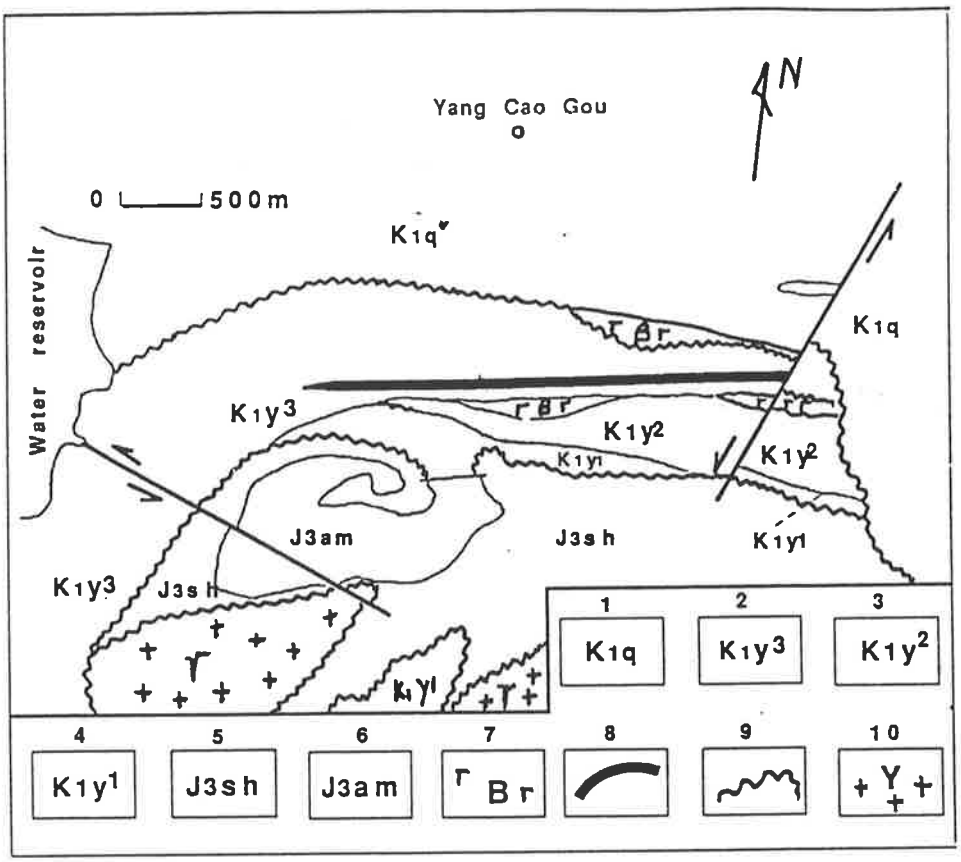

Fig. 4.1 Geological map of the Yang Cao Gou coal sub-basin

1. Quan Tou Formation; 2. Upper member of Ying Cheng Formation;
3. Middle member of Ying Cheng Formation; 4. Lower member of Ying Cheng Formation;
5. Sa He Zi Formation; 6. An Min formation;
7. Basalt; 8. Coal; 9. Unconformity; 10. Granite.

which the upper one is the thickest and contains the most important coal seams (Geological Survey of Jilin, 1986).

The lower member (K_1Y^1), ranging up to 308 m in thickness, consists of acidic volcanic rocks and contains gray-white rhyolite, spherulitic rhyolite, lava and bentonite layers. Seams of zeolite and bentonite, plus pearlite, are important indicators for identifying the Yingcheng Formation. This member generally measures more than 290 meters in thickness.

The middle member (K_1Y^2) is up to 300 m thick. Distributed in the east of the study area, it consists mainly of gray tuffaceous sandy conglomerate, tuffaceous sandstone interlayered with some bentonite lenses, gray-white tuffaceous muddy sandstone and siltstone, gray to black carbonaceous muddy sandstone intercalated with some thin coal seams, gray-white tuffaceous conglomerate, sandstone with a few bentonite lenses, and at the top, andesitic basalt and basaltic- conglomerate.

The upper member (K_1Y^3) contains the upper coal which is distributed throughout the Yang Coa Gou Basin. This unit contains 5 economic seams ranging from 1 to 13 meters in thickness. This economically significant member can be subdivided into 6 sub-units as illustrated in Table 4.1.

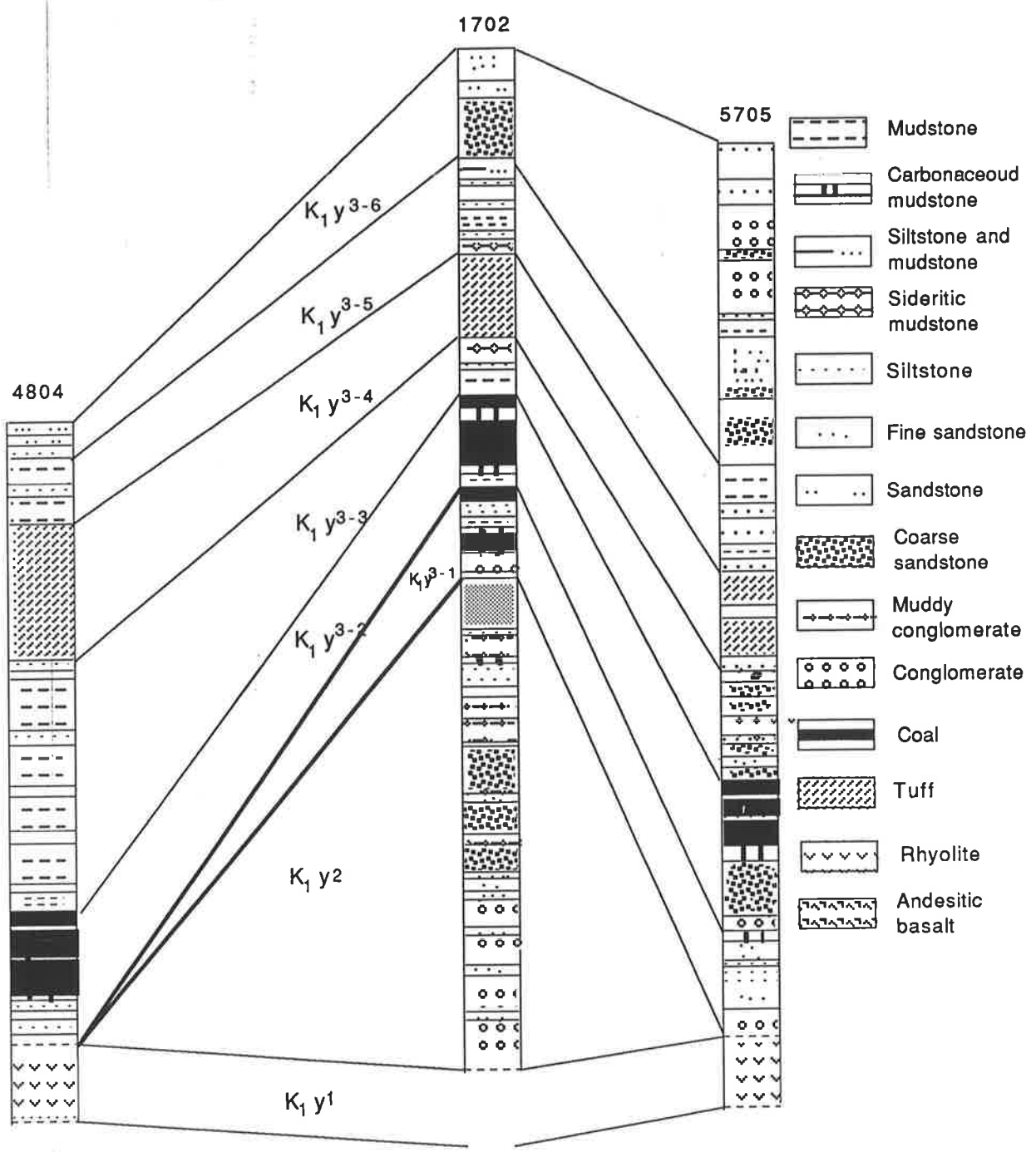

Fig. 4.2 Correlation of coal-bearing sequences of the Yingcheng Formation, Yang Cao Gou Basin. For borehole location see figures 4.6 and 5.24.

Table 4.1 Lithology of units in the upper member of the Yingcheng Formation (modified from Yang, 1987).

Sub-units	Lithology	Thickness (m)
K_1Y^{3-6}	grey - white, thickly-bedded tuffaceous sandstone, common sandy conglomerate, no bedding.	8-80
K_1Y^{3-5}	grey-black carbonaceous mudstone, shale, and muddy siltstone, interlayered with sandstone, horizontal bedding and abundant plant fossils.	11-85
K_1Y^{3-4}	grey to greyish green, tuffaceous sandstone, predominantly massive, scattered carbonaceous fragments.	3-40
K_1Y^{3-3}	dull grey and greyish black mudstone, intercalated with light grey to grey- white sandy conglomerate, 5-15 cm thick siderite thoughout, laminated and contorted bedding, slump structures, plant fossils.	1-60
K_1Y^{3-2}	sandy conglomerate, sandstone, thick superincumbent coal seams, interbedded with carbonaceous mudstone.	5-40
K_1Y^{3-1}	grey-white tuffaceous sandy conglomerate, carbonaceous siltstone, 1 - 3 workable coal seams, breccias, tuffs	31-187

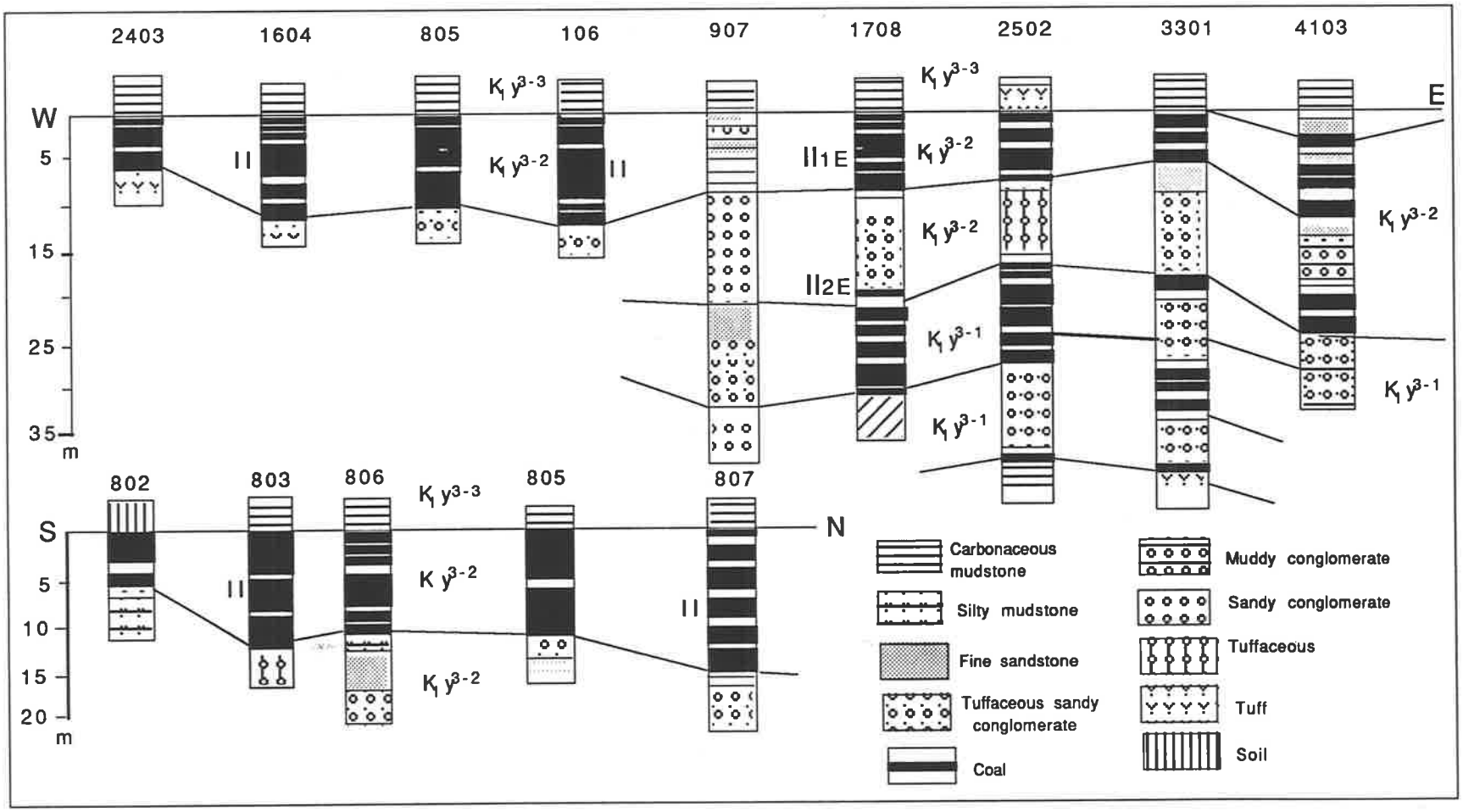

Fig. 4.3 Correlation and seam distribution of Group II coal beds in the upper member of the Yingcheng Formation (modified from Zhou et al., 1985). See Figs. 4.6 and 5.24 for location of boreholes

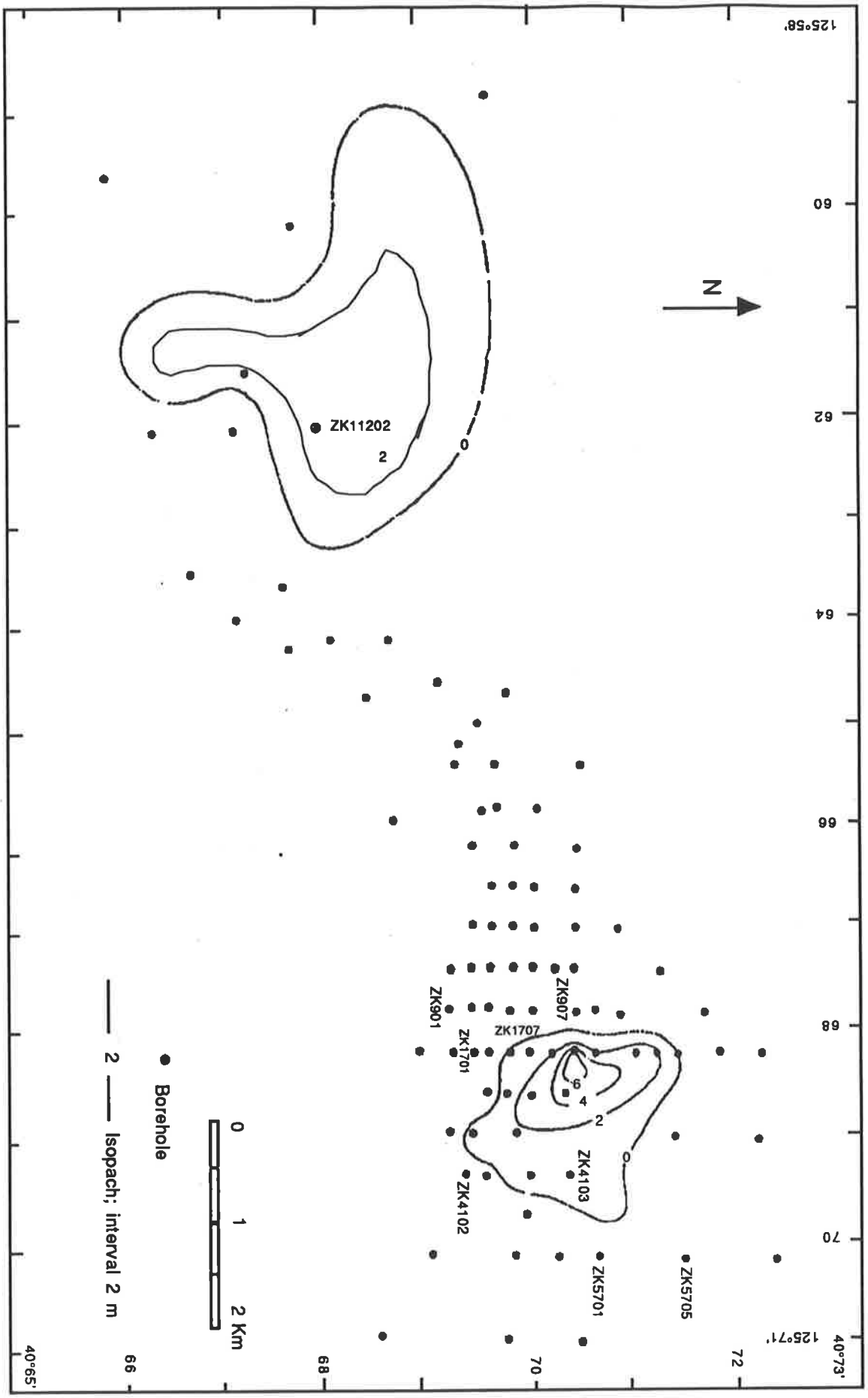

Fig. 4.4 Isopachs of the Lower Group coals, Yang Cao Gou Basin (modified from Zhao, 1989)

The Ying Chen Formation is overlain by the Quan Tou Formation which is distributed in the central and southern parts of the basin and is over 1,000 m thick. It consists chiefly of basalt with interbeds 20-60 m thick of muddy conglomerate, grey-green sandy conglomerate and purple-red sandstone and mudstone.

K-Ar dating of volcanic rhyolite in the Yingcheng Formation gave a minimum age of 105 Ma (Yang, 1986).

4.2 COAL SEAM NOMENCLATURE, COAL DISTRIBUTION AND QUALITY

During the time of deposition of the Yingcheng Formation, there were three periods of coal accumulation. They are K_1Y^2 (middle member), K_1Y^{3-1} (unit 1 of upper member) and K_1Y^{3-2} (unit 2 of upper member), respectively. Coal formed in various swamps: fringing lakes, between stream channels, between deltaic distributaries, and between alluvial fans (Zhao et al., 1987). The most extensive coal seams (in sub-unit K_1Y^{3-2}), are thickest in the western centre and east of the basin. The Geological Survey of Jinlin classified the Upper Cretaceous coal measures of the Yang Cao Gou Basin on the basis of quality characteristics into a lower group of coals (in member K_1Y^2) and an upper group of coals (in member K_1Y^3). The latter one is further divided into Group I coals (in sub-unit K_1Y^{3-1} , including seam I_1 to seam I_5) and Group II coals (in sub-unit K_1Y^{3-2}, including seam II, II_1 and II_2). The coal seam correlations are shown in Figure 4.3. This classification for the Yang Cao Gou Basin is widely accepted by the coal industry in China and is followed in the present study. The aggregate thickness of the lower group of coals, the Group I coals, and the Group II coals ranges from 0.15 m to 11 m, 4.22 m to 7.64 m, and from 1.8 m to 14.52 m, respectively, depending on borehole locality.

The K_1Y^2 sequences (middle member) consist of mainly coarse clastic rocks; beds of carbonaceous mudstone and siltstone are few and relatively thin. Coal seams observed in this unit have very limited persistence, and in most cases, are unworkable. The isopachs of the lower coal group are

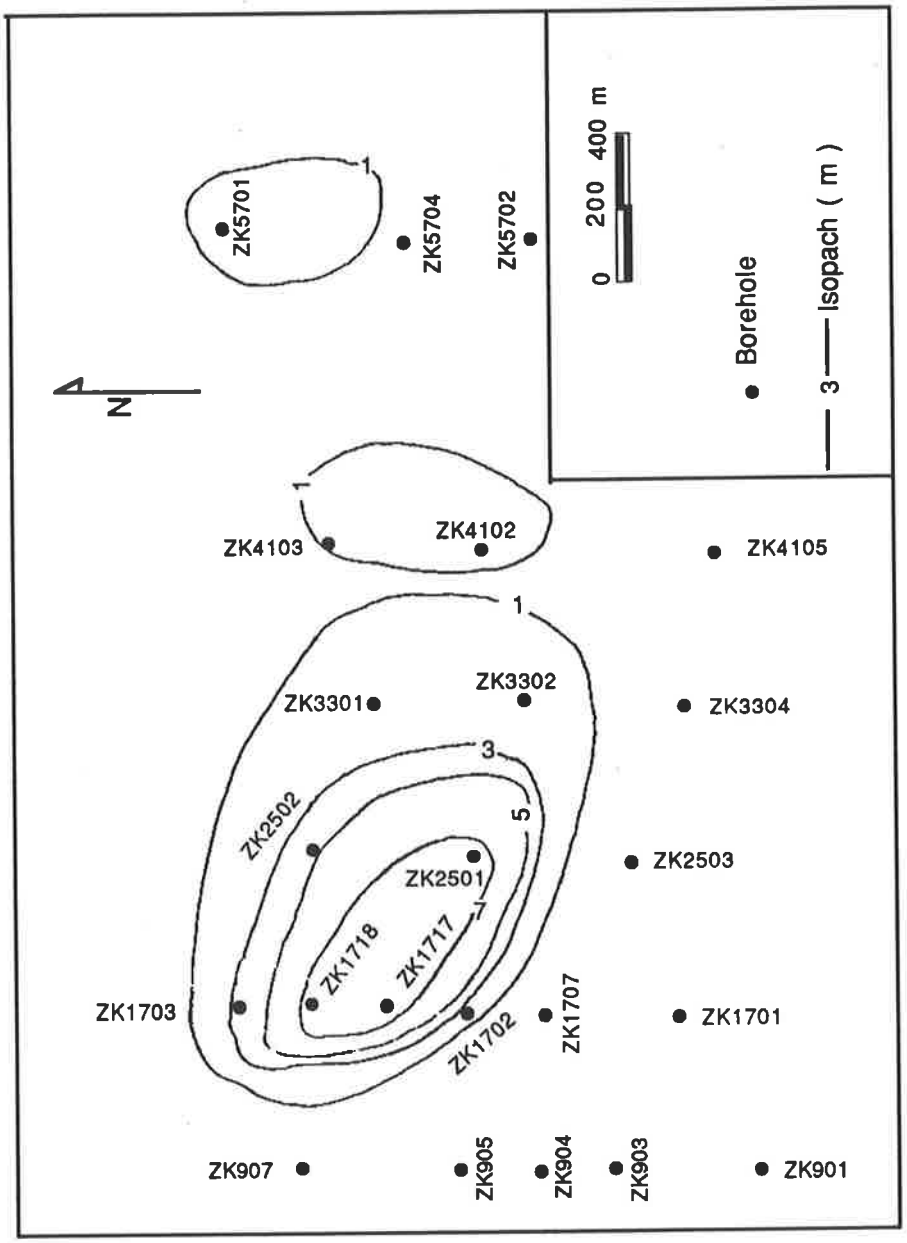

Fig. 4.5 Isopachs of Group I coals, in lower member of Yingcheng Formation , Yang Cao Gou Basin

shown in Figure. 4.4. However, coals in this unit account for only 0.8% of the coal resources in the basin.

The Group I coals in K_1Y^{3-1} occur in 5 seams which comprise about 12% of the coal resources in the basin. Of those coal seams, I_2, I_3, I_4 and I_5 are workable and seam I_1 is unworkable. These coals are concentrated in the eastern part of the basin. Proximate analyses of selected Group I coals are shown in Table 4.2. Most of the coals are sub-bituminous with volatile matter contents (calculated on a dry ash-free basis) ranging from 41.13 to 52.45 per cent. The moisture content of the seams varies from 5.42 per cent to 11.02 per cent, and rises markedly as the sequence is ascended pointing to depth of burial by younger rocks as the cause of this variation. The calorific value of the Group I coals ranges from 2830 to 5485 Kcal/kg, and in most cases this increase is proportional to increasing carbon and decreasing moisture contents. The ash content varies from 25.67 to 58.23 per cent, with an average value of 43.33. Where the isopachs of the lower coal group (Fig. 4.4) are compared with the isopachs of the Group I coals (Fig. 4.5), it is apparent that the coal depocentre migrated northwestward.

The coals in K_1Y^{3-2} are referred to as Group II coals; these are economically the most important and they are well developed over the whole deposit, averaging about 7.2 m in thickness (Fig. 4.6). The Group II coals conformably overlie the uppermost clay bed of K_1Y^{3-1} and constitute the major resource in the study area (93.2%). In places, the seam appears to split into two subseams, referred to as the II_{1E} and II_{2E} coal seams on eastern part and II_{1W} and II_{2W} coal seams on western part of the basin(Fig. 4.7). Elsewhere in the field area it remains as one seam (referred to as II_1 coal seam). Seam thickness varies from 2.74 to 8.54 m in the east (II_2 coal seam), 7.68 to 10.90 m in the center (II_1 coal seam), and 3.61 to 10.91 in the west (II_3 coal seams). Proximate analyses, Rmax data and petrographic analyses of samples from boreholes ZK1717, ZK1718, ZK1703, ZK2501, ZK2502, ZK3302, ZK3301, ZK4105, and ZK4103 are shown in Table 4.3. All the coals are sub-bituminous with volatile matter content, calculated on a dry ash-free basis, ranging from 36.53 to 44.97%. Weighted average moisture and ash contents for the whole seam range from 20.5 to 41.18 % and from 25.96 to 41.18%, respectively. Coal seam II has an average calorific value of from 3874 to 5070 Kcal/kg,

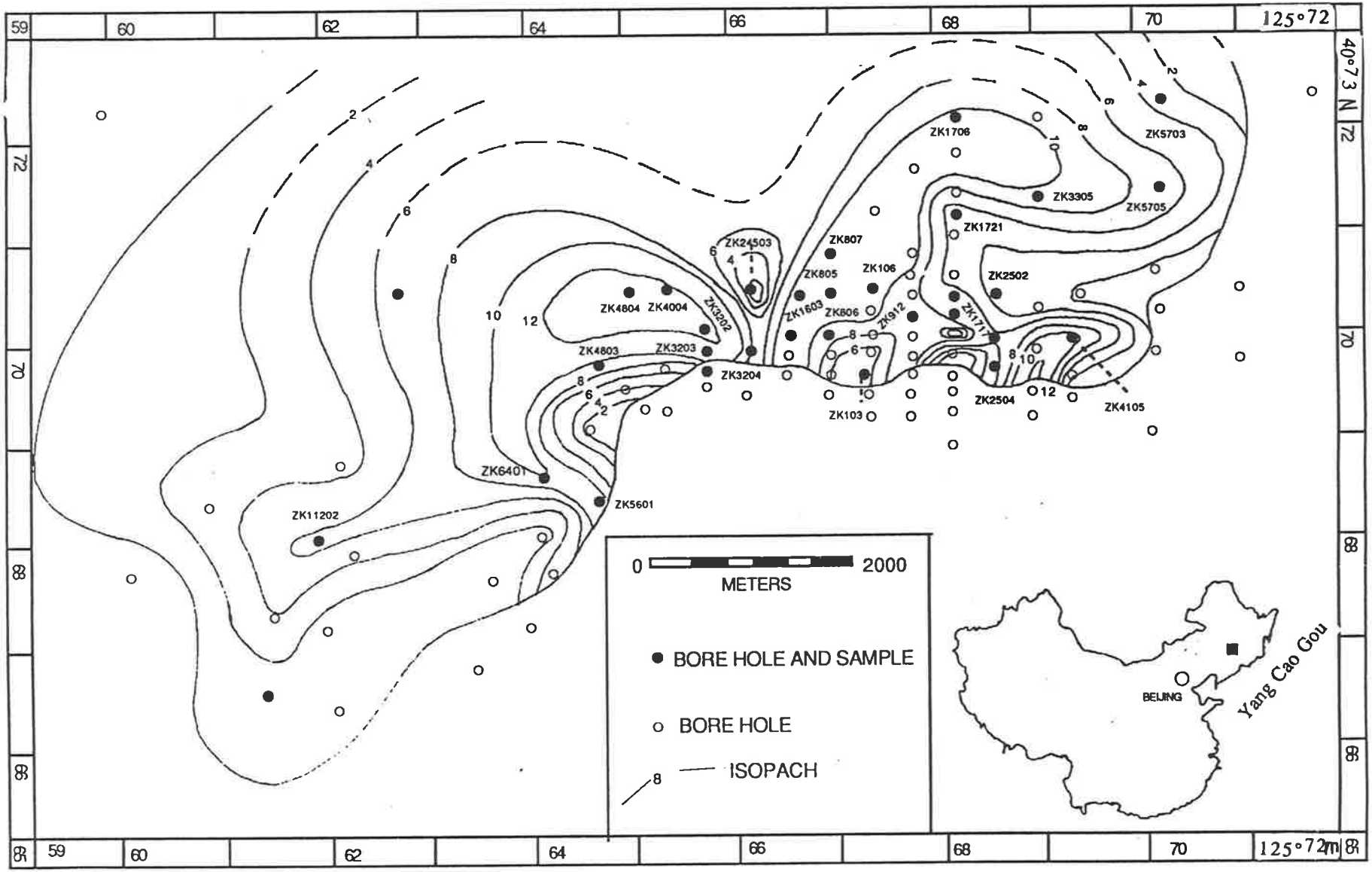

Fig. 4.6 Sample localities and isopach map of the Group II coals in Ying Cheng Formation, Yang Cao Gou Basin (modified from Zhao et. al., 1989).

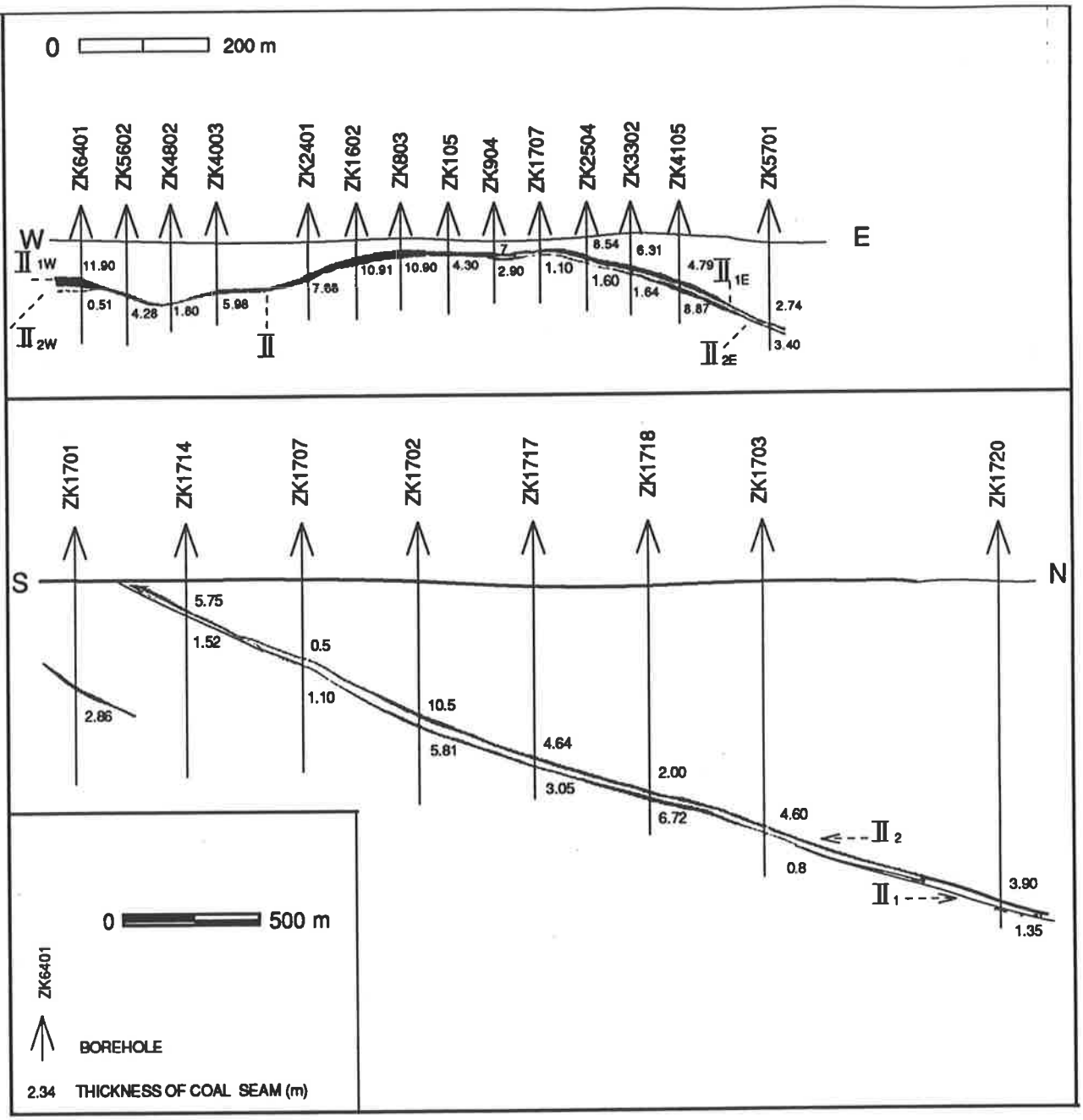

Fig. 4.7. Distribution of Group II coals in the upper member of the Yingcheng Formation. modified from Zhao, 1989. Borehole locations are shown in figures. 4.6 and and 5.24

Table 4.2 Proximate analysis data for some Group I coals and shales the Yang Cao Gou Basin (analyses by the Geological Survey of Jilin)
Yangcaogou basin (analysis by The geological Survey of Jilin)

Borehole Number	Sample Numbe	Seam	M	Ash (db)	V.M (db)	Tot. S	C. V
			% by weight				
ZK1717	1	I_1	8.28	25.67	28.89		5485
	2	I_2	8.24	33.62	43.93		4759
	3	I_3	5.56	58.23	49.30		2830
ZK1718	4	I_1	8.29	45.74	52.45		3845
	5	I_2	6.65	51.23	50.47		3172
	6	I_3	10.1	33.62	45.55		4711
ZK1703	7	I_2	9.73	34.93	51.38		4323
	8	I_3	6.81	53.54	50.88	0.47	2717
	9	I_4	9.09	39.47	43.70	0.54	4126
ZK2501	10	I_2	5.91	42.32	48.30	0.40	4007
	11	I_3	6.41	33.30	48.03		4386
	12	I_4	5.42	62.00	52.56		2399
ZK2502	13	I_2	8.40	33.14	47.49		4844
	14	I_3	11.02	37.57	48.58		4304
	15	I_4	7.36	36.45	44.25		4634

Key to the Table; M: Moisture content (db)
V. M: Volatile matter content (db)
Tot. S: Total Sulpher (daf)
C. V: Calorific value (gross) (*daf*)

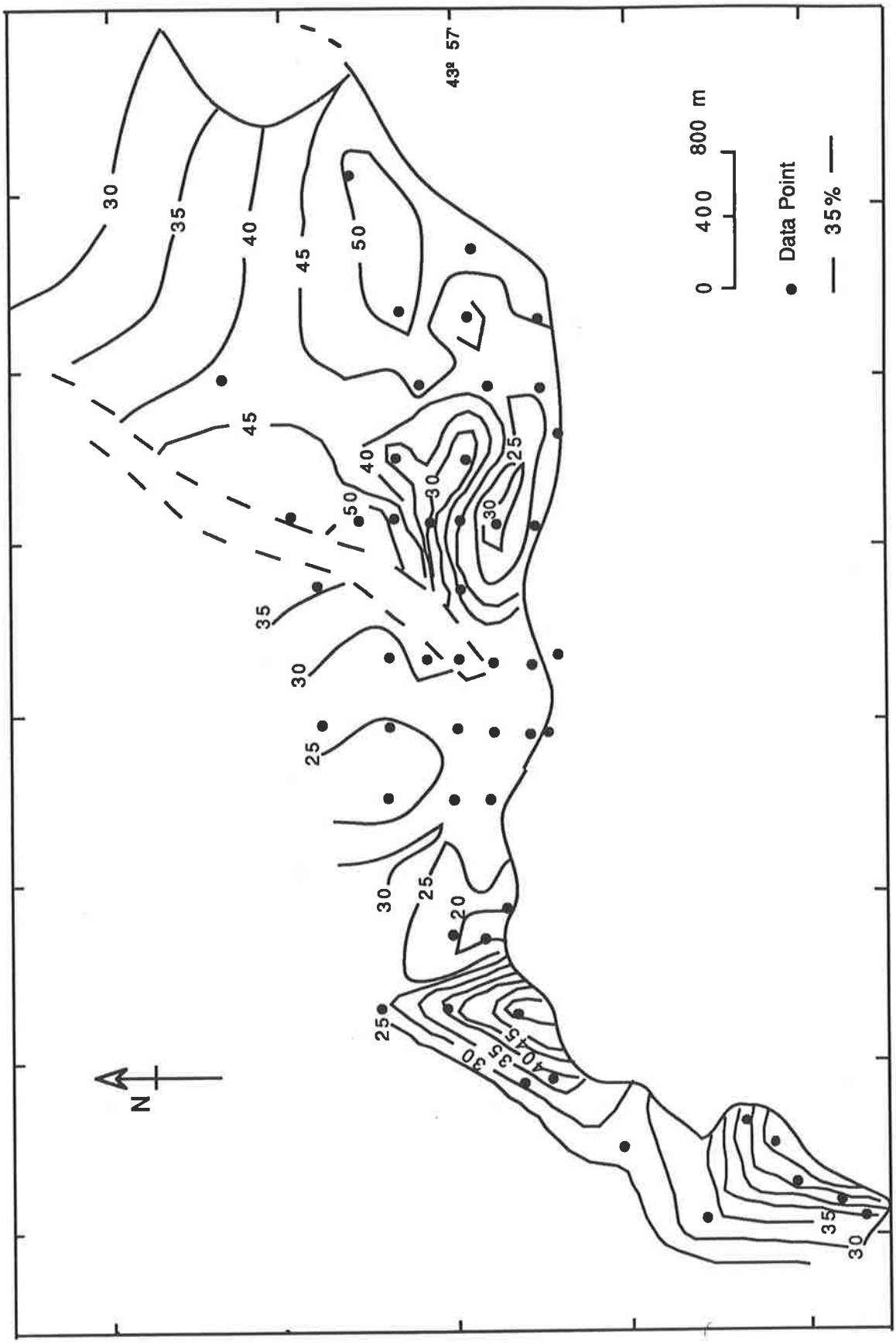

Fig. 4.8 Contours of ash contents of Group II coals, Yang Cao Gou Basin (modified from Liu, 1988 and Zhao, 1989)

depending on depth of burial. However, the total sulphur contents are low (0.42 to 0.55 %); and this is a characteristic feature of the Group II coals in the study area. The contours of ash content (Fig. 4.8) and calorific value (Fig. 4.9) indicate that the peat environment was a stable swamp, as the ash content decreases and calorific value increases toward the coal depocentre. Coal seam II has several lenticular black mudstone and sideritic mudstone partings and rests on a thin carbonaceous mudstone, or in places, on siltstone, sandstone, or tuff. This indicates that coal seams result from shallow lake deposits (Fig. 4.10).

4.3 DEPOSITIONAL ENVIRONMENTS OF THE COAL MEASURES

The sediments in the Yang Cao Gou Basin are terrestrial in origin. The coal measures were deposited in a variety of environments ranging from alluvial fan to fluvial, deltatic and lacustrine (Zhao et al., 1989).

Liu (1988) considers that there are two types of alluvial fan deposits in the basin: dry alluvial fans with no coal accumulations and wet alluvial fans with coal accumulation. The dry alluvial fan facies is present in the sequences of the Shahezi Formation on the southern margin of the basin. These sediments are red in colour and contain no plant fossils. The wet alluvial fan facies, which was deposited under humid climate conditions where ground-water levels were high, is represented by the lower coal member (K_1Y^2) sediments of the Yingcheng Formation (Fig. 4.11). Zhao et al (1989) agreed that K_1Y^2 mostly formed in wet alluvial fan environments, and suggested that the coals in this sequence accumulated in the inter-lobe depressions of alluvial fans. The K_1Y^2 sequence consists of debris flow, river channel and flood plain deposits, showing massive bedding, clast imbrication and graded bedding, and in addition some parallel bedding, horizontal bedding and small scale cross bedding (Liu, 1988). The coals formed in this environment (lower coal group) are of very limited extent and hence mostly unworkable.

Table 4.3 Proximate analysis data for some Group II coals and shales in the Yang Cao Gou Basin (analyses by the Geological Survey of Jilin)

Borehole Number	Sample Numbe	Seam	M air dried	Ash db	V. M db	Tot S daf	C. V daf
			% by weight				
ZK904	16	II	11.95	40.93	44.03	0.27	3663
	17	II	10.13	44.22	46.41	0.33	3582
ZK905	18	II	8.38	45.73	46.08	0.39	3595
	19	II	8.57	34.29	46.39	0.35	4138
ZK1702	20	II 1E	7.69	51.29	48.26	0.36	3084
	21	II 2E	9.82	32.39	45.39	0.43	4506
ZK1714	22	II 1E	11.57	47.63	41.85		3573
	23	II 2E	10.72	33.31	42.83	0.39	4694
ZK1717	24	II 1E	8.52	22.78	43.31		5604
	25	II 2E	7.8	31.94	47.99		4769
ZK1718	26	II 2E	4.73	44.81	55.35		3761
	27	II 2E	6.84	46.89	47.11		3739
ZK1720	28	II 1E	2.04	42.09	49.82	0.74	4222
	29	II 2E	2.03	42.09	49.82		4172
ZK2501	30	II 1E	10.86	19.72	44.23	0.61	5873
	31	II 2E	7.61	29.12	43.38		5209
ZK2502	32	II 1E	7.32	34.59	47.08		4642
	33	II 2E	8.19	26.42	46.47		5368

Table 4.3 (CONTINUED)

Borehole Number	Sample Numbe	Seam	M	Ash	V. M	Tot. S	C. V
			% by weight				
ZK3302	16	II 2	6.62	62.64	48.72		2491
	17	II 3	9.56	40.77	46.07		4192
ZK3301	18	II 2	8.02	47.36	42.44	0.45	3239
	19	II 3	8.43	46.76	41.93		3287
ZK4106	20	II 2	8.51	43.33	43.13	0.42	3800
	21	II 3	8.31	46.32	40.82	0.40	3725
ZK4105	22	II 2	8.32	40.44	44.65	0.34	4267
	23	II 3	8.99	32.99	44.88		4898
ZK4103	24	II 2	5.92	46.40	43.90	0.64	3631
	25	II 3	5.06	53.14	55.09	0.52	2587
ZK5703	26	II_1	3.47	26.20	41.13	0.49	6678
ZK3305	27	II_1	1.51	38.14	44.64	1.23	5275
ZK910	28	II_1	4.15	35.20	47.56	0.78	4770
ZK103	29	II_1	12.55	25.50	45.53	0.40	5061
ZK105	30	II_1	13.22	26.29	44.37	0.40	5052
ZK801	31	II_1	9.96	4.74	31.95		7142
ZK806	32	II_1	6.21	26.68	46.24		5343

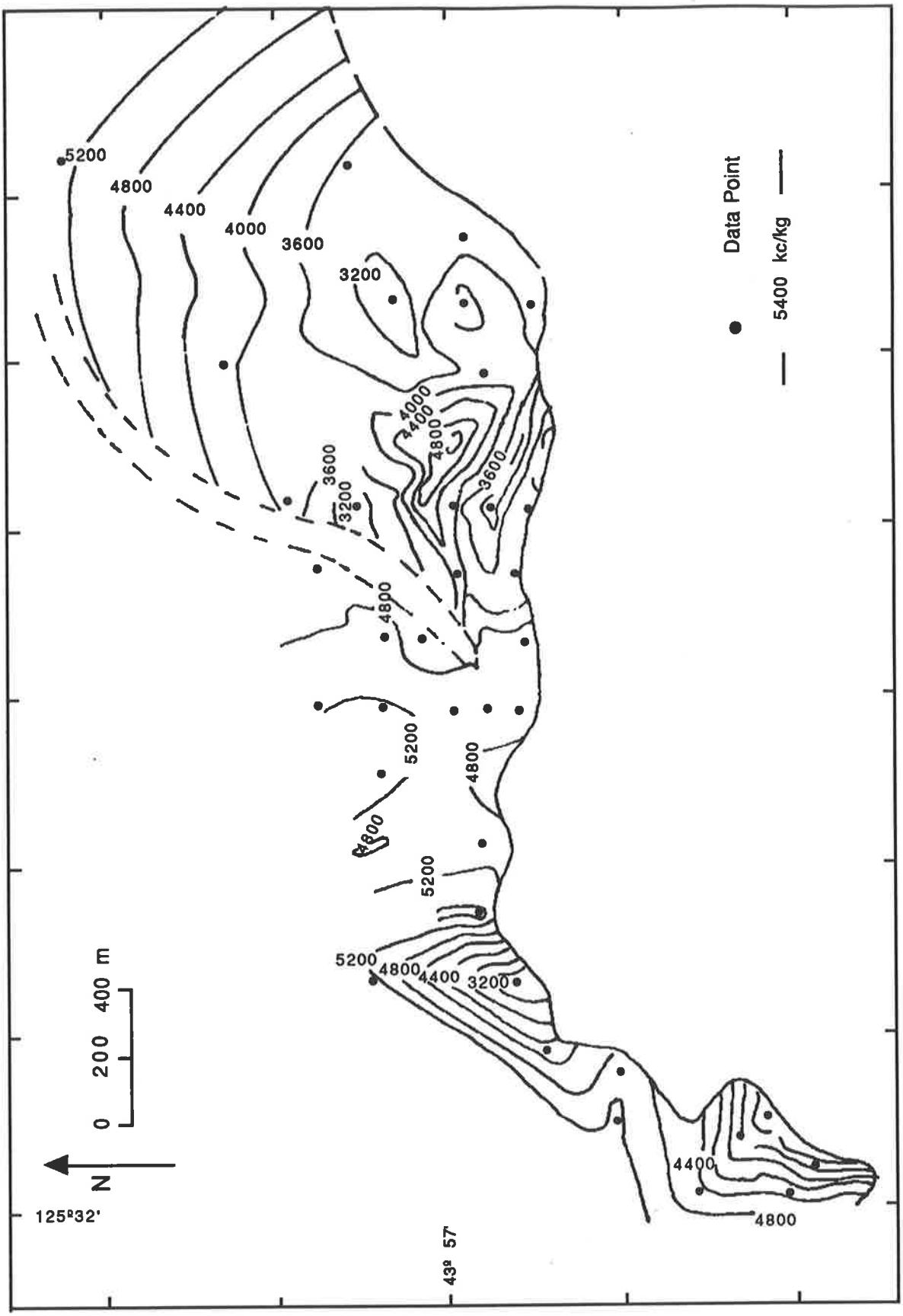

Fig. 4.9. Contours of calorific value of the Group II coals, Yang Cao Gou Basin (modified from Liu, 1988 and Zhao, 1989).

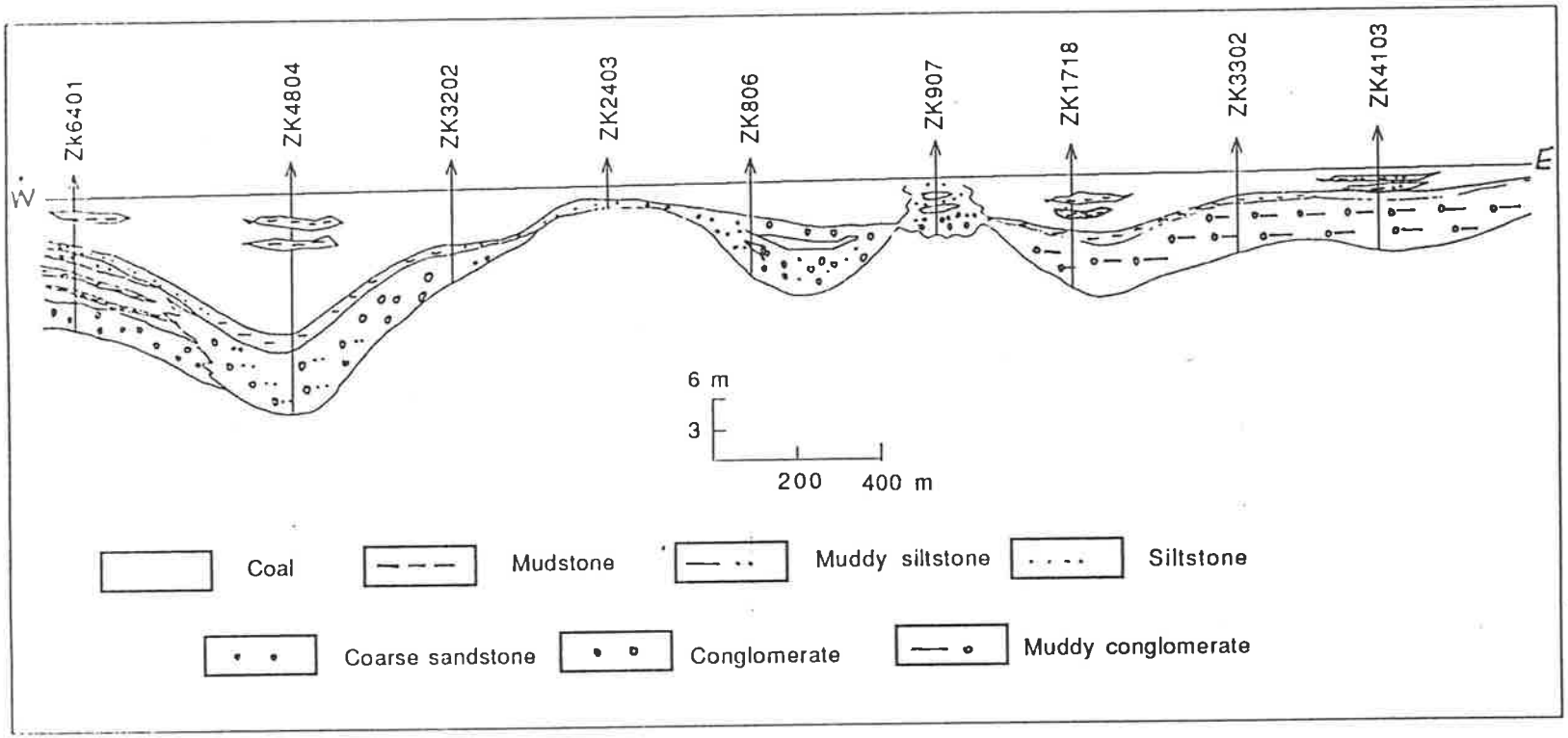

Fig. 4.10 Cross section of the K_1y_{3-2} sequences, Yang Cao Gou Basin

Fluvial sediments are also found in K_1Y^2 on the eastern and southwestern margins and some parts of the basin centre. Two subfacies are recognized: 1) channel facies, and 2) flood plain facies.

The channel facies, up to 6 m thick, contains greyish white fine-grained conglomerate with imbricated structures, sandy conglomerate, and fine-grained sandstone with small-scale cross bedding.

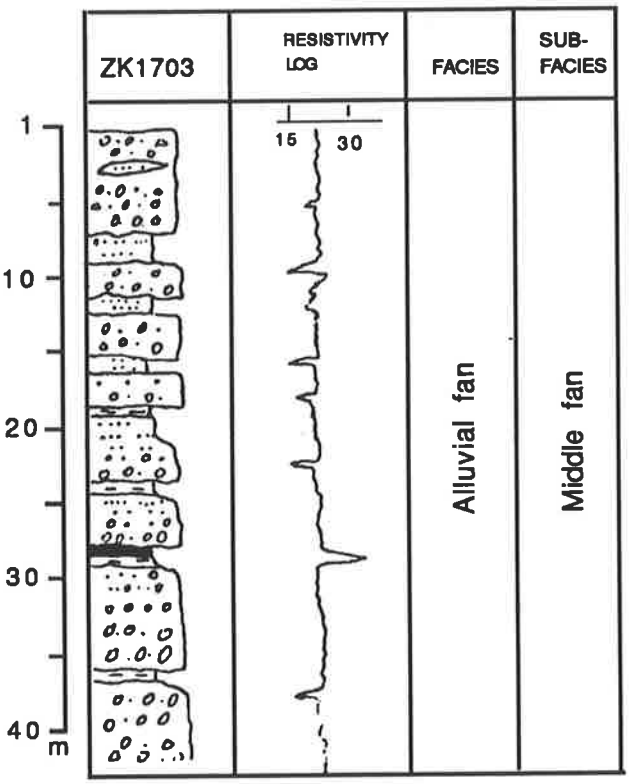

Fig. 4.11 Stratigraphy of the alluvial fan sequences (in borehole ZK 1703), lower coal member (K_1y^2) of the Ying Cheng Formation, Yang Cao Gou Basin (modified from Liu, 1988 and Zhao, 1989).

The flood plain sediments comprise natural levee, overbank, and swamp deposits (Fig. 4.12). The levee deposits are composed mainly of siltstone, in places as muddy or interbeded with fine-grained sandstone. The overbank facies consists mainly of black mudstone intercalated with

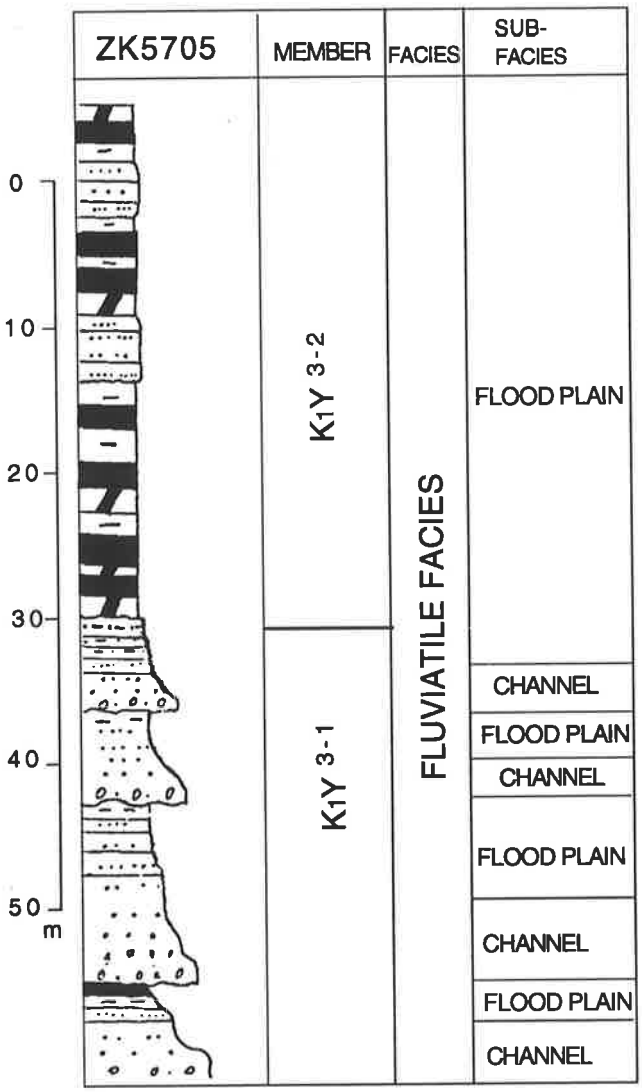

Fig. 4.12 Stratigraphy of the fluvial deposition, K y $^{3-1}$ and K$_1$ y$^{3-2}$ of the Yingchen Formation, Yang Cao Gou Basin modified from Liu, 1988 and Zhao, 1989).

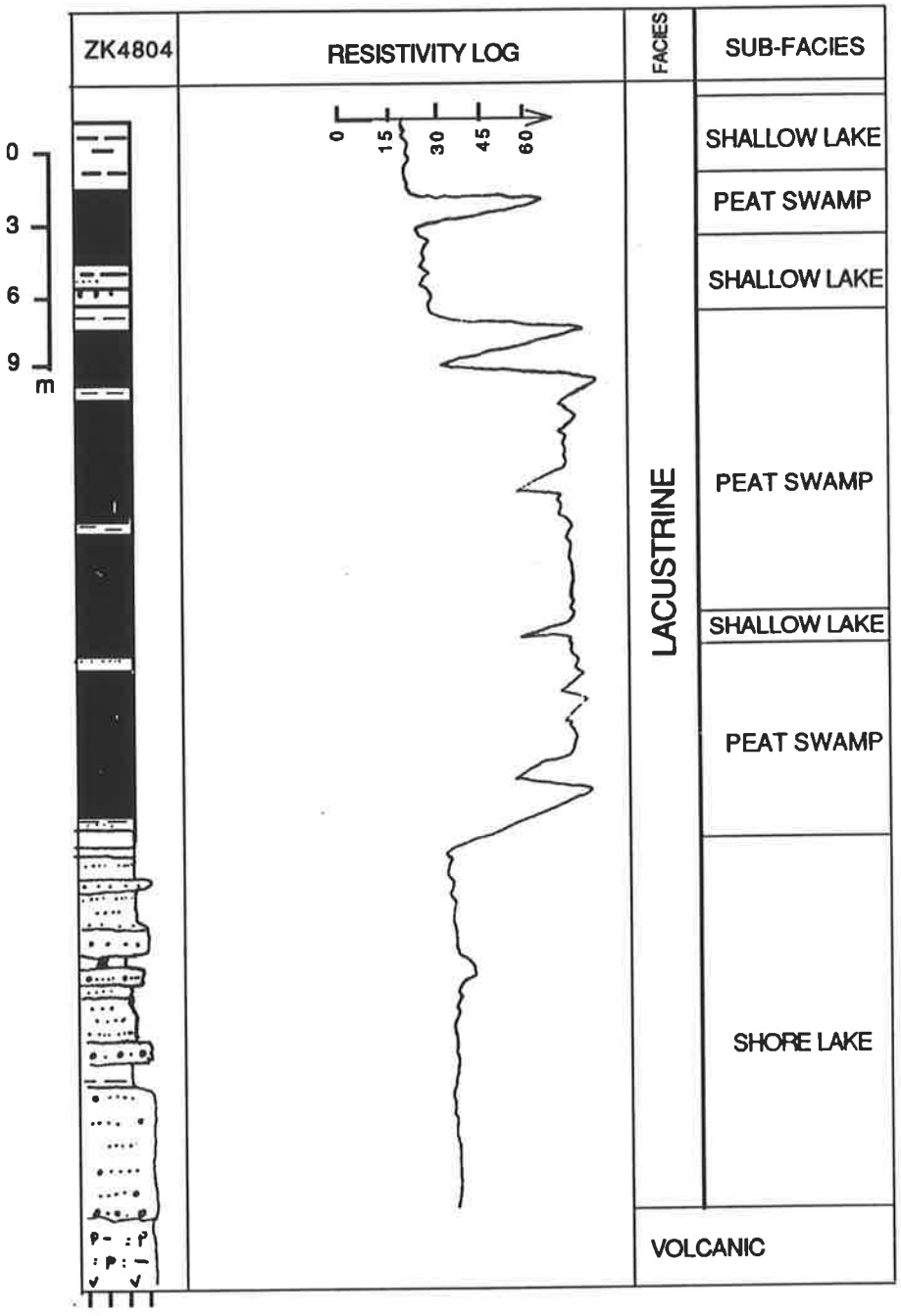

Fig. 4.13 Stratigraphy of the lake shore sequence, K_1Y^{3-2} Yingcheng Formation (modified from Lui, 1988 and Zhao, 1989)

siltstone displaying horizontal and current bedding, and containing abundant carbonaceous debris and plant fossils.

The swamp sediments are chiefly carbonaceous mudstone and coal (lower Group coal). Much plant debris and many small root fossils are found in the mudstone. This coal is thin and readily splits (Liu, 1988).

Lacustrine deposits are widely represented in the Yang Cao Gou Basin. The most important coal seams were deposited in lake shore (coal Group II coal) and delta fan (Group I coal) environments. From Figure 4.13, the sequence of lake shore sediments begins with a thin conglomerate overlying rhyolite, followed by intercalated black siltstone and thin mudstone, coal with black mudstone partings, and thick mudstone interbedded with shale and sideritic mudstone. Mudstone and siltstone show horizontal bedding. The delta fan is composed of delta fan plain, and delta fan-front (Fig. 4.14). The grain-size of delta fan sediments grades from fine in the lower part to coarse grained in the upper part.

4.4 PALAEOCLIMATE

Evidence from oxygen isotopes, palaeobiogeography and rock distribution suggests that the late Jurassic to Cretaceous global climate was characterized by high mean global temperatures and low precipitation, with global warming culminating in the late part of the Early Cretaceous (Frakes, 1979). Based on the evidence from the Cretaceous fossil flora and fauna of the Songliao Basin, Wang et al., (1979) suggested a humid temperate climate for the Jurassic-Cretaceous transition, followed by humid subtropical to warm temperate climate conditions through most of the Cretaceous. Table 4.4 summarises the climatic variations during the Jurassic to Cretaceous in Northeast China.

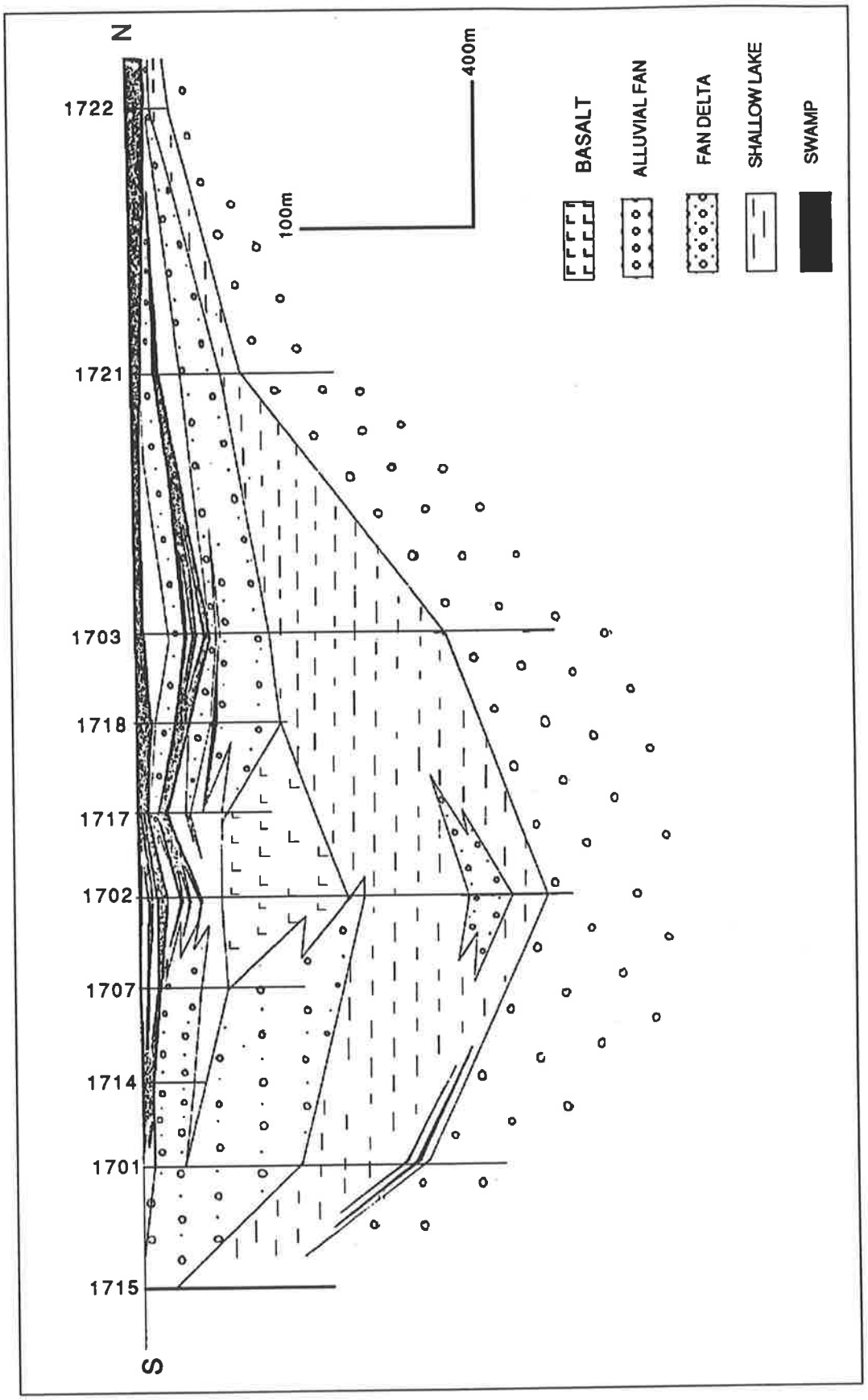

Fig. 4.14 Sedimentary facies variation, Ying Cheng Fornation, Yang Cao Gou basin (modified from Zhao, 1989).

TABLE 4.4 Jurassic to Cretaceous climate variations of North China (after Wang et al., 1979)

LATE CRETACEOUS	humid subtropical to warm temperate
EARLY CRETACEOUS	humid warm to temperate
LATE JURASSIC	humid temperate
MIDDLE JURASSIC	humid temperate
EARLY JURASSIC	humid temperate

CHAPTER 5. PETROLOGY AND GEOCHEMISTRY OF COALS FROM THE YANG CAO GOU BASIN

5.1 INTRODUCTION

A total of 205 samples from 43 boreholes (drill core samples) and 3 mines (coal face channel samples) in the Yang Cao Gou Basin were collected and analysed chemically and petrologically. The core samples were cut into halves. One half was utilised for petrographic determinations, and the other for chemical analysis. The face channel samples represent whole coal seams at the sampling sites. The maceral content of each of the 205 samples was determined microscopically and the results are listed in Table 5.1. Maceral analyses were determined by reflected light microscopy on polished specimens made from crushed samples mounted in epoxy resin, in accordance with AS 2646.6 (1984). The analyses are based on counting of at least 500 points on each sample and the results are expressed as volumetric percentages of the various macerals on a mineral-free (m.f.) basis. Maceral group analyses of the coals and parting samples were undertaken to document stratigraphic changes in these parameters, and to relate these changes to sedimentary environments.

Teichmüller et al. (1950) claimed that different swamp types yield different coal lithotypes. Tasch (1960) connected the lithotypes to a range of wet and dry conditions reflecting differing subsidence rates. He claimed the fusain represents the driest conditions and durain the wettest. Based on the different types of sporinite, Wanless and Macrae (1943) differentiated two types of durain with distinctive compositions. In his study of the petrography of the Permian Liddell Seam of eastern Australia, Marchioni (1980) found that most dull coals occurred in close vertical proximity to clastic beds. He concluded that these dull lithotypes were formed during periods of elevated water levels and circulation within the mire and they were assigned to formation in the reed moor and

Table 5.1 Results of petrographic analyses of coal and shale samples from Yang Cao Gou Basin

(m m f)

Borehole Number	Sample No.	Seam	Depth (m)	VITRINITE					LIPTINITE						INERTINITE				
				TeloV	At/Der	Desm	Gelov	Tt V	Spor	Cutin	Lipto	Algin	OL	Tt L	Fusin	Semi F	Iner	Other	Tt I
				(m.m.f. vol. %)															
ZK11202	1	II1w	494 -494.4	30.1	36.4	26		92.4	0.4	1.3	10			12.3	0.2		0.7		0.9
	2	" "	494.5-495.3	76.8	13.8	0.2		90.6	3.1	2.9	2.1			8.1	0.2	0.2	0.8		1.3
	3	" "	495.4-495.9	72.5	11.2	5		88.7	1	1	4.3		0.2	6.7	0.2	4	0.4		4.6
	4	" "	496.3-497.3	46	18.4	16.2		80.6	3.5	3.8	5.1			12.4	2.5	3	1.5		7.1
	5	" "	497.6-499	41.9	24.5	3.1		69.5	1.8	2.4	3.1		0.2	7.6	5.4	16.8	0.7		23
	6	II2w	521-522	56	13	2.3		71.3	0.7	2.3	1.5			4.5	1.8	21.3	1.2		24
ZK6401	1	II1w	368.9-370.4	49.8	26.7	13.4		89.9	1.3	2.2	2.7			8.2	0.2		1.7		1.9
	2	" "	368.9-370.4	56.5	13.2	6.9		76.6	2.8	1.6	6.3		0.4	11.1	1.7	7.9	0.6		12
	3	" "	372.5-373.7	61.6	25.7	3.6		90.7		0.4	6.1			6.5	0.5	1.4			2.9
	4	" "	373.7-375.4	65.2	26	2.1		93.3	1.1	2.6	2.4			6.1			0.6		0.6
	5	" "	375.4-376	32.9	30.2		1.4	65.5	1.2	0.6	11	0.6	0.3	13.6	8.2	9.1	3.5	0.1	21
	6	" "	376.3-376.8	29.2	44.3	8.3		81.8		0.1	0.9	0.1	0.3	1.5	4	5.7	5.7	1.4	17
	7	" "	376.8-378.1	31.3	14.3	10.5		56.1	3.2	1.4	6.3			10.9	2.9	9.7	20	0.5	33
	8	II1w	387.9-388.2	51.2	10.2	6	0.1	64.2		0.2	13	0.6		14	6.4	12.8	2.1		22
	9	" "	388.2-388.7	53.1	13.1	5.6		71.8	4.8	0.4	6			11.2	4.5	4.2	7	1.1	17
	10	" "	388.2-389.5	48.9	16.1	9.8	0.6	75.4	4.2	3.6	6.3	0.4		14.5	2	1.7	7.3		11
	11	" "	389.5-392.5	25.8	56.9	0.5	0.8	84	0.3	0.3	1.1	0.5		2.1	2.4	7.7	3.5	0.3	14
ZK4803	1	II1w	841.5-843.3	89.3	0.6	2.1		92	1.9		4.2			6.1			1.9		1.9
	2	" "	843.5-843.9	88.2	2.2	0.7		91.1	0.7	1	0.7		0.2	4.2	0.3		4.2	0.3	4.8
	G02	P	844.3-845.2	3.1	2.1			5.1	15.9	5.1	32	4.6		66.7			16		28
	3	II2w	849.7-851.3	88.4	0			88.4	1.1	4.6	3			8.7			2.5	0.2	2.7
	4	" "	851.3-852.3	88.6	0.7	4.1		93.4	0.5	1.4	1.7			3.6	1.4		1.4	0.4	3.2
	5	" "	852.3-853.3	90.9	0.9	0.4		92.2	0.4	0.6	3.7	0.4		5.1	0.8		2.1		2.9
	6	" "	853.3-855.4	93.8	0			93.8	0.5	3	1.6	0.2		5.3	0.2		0.4		1
	7	" "	855.4-856.2	89.4	0.2			89.6	0.2	2.1	5.2	0.2	0.4	8.1	0.2		2.1		2.3
	8	" "	856.9-857.1	43.7	25.7			69.4	0.2	10.6	4.7	0.2		15.8	0.2		15		15
	9	" "	857.4-859.4	55.1	3.1	10.6		87.8	0.2	0.7	6.9	0.4		8.2	1.3		1.8		5.1
	10	" "	860.6-861	88.3	0.2	1.7		90.2	0.3	2.2	5		0.2	7.8	0.7		1.2	0.2	2.1

Table 5.1 (continued)

Borehole Number	Sample No.	Seam	Depth (m)	TeloV	At/Der	Desm	Gelov	Tt V	Spor	Cutin	Lipto	Algin	OL	Tt L	Fusin	Semi F	Iner	Other	Tt I
ZK4804	1	II1w	1004.8-1006	55.2	13.1	9.8	0.2	78.3	1.9	9.2	8.7	0.2	0.8	20.8	0.3	0.6	0.4	0.3	1.6
	G02	P	1006-1008.4	54.3	18.8		0.4	73.4	2.3	10.9	7		2	22.3	0.8	2.7	0.8		4.3
	2	II2w	1008.4-1010	53	6.7	31	3.3	94.1	1.3		2		0.2	3.5	0.9	0.7	0.7	0.2	2.4
	3	" "	1010.4-1012	77.1	1.7	0.2	4.3	83.4	0.4	1.8	6.6	0.5	0.7	9.9	1.1	4.1	0.7	0.9	6.7
	4	" "	1012.4-1014	72.6	0	4	3.1	90.7	1.5	1.5	4	0.4		7.4	0.4	0.9		0.5	1.9
	5	" "	1014.4-1015	31.3	27.8	26.1	1.7	87			3.4	0.2	6.9	8.7		1.7	0.3	0.7	2.6
	6	" "	1015.8-1017	58.7	30.1	4.3	0.1	93.2		0.2	2.7	0.4	0.1	3.4	0.2	2.8	0.4		3.4
	7	" "	1017.8-1019	51.7	26.9	3.1	2	83.7		0.2	2.7	0.2	0.2	3.2	0.4	11.4	1.2		13
	8	" "	1019.8-1021	50.6	24.6	6.1	2.5	83.7			6.1	1.1	3.8	11		4.7	0.5	0.1	5.3
	9	" "	1021.8-1022	54.8	7.1	14.5	0.2	76.7	2.3	8	8	0.8	1.3	20.4		2.9			2.9
	10	" "	1022.7-1023	61.5	10.7	2.9		75.1	0.1	1.2	19	1.8		22.3	1.8	1.7	0.2	0.1	3.8
ZK4004	1	II1w	980.4-980.8	48.2	10.5	8.5		67.4	0.4	0.8	9.3		0.8	11.3		20.2	0.8	0.4	21
	2	II2w	986.4-987.5	70.2	7.5	7.5	0.4	85.6	1.7	4.3	5.4	1.1	1.3	13.8	0.2		0.6		0.8
	3	" "	987.5-988.8	79.7	0.9	13.4	0.5	94.5			3.7	0.5		4.2	0.2	0.9			1.4
	4	" "	988.8-990.6	77.6	0.4	4.8	0.5	83.3	0.7	0.5	8.5	1.9	1.1	12.7	0.3	3.2	0.4		3.9
	5	" "	995.2-996.7	81.5	1.4	4.2	0.7	87.8	1.2	0.5	6.1	0.7	1.6	8.7	0.7	1.1	0.4		2.2
	6		996.7-998.4	74.1	1.3	5	0.8	81.2	0.5	1.6	8	0.5	2.1	12.7		4.8	1.1		4.7
	7	" "	998.4-999.6	83.2	0.6	3.7	1.1	88.6	1.1	0.2	7.1	0.2	1	9.6	0.6	0.8	0.4	0.2	2
	8	" "	999.6-1001.4	87.4	1	1.9		90.4	0.9	3.6	4	0.3	0.7	9.5			0.2		0.2
	9	" "	1001.36-100	81.5	0.9	4.6	0.8	88.4	1.7	3.3	5.7	0.3	0.5	11.5	0.2		0.5	0.3	1
ZK3202	1	II	510.42-512.4	75	2.9	4.9		82.7	1.8	5.4	4.4		0.7	12.4		4.5	0.3		4.9
	2	" "	512.5-515	88	1.3	0.6		89.9	2.1	3.4	2.6		0.4	8.6	0.2	0.4	0.9		1.5
	3	" "	515.04-516.3	73.8	0.7	8.6	0.5	83.6	1	5.4	5.1		0.2	11.8	3.4		1.2		4.7
	4	" "	516.3-517.2	69.9	1.4	15.8	0.3	87.4	0.7	3.6	4		0.1	8.4	2.8	0.4	1.6		4.8
	5	" "	517.2-518.4	54.3	6.8	30.4	1.8	93.4	0.6	2.5	2			5	0.3	0.7	0.4		1.4
	6	" "	518.4-519.8	63.9	2.1	20.1	0.9	87	0.5	4.1	7.1		0.4	12.1	0.4	0.5			0.9
	7	" "	519.8-521.3	69.4	6.4	10.4	0.5	86.7	1.1	3.4	6.9		0.6	12	0.4	0.2	0.5		1.1
	8	" "	521.3-522.9	63.7	1.2	24.6		77.3	2	6.5	7.2	0.2	0.2	15.9	2.2	3.5	1.1		6.8
	9	" "	522.4-523.7	67.4	2.3	15.1		89.4	1.8	1.8	5		0.4	9	0.4	0.6	0.6		1.6
	10	" "	523.7-525.3	68.1	7.2	9.6		84.9	1.7	6.6	2.3		0.6	11.2		3.9			3.9
	11	" "	525.3-528.2	72.6	5.3	7		84.9	1.8	4.6	6.1	0.4	0.9	13.8	0.4	0.2	0.7		1.3

Table 5.1 (continued)

Borehole Number	Sample No.	Seam	Depth (m)	TeloV	At/Der	Desm	Gelov	Tt V	Spor	Cutin	Lipto	Algin	CL	Tt L	Fusin	Semi F	Iner	Other	Tt I
ZK2401	1	II	279-281	35.5	0.9	50.5	1.8	88.7	0.2	0.2	9.3	0.1	0.2	9.8		0.5	0.8	0.3	1.5
	2	" "	281-283.3	80.9	0	7.8	2	90.6	1.6	1.6	3.6		1.6	8.8		0.4	0.2		0.6
	3	" "	283.3-284.7	72.9	0.9	10.6		84.4	0.5	0.1	12	0.6	1.7	14.7	0.3		0.5	0.1	0.9
	4	" "	284.7-285.5	61.8	2.3	13.5	1.5	79.2	0.4	4.8	3.5		1	9.6	4.1	4.6	2.5		11
	G01	P	285.5-285.8	31.6	21.2	10.5		63.3	6.6	9.8	16	1.2		33.9			2.8		2.8
	5	" "	285.8-286.7	60	3.1	17.4	1.2	71.4	0.8	3.7	6.9	0.2	0.6	12.2	2.2	2.6	0.8		5.6
ZK1603	1	II	308-309.1	70.9	1.3	10.7		83	1.9	2.7	4		1.4	10	5.1	1.7	0.2		6.9
	2	" "	309.1-310.5	55.7	1.3	19.4	0.2	75.5	3.5	8.6	5.8			17.5	3	0.7	1.5	0.2	5.4
	3	" "	310.5-312.3	68.3		21.5		86.8	1.1	3	5.8			9.9	1.3	1.1	0.9		3.4
	4	" "	312.3-313.8	51.7	11	19.8		82.4	0.8	5.9	5.9		0.6	13.1	1.2	1.6	1.6	0.2	4.5
	5	" "	313.8-316.4	74.4	0	12.8		87.2	2.4	4.4	3.7			10.4	0.7	0.9	0.7		2.4
	6	" "	316.4-319.1	58.9	6.7	14		79.6	3.8	2.9	5.1	0.4		12.2	0.6	2.4	5.2		8.2
	7	" "	319.1-320.4	57.1	8.1	23.4		86.5	1.4	6.6	3.6		0.8	12.4	1		0.2		1.2
	8	" "	320.4-321.6	49.4	13.1	16.9	0.3	79.7	2.3	4.5	3			9.8	2.4	1.6	6.5		11
	9	" "	321.6-322.9	68	2.9	15.4		86.5	1.1	3.1	3.7	0.2	0.7	8.7	0.7	3.1	1.1		4.8
ZK806	1	II	232.9-233.9	41.8	16.3	32.8		90.9		1.4	3.3		0.2	5		2.9	1.2		4.1
	2	" "	233.9-234.4	54.9	25.7	11.6	1.6	93.8	1	0.9	2.5	0.1	0.3	4.8		0.5	0.2	0.7	1.4
	3	" "	234.4-235.4	55.9	14.6	16.8		87.3	1.7	0.8	3	0.2	0.7	6.4	1.1	1.9	2.6	0.4	6
	4	" "	235.4-237.7	56.1	15.8	18.7	1.1	91.7	0.8	1.2	3.5		0.4	5.9	1.9	0.2	1.9	0.6	4.6
	5	" "	237.7-238.2	61.2	2.2	26.9	2	92.3	0.7	1	2.7	0.2	0.7	5.3		0.8	1.2	0.2	2.2
	6	" "	238.3-239.8	34.8	31.5	12.4	1.3	80	0.1	0.3	6.3			6.7	2.5	5.8	4.6	0.1	13
	7	" "	239.8-241	57.6	0.8	11.1	0.6	70.1	1.6	5.8	5.8		0.3	13.5	3.7	10	2.7		16

Table 5.1 (continued)

Borehole Number	Sample No.	Seam	Depth (m)	TeloV	At/Den	Desm	Gelov	Tt V	Spor	Cutin	Lipto	Algin	OL	Tt L	Fusin	Semi F	Iner	Other	Tt I
ZK2501	1	II1e	276.8-278	68.5	3.6	11.1		83.2	1.4	6.9	2.1		5.9	16.4	0.2	0.2			0.4
	2	" "	278-279.3	49.8	14.9	21.8		86.5	2.8	1.6	3.7		3	11.1	0.4	0.3	1.4		2.4
	3	" "	280.6-281.9	60.3	2.2	24.8		92.9	2.3	2.3	1.6			6.1		0.6	0.3		1
	4	" "	281.9-284.2	52.4	16	15.8		84.2	5.1	7.8	1.5			14.4	0.6	0.5	0.3		1.4
	5	II2e	286.6-288.5	53.8	8.8	15.7		78.3	3.4	7.5	6.7			18.4	1.1	0.7	1.5		3.4
	G02	P	289-289.9	29.9	18.5	16.4		64.8	6.9	9.3	17	0.7		34.1	0.2		0.9		1.1
	G03	P	290.2-291.2	30.3	21.1	9.9		61.3	10.8	8.1	17	0.2		36.4	0.3	0.4	1.6		2.3
	6	I1	292-292.2	37.2	17.9	16.1		71.2	7.1	7.8	14			28.9	0.9				0.9
	G04	P	296.5-298.5	40.3	19.9	21.6		81.8	3	2	13			18.2					
	7	I2	304.9-305.3	59.4	1.6	17.8		78.8	8	5.9	5.7			19.4	0.4	0.6	0.6		
	8	I3	315.8-316.4	48.8	19.5	15.2		83.5	0.8	9.6	2.9		2.7	16		0.3	0.3		0.6
ZK3305	1	II1e	777.1-778.6	51.4	31.9	11.7		95	1.2	1.4	1.6		0.4	4.6			0.4		0.4
	2	" "	778.6-780.8	57.3	28.6	4.9		91.9	0.5	3.5	1.4	0.3		5.7	0.5	1.9			2.4
	3	" "	780.8-782.8	90.5	0.8	2.2		93.5	1	2.9	0.6		1.2	5.7			0.8		0.8
	4	" "	782.8-785.5	64.3	19.8	8.9		93	1.6	1.6	1.5	0.9		5.6	0.4	0.7	0.3	1	2.4
	G01	P	790.7-792.3	49.7	35.5	1.8	0.5	87.5	0.7	4.5	6.1	0.4	0.2	11.9	0.2	0.3	0.2		0.7
	5	II2e	792.3-793.3	76	1.1	14	0.6	91.7	2.5	2.8	1.4	0.2	0.5	7.3		0.5	0.5		1
Zk5705	1	II	920.4-920.8	63.2	19.8	0.2	0.1	83.3	5.5	4.3	3.9	0.4	0.2	14.3	0.2	1.1	0.5	0.3	2
	G01	P	920.8-922.5	59.1	25.6	0.4		85.1	4.2	5	4.6			13.7		0.8	0.4		1.1
	2	II	922.5-923.6	39.2	14.5	7.4		61.2	0.8	1.2	16	0.3	0.2	18.5	0.3	4.5	12	3.8	20
	3	II	924.6-925.1	46.8	16.1	14.3		77.2	0.1	0.1	12	1.1		14.3	4.1	2.3	1.7	0.3	8.5
	4	II	925.6-926	37.7	17.8	15.8		71.3	2.6	10.1	4.5	1.2	2.4	20.9	2.4	2.8	2.4	0.2	7.9
	5	II	932.1-935.8	39.8	44.5	1.1	0.5	85.8		0.8	10	0.3	0.3	11.4		2	0.5	0.3	2.8
	6	II	935.8-935.1	65.5	3.7	15.2		84.5	4.1	4.7	2.4		1	12.3	1.5	1.3	0.4		3.3
	7	II	935.7-936.2	53.1	26.5	2.3		81.9		0.2	12	0.2	1	12.9	1.9	2.4	0.3	0.5	5.2
	8	I	942.9-944.28	41.7	31.1	2.2		75			5.6	0.6	7.8	14	0.6	8.9	1.1	0.6	11
	9	I	947.3-948	70.9	8	6.1	2.3	93.3	0.9	1.8	2.6	0.4	0.6	6.3		0.3	0.1		0.4
	10	I	948.1-948.8	67.4	20.4	3.5		91.3			1.2		0.2	1.4	2.1	4.3	0.8		7.2

Key to table: TeloV= telovitrinite At/Den=attrinite plus densinite Desm=desmocollinite Gelo V= gelovitrinite TtV=total vitrinite
Cutin=cutinite Lipto=liptodetrinite Spor=sporinite Algin=alginite OL=other liptinite TtL=total liptinite Fusin=fusinite
Iner=inertidetrinite Semi=simifusinite Other I=other inertinite TtI=total inertinite P= parting G01=shale

open moor environments. Hagemann and Wolf (1987) suggested that different lithotypes are mostly the result of varying degrees of plant decomposition rather than differences in the peat-forming plant communities. Based on maceral characteristics, Diessel (1982) concluded that the "dullness" in coals may be caused either by macerals ascribed to dry conditions (structured inertinites, ground mass macrinite), where oxidation of vegetation is due to sub-aerial exposure, or by "wet" macerals (inertodetrinite, discrete macrinite, sporinite, and alginite) and mineral matter, indicative of high water levels and transport of maceral precursors. Based on her petrographic analysis, Teichmüller (1989) claimed that most brightness is attributable to vitrinite, particularly structured vitrinite, and in most cases dullness has been attributed to either liptinite or inertinite contents.

The lithotypes are thought to reflect various proportions of organic components (vitrinite, liptinite, inertinite) and mineral matter contents. The variations of the lithotypes are also used to assess the environment of deposition when the peat swamp was formed. In particular they are thought to indicate subsidence rates and related changes of the water table.

5.2 MICROSCOPIC CHARACTERISTICS- MACERALS

Table 5.1 summarises the maceral composition of Yang Cao Gou coal samples. The relative proportion of the three maceral groups, vitrinite, liptinite, and inertinite, on a mineral-free basis (mf.) are illustrated in ternary diagrams (Figs 5.1, 5.2 and 5.3). Figure 5.1 is for all samples regardless from which group or which seam. Figures 5.2 and 5.3 are for some specified coal seams. The general type, morphology, and common associations of the coal macerals from samples of the region are photomicrographically shown in Plate 5.1. The outstanding characteristic of the Yang Cao Gou coals is their high vitrinite content. With the exception of two samples from seam II_{2w} and some parting samples, the vitrinite content ranges from over 56% to about 99% and the mean content is about 85% (by volume, mf.). Within the vitrinite group, the main

components were found to be telocollinite and eu-ulminite (Plate 5.1), together comprising 29-91 vol. % (except in some samples of parting). For all coal samples, liptinite ranges from 1.4 to 28.9 vol. % and consists mainly of liptodetrinite, sporinite, and cutinite. Parting samples, containing similar liptinite macerals, have liptinite contents ranging from 5 to 67 vol % (Plates 5.2 and 5.3). Inertinite in these coals mainly comprises semifusinite, fusinite, and inertodetrinite (Plates 5.4). A few sclerotinite bodies, and some macrinite are also present (Plate 5.4). Micrinites are rarely found in these coals.

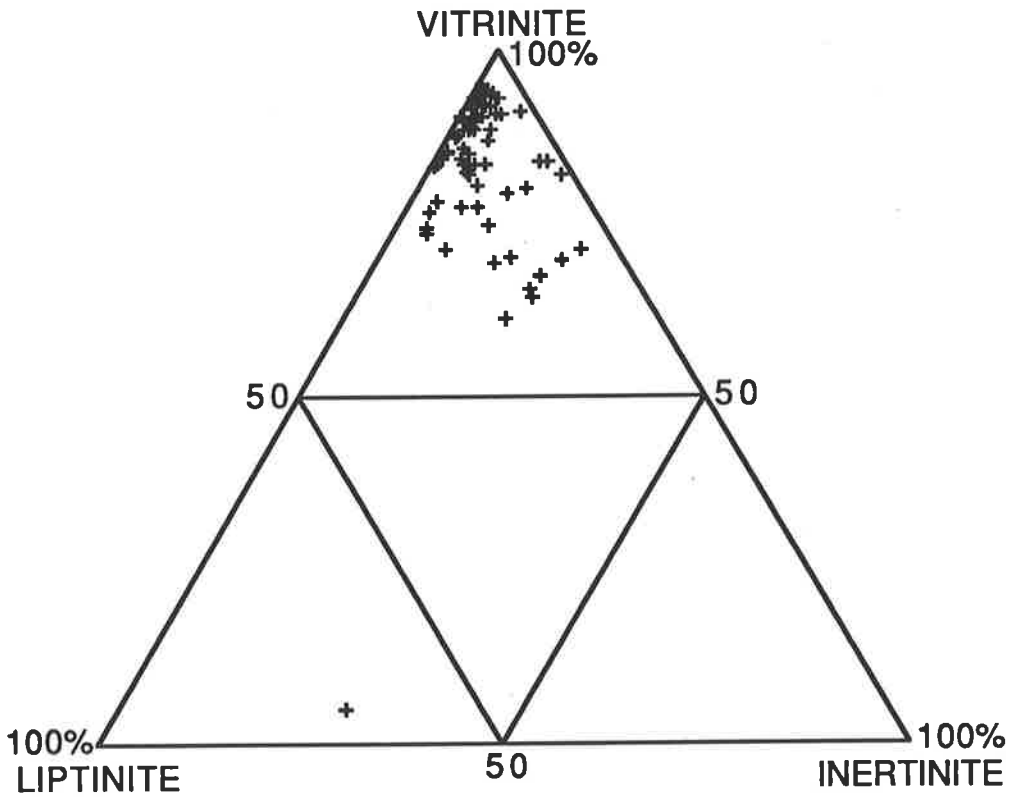

5.1 Maceral compositions of the coals from Yingcheng Formation, Yang Cao Gou Basin

Frequency distributions of the maceral group compositions (Fig. 5.4) show some regularities in that they each display one main mode. Vitrinite is mostly in the range of 75 - 95%. Liptinite in most samples falls in the range 5-15% (Fig. 5.4). Inertinite content, which is very low throughout

the basin, has two modes, between 0.1-5% (major) and 15-20% (minor) (Fig. 5.4).

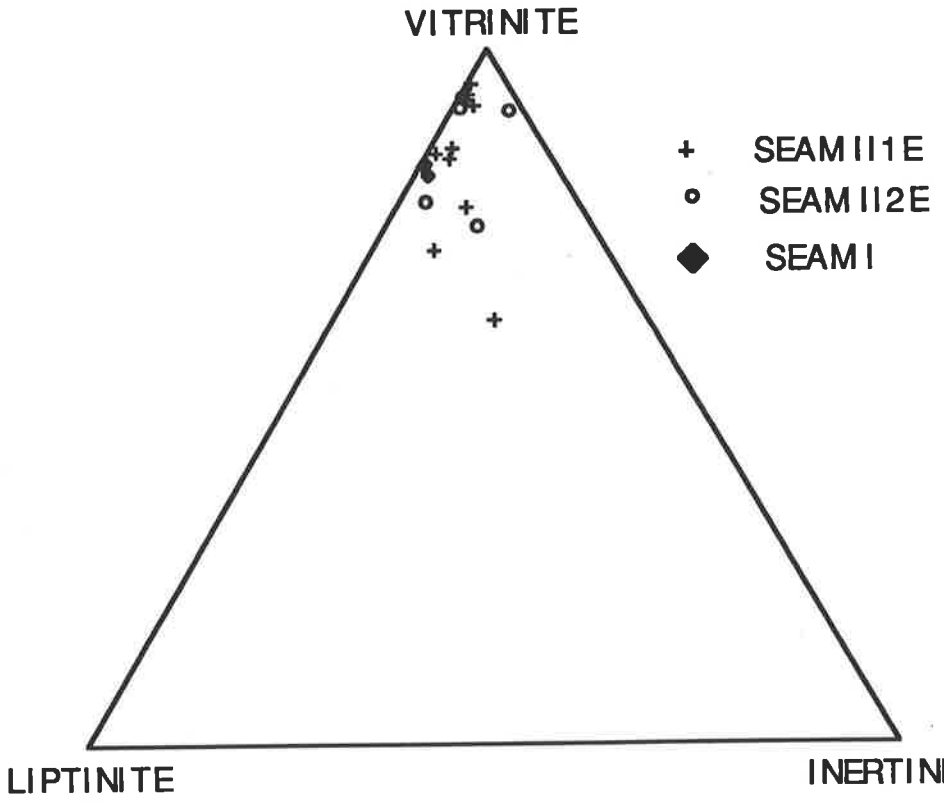

Fig. 5.2 Maceral compositions of the coal seams II1e, II2e (Group II coals) and, seam I (Group I coal) of the Yingcheng Formation, Yang Cao Gou Basin.

Two types of vitrinite are easily distinguished as vitrinite A and vitrinite B. The first one corresponds to the telovitrinites, present as centimetre thick layers of vitrite. Its Ro is very constant within an individual coal seam, and is very characteristic of rank. Vitrinite B is more widespread and is particularly well seen in the exinite-rich layers. The vitrinite B has a lower Ro than vitrinite A of the same rank. Stach (1970) stated that the difference between the Ro of vitrinite A and B may be as high as 0.3 to 0.4% at low ranks, and he showed that these variations are due to a difference in their original composition: vitrinite A originates from a more ligneous material, whereas vitrinite B is mainly derived from cellulose. The most typical telocollinite in the Yang Cao Gou Basin belongs to the type rich in the products of ligneous decay, i.e. it is vitrinite A.

Thin-walled sporinite is the dominant liptinite component in the Yang Cao Gou coals.

Semifusinite, fusinite, inertodetrinite and macrinite are the most common inertinite macerals found in the Yang Cao Gou Basin coals. Teichmüller (1982) stated that inertinite macerals, in contrast to vitrinite, are formed by more intensive oxidative alteration of plant tissues during peatification. The inertinite content thus is an indicator of the degree of oxidation within the environment of peat formation. Semifusinite is dominant over other inertinites. It occurs as layers, large lenses or as isolated fragments and is generally associated with vitrinite and fusinite. Fine angular fragments of inertodetrinite are present in all Yang Cao Gou coals and are asociated with all maceral types.

5.2.1 VITRINITE GROUP

In the Yang Cao Gou Basin significant variations occur across the area studied although the coals show a limited and characteristic range of organic matter type. In particular, the proportion of telocollinite increases and the detrovitrinite decreases from margin to basin centre.

Vitrinite is the most abundant maceral in the Yang Cao Gou coals. It comprises more than 56 % by volume of the macerals in these coals, and is mainly eu-ulminite, telocollinite, densinite, and desmocollinite. Clay minerals, carbonates, and quartz are commonly associated with the vitrinite.

The detrovitrinite content increases greatly down sequence from Group II coals through Group I coals, to Lower coals, and decreases toward the centre of the basin (Fig. 5.5).

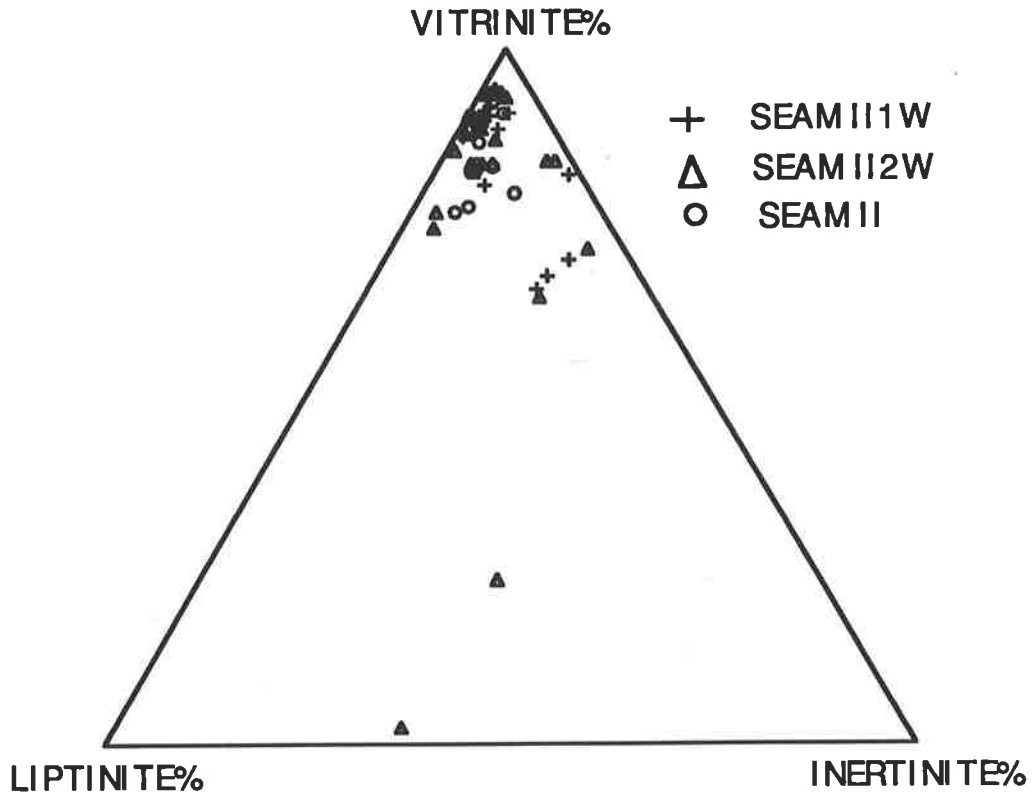

Fig. 5.3. Maceral composition of coal seams II1w, II2w and, II (Group II coals) of the Yingcheng Formation, Yang Cao Gou Basin

Telocollinite is dominant and occurs as a homogeneous mass in the form of sheets and layers (especially in Group II coals), or strips and fragments (especially in Lower coals and Group I coals). It is medium to dark grey in colour with R_o of about 0.5 to 0.6%. It may contains syngenetic resinite and mineral matter (Plates 5.1 and 5.5).

The term desmocollinite is used here to describe matrix-forming vitrinite macerals. Large detrital components often associated with mineral matter are described as vitrodetrinite.

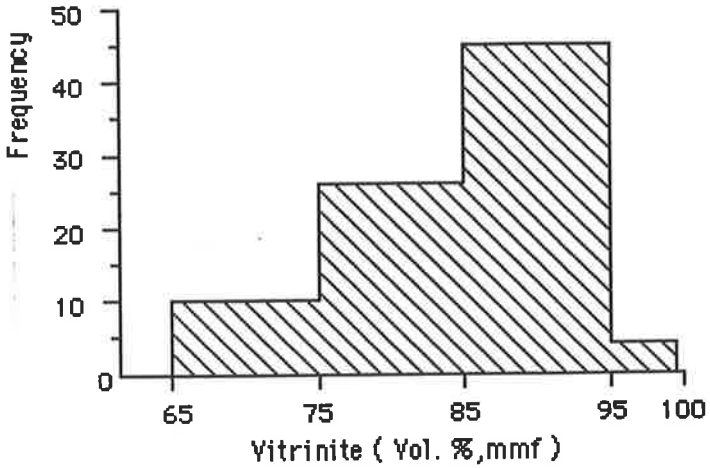

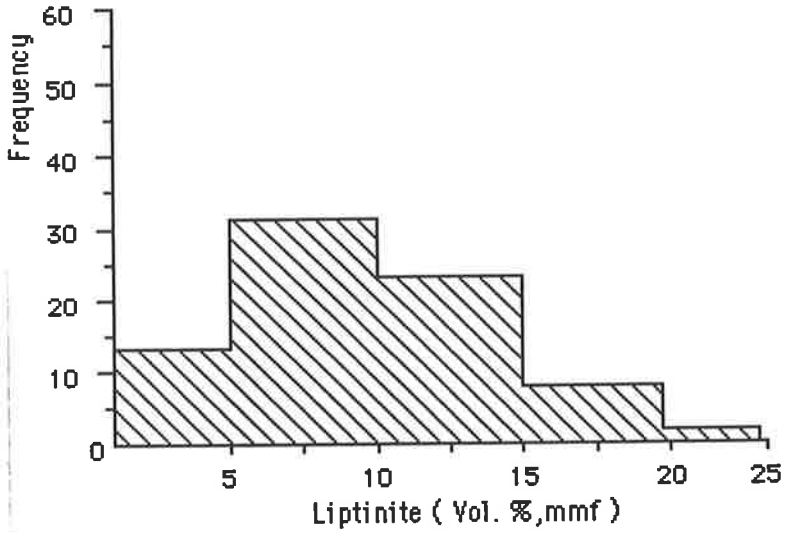

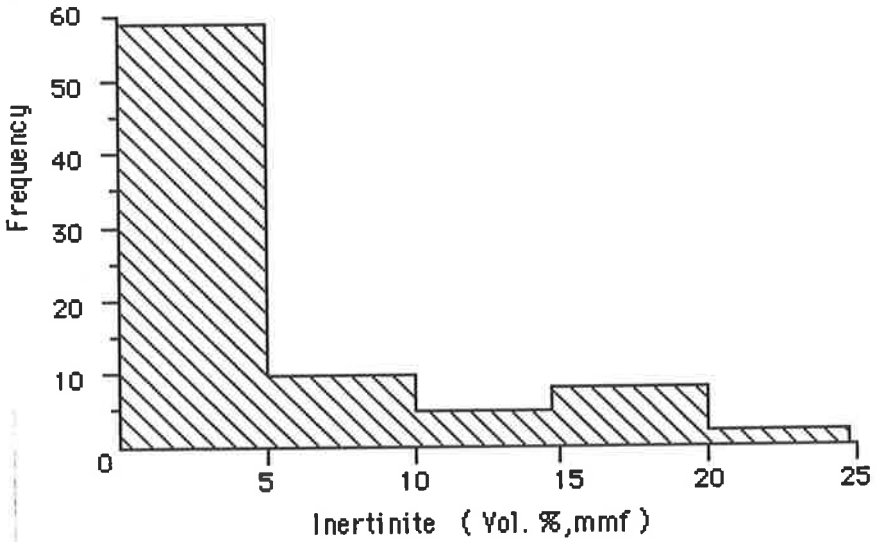

Fig. 5.4 Frequency distribution of macerals in the Yang Cao Gou Basin

5.2. 2 INERTINITE GROUP

The inertinite is characterized by its higher reflectance compared with other macerals. It ranges up to 33% in abundance, but in most cases the inertinite content is less than 5%. The most common inertinite macerals are semifusinite, fusinite, and inertodetrinite.

The semifusinite is very similar to fusinite with properties intermediate between those of vitrinite and fusinite. It is the dominant inertinite maceral. Cellular structure in semifusinite is usually not well preserved, but occasionally intact cell walls and lumens have been observed. Some of the semifusinite occurs as isolated fragments, and some as large bands of oxidised vitrinite. Cell walls in the semifusinite
are thicker than in the fusinite. Other macerals of this group include macrinite (< 0.9%), and sclerotinite (< 0.9%). The cellular structure of vascular plant tissue in fusinite may be preserved in great detail, both as regards cell morphology and the layered structure of the cell walls (Plate 5.4). Fusinite always shows cell structure (bogen structure) and in most cases the pores are empty. Semifusinite, together with fusinite, represents the non-humified and more oxidised remains of woody tissue in which the cellular structures are preserved. Inertodetrinite consists of the broken fragmentary oxidised material, perhaps redeposited debris (Stach et al., 1975).

5.2.3 LIPTINITE GROUP

Liptinite macerals average 17 % by volume of the organic matter in these coals. They are distributed irregularly, often concentrated in discrete layers but absent elsewhere. They occur in intimate association with detrovitrinite and comprise mainly sporinite, cutinite, liptodetrinite, and resinite. In both reflected white light and fluorescence mode, cutinite, sporinite, resinite, alginite, and liptodetrinite were counted separately, while the other liptinite macerals were grouped as "other liptinite macerals". Sporinite, cutinite, and liptodetrinite are among the most

Table 5.2 Results of the ultimate analysis of Group II coals, Yang Cao Gou Basin (as received)

Sample No.	O	C	H	S	N
Zk2501(5)	20.53	73.24	4.55	0.13	1.02
Zk4106(1)	29.18	76.19	5.11		0.87
ZK3304(1)	25.18	67.75	5.28	0.11	0.93
ZK3304(2)	18.37	75.41	4.63	0.11	0.86
ZK3304(3)	19.21	74.92	4.21	0.1	0.84
ZK1720(2)	16.99	74.62	5.55		
ZK908(3)	18.21	71.16	5.65		1.03
ZK1714(3)	18.16	74.39	5.01	0.19	1.1
ZK6401(10)	20.35	79.29	5.44	0.3	1.22
ZK3304(6)	23.67	69.86	4.7	0.08	1.02
ZK1720(2)	16.99	74.62	5.55		1.32
ZK2503(3)	19.65	72.64	5.38		0.96
ZK2501(4)	17.18	75.79	5.24	0.18	1.05
QZ908(3)	18.21	71.16	5.65		1.03
ZK107(1)	21.39	70.88	5.39		1.07
ZK107(2)	16.41	76.19	5.35		1.1
ZK107(3)	18.28	74.73	5.17		1.07
ZK107(4)	18.63	74.54	5.16		1.12
ZK107(5)	17.1	76	5.2		1.02
ZK107(8)	19.79	73.18	5.24		1.05
ZK107(9)	18.76	74.17	5.43		0.98
ZK107(10)	23.15	69.9	5.43		1.05
ZK806(3)	16.99	75.77	5.56	1.08	1.2
ZK806(4)	16.03	76.32	5.74	0.21	1.42
ZK1602(2)	17.59	75.79	4.98		1.32
ZK1602(4)	17.59	75.81	5.03	0.38	1.14
ZK1602(6)	17.82	78.3	4.99	0.27	1.16
ZK4803(1)	18.18	71.71	6.31	0.08	1.59
ZK4803(2)	15.57	76.16	6.6	0.08	1.17
ZK2401	16.42	75.95	5.57	1	1.37
ZK3305(1)	17.2	74.32	5.86	0.29	0.61
ZK3305(2)	18.57	72.04	5.86	1.15	0.54
ZK3305(3)	15.13	76.7	5.61	0.14	0.77
ZK3305(4)	14.51	75.9	5.57	0.7	0.61
ZK3305(5)	15.68	76.5	5.75	0.43	0.72

common liptinites in all seams. Large megaspores (up to several millimeters long) can easily be distinguished from small microspores (less than 0.1 mm long).

The cutinites are long and slender with serrated margins on one side. They occur as persistent layers or sporadic broken fragments and streaks. In the Group II coals, cutinite has a brownish yellow autofluorescence, and is larger and thicker than of that in Lower Group coals and Group I coals. In contrast, the sporinites of the latter coals are much smaller and, in most cases appear yellow in fluorescence mode.

Sporinite is the lightest component of the coal. Its density rises with rank, and an important physical property of sporinite is its toughness. In Yang Cao Gou coals, most sporinite occurs as microspores and subordinate megaspores are rare. The sporinites have similar fluorescence colours to cutinite. The microspores are of dumb-bell or spherical shape, and the megaspore exines are elongate to lanceolate (Plate 5.2).

Liptodetrinite consists of liptinitic detritus, which has no definite shape but is copmmonly elongated. In most cases, the liptodetrinites seem to have been derived from microspores, because they display similar fluorescence colours. Larger fragments of liptodetrinite often show the porous structure of the megaspores which are their probable precursors (Plate 5.3).

Bodies of resinite are oval in shape and often less than 0.2 mm across. Under blue light irradiation, they commonly show a bright yellow centre and a thin rim that appears brown and rather dark. Resinite cell fillings generally appear as regular oval bodies within telocollinite. They are only slightly darker than vitrinite and lighter than any other liptinitic maceral.

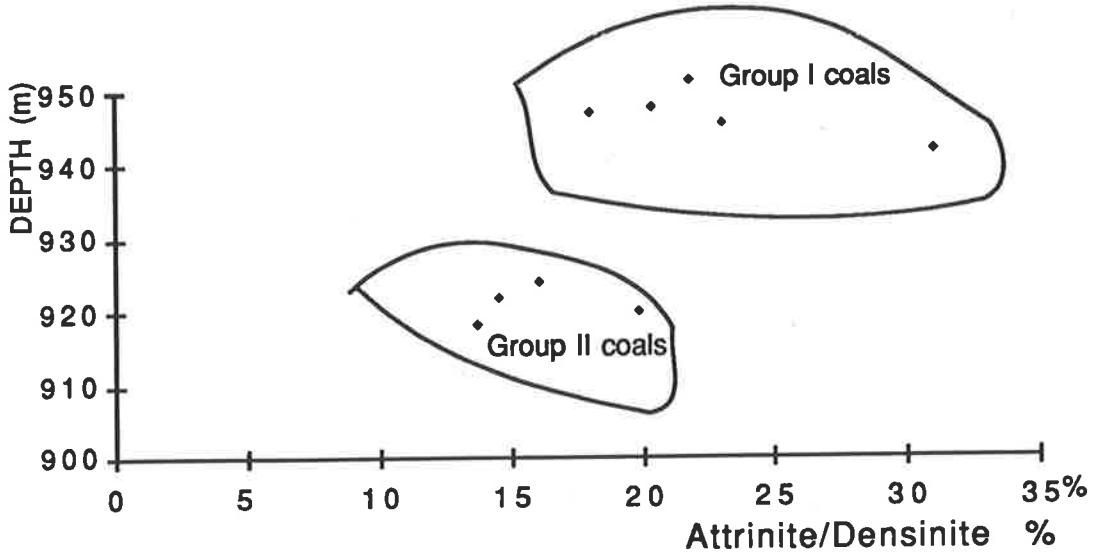

Fig. 5.5 Densinite plus attrinite vs depth for Groups I and II coals from borehole ZK5705

5.2.4 MINERALOGY AND COAL GEOCHEMISTRY

5.2.4.1 MINERALOGY

Mineral matter in the Yang Cao Gou coals was found to consist mainly of clay, quartz, unspecified carbonate, siderite, and pyrite, with clay and carbonate being the most abundant. Clay is present as fine disseminations within vitrinertite (both vitrinite-rich and inertinite-rich), vitrite and clarodurite. Clay also occurs infilling cell lumens of semifusinite, fusinite and vitrinite. Siderite occurs as spheroidal nodules (Plate 5.5). Pyrite and elemental sulphur in the Yang Cao Gou Basin were found to occur as individual euhedral crystals, framboids, and thin crusts or minute crystals. With respect to different coal groups and within the coal seams, pyrite content was found to be highest in the Group II coals which formed in lake shore and shallow lake environments. Pyrite also increases towards the coal depocentre. The lowest pyrite content was found in Lower Group coals that formed in inter-lobe depressions of alluvial fans.

Examination of mineral matter under the microscope suggests that most was introduced into the peat as detrital grains, or as minerals precipitating out of solution. The majority of mineral matter occurs as finely disseminated particles in the coal matrix, and often is concentrated in gelified plant tissues such as gelinite cellular infillings. Such mineral matter is very difficult to remove by physical coal washing techniques.

5.2.4.2 COAL GEOCHEMISTRY

The coal samples collected from boreholes and mine sites were analysed chemically, and their proximate and ultimate analyses, calorific value, and trace elements were determined by the Chemical Laboratories, Geological Survey of Jilin, P. R. China. The telocollinite reflectance data are here compared with results from determination of volatile matter, calorific value and elemental analysis.

The ultimate analysis data (Table 5.2) show that C content ranges from 68 - 79%; H from 4.2 - 6.6%; O from 14.5 - 25.2%; and N from 0.5 - 1.6%, on dry mineral-matter-free basis. Sulphur content is very low, being less than 0.8%. The above parameters therefore, indicate that the Yang Cao Gou coals can be assigned to subbituminous rank.

Figure 5.6 shows the relationship between vitrinite reflectance and volatile matter content. It can be seen that vitrinite reflectance increases with decreasing volatiles content.

In Figure 5.7 the H/C and O/C atomic ratios of the Yang Cao Gou coals are plotted on a van Krevelen diagram. This diagram shows clearly that for the low coalification range of Yang Cao Gou coals, the hydrogen content only decreases slightly, whereas the oxygen content decreases rapidly due to loss of water and carbon dioxide with increasing rank.

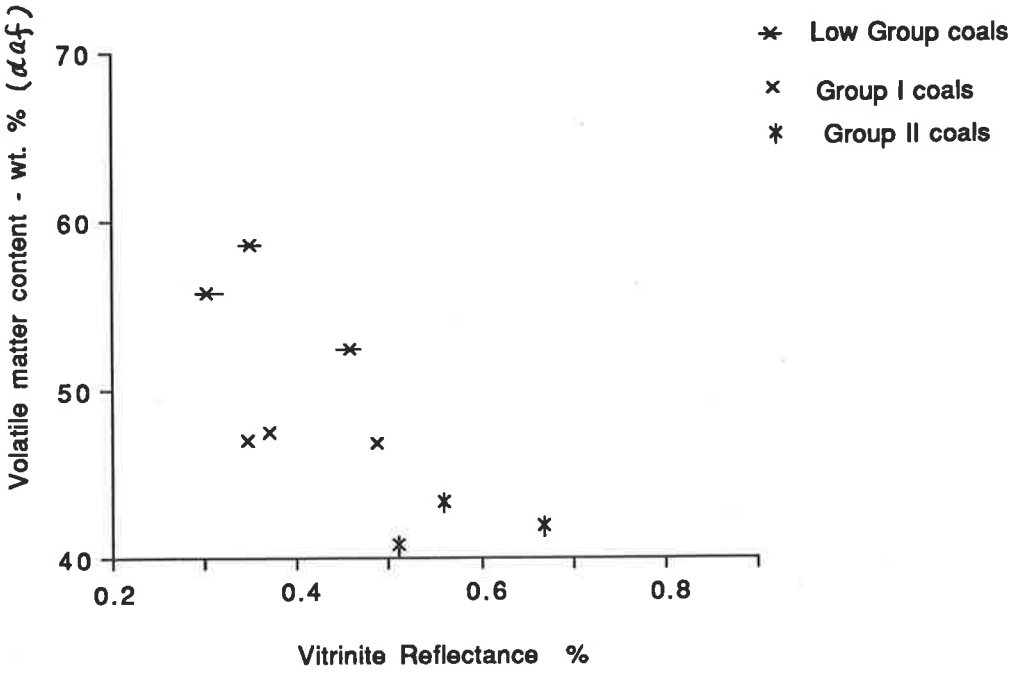

Fig. 5.6 Vitrinite reflectance vs volatile matter content for Yang Cao Gou coals

Calorific value (specific energy) is a good rank parameter in low-rank coals. Patteisky and Teichmuller (1960) observed that in brown coals and low- rank bituminous coals, the calorific value increases rapidly with increase of carbon content. The maximum calorific value is reached at a carbon content of 89.6% in low volatile bituminous coals. At higher rank the calorific value decreases slightly with further increase of coalification into the semi-anthracite and anthracite range. The calorific values range from 2000 to 6580 Kcal/kg. In Figure 5.8 calorific value is plotted against the reflectance of telovitrinite. This diagram shows that calorific value increases with increasing reflectance of the vitrinite.

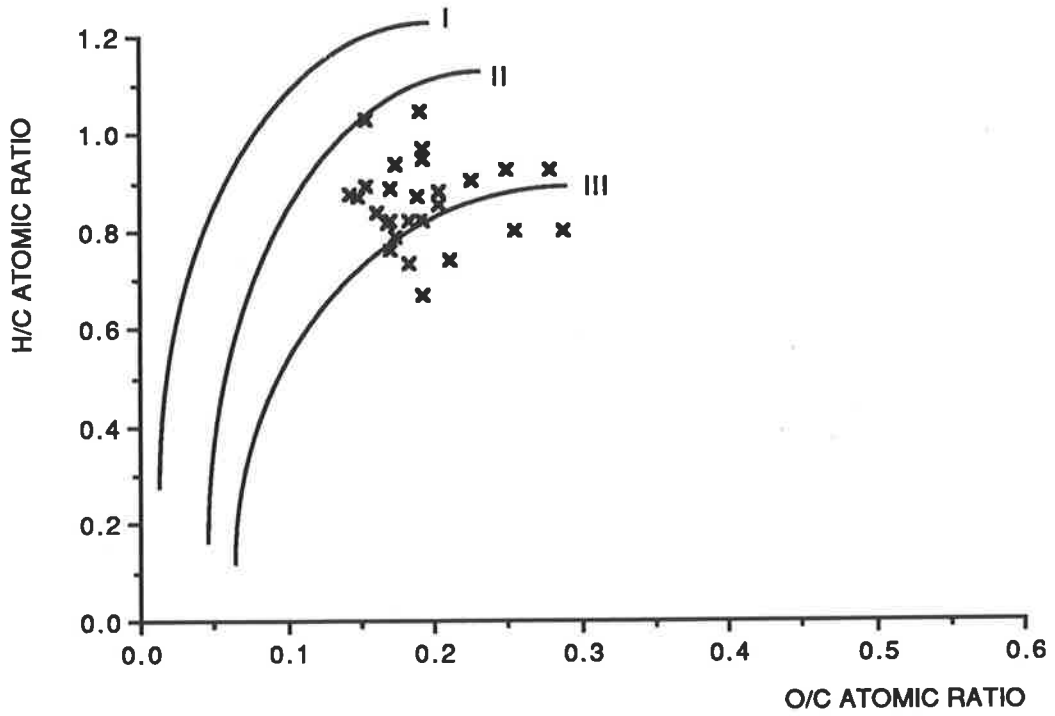

Fig. 5.7 H/C and O/C atomic ratios for Group II coals

5.3 LITHOTYPES AND MICROLITHOTYPES OF THE YANG CAO GOU COALS

Lithotype and microlithotype analyses of the Lower, Group I and Group II coals were undertaken to determine the stratigraphic variation in these parameters and to relate these changes to sedimentary environments. The coal seams were logged visually in terms of the proportions of bright coal, banded bright coal, banded coal, banded dull coal, dull coal, and fibrous coal, and in terms of vitrain, clarain, durain and fusain. After the lithotypes were described, samples of each macroscopic coal band were collected for petrographic and microlithotype analyses. For the lithotype analysis, all the samples were taken at four localities in the Yang Cao Gou Basin where the thickest coals are located, and from freshly mined faces to reduce the possibility of oxidation and contamination. Most of these samples were also subjected to microlithotype analysis, involving the counting of at least 500 points.

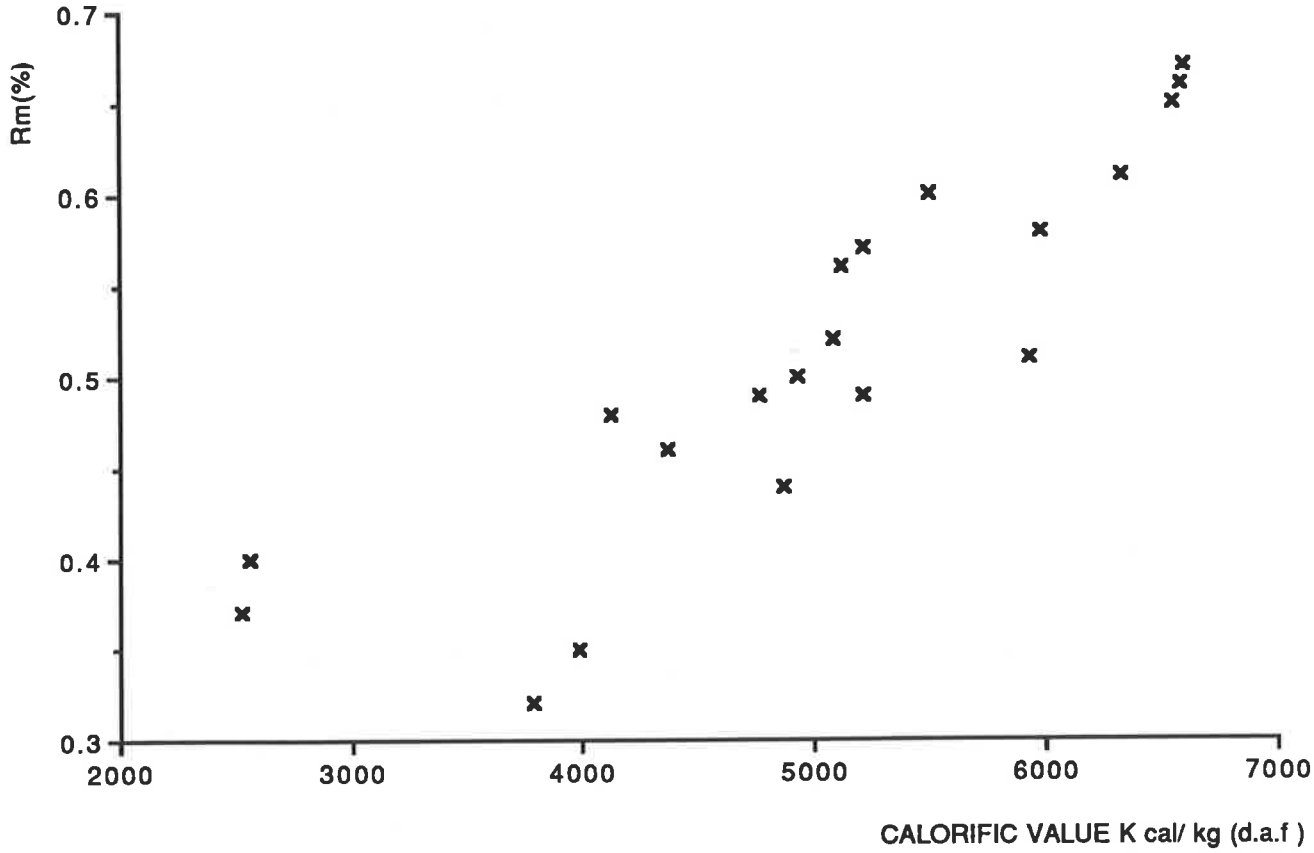

Fig. 5.8 Relationship between vitrinite reflectance and calorific value in Group II coals

5.3.1 MEGASCOPIC CHARACTERISTICS- LITHOTYPES

5.3.1.1 INTRODUCTION

In order to determine the petrographic composition of coal lithotypes, to interpret the original peat- forming environments, and to document lateral and stratigraphic variation in lithotype and maceral composition, a comprehensive field and laboratory investigation of the coal seams in Yang Cao Gou Basin was carried out. This investigation focused on both intra- and inter-seam variations. So far, in terms of coal facies, most coal

petrologists have focused on Carboniferous (Hacquebard and Donaldson,1969), Permian (e.g. Marchioni, 1980; Smyth, 1984; Diessel, 1986), or Tertiary (Teichmüller, 1962, 1982) coal deposits. Little has been published concerning the facies of Lower Cretaceous coals. It is very true, as Cameron (1978) stated, that the lithotype description of coals and the use of lithotype nomenclature was not intended as a substitute for detailed analysis by microscope but is intended to give a gross indication of coal composition and, in particular, to assess the internal stratigraphy of a coal seam. The lithotype variations can be used to determine depositional environments in the ancient peat swamp; in particular they are good indicators for subsidence rates and related changes of the water table.

5.3.1.2 LITHOTYPE NOMENCLATURE AND SAMPLE COLLECTION

Several coal lithotypes were recognized in this work. Vitrain was introduced by Stopes (1919) to designate the very bright bands or lenses, usually a few mm in width, in bituminous coals. The term clarain was likewise coined to describe the bright lustrous constituent of coal which is intrinsically striated by dull intercalations. Clarain generally has bands of variable thickness and a lustre between that of vitrain and durain. Conventionally, the thickness of the fine, bright and dull striations should be less than 3 mm. Only bands having a thickness of several mm are usually defined as clarain. The term fusain was introduced by Grand' Eury (1962) for the black silky, lustrous bands in coal. The term durain was used by Stopes (1919) for the macroscopic dull bands in coals. These are characterized by their grey to brownish black colour and rough surfaces with dull or faintly greasy lustre. They are markedly less fissured than bands of vitrain and generally show granular fracture (Bustin et al., 1983). All coal seams at the mining sites were described according to a modified Australian lithotype classification scheme (Table 5.3).

Table 5.3 Lithotype terminology used in this study (adapted from Diessel, 1965 and Marchioni, 1980)

Divisions after Stopes(1919)	Divisions used in this study	Description
vitrain	bright coal	subvitreous to vitreous lustre, conchoidal fracture, less than 10% dull coal laminae
	banded bright coal	predominatly bright coal with 10 to 40% dull coal laminae
clarain	banded coal	bright and dull coal interlaminated in approx. equal proportions
	banded dull coal	predominately dull coal with10-40% bright laminae
durain	dull coal	matt lustre, uneven fracture, less than 10% bright coal laminae
fusain	fibrous coal	satin lustre, very friable

Coal samples from mines and from boreholes were prepared for petrographic analysis as follows: the megascopically recognizable subunits of the coal seams were logged and described visually in terms of the proportions of bright, dull and lustrous coal. Then each of the lithotype was also described in terms of the thickness of vitrain layers and detrital layers, abundance of vitrain, fracture types, relative hardness of the coal, thickness of the fusain, cleat spacing, and occurrences of mineral matter (focused on pyrite and calcite). The samples were taken from 3 collieries in Yang Cao Gou Basin (Changchun city colliery, Jutai colliery and, Artillery colliery: Figure 5.24). Each of the macroscopic coal bands were sampled for petrographic analysis.

Table 5.4 Microlithotype compositions of Group II coals

WELL	SAMPLES	VITRITE	LIPTITE	INERTITE	CLARITE	DURITE	VITRINERTITE	TRI-MACERITE	V,E,I +M	MINERALS
CC	892-2	98.2	0.2						1.2	0.4
	892-3	96		0.8			1.8		1.4	
	892-4	52.9	0.2	1	38.7		0.6	5.5	11	
ZK4004	892-39	18.4		8.6	7.7		0.4	0.4	30	34.5
	892-40	56.8	0.2	0.2	17.3		0.4	0.2	13.3	11.6
	892-41	17.6		0.1	0.1				14	67.2
	892-42	57.8		1.9	28.1		1.9	0.6	8.6	1.1
	892-43	50.8		0.6	27.4		1.3	0.1	12.5	7.3
	892-44	35.7	0.1	3.1	32.9		1.8	0.3	14.3	11.9
	892-45	56		4.3	33.9	0.4	0.7	0.7	3.2	0.5
	892-46	33.8		30.5	4.6	19.1	4.5	0.3	7.1	
	892-47	50.3	0.1	10.2	21.3	9.7	0.9	0.4	4.1	3
ZK4803	892-48	11		41.8	3.7	11.3	0.2	0.4	19	12.8
	892-49	1.8	0.2	46.1	0.8	10.3		0.5	15.8	24.5
	892-50	3.2		58.8		25.5			12.2	0.3
	892-51	37.4		27.7	5.1	9.2	8.7	2.1	6	3.8
	892-52	4.6	0.5	62.3	0.2	14.2	5.1		5.8	7.5
	892-53	17.8		46.7	2.3	13.5	8.5		10.5	0.7
	892-54	14		33.2	1.7	10.7	9	0.3	22.1	9
	892-55	3.9	0.2	27.4	0.3	15.1			39.7	13.4
	892-56	37.2	0.3	25	3.7	14.5	4		11.2	4.2
	892-57	22.7		42.2	1.2	21.2	3.2	0.9	8.3	0.5
	892-58	1	0.9	3.3		0.3			57.5	37
ZK6401	892-64	11.9	0.2	5.2	1.4	0.1	0.5	0.2	40.9	39.6
ZK5705	892-73	53.1		23.8	14.6		0.4		7.9	0.2
ZK806	892-87	36.3		6.7	18.6	0.7	3.9	3.4	20.8	9.5
ZK5601	892-90	85.3			11.3		0.9	0.2	1.3	0.8
	892-91	84.7	0.3	0.8	9.2		0.3		2.1	2.6
ZK3202	892-93	67.2	0.3	4.3	25		0.5	0.3	1	1.3
	892-94	56.2		0.2	27.6	0.2	0.4	0.6	14.3	0.6
	892-95	76.8	0.6	0.9	4.3	0.3	3.1	1.9	10.2	1.9

Table 5.4 (continued)

WELL	SAMPLES	VITRITE	LIPTITE	INERTITE	CLARITE	DURITE	VITRINERTITE	TRI-MACERITE	V,E,I +M	MINERALS
	892-96	52.8	0.2	11.1	23.1	0.4	6.8	2.1	0.2	1.4
	892-97	49.5	0.2	4.6	33.3	0.2	3.3	0.8	0.6	0.2
ZK3202	892-98	64.4		0.8	29.6		1.6	0.4	9	5
	892-99	70.4		3	23.8	0.6	0.6		5.4	3
	892-100	52	0.2	0.6	31.7		1	0.8	16.7	4.2
ZK4804	892-108	40.5	0.4	2.8	47.6	0.2	0.2	1.2	11	
	892-109	39.5	1	2.9	34.4		0.5	1.8	7.3	0.6
ZK3203	892-112	52.8		2.2	25.7	0.2	6.9	1.6	12.1	0.8
	892-113	58.4		3.6	24.1		4.3	0.4	53.2	14.6
	892-115	56.5	2.9		26.2			8.9	19.9	4.4
ZK2501	892-116	22.6		0.4	8.4		0.4	0.7	14.8	3.9
	892-118	36.9	0.3	0.9	26.5	0.3	1.9	2.2	18.7	9.3
	892-119	47.8	2.5		29.6		0.7	0.3	13.3	6.5
ZK2502	892-120	47.3	0.4	0.6	20.1		1.4	0.8	9.5	2.8
	892-122	61.4			18.5			2.7	10.8	2.9
ZK2505	892-124	82.1		1.9	7.8		2.9	3.3	1.6	0.3
	892-126	57.3		5.6	22.8		1.2	6.2	2.9	1.1
	892-127	42.7		1.9	37.7		1.4	11	6.2	7.6
	892-128	62.7		0.2	23.4		2	8.4	0.6	1.1
ZK1603	892-129	41	0.4	1.8	25.3	0.4	6.5	2.4	0.4	
	892-129a	60.2		1.1	26.6		0.2	0.2	31.7	2.8
	892-130	61		0.8	35.2		0.2	2.6	11	2.8
	892-132	46.5	0.2	4.2	14.2		0.2		25.6	6.5
ZK11202	892-134	62.1			19.7		1.8	0.8	3.8	
	892-135	57.3	0.4	0.2	6.3		3.6	1.2	28	3
ZK3305	892-141	78.5			16.3		0.6	6	2.6	
	892-143	44.2	0.4		22.2		1	0.8	38.3	1.5
ZK3204	892-144	49		3.2	36.3	0.2	2.8	2.4	24.9	2.4

Table 5.4 (continued)

WELL	SAMPLES	VITRITE	LIPTITE	INERTITE	CLARITE	DURITE	VITRINERTITE	TRI-MACERITE	V,E,I +M	MINERALS
ZK1718	892-157	46	0.2	1.2	22.7		0.2	1.4	7.9	1.5
QZ8001	892-168	19.3		3	0.2			1.6	4.6	4.2
ZK805	892-170	56.7		6.3	24.7		1.5	1.2	8	5
ZK5604	892-175	52		8.6	25.8		3.1	0.6	3.2	
	892-176	63		2.9	17.1	1	1.8	0.6	7.4	0.9
ZK2401	892-178	69.2			27.1					
	892-179	49.9	0.1	0.3	40		0.9			
ZK1718	892-156	43		1.3	15.3		0.3		34.9	42.5

5.3.1.3 RESULTS AND DISCUSSION

Table 5.3 shows the Diessel (1965) and Marchioni (1980) classifications. This system is the basis of the lithotype profiles of Lower coals, Group I coals, and the Group II coals (Figures 5.9 to 5.12) in which are shown the vertical and lateral variations in the coal lithotypes of the Yang Cao Gou Basin.

Generally speaking, Early Cretaceous coals in the Yang Cao Gou Basin are very finely banded, compact, hard, and lustrous. Lenticular bands of up to 45 mm in thickness occur in the coal. Clarain is most abundant lithotype, durain is common and fusain is rare to sparse. In most cases, the bright coal bands are composed dominantly of vitrinite, in particular, telovitrinite. The dull coal matrix contains varying amounts of vitrodetrinite, liptinite and inertinite.

As mentioned in Chapter 4, Group II is the main coal-bearing unit in the basin. It locally includes 3 seams. The major measured seam is 5.27m thick. The petrographic composition of this coal unit shows relatively little variation around the basin. Most samples examined are composed of structureless vitrinite with minor liptinite and rare inertinite. Clay and carbonate veins occur in most samples. Pyrite is conspicuous in many samples as framboids or as massive partings. According to the modified Diessel and Marchioni classification (Table 5.3) most of the Yang Cao Gou coals are bright to banded bright. That is to say, the greater part of the coal consists of clarain and vitrain, with durain occurring in relatively thin bands.

The lithotype profile in Figure 5.9 contains a composite log of seam II (Group II coal), based on the examination of coal seams in the Changchun coal colliery in Yang Cao Gou Basin. The sequence of lithotypes in the Group II coal seams range from dull coal to bright coal. Fusain, as one end member, represents a low subsidence rate, with shallow water cover and periodic dry conditions, whereas dull lithotypes (except fusain) on the other hand are thought to represent a much higher water level and grade with increasing subsidence rates into carbonaceous shale or other

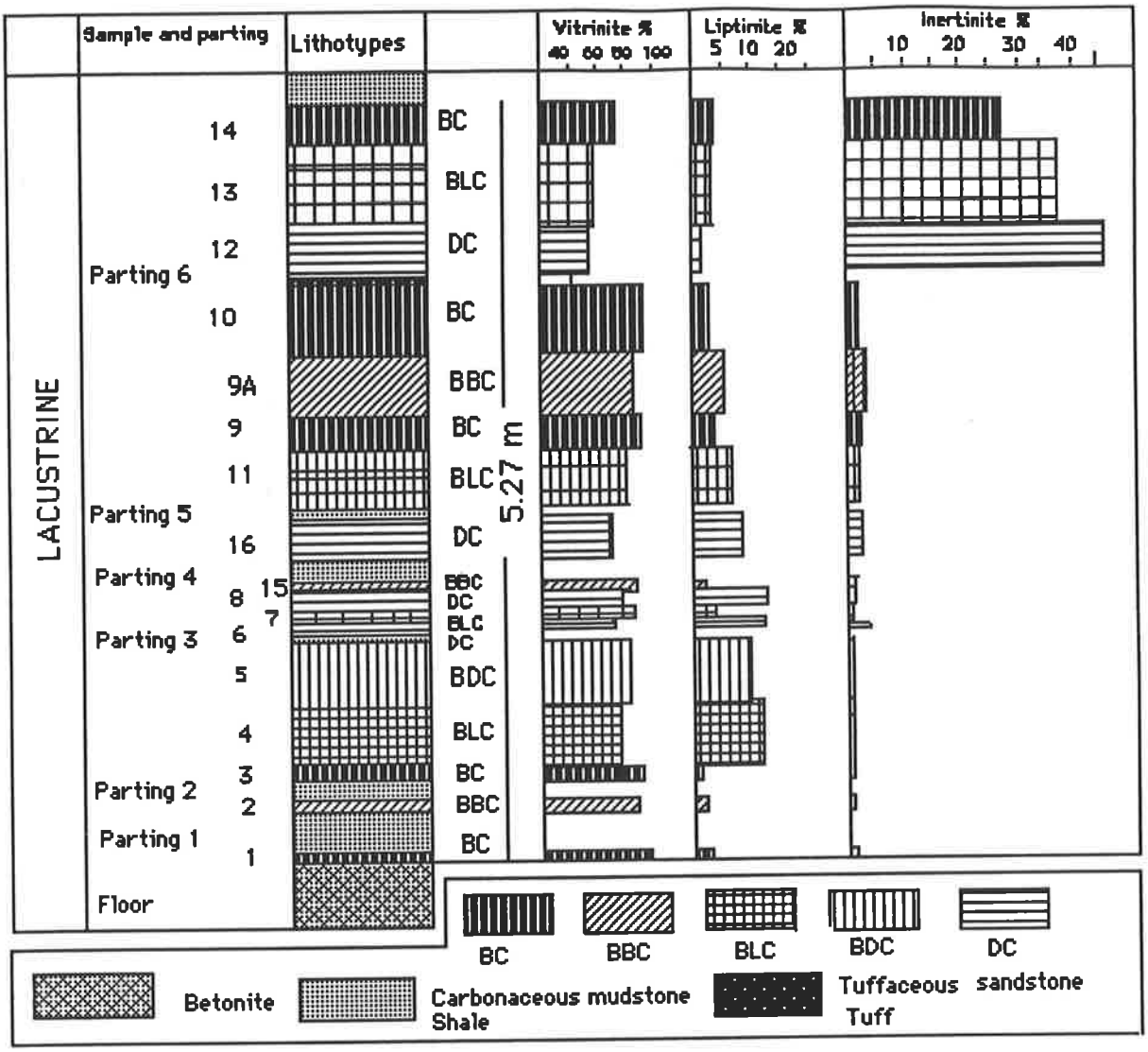

Fig. 5.9 Variation in lithotypes and macerals of the Group II coals at Changchun colliery in the Yang Cao Gou Basin

The following symbols are also used to describe the coal: BC= bright coal; BBC=banded bright coal; BLC=banded coal; BDC=banded dull coal; DC=dull coal

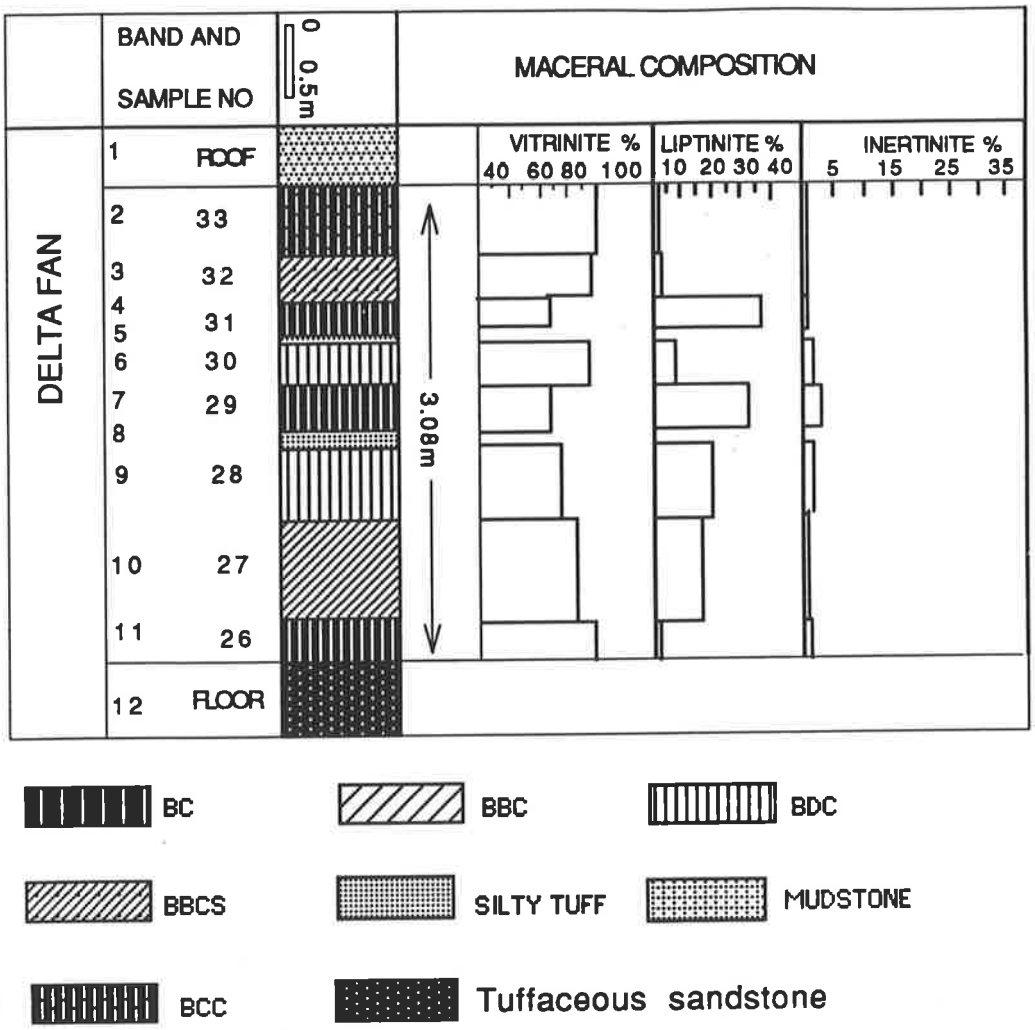

Fig. 5.10 Variation in lithotypes and macerals of the Group I coals, at Jiutai colliery in the Yang Cao Gou Basin

See Fig. 5.9 for an explanation of symbols except BBCS=Banded bright coal interlaminated with thin siltstone beds and BCC= Bright coal interlaminated with thin siderite lenses

partings. The bright, banded bright and banded coal layers represent intermediate water levels. From Figure 5.9 it is apparent that the seams are characterized by a predominance of banded lithotypes indicating that intermediate water levels occurred during deposition. The dull coal type occurs in the upper half of the seam, and the inertinite content increases dramatically above parting 6 to the top of the seam, indicating a trend to somewhat drier conditions within the swamp. The increase in inertinite, and the decrease in vitrinite and liptinite contents of the coal from the bottom to the top of the seam resulted from the slower subsidence of the peat swamp, and corresponded with a lowering of the water table. This indicates that the amount of clastic influx into the basin during peat accumulation was low at first, and then increased with time. The high vitrinite content through the coal seam suggests that the rate of subsidence of the peat swamp kept pace with the rate of peat accumulation. This depositional condition allowed the peat to remain beneath the water table, and therefore to accumulate in anoxic conditions. The occurrence of bright layers (bright coal) is also a indication of periods of wetter conditions, in particular at the base and top of seam II where bright layers grade into carbonaceous mudstone/shale; this indicates that the subsidence rate increased. Fusain (the end member representative of a very dry environment of deposition) was not observed. The base of Group II coal seams is a mineral-matter-rich zone which indicates that a gradual changeover from shallow lacustrine conditions to a swamp environment occurred.

Figure 5.10 shows a section at Jutai colliery in the Yang Cao Gou Basin. The bright coal type occurs at both the top and bottom of the seam, inertinite is rare, and the liptinite content increases from the bottom to the middle part of the seam and then decreases dramatically to the top of the seam. The changes in liptinite and vitrinite content of the coal suggest rapid initial subsidence followed by slow subsidence of the peat swamp.

There are some differences in the composition of macerals and in the proportion of the lithotypes between the Lower Group coals (Figure 5.11) and Group II and I coals. The Lower Group coals have a very limited extent and were formed in a high-energy environment, because they were deposited in the inter-lobe depression of an alluvial fan (Zhao, 1989). One

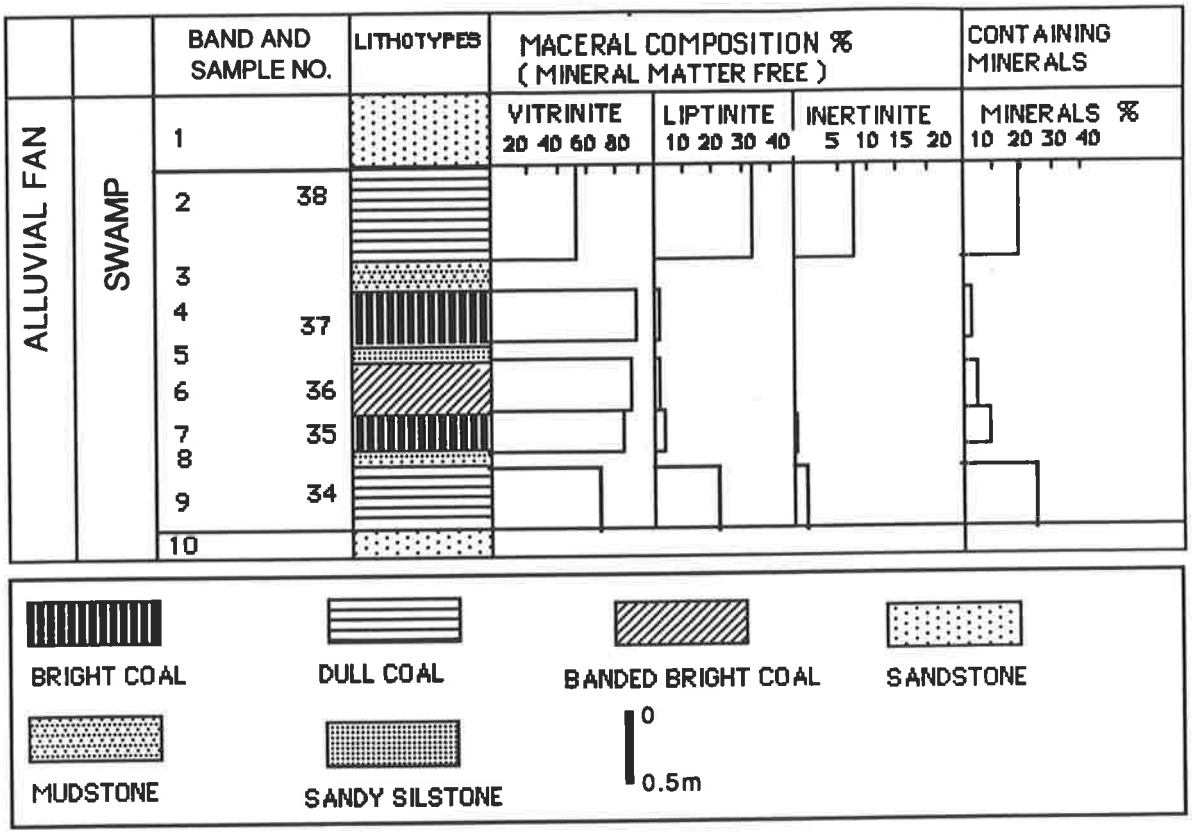

Fig. 5.11 Variation in lithotypes and macerals of the Lower Group coals at Rural colliery in the Yang Cao Gou Basin

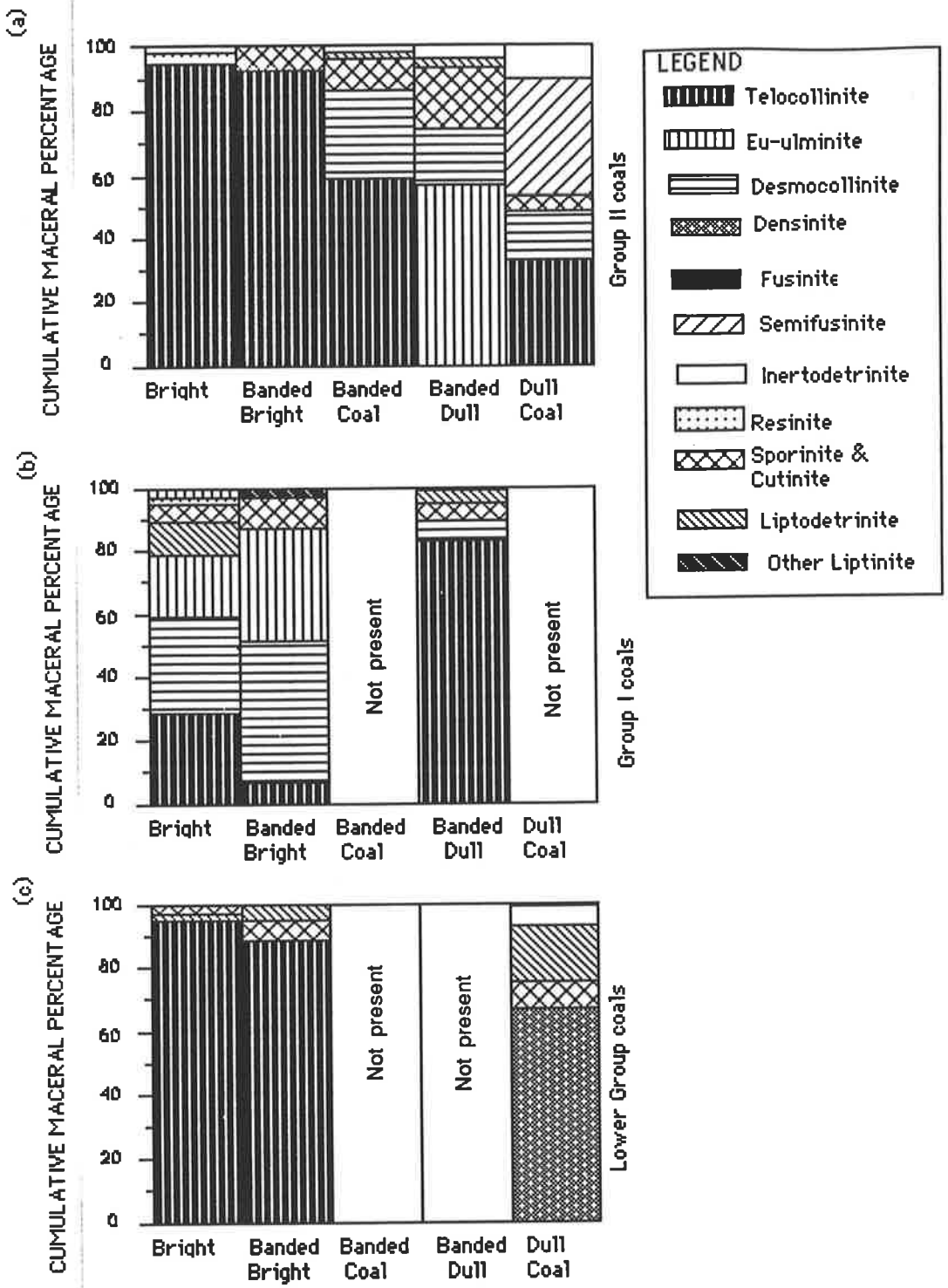

Fig. 5.12 Average maceral composition of Ying Cheng Formation on a mineral matter-free basis. (a) Group II coals; (b) Group I coals (c) Lower Group coals. (only maceral > 0.5% taken into acount)

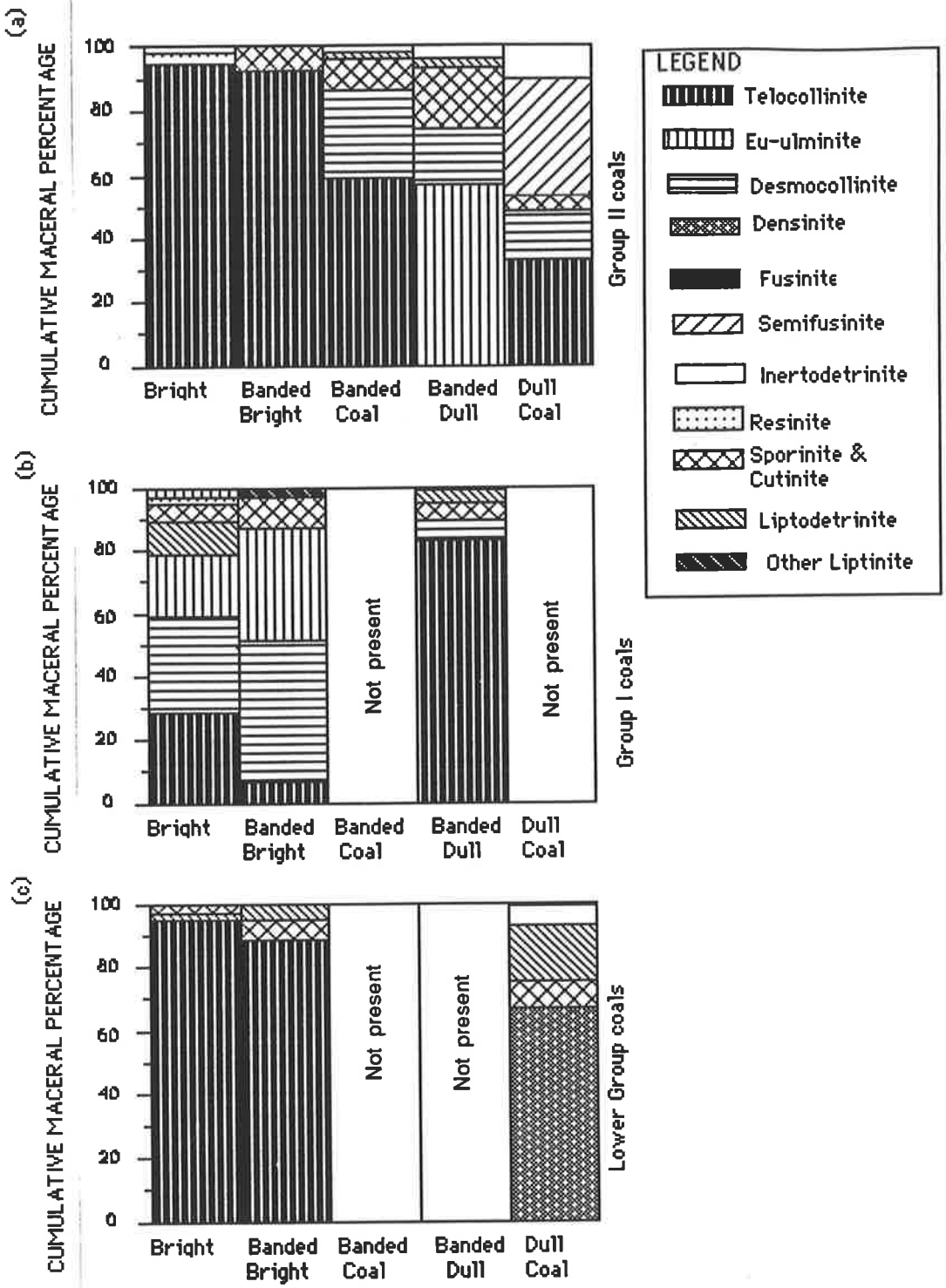

Fig.5.12 Average maceral composition of Ying Cheng Formation on a mineral matter-free basis. (a) Group II coals; (b) Group I coals (c) Lower Group coals. (only maceral > 0.5% taken into acount)

of the causes for petrographic variation within a mire is water level, which can influence both the type of plant community and the degree of degradation of maceral precursors. The Lower Group coals contain numerous clastic beds (Fig. 5.11) indicating that flooding was common and that insufficient time was available for the build-up of the mire above the water table. Petrographically, these coals contain better preserved cell structures in the vitrinite (textinite and texto-ulminite) and less inertinite.

The petrographic compositions of lithotypes from the three groups of coals are summarised in Figure 5.12. It is clear that the inertinite and detrovitrinite (vitrinitic groudmass material) contents increase, and the vitrinite content decreases, from bright to progressively duller lithotypes.

5.3.2 MICROLITHOTYPES

The microlithotype compositions of the seams from the Yang Cao Gou Basin are shown on a ternary diagram in Figure 5.13, and in Table 5.4. The microlithotype analyses provide data pertinent to an interpretation of Yang Cao Gou coal facies. The most abundant microlithotypes are vitrinite-rich (vitrite, clarite, vitrinertite, and duroclarite). As in most coals, vitrite is the most abundant constituent. In many cases the vitrinitic groundmass contains some liptinite, thus forming clarite.

Vitrinertite, in which the vitrinite is closely associated with inertite, occurs in two forms. The most common one is vitrinertite rich in vitrinite, and is characterized by inertinite dispersed within a vitrinitic matrix. The second form is vitrinertite rich in inertinite.

Trimacerite is present in all seams with an abundance of 3 - 7%. In most cases it occurs as the vitrinite-rich variety duroclarite, which in places has a high proportion of liptinite.

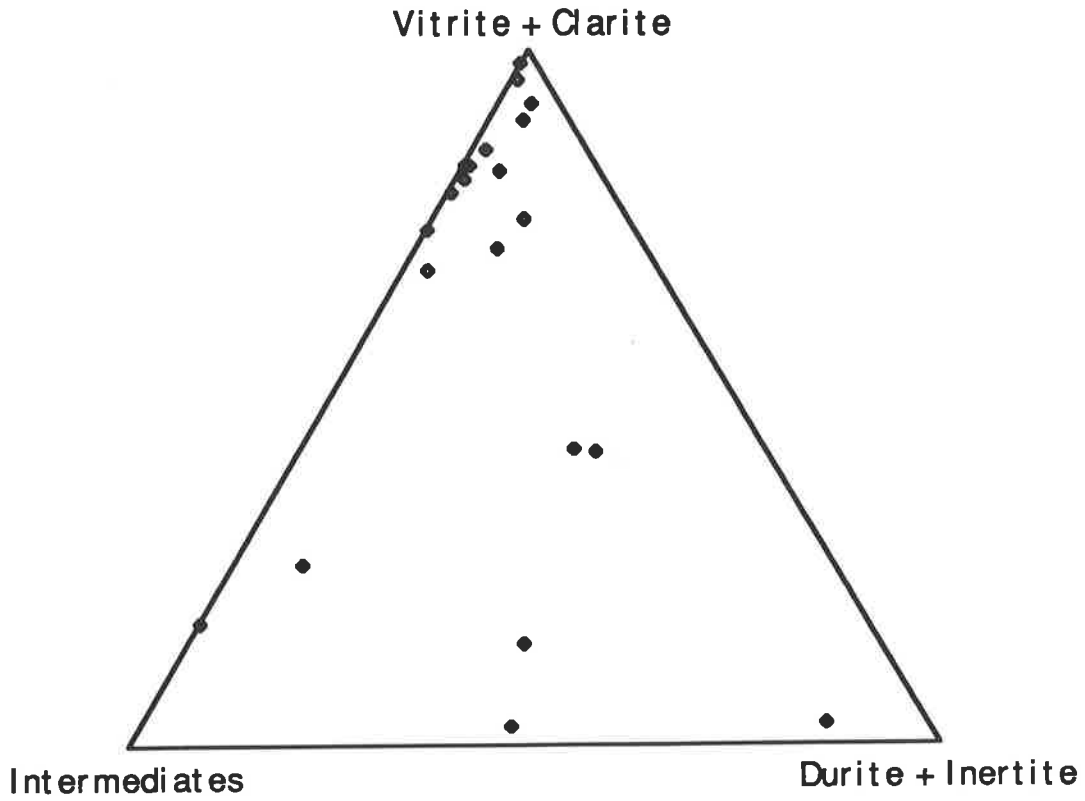

Fig. 5.13 Microlithotype composition of the Yang Cao Gou coals

5.4 DEPOSITIONAL ENVIRONMENTS OF THE YANG CAO GOU COALS

Generally speaking, the Yang Cao Gou coal displays a high vitrinite content. The high vitrinite content throughout the coal sequence indicates that the rate of subsidence of the peat swamp kept pace with the rate of peat accumulation. This environment allowed the peat to remain beneath the water table, and therefore to accumulate in anoxic conditions. In terms of microlithotypes, the high content of vitrite and liptinite-poor clarite is generally considered to be derived from woody tissues like stems, branches, and roots, in a forest swamp environment (Teichmüller, 1982). The extensive, thick, homogeneous and structureless telocollinite in the Group II coals also indicates that the thick coal beds are derived from large amounts of plant material accumulated under conditions of minimum organic degradation, and in most cases they formed *in situ* (i.e. they are autochthonous). High ground water levels can protect vitrinite

from oxidation. In contrast, the much thinner, relatively abundant telocollinite, and the higher detrovitrinite, inertodetrinite and liptodetrinite contents in the Lower coals and Group I coals indicate these coals formed either from small amounts of accumulated plant debris under minimum conditions of degradation, or from large amounts of plant debris under conditions of maximum organic degradation. On the other hand, they may have originated as *allochthonous* peat (Lower Group coal), or been transported a very short distance *(hypautochthonous)* prior to deposition in the basin (Group I coal). This is borne out by microscopic evidence, such as many scattered inertinite (fusinite) phytoclasts within the vitrinite. These are angular whilst others are rounded indicating that they have been subjected to abrasion during transport. Also supportive of this interpretation are the high mineral-matter content and high inertodetrinite and vitrodetrinite contents, as well as the occurrence of vitrinite with oxidized rims. Some supporting geological evidence is also found in the Lower Group coal. In two boreholes in the south of the basin, the coal rests directly on rhyolite, and there are no plant rootlets on the floor of the coal beds.

As discussed before, Groups II, I and Lower Group coals accumulated in lacustrine, delta plain and alluvial fans environments, respectively. At the coal group level (not the individual coal seam level), considerable differences in maceral composition from fluvial - deltaic environments are apparent (Fig. 5.14).

Some Group II coals have higher vitrinite and inertinite than Group I and Lower group coals. Thickening of the Group II coals around borehole ZK4004 suggests more prolonged subsidence favorable to peat development at this locality. Zhao (1989) found that the best and thickest coal was developed in a local depression on a basement high. The high content of telovitrinite of the Group II coals (Figs. 5.10 and 5.11) can be considered as an indication of the original composition of the coal. The relatively high liptinite content in the upper coals (Fig. 5.9) confirmed the former existence of a lake because the spore exines and leaf cuticles, the precursors of the two most abundant types of liptinite, are very resistant to degradation and are the lightest elements of the coal, and thus can be transported to concentrate in the lake. Most other plant remains are easily

decomposed during water transport (except for the inertinite). By microlithotype, the majority of the Group II coals comprise liptinite-poor clarite and vitrite that were typically formed in forest swamp environments and represent the detritus of stems, branches, barks, and spores (Teichmüller, 1982).

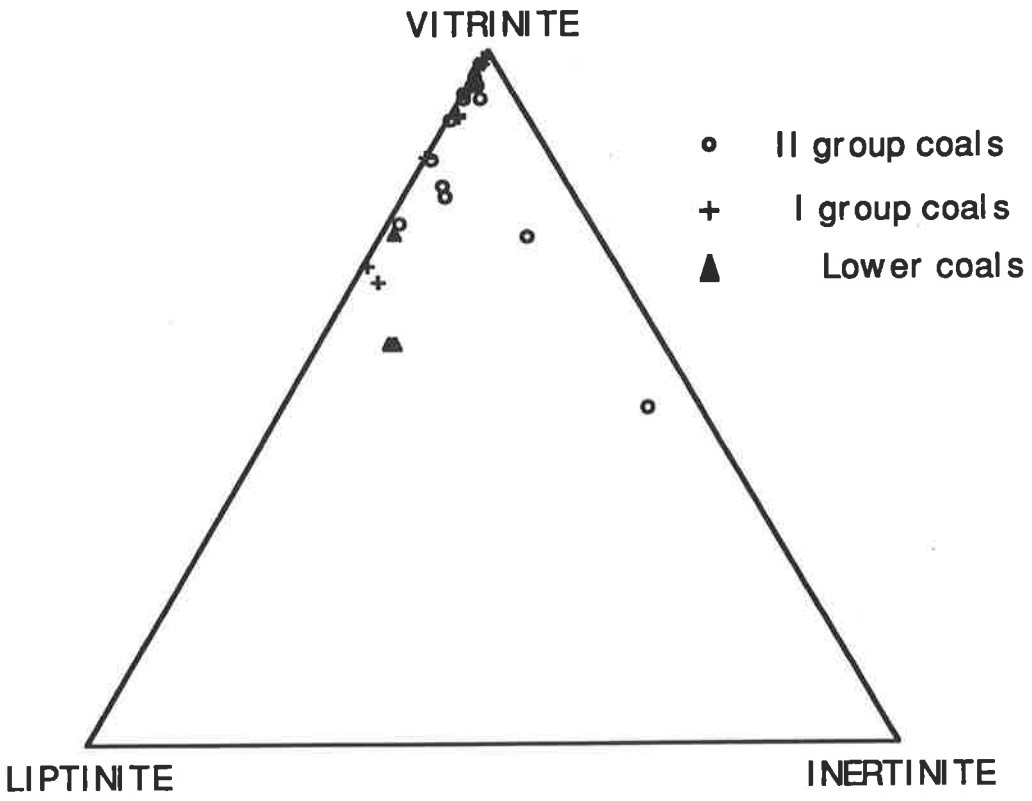

Fig. 5.14. Maceral compositions of the coals from the Group II, Group I, and Lower Group coals

As discussed in Chapter 4, the Lower coals were deposited in an alluvial fan setting, and are thinner than the upper coals (Groups II and I coals). They are discontinuous and cannot be traced for any great distance, as can the upper coal seams. The water level of the mire changed periodically under the influence of flooding. Correspondingly, the inertinite and vitrodetrinite contents fluctuated vertically within the coal seam. The Lower coals consist mainly of vitrinite, minor amounts of liptinite and sparse inertinite.

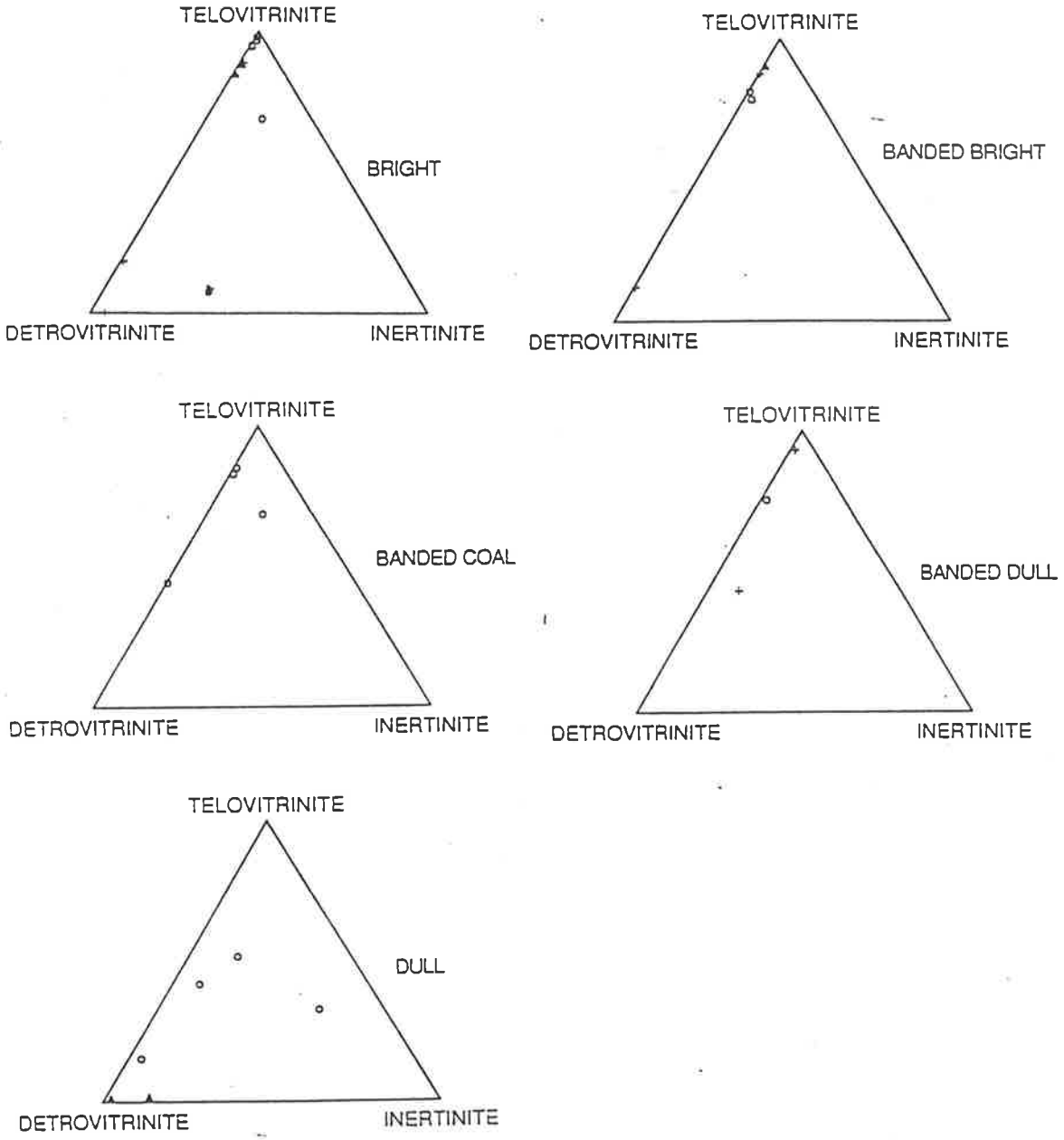

Fig 5.15 Ternary composition diagrams by lithotype, mineral matter free basis. o Group II coals; + Group I coals; ▲ Lower Group coals

The following three petrographic indices were introduced by Diessel (1982) as facies indicators and are adopted for use here:

(1) tissue preservation index (TPI) = $\frac{\text{eu-ulminite + telocollinite + semifusinite + fusinite}}{\text{desmocollinite+ macrinite + inertodetrinite}}$

(2) gelification index (GI) = $\frac{\text{vitrinite + macrinite}}{\text{semifusinite + fusinite + inertodetrinite}}$

(3) wetness (or dryness) of forest moor:

wetness index(WI)= $\frac{\text{eu-ulminite + telocollinite}}{\text{semifusinite + fusinite}}$

The ratio $\frac{\text{eu-ulminite + telocollinite + semifusinite + fusinite}}{\text{sporinite + inertodetrinite}}$

indicates the input of oxidized material to the coal (Diessel, 1982), but this is only true when the semifusinite and fusinite formed in situ (i.e. are not allochthonous).

To determine the facies and depositional environments of the Yang Cao Gou coals, the present study focused on the facies-critical macerals or maceral subgroups encountered in these coals. Gelification and preservation indices are used to define swamp types and depositional environments. Figure 5.16 shows the facies diagrams for the Yang Cao Gou lithotypes. These indicate that most of the lithotypes were formed in wet forest swamps, except some dull coals in Group I and Lower group which were formed in limited clastic marsh environments. The Yang Cao Gou

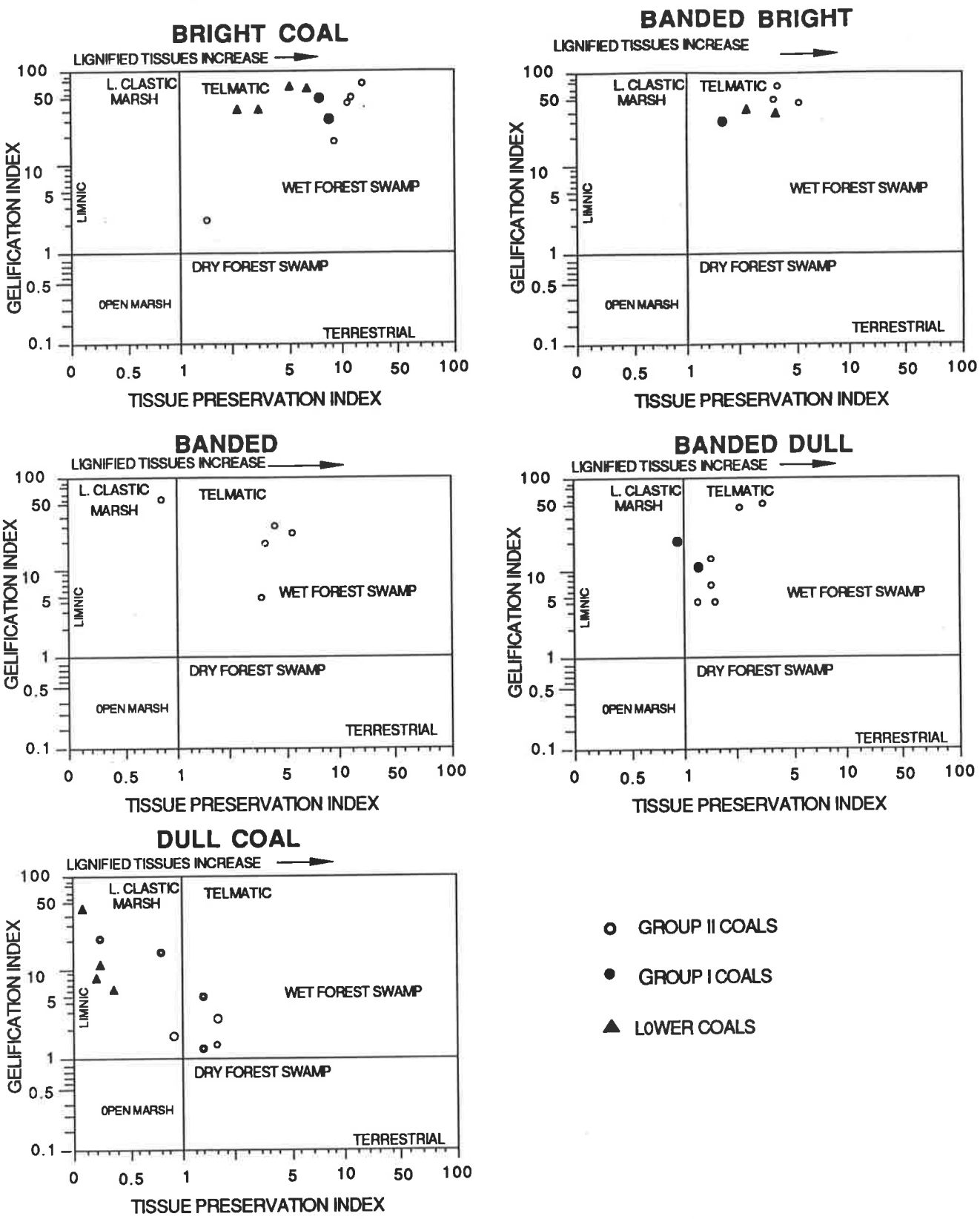

Fig. 5.16. Coal facies diagrams for Yingcheng Formation lithotypes (modified from Diessel, 1986). L.=limited influx.

coals are enriched in telovitrinite, so both the gelification index (GI) and

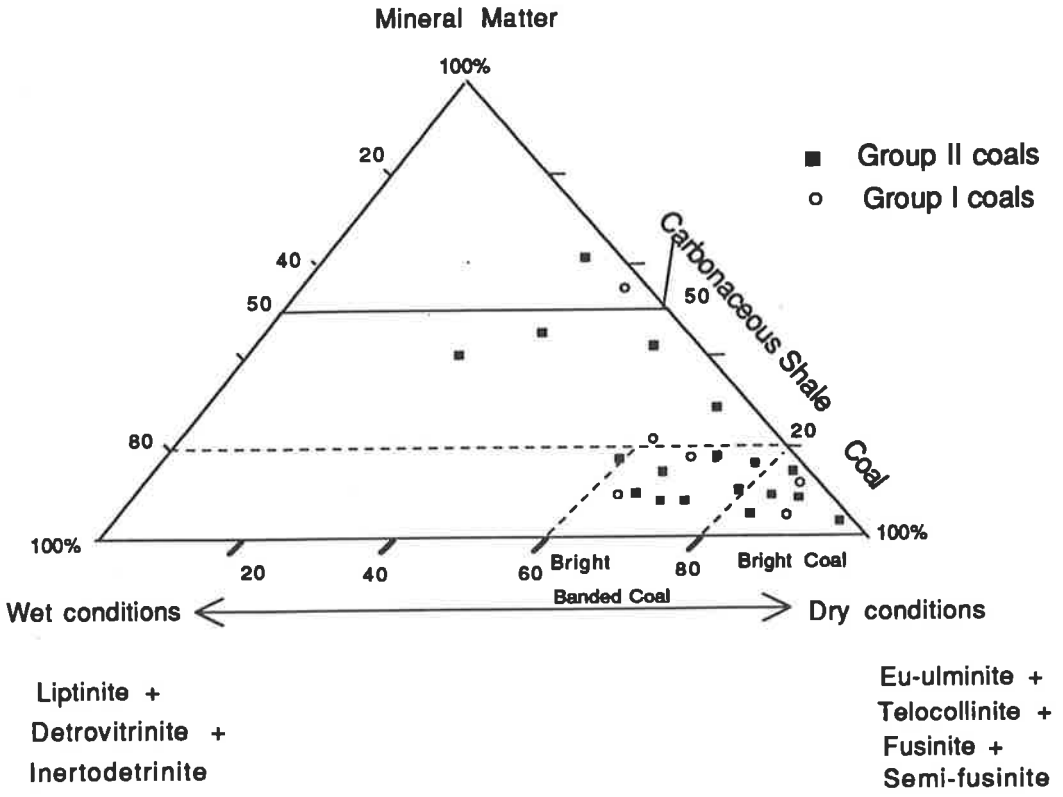

Fig. 5.17 Maceral compositions of coal samples (Group I and II), indicating depositional environment based on inferred lithotypes (after Goodarzi and Gentzis, 1987)

the tissue preservation index (TPI) are high to very high. These data indicate wet forest moor conditions. Goodarzi and Gentzis (1987) have used maceral composition to deduce lithotypes of coal, referred to as dull, banded, and bright coal. Their maceral composition diagram (Figure. 5.17) indicates that the Yang Cao Gou coal consists of bright banded and bright coals, that is to say, the peat formed in a shallow water environment and contains high amounts of eu-ulminite and telocollinite and low amounts of inertodetrinite and liptinite. When peat was forming, conditions must have been favourable for the preservation of organic matter; only limited biological degradation of the woody tissue took place. Figure 5.18, a ternary facies diagram (after Diessel,1982), also shows that the Yang Cao Gou coals plot mainly in the area of high proportions of eu-ulminite and thus are of forest moor origin.

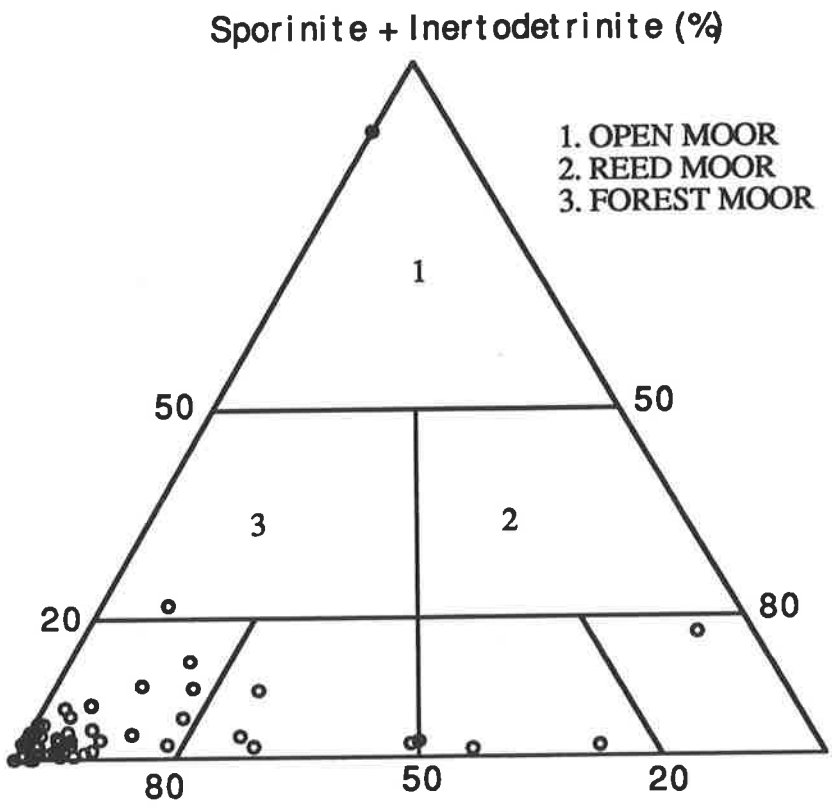

Fig. 5.18 Ternary facies diagram (after Diessel, 1982) for the Yang Cao Gou Basin coals.

Smyth (1979) examined microlithotype compositions of coals from the Permian Cooper Basin, and related them to specific depositional environments interpreted from sedimentological investigations by Thornton (1978, 1979). She concluded that the lacustrine coals are typically rich in inertinite (area A). Also area B in her model relates to fluvial systems with a large sediment load, and area C represents coals deposited in brackish environments (Fig. 5.19). Furthermore, the deltaic coals are typically rich in intermediate microlithotypes (duroclarite, clarodurite and vitrinertite).

Table 5.5 Reflectance data from Yang Cao Gou and adjacent basin coals

Sample No.	Location	Depth(m	Rvmax (%)
892-164	ZK103	28.00	0.39
892-168	QZ8001	73.10	0.49
892-83	ZK806	233.89	0.50
892-175	ZK5604	262.72	0.49
892-115	ZK2501	276.80	0.59
892-178	ZK2401	281.01	0.49
892-127	ZK1603	309.11	0.56
892-170	ZK805	328.00	0.51
892-157	ZK1718	367.79	0.51
892-120	ZK2502	402.59	0.48
892-122	ZK2502	428.42	0.61
892-134	ZK11202	494.52	0.54
892-96a	ZK3202	518.44	0.55
892-140	ZK3305	778.60	0.61
892-52	ZK4803	853.26	0.54
892-58	ZK4803(G)	844.33	0.45
892-167	ZK5703	916.98	0.74
892-81	ZK5705	948.13	0.62
892-39	ZK4004	980.44	0.58
892-44	ZK4004	998.40	0.50
892-71	ZK1721	549.00	0.53
892-184	ZK108	789.00	0.62
892-101a	ZK4804	1006.00	0.67
892-102	ZK4804	1012.40	0.59
892-107	ZK4804	1019.80	0.61
892-112	ZK3203	351.30	0.54
892-119	ZK2501	316.40	0.32
892-129a	ZK1603	316.40	0.57
892-188	ZK108	400.00	0.63
892-59	ZK6401	373.70	0.48
892-68	ZK912	291.00	0.35
892-L6	Liufangzi	*	0.61
892-Y5	Yingcheng	*	0.67
892-J6	Jiutai	*	0.58
892-X5	Xinlicheng	*	0.68

*= coalface sample

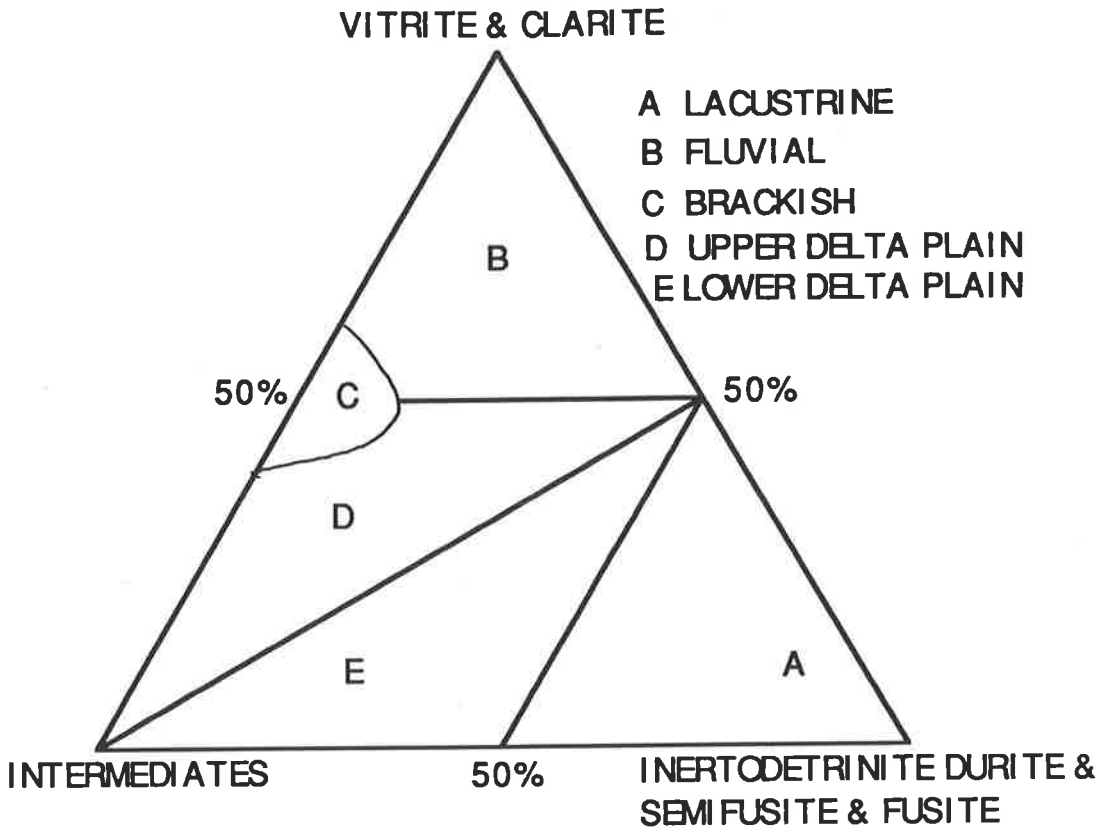

Fig. 5.19 Ternary diagram showing depositional environments of Permian coals from the Cooper Basin interpreted from microlithotype compositions (after Smyth, 1979).

Most Yang Cao Coal coals fall in area B (fluvial) on Smyth's model (Figure 5.20). This suggests that most coal facies in Yang Cao Gou Basin are related to high energy fluvial palaeoenvironments. Some of the coals plot in areas D and E, may be suggesting that the environment of deposition was partly delta plain. In fact, as already shown, the Group II, Group I coals and Lower coals were of lacustrine, fan delta and alluvial fan origin, respectively. The limited value of Smyth's model may result from the fact that it is based on Australian (Gondwana) coals that are rich in inertinite, whereas the Yang Cao Gou coals are inertinite-poor.

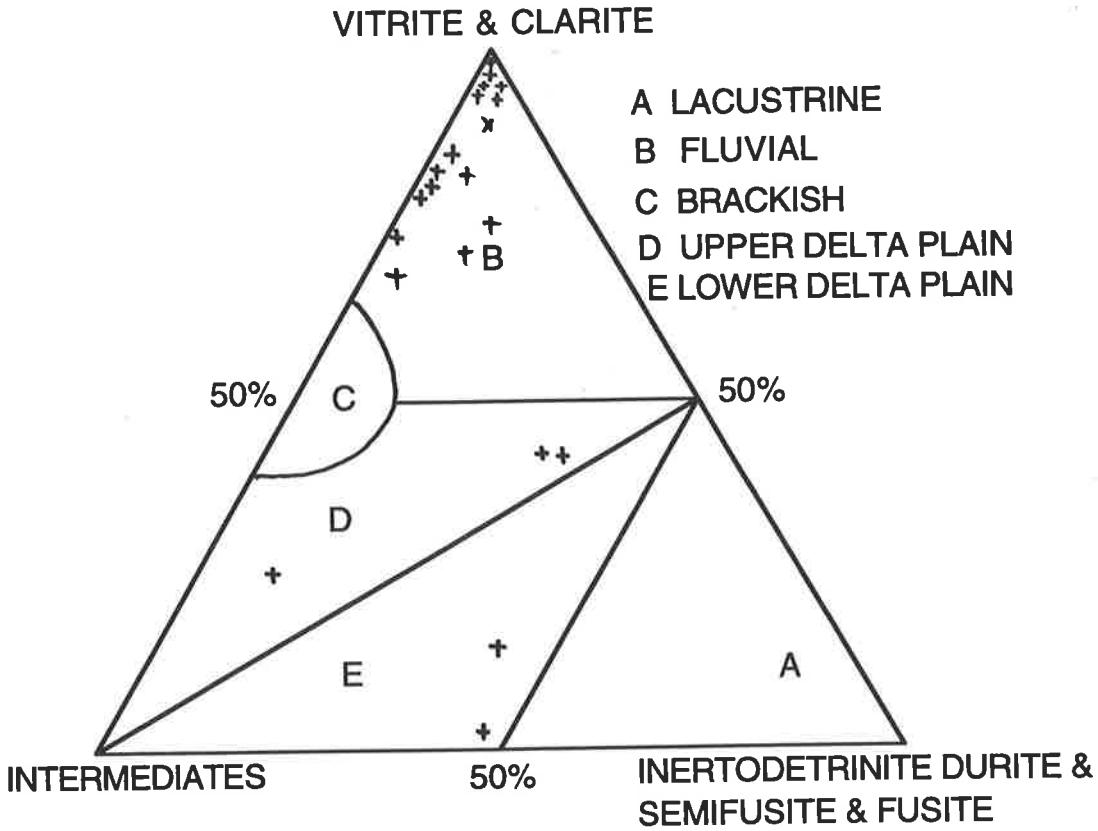

Fig. 5.20 Ternary diagram of the microlithotype compositions of coals in Yingcheng Formation, Yang Cao Gou Basin plotted on the Smyth (1979) model.

Figures 5.21 and 5. 22 are maceral profiles of the Group II and Group I coals in the Yingcheng Formation. These figures represent vertical and lateral changes of maceral composition around the basin. Figure 5.24 is a location map for these profiles.

Seam II of Group II coals contains thick intervals of clean, bright coal resulting from peat accumulation which remained uninterrupted for a long period of time (Fig. 5.21, ZK3202 and ZK2401). Relatively constant reducing environments are indicated by a trend of upward-increasing telovitrinite content in the seam which is observed in Figure 5.21 between two partings and by the persistently high ratio of vitrinite macerals to liptinite and inertinite macerals. It can be seen that peat accumulation was disrupted by a influx of sediments represented by a parting, and then

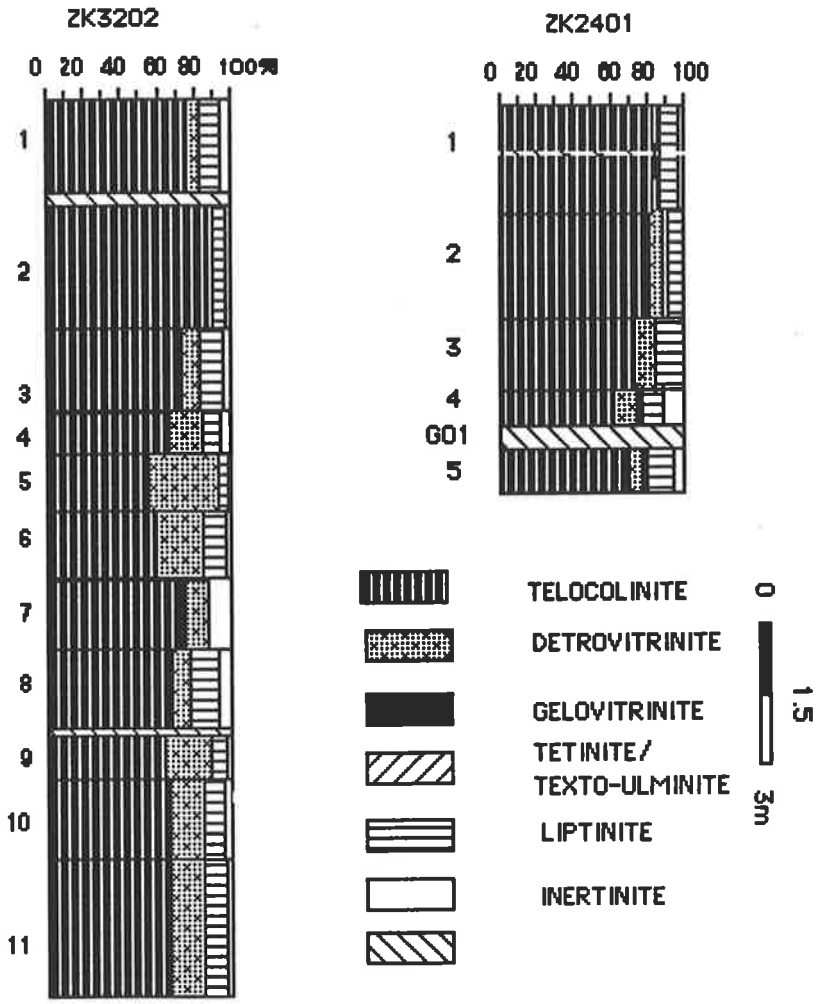

Fig. 5.21 Variation and distribution of average maceral compositions of seam II (group II coals), Yingcheng Formation, Yang Cao Gou Basin

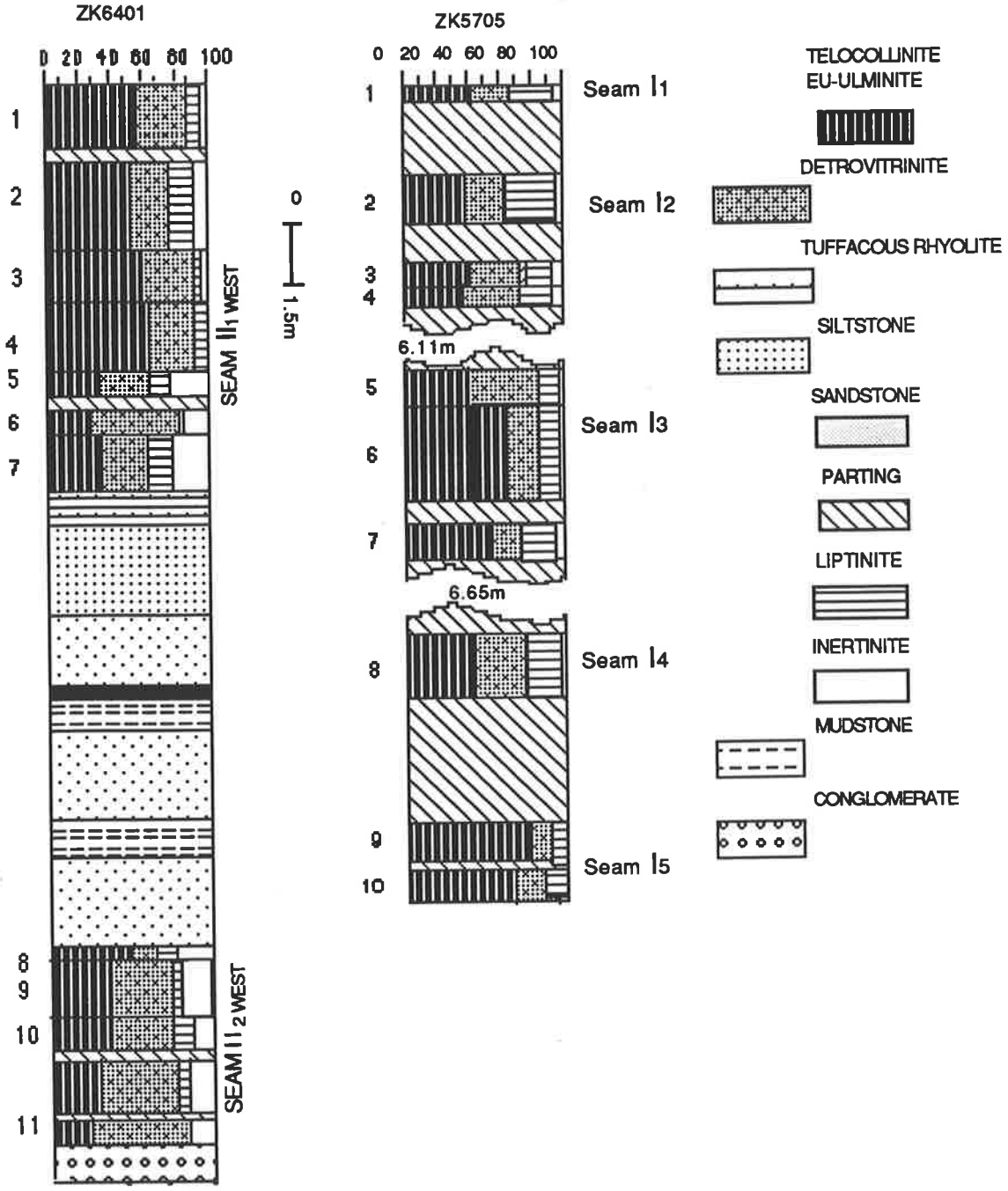

Fig. 5.22 Variation of average maceral compositions of Seams II_1 and II_2 and Seams I_1, I_2, I_3, I_4, and I_5 in west to east direction. Location of sections shown in Fig. 5.24

conditions for peat accumulation returned, resulting in the formation of a thick seam.

The petrological profiles of sections for seams II_1 E, II_{2E}, II_1 w, II_{2W} and group I coals are presented in Figure 5.22. Seams II_{2E}, and II_1 w contain numerous intervals rich in inertinite with less liptinite at the base. The presence of the thick sandstone between II_1 w and II_{2W} indicates the "drowning" of the peat surface due to the sudden influx of siliciclastic sediments (Fig. 5.22, section ZK6401). The Group I coals (seams I_1, I_2, I_3, I_4,and I_5) in general are liptinite-rich and inertinite-poor as compared to the Group II coal seams (Fig. 5.22, section ZK5705).

Generally speaking, Group II coal seams are similar in maceral composition, except for the following differences, which indicate some local events. Section ZK1603 in Figure 5.21 has relatively more liptinite than other sections, particularly in the upper part of the seam, indicating possible differences in accumulation of plant debris. Sections in Figure 5.21 have clean coals (relative to those sections in Figure 5.22) due to fewer partings.

Variations in the plant communities can be caused by water level variation in the peat swamp due to flooding or drying. In return, the relative diversity of the peat-forming communities could influence re-establishment of peat formation given environmental fluctuation. Detrovitrinite, comprises plant debris derived from plant tissues, and is comminuted into fine-grained attritus. As it formed (at least in part) during transportation to its site of accumulation, it could represent high energy aquatic regimes. Figure 5.25 shows that the detrovitrinite content increases proportionally with the ash content. Based on detrovitrinite content, three zonations are proposed with respect to water-energy regime. Zone I (detrovitrinite < 10%, telovitrinite> 60%), represents the low energy, stagnant water, distal lacustrine environment (basin depocentre). In Zone I, because of strong alkaline conditions which promote fungal and bacterial activities, a peat with less structured vitrinite is formed. Zone II (detrovitrinite = 10%-20%), with limited clastic influx, represents a high-energy, transitional area between stagnant and open water areas; Zone III (marginal parts of the basin), in

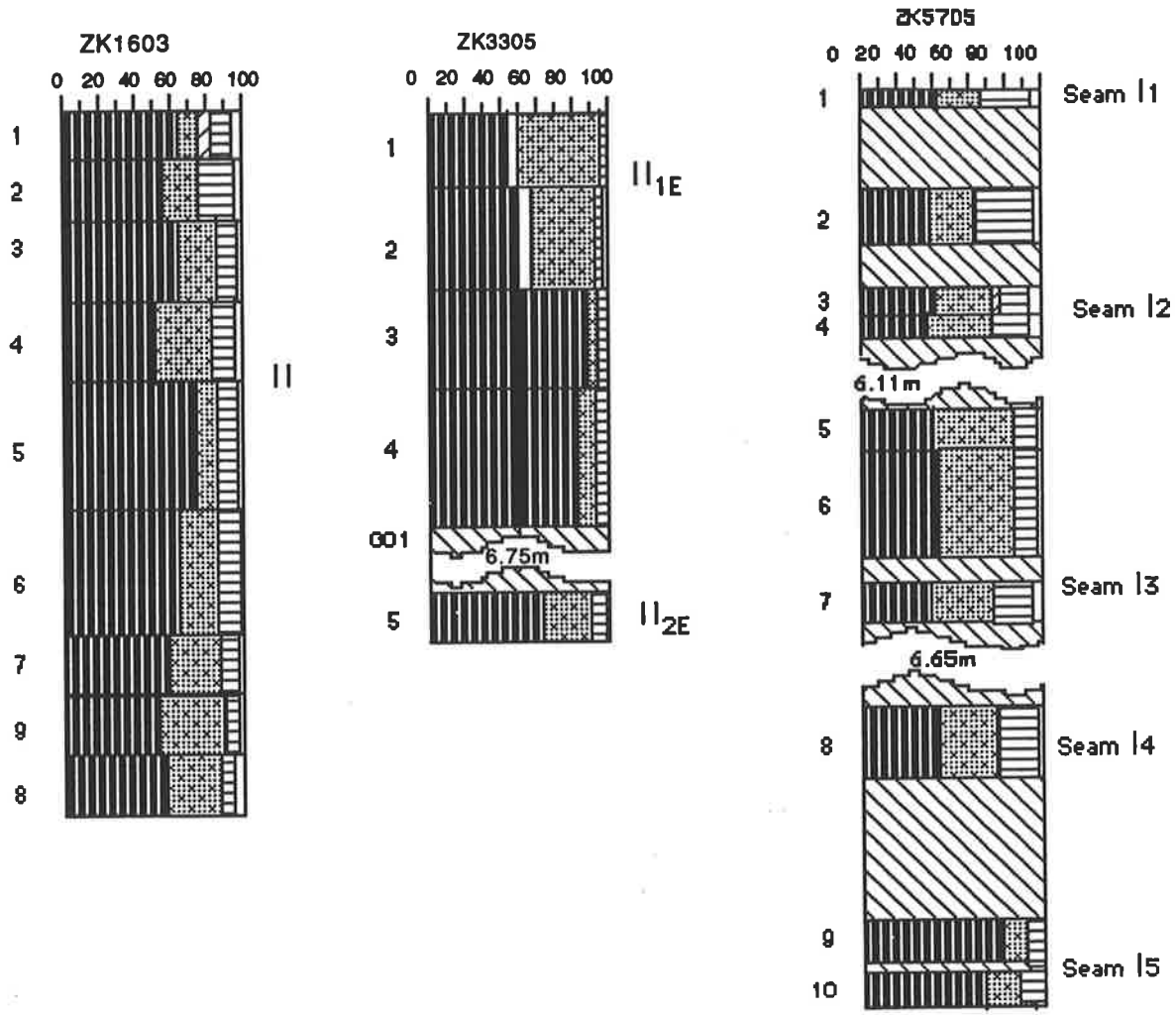

Fig. 5.23 Variation and distribution of average maceral composition of seams II, II_{1E}, II_{2E}, I_1, I_2, I_3, I_4 and I_5, Yingcheng Formation.

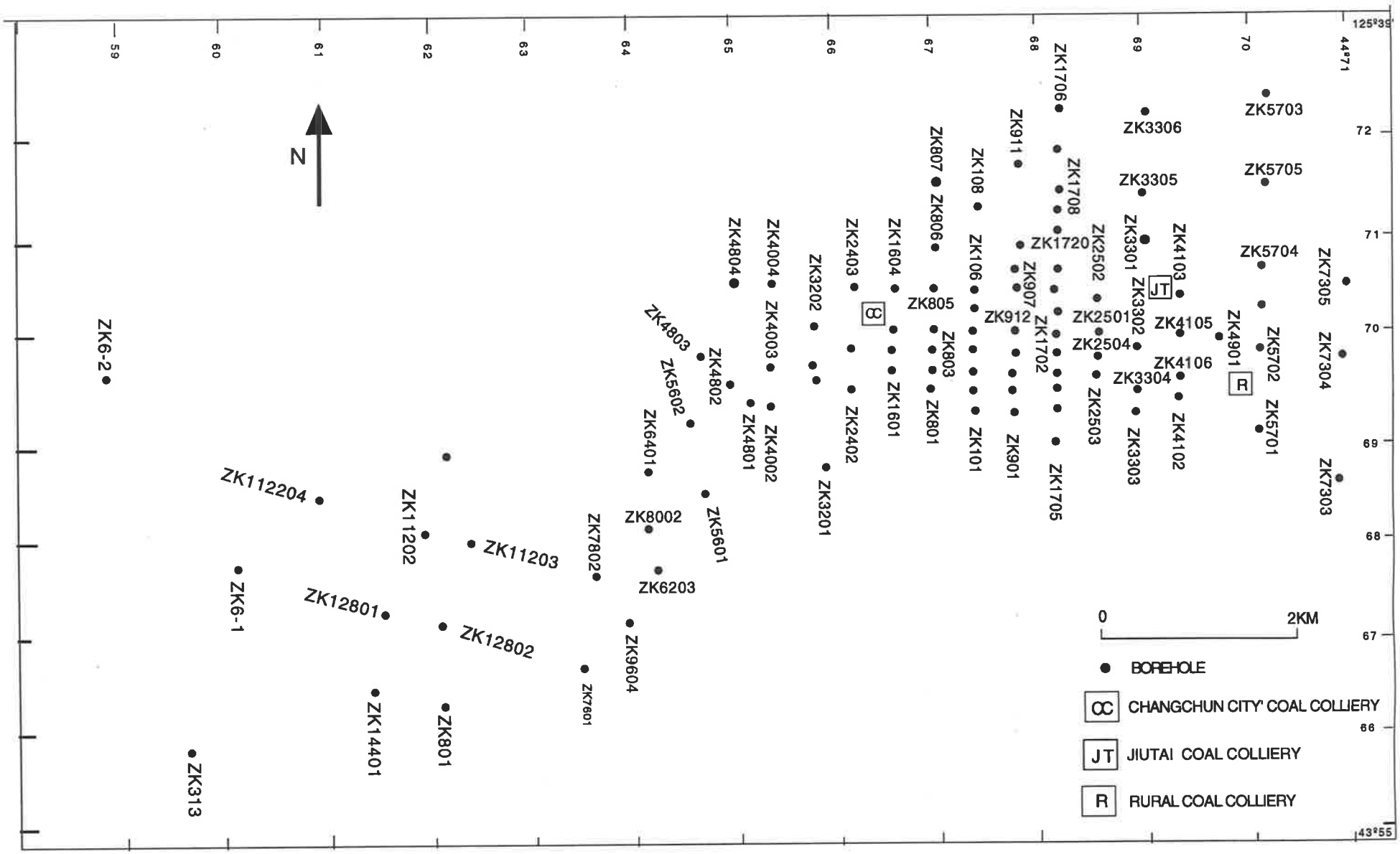

Fig. 5.24 Borehole and coal collieries location map

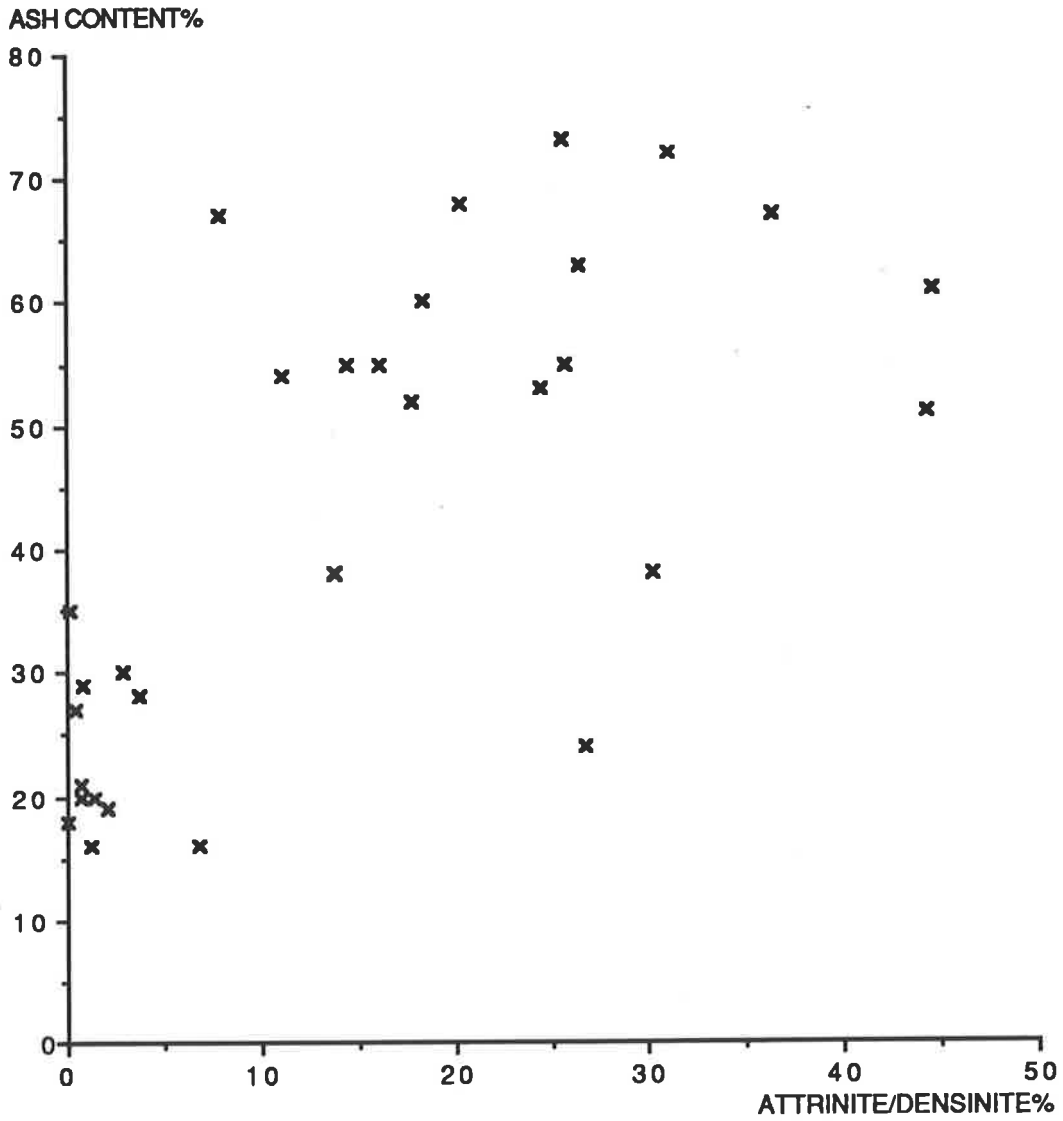

Fig. 5.25 Relationship between ash content and attrinite plus densinit

which detrovitrinite content is generally less than 30%, represents the highest-energy fresh water area, where rapid burial and slight oxidation would form a vitrodetrinite-rich, relatively more-structured vitrinite peat with lesser telocollinite, liptinite and minor inertinite. The telovitrinite content increases with decreasing detrovitrinite (Fig. 5.26). The maceral compositions of the coals in the three zones are shown in Figure 5.27. It can be seen that vitrinite increases from Zone III to Zone I, and in contrast, the coals tend to have the highest inertinite content in

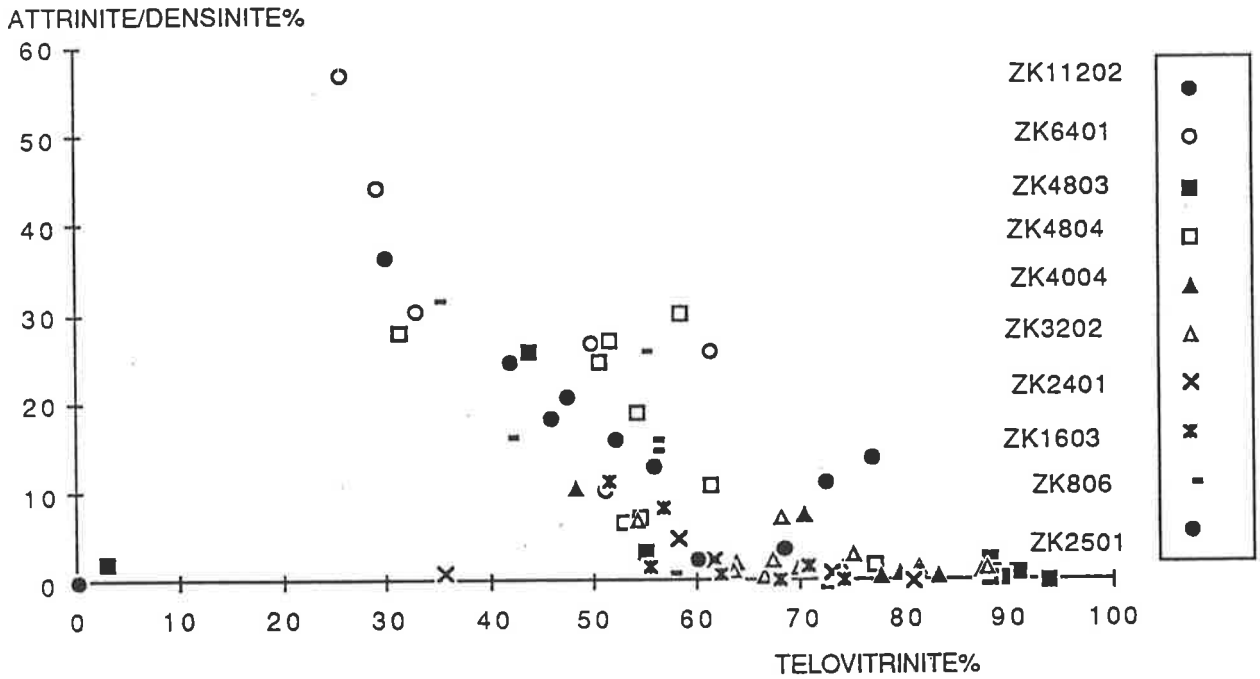

Fig. 5.26 Relationship between telovitrinite and attrinite plus densinite

Zone 3 and highest liptinite in Zone 2. These zonations are significant for targeting the coal depocentre during exploration. The fluvial-associated coal has a wide range of detrovitrinite content, from zone I to zone III. Figures 5.28 - 5.30 are the palaeoenvironment maps for Group II, Group I, and Lower coals, based on thickness, chemical characteristics and the above petrographic analysis.

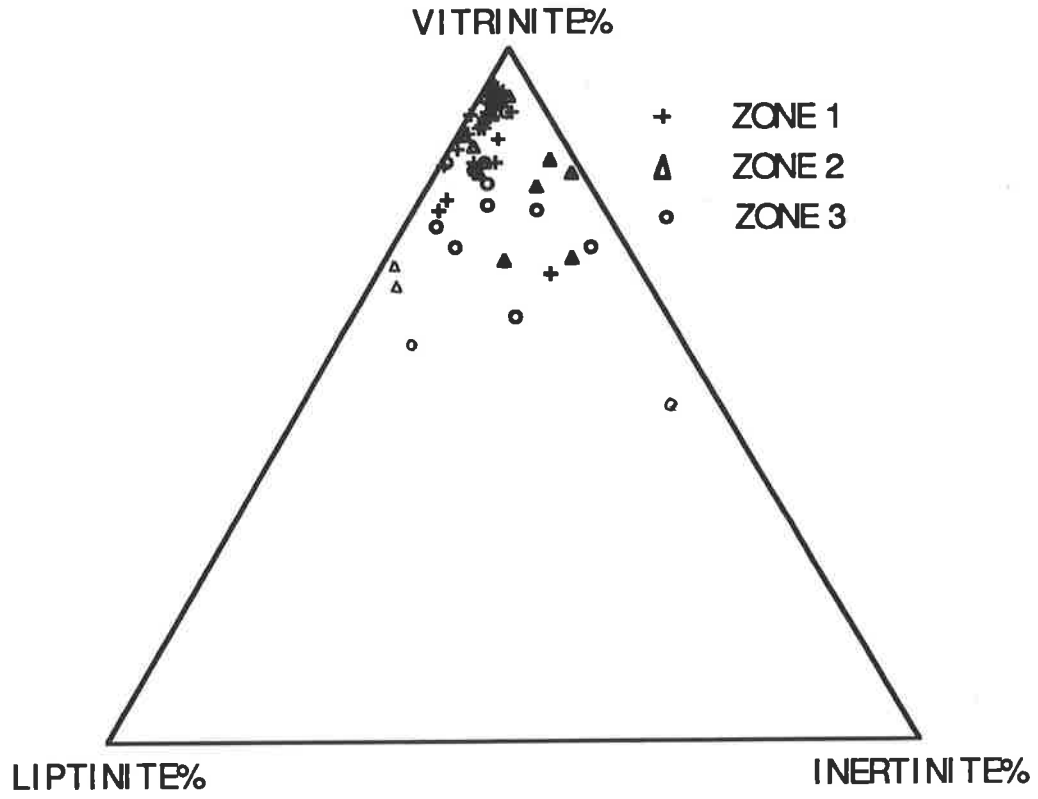

Fig. 5.27 Maceral compositions of the Zone 1, Zone 2 and Zone 3 of the coals in Yingcheng Formation, Yang Cao Gou Basin

The Yang Cao Gou Basin resulted from the Yenshan movements in the middle Jurassic. After early subsidence, andesite (An Min Formation) was deposited on basement granite. During further subsidence, the sediments of Sha He Formation, mostly alluvial sandstone and conglomerate, were formed. During K_1Y^1 time (volcanic member of Yingcheng Formation), the basin was enlarged again due to rifting, and rhyolites, the basement for the Yingcheng coal measures, were deposited.

During deposition of K_1Y^2, the basin floor subsided rapidly, causing two perennial lakes to form within the basin. Large scale alluvial fan to fan delta sediments were developed on the southeast and northwest margins of the basin. These alluvial fan sediments entered the lakes at the margins to form fan delta and shallow lacustrine sediments. In the centre, only rhyolite was deposited. The Lower coals were formed in inter-lobe depressions of the fans. Petrographically, most of the Lower coals have more than 30% detrovitrinite and contain relatively more mineral matter. Therefore, coals were formed in zone 3 (swamps; Fig. 5.28).

During deposition of K_1Y^{3-1}, sequences consisting mainly of alluvial, fan delta and swamp sediments, were laid down. The fan delta sediments were distributed around the southwest, east and northeast parts of the basin (Fig. 5.29). Thin coal seams were formed in the northwestern part (zone 2) where a well drained swamp occurred. A poorly drained swamp occupied a small area in the central east where the most important coals along Group I coals accumulated (Fig. 5.29). Coals mostly belong to zone 1 at this position.

In the early stages of K_1Y^{3-2}, two separate depocentres coalesced, and subsided as a whole. Except for the southern margin area, shallow lacustrine sediments were widespread. Thick alluvial fan and fan delta sediments were deposited on the eastern and southern margins of the basin. The central part of the basin (between ZK1706 and ZK3306, and between ZK2401 and ZK6401) was slightly domed (palaeo-highs) in the K_1Y^{3-1} period (Fig. 5.30). This area was covered by swamp, and became the most favourable site for the formation of late stage coals. Coal seams here are thick, have low ash and contain abundant well-gelified telovitrinite and less detrovitrinite. This area is in zone 1 (Fig. 5.30).

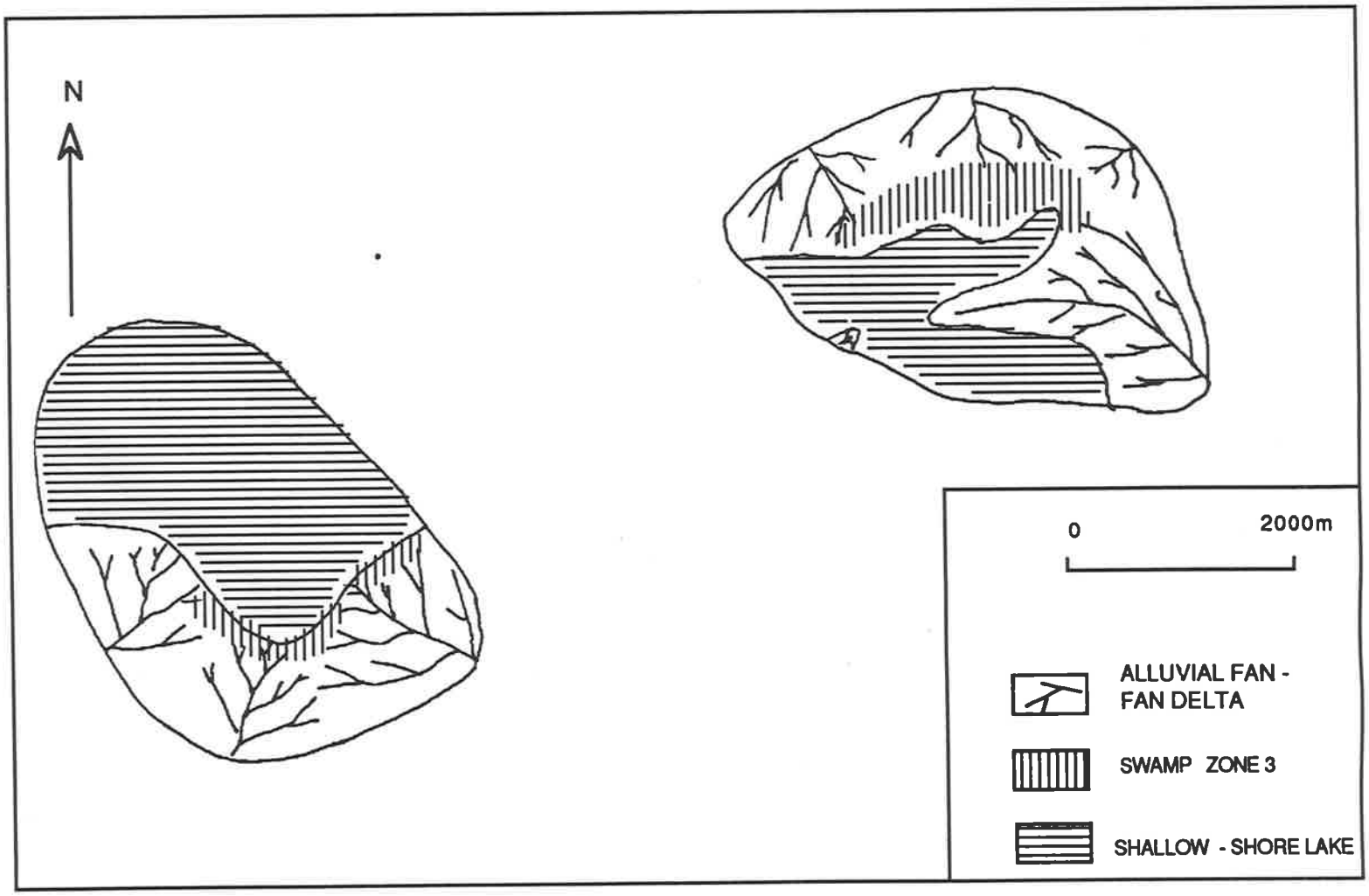

Fig. 5.28 Palaeogeographic map of $K_1 Y^2$ (including Lower coals), Yingcheng Formation, Yang Cao Gou Basin

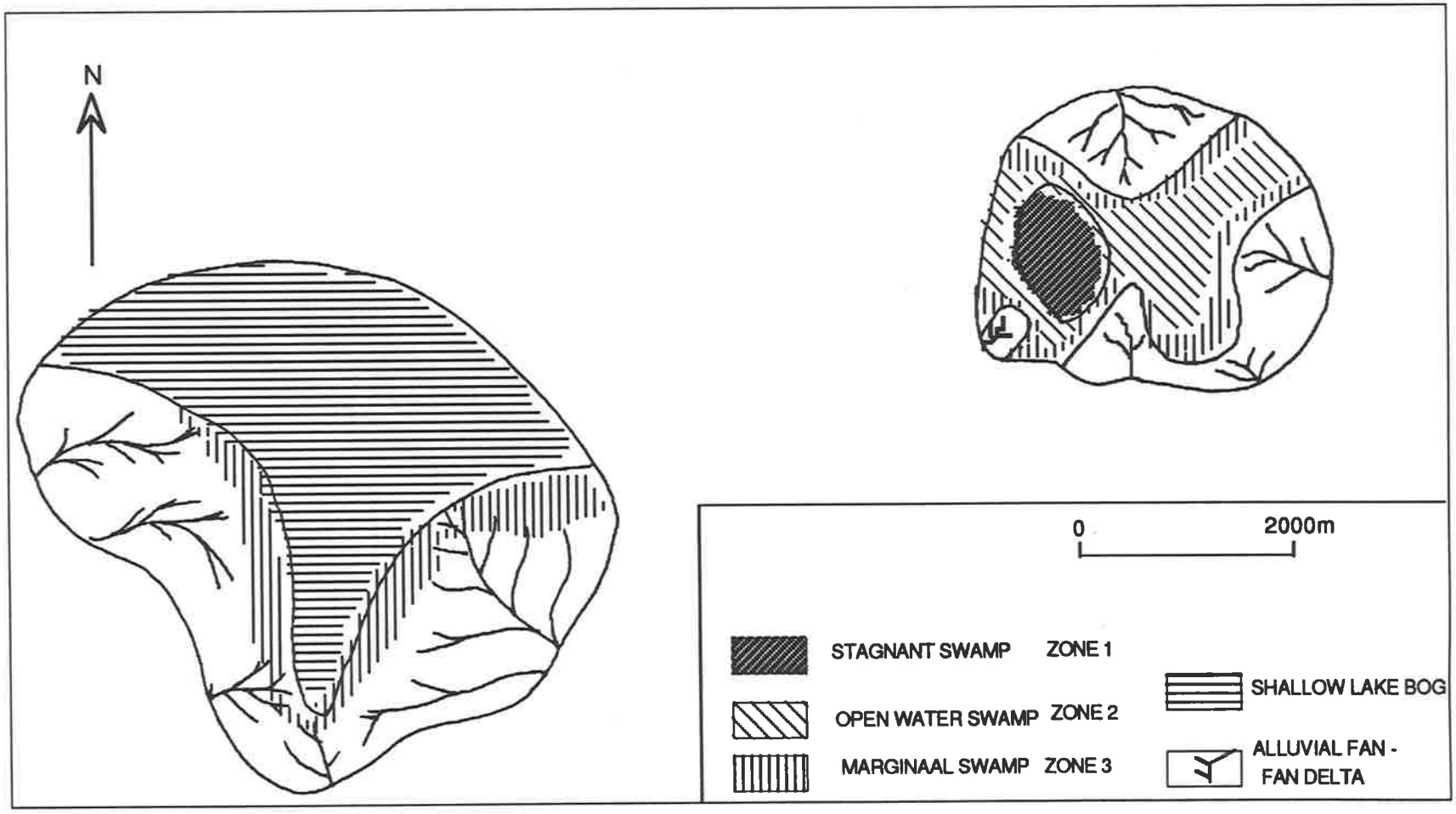

Figh. 5. 29 Palaeogeographic map of K_1Y^{3-1} (including Group I coals), Yingcheng Formation, Yang Cao Gou Basin

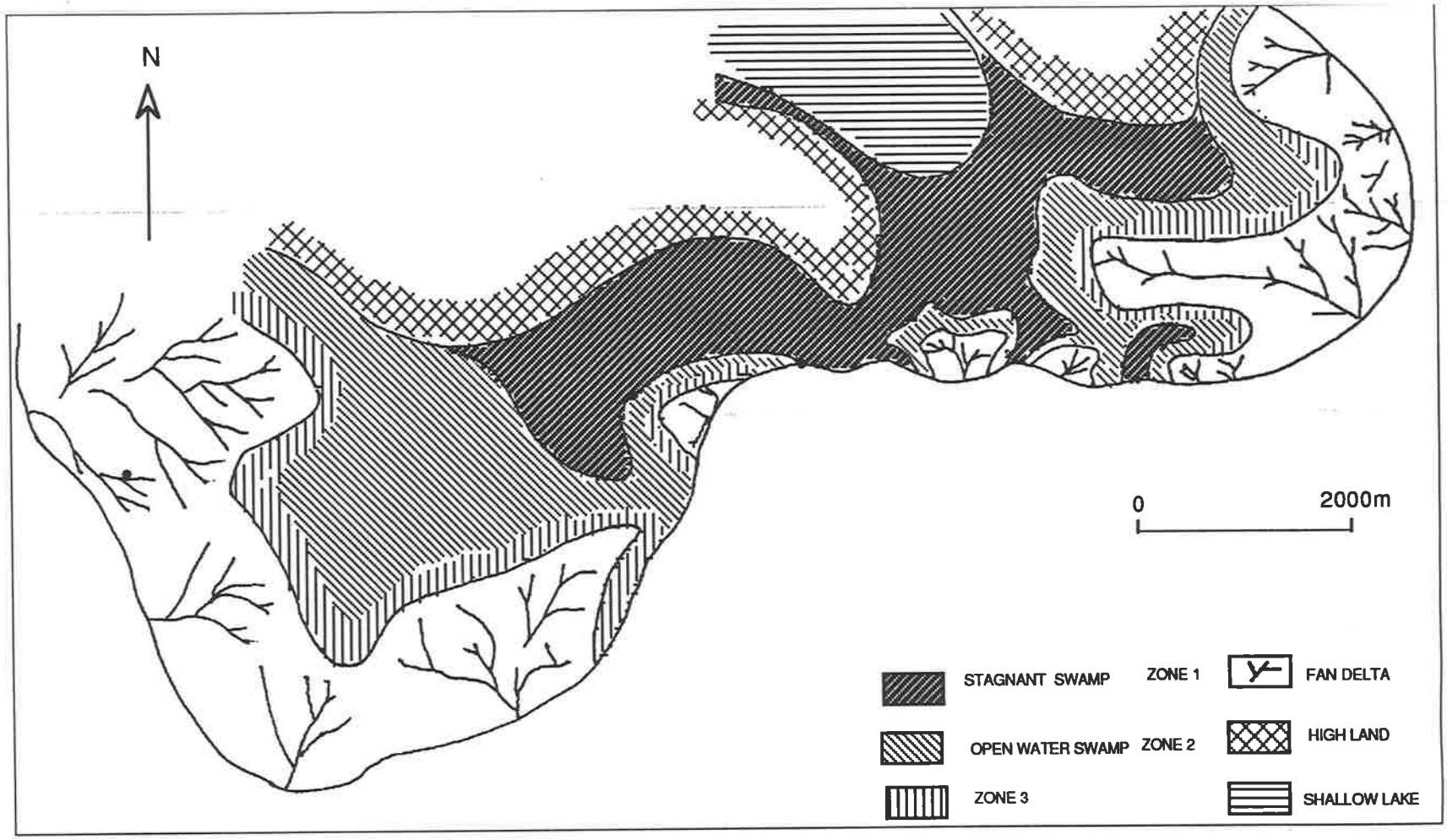

Fig. 5.30 Palaeogeographic map of K_1Y^{3-2} (including Group II coals), Ying Cheng Formation, Yang Cao Gou Basin

5.5 RANK DETERMINATION BY MICROSCOPICAL METHOD

Low rank coals, such as most of the coals of this study, are typically classified using volatile matter and calorific value in China. Based on the average volatile matter contents of greater than 40%, the Yang Cao Gou coals are Long Flame coals under the Chinese classification (roughly equivalent to subbituminous B rank in the ASTM system).

The mean maximum reflectance of the vitrinite is normally used as a measure of the rank. In contrast to chemical parameters these measurements can be undertaken on both coal layers and on clastic rocks which contain finely dispersed vitrinite.

In order to determine the correlation between vitrinite reflectance and other coal parameters (e.g. proximate analysis), telocollinite reflectance was measured on 40 samples from 9 wells. The results are summarized in Table 5.5. Figure 5.31 is a plot of mean maximum vitrinite reflectance against depth for the 40 coal samples shown in Figure 5.7. The most obvious trend is the increase of $R_{V\,max}$ with depth from about 0.39% to 0.74%. The values of $R_{V\,Max}$ are mostly in the range 0.45 - 0.60% and indicate that the samples have attained the sub-bituminous A and B rank stage. Thus on the basis of these coalification parameters, the coals do not fall within the main phase of oil generation, i.e. the "oil window" for Type III kerogen (Robert, 1981).

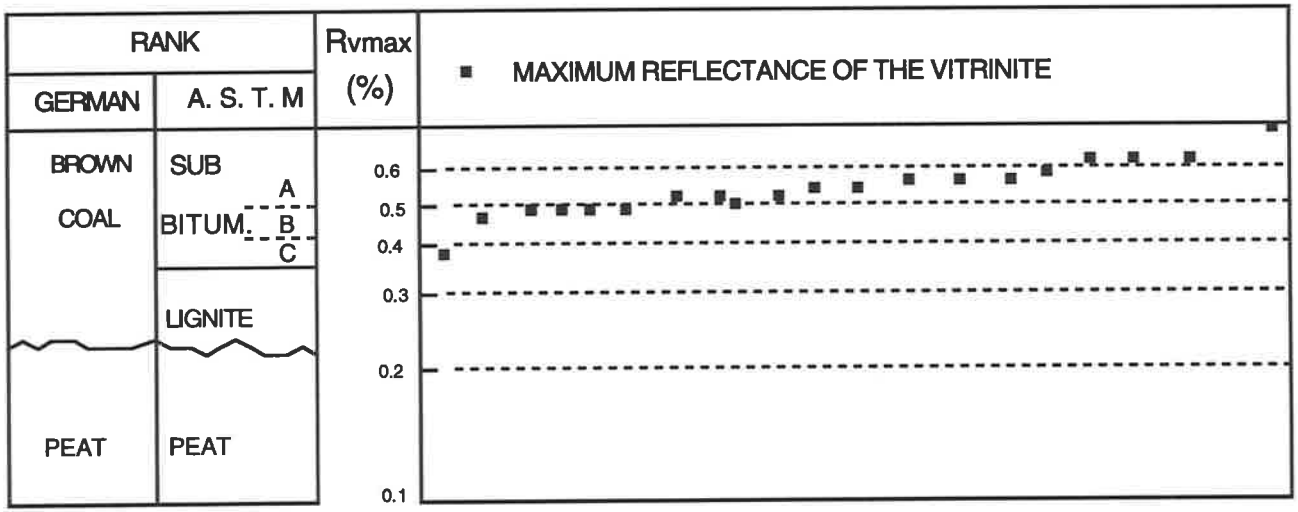

Fig. 5.31 Reflectance of vitrinite in Yang Coa Gou Basin coals in relation to the German and A. S. T. M. rank classifications of coals

CHAPTER 6 ORGANIC GEOCHEMISTRY AND OIL SOURCE POTENTIAL

6.1 INTRODUCTION

Hydrocarbon generation from coal measures and coal macerals has been the subject of extensive studies by many authors (Tissot and Welte, 1978; Powell and Snowdon, 1980; Thomas 1982; Durand and Paratte (1983); Thompson; 1985; Saxby & Shibaoka 1986; Teichmüller 1986; McKirdy et al., 1986; Cook,1982, 1986; Powell et al., 1991), It seems that coal and coal-bearing strata are a major source of oil in the Gippsland Basin, Australia (Thomas, 1982; Shanmugam, 1985), and the Mahakam Delta, Indonesia (Monthioux et al., 1985, 1987; Hvoslef et al., 1987). In China, many hydrocarbon accumulations associated with Jurassic coal-bearing strata have been found. These include Lenghu oil field in the Qaidam Basin, the Qigu oil field in the Junggar Basin and the Qiketai oil field in the Turpan Basin (Huang et al., 1980; Huang Wen-Yen et al., 1989). The oil/gas fields in Eocene coal measures beneath the East China Sea and South China Sea are also apparently sourced from coal. This organic matter includes plant remains deposited in swamps, and plant detritus that was washed into lakes and fluvial systems from surrounding highlands. During the last decade, terrestrial petroleum has been discovered in many sedimentary basins. It is widely accepted from geological and chemical evidence that hydrocarbons result from alteration of organic matter within sedimentary rocks under the influence of temperature and pressure (Tissot and Welte, 1978; Hunt, 1979; Cook, 1982). Source potential for hydrocarbons is dependent on the type and quantity of the organic matter, whereas the actual generation of hydrocarbons is controlled by the extent of thermal evolution of organic matter. For coals and terrestrial organic matter to become hydrogen-rich and oil-prone, a process of liptinite enrichment is required (Thompson et al., 1985; Khavari Khorasani, 1987). Khavari Khorasani (1987, 1989) also claimed that the deposition of organic matter under suboxic conditions favours the formation of hydrogen-rich, oil-prone vitrinites.

Using data based mainly on Chinese locations, Powell (1986) discussed the petroleum geochemistry and depositional setting of lacustrine source rocks. He acknowledged the wide variety of rock types that can develop as a result of differing depositional environments, ranging from fresh water lakes in a humid climate through fresh-to brackish water lakes in a semi-humid climate and saline lakes in a semi-arid climate, to hypersaline lakes in arid climates (Tian et al., 1983; Huang et al., 1984). An extremely high wax content is the most significant characteristic of the Chinese non-marine oils (Powell, 1986). Deep-water lacustrine facies containing Type I kerogens, which are dominated by degraded terrestrial organic matter with a varying contribution from bacterial and algal remains, are the best source rocks in the Songliao Basin (Tian et al., 1983; Huang et al., 1984; Powell, 1986).

Petrographic examination of a coal also can help determine whether it has the capacity to generate oil. Direct petrographic evidence of oil generation includes green fluorescing material similar to crude oil, oil droplets, micrinite and exsudatinite (secondary macerals). Oil droplets and yellow to green fluorescing bitumen seem to occur in vitrite and clarite in the Yang Cou Gou Basin coals. Teichmüller and Durand (1983) concluded that secondary vitrinite fluorescence is caused by these bitumen-related products.

This chapter discusses the oil potential of coal in the Yang Cao Gou Basin and examines the relationship between pyrolytic behaviour and petrographic characteristics of these coals.

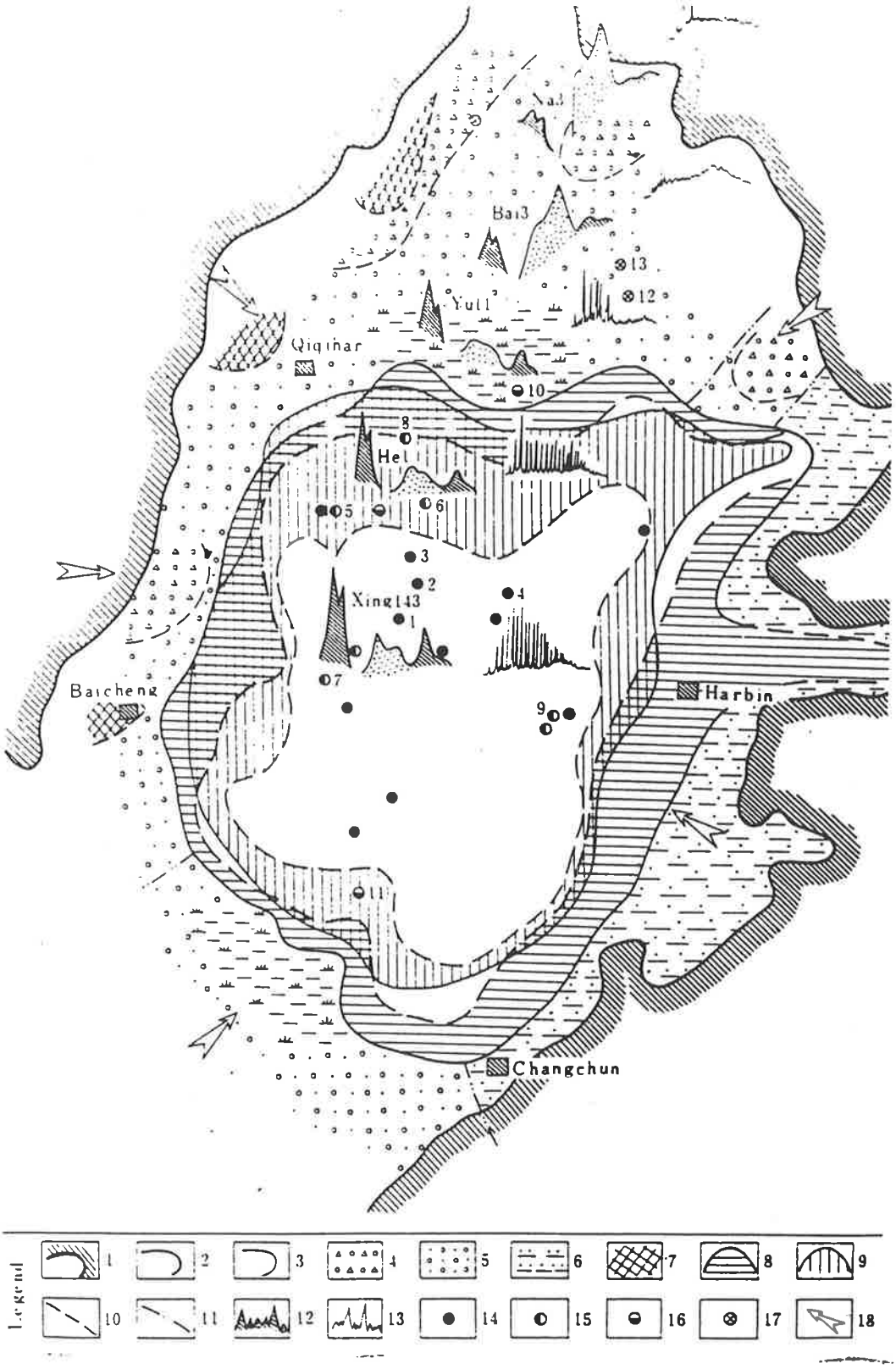

Fig 6.1 Kerogen type and n-alkane distribution, Songliao basin(after Yang et al., 1985)
Legend: (1) boundary of basin, (2) Qin 1 lake shoreline, (3) Qin 2 + 3 lake shoreline, (4) diluvial, (5) fluvial, (6) foothill alluvial, (7) trucated area, (8) Qin 1 shallow lakeshore, (9) Qin 2 + 3 shallow lakeshore, (10) facies boundary line, (11) systerm boundary line, (12) infrared specta of kerogen, (13) gas chromatography of extracts, (14) type I kerogen, (15) subtype IIA kerogen, (16) subtype IIB kerogen, (17) type III kerogen, and (18) direction of source material.

6.2 PREVIOUS WORK

After more than 25 years of exploration and research, large accumulations of petroleum and coal have been found in the Songliao Basin. Although no previous geochemical work has been done in the Yang Cao Gou Basin, there has been much undertaken on other parts of the Songliao Basin.

Yang et al. (1985) investigated the formation and evolution of nonmarine petroleum in the Songliao Basin, and found that there is a gradation from Type III organic matter in the lake margin sequence to Type I in the central deep-lake facies (Fig. 6.1). They noted that this gradation in kerogen type is accompanied by a decreasing proportion of recognisable vitrinite under the microscope. Based on analysis of the kerogen from the Songliao Basin, they found that source beds containing sapropelic kerogen occur mainly in lacustrine deposits, and that their maximum transformation ratio and total genetic potential for petroleum may be even higher than that of marine source rocks. Tian et al. (1983) have attributed the lacustrine source facies of the Songliao Basin to deposition in fresh- brackish lakes under a semi-humid climate. The main phase of source bed genesis corresponds to the period of maximum lake development and is represented by the Cretaceous Qingshankou Formation.

6.3 EXPERIMENTAL

In addition to the petrographic analysis, coal samples from the Yang Cao Gou Basin and five other nearby subbasins along the eastern edge of the Songliao Basin were examined using the organic geochemical methods described in Chapter 3. The samples from other basins (Fig. 2.2) are listed in Table 6.1. The resulting geochemical data are presented in Tables 6.2 - 6.5 and Figures 6.2 - 6.17.

Based on the results of Rock-Eval and TOC analysis, 20 coal samples (Table 6.3) were chosen as representative of the coal samples of the Yang

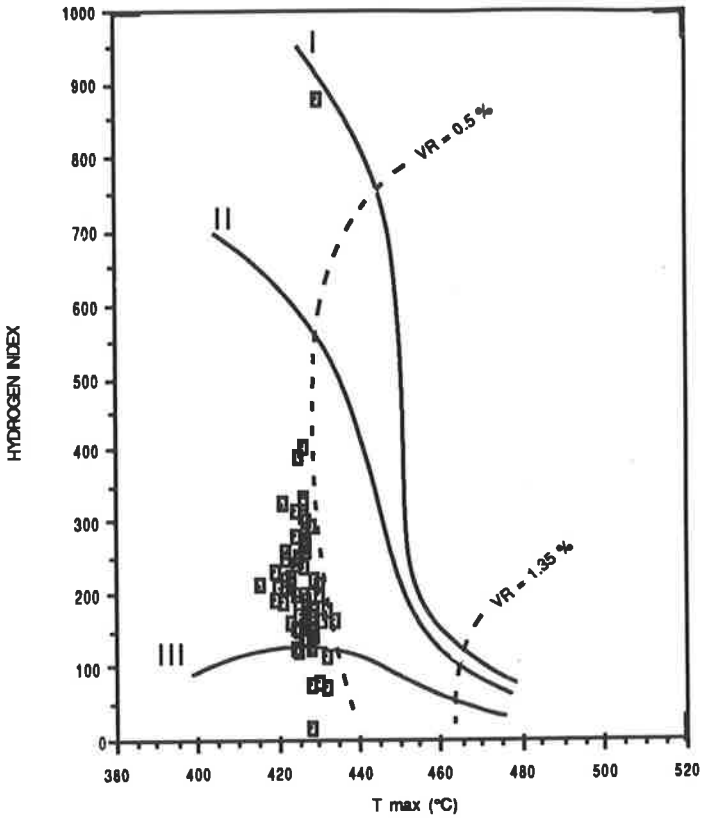

Fig. 6.2 Kerogen type and maturity in coals and carbonaceous shales from Yang Cao Gou and adjacent sub-basins

Cao Gou Basin for molecular typing of their kerogen by pyrolysis-gas chromatography (Larter and Sentfle, 1985; Powell et al., 1991).

Table 6.1 Location of samples other than Yang Cao Gou Basin coals

Sample No	Coal Basin	Age	Formation	Depositional Environment
Y5	Yingcheng	Late J	Shahezi	Delta plain
L6	Liufangzi	Early K	Yingcheng	Fluvial
J5	Jutai	Late J	Shahezi	Fluvial
X5	Xinlicheng	Late J	Shahezi	Alluvial fan

6.4 RESULTS AND DISCUSSION

6.4.1. HYDROCARBON GENERATION POTENTIAL AND ORGANIC MATTER TYPE

The total organic carbon and Rock-Eval data for coal samples from 5 sub-basins are summarized in Table 6.2. Hydrogen index and Tmax data are plotted in Figure 6.2. The majority of the samples analyzed contained at least 40% TOC and can be classified as true coals. The 35 samples with less than 40% TOC values may be better termed carbonaceous shales. According to Table 6.2, the Yang Cao Gou coals have Hydrogen Indices ranging from 16 (sample 892-71) to 879 (sample 892-101a). Most are between 71 and 300 mg HC/g TOC, which is typical for sub-bituminous humic coals. The total organic carbon content of the coals and shales varies between 13.5 and 63 %, but for most of the samples it is greater than 20% (Table 6.2). The variation of Hydrogen Index with reflectance is shown in Figure 6.3, from which it is clear that decreasing HI is only partly due to increasing thermal maturity.

Typing of organic matter is achieved using the hydrogen index and Tmax (Fig. 6.2), H/C and O/C atomic ratios (Fig. 5.7) and petrographic composition (e.g. Fig. 5.27). Type I and Type II kerogens derived from continental and marine debris, are liptinite-rich. Depending on the individual liptinite macerals present, they may have high to very high oil yields (Cook, 1982). Type III kerogen consists of mainly vitrinite which can yield moderate amounts of oil (Tissot & Welte, 1978; Durand, 1980).

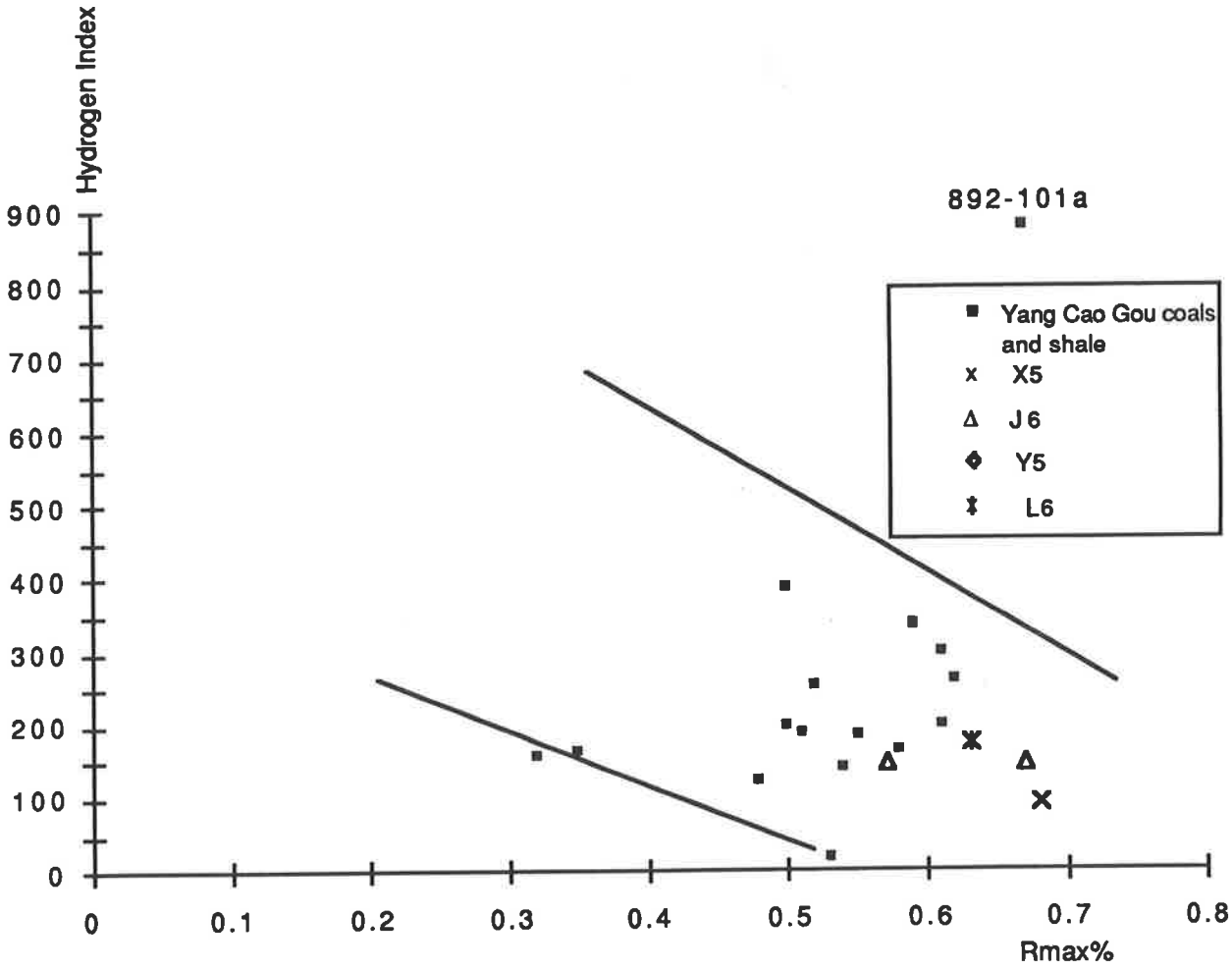

Fig. 6.3. Rmax vs Hydrogen Index as determined by Rock-Eval pyrolysis

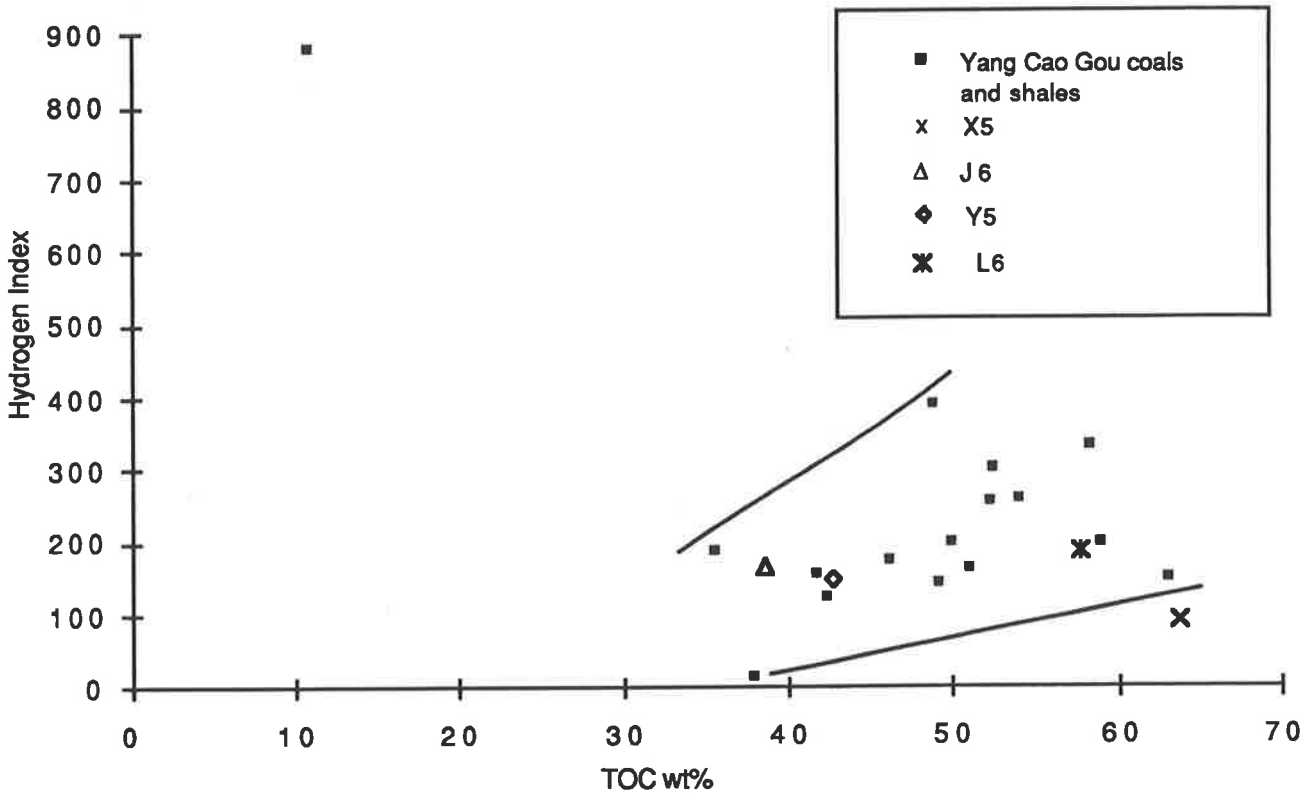

Fig. 6.4. TOC vs Hydrogen Index as determined by Rock-Eval pyrolysis

Table 6.2 Rock-Eval and TOC data from coals and carbonaceous shales in the Yang Cao Gou Basin

Sample No.	Location	Depth (m)	TOC(%)	Tmax(°C)	HI	S1	S2
892-20	CCCC	275.0	50.0	425	174	1.23	87.42
892-25	JTCC	301.0	3.2	429	222	0.05	7.08
892-39	ZK4004	980.4	22.2	415	213	1.97	47.29
892-43	ZK4004	995.0	49.6	426	269	3.77	133.77
892-44	ZK4004	996.7	48.8	425	389	3.88	190.00
892-46	ZK4004	999.6	75.9	429	201	4.95	153.06
892-47	ZK4004	1001.4	59.4	427	260	3.77	154.71
892-48	ZK4803	841.5	49.6	422	263	2.83	130.94
892-49	ZK4803	843.5	36.9	428	295	1.82	109.13
892-52	ZK4803	852.3	52.3	425	255	2.36	133.45
892-57	ZK4803	860.6	51.8	426	278	3.67	144.15
892-58	ZK4803	844.3	12.7	421	325	1.76	41.29
892-59	ZK6401	372.5	42.4	428	124	1.29	52.87
892-63	ZK6401	388.7	16.7	424	151	0.36	25.25
892-64	ZK6401	389.5	16.8	424	123	0.34	20.77
892-68	ZK912	289.0	51.0	427	164	1.71	84.09
892-69	ZK1712	576.0	54.9	422	247	2.31	135.74
892-71	ZK1712	578.9	38.0	428	16	0.07	6.13
892-72	ZK5705	920.4	32.2	430	202	1.16	65.24
892-78	ZK5705	935.7	25.0	432	177	0.99	44.25
892-81	ZK5705	948.1	22.0	428	168	1.05	37.04
892-86	ZK806	235.4	42.8	426	202	2.22	86.56
892-88a	ZK806	237.1	13.1	426	235	0.37	30.85
892-89	ZK5601	202.1	44.4	427	170	1.22	75.75
892-92	ZK5601	215.1	43.8	428	127	1.07	55.78
892-93	ZK3202	510.4	43.3	427	185	1.58	80.39
892-96	ZK3202	516.3	57.6	425	187	2.59	108.05
892-100	ZK3202	525.3	45.9	422	207	1.40	95.04
892-101a	ZK4804	1004.8	10.8	430	879	6.24	95.02
892-101	ZK4804	1008.4	45.9	426	405	5.09	186.03
892-102	ZK4804	1010.4	58.3	426	335	4.12	195.77
892-103	ZK4804	1012.4	58.5	427	272	3.45	159.62
892-107	ZK4804	1019.8	52.4	427	300	4.27	157.28
892-108	ZK4804	1021.8	56.6	426	311	5.08	176.33
892-109	ZK4804	1022.7	46.7	427	267	3.55	124.85
892-111	ZK4804	1006.0	23.0	419	233	2.33	55.54
892-112	ZK3203	349.5	49.2	427	141	0.73	69.44
892-114	ZK3203	354.2	53.2	426	142	1.32	75.56
892-115	ZK2501	276.8	43.0	427	172	1.40	74.20
892-118	ZK2501	286.6	33.8	426	152	0.85	51.52
892-119	ZK2501	315.8	41.7	426	157	1.16	65.63
892-120	ZK2501	402.6	38.7	427	159	0.38	61.52
892-123	ZK2505	51.6	42.7	423	160	1.63	68.54
892-124	ZK2505	52.9	50.2	420	207	6.22	104.28
892-126	ZK1603	308.0	37.4	428	148	0.49	55.58

Table 6.2 (continued)

Sample No.	Location	Depth (m)	TOC(%)	Tmax(oC)	HI	S1	S2
892-128	ZK1603	310.53	29.70	423.00	226.00	0.80	67.30
892-129	ZK1603	312.26	63.00	425.00	149.00	1.55	94.27
892-131	ZK1603	320.39	27.30	426.00	324.00	0.83	88.51
892-133	ZK11202	493.97	21.18	428.00	141.00	0.25	28.89
892-134	ZK11202	494.52	40.90	428.00	173.00	0.83	70.92
892-135	ZK11202	495.42	45.80	430.00	82.00	0.35	37.67
892-137	ZK11202	497.57	48.80	426.00	202.00	1.26	98.83
892-138	ZK11202	521.00	32.80	432.00	118.00	0.19	38.84
892-139	ZK3305	777.05	34.56	434.00	166.00	0.60	57.47
892-142	ZK3305	782.76	46.90	428.00	199.00	2.23	93.49
892-144	ZK3204	790.00	61.60	423.00	213.00	4.11	131.27
892-145	ZK3204		51.90	427.00	191.00	1.20	99.25
892-146	QZ908	40.76	13.44	427.00	169.00	0.35	22.76
892-148	QZ908	42.40	39.20	425.00	120.00	0.98	47.05
892-149*	QZ908		14.60	428.00	154.00	0.34	22.49
892-150	QZ6204		24.70	428.00	76.00	0.09	18.79
892-152	QZ6204		15.30	432.00	71.00	0.05	10.96
892-154	QZ7201		22.84	423.00	160.00	0.56	36.68
892-155	ZK1717	316.77	19.80	421.00	190.00	1.38	37.72
892-156	ZK1718	366.09	22.84	426.00	140.00	0.51	31.99
892-157	ZK1718	368.86	35.61	425.00	189.00	0.84	67.35
892-158*	ZK1718	396.03	22.15	422.00	219.00	1.13	48.65
892-159	ZK807	512.50	48.53	424.00	241.00	2.89	117.00
892-160	ZK807	514.45	50.63	424.00	199.00	1.37	101.19
892-161	QZ1702		24.41	420.00	113.90	1.26	27.81
892-162	ZK2501		33.09	430.00	139.47	0.57	46.15
892-163	ZK2403	524.19	13.40	429.00	145.00	0.27	19.55
892-164	ZK103	28.00	41.98	427.00	185.00	7.01	77.98
892-165	ZK4105	416.47	41.11	427.00	165.05	1.16	67.85
892-166	ZK4901	432.45	33.26	427.00	195.28	0.95	64.95
892-172	ZK106	322.70	46.60	419.00	194.00	1.78	90.59
892-183	ZK108		44.40	424.00	316.00	3.27	140.54
892-184	ZK108		54.00	424.00	260.00	2.65	140.51
892-185	ZK108		51.27	424.00	282.00	4.25	145.00
892-187	ZK108		60.10	425.00	251.00	1.63	151.02
892-188	ZK108		46.20	429.00	175.00	1.13	80.94
892-189	ZK108		36.70	430.00	211.00	0.76	77.78
892-190	ZK108		44.78	431.00	165.00	1.19	74.03
892-L6	Liufangzi		49.90	483.00	198.00	9.26	98.99
892-Y5	Yingcheng		42.70	435.00	148.00	1.03	63.30
892-J6	Jutai		38.60	438.00	166.00	0.66	64.09
892-X5	Xinlicheng		63.70	430.00	94.00	0.36	60.18

Key to symbol: CCCC=Changchun City's colliery in Yang Cao Gou basin .

JTCC= Jui Tai Colliery in Yang Cao Gou basin .

HI= hydrogen Index(milligrams per gram organic carbon

TOC= total organic carbon (%) .

Because of the alteration of its organic matter by oxidation, inertinite contains little hydrogen and hence yield little or no oil. The T_{max} values from Rock-Eval pyrolysis (Table 6.2) and the Hydrogen Index- Tmax cross plot (Fig.6.2) indicate that the majority of the samples are immature and contain Type II/III or Type III kerogen. Elemental analysis data also indicate Type III or Type IIB (see Yang, 1985) kerogen. Most samples have measured vitrinite reflectance values < 0.6% which are therefore in reasonable agreement with the maturity indicated by Rock-Eval pyrolysis (Fig. 6.2). Those with Rv max values in the range 0.61 - 0.74% (Table 5.4) appear abnormally immature in Figure 6.2.

Durand and Paratte (1983), Thompson et al. (1985) and Bertrand (1984) have concluded that the relationship between the petrographic and geochemical characteristics of coals often appears variable and is not systematic. The determination of the petrographic compositions of the coals from Yang Cao Gou coal basin shows that the vitrinite content is from 29 - 97%, liptinite content varies from 1 to 67% and inertinite content ranges from 2 to 27%. The liptinite consists mainly of sporinite, cutinite and liptodetrinite. These petrographic compositions represent typical humic kerogens (Type III or II/III). Their precursors were terrestrial plants which contributed organic matter to the shallow-water sediments of lake basin bogs or flood plains. Yang et al. (1985) found that most marginal coals in the Songliao Basin comprise Type III kerogen which is hydrogen-poor and oxygen-rich (H/C atomic ratio <0.8 and the O/C ratio >0.2). A very weak aliphatic C-H peak and strong absorption of carbon C=O and aromatic C=C bonds are characteristic features of their infrared spectra.

The Rock-Eval pyrolysis data indicate that most of the examined coal and shale samples have the ability to generate significant quantities of hydrocarbons (HC). Total generation potentials (S1 + S2) are all greater than 50mg HC/g rock, and mostly greater than 100 mg HC/g rock (Table 6.2).

Figure 6.4 shows that the hydrogen index increases with increasing TOC. Figure 6.5 is a graph of Hydrogen index vs % three maceral groups. It is

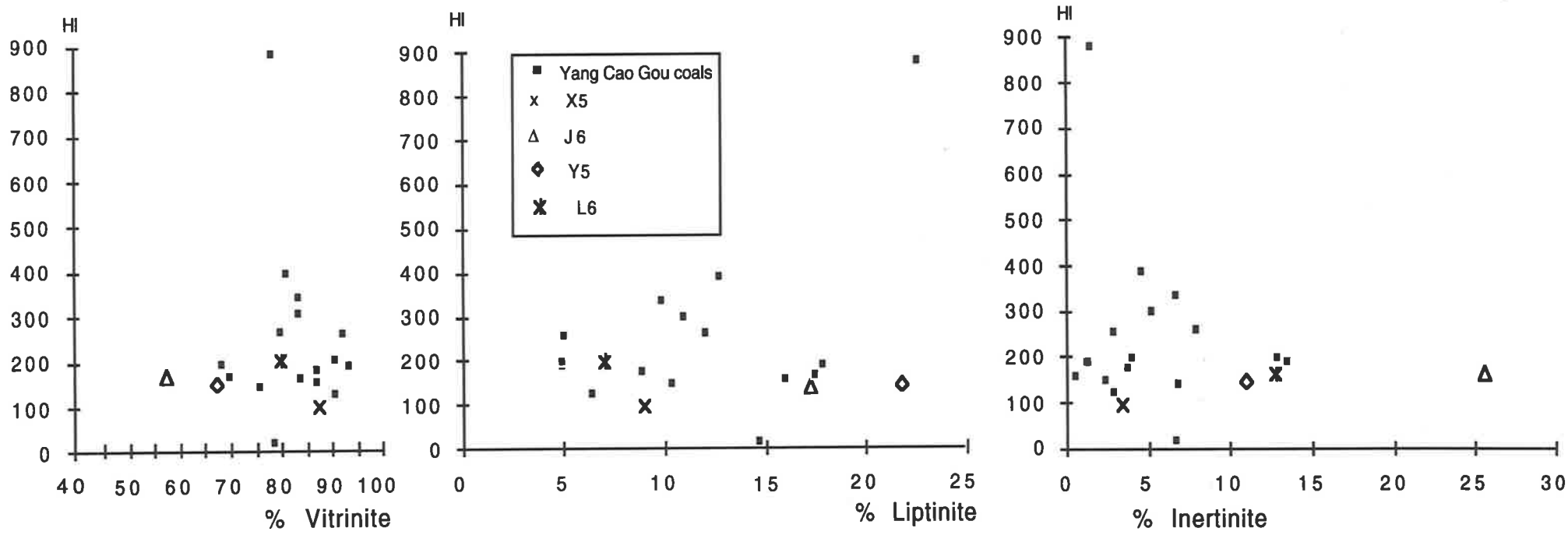

Fig. 6.5. Hydrogen Index vs three maceral groups (mmf) for samples from Songliao Basin

evident from Figures 6.5 and 6.9 that the HI of a coal is only weakly dependent on the amount of liptinite.

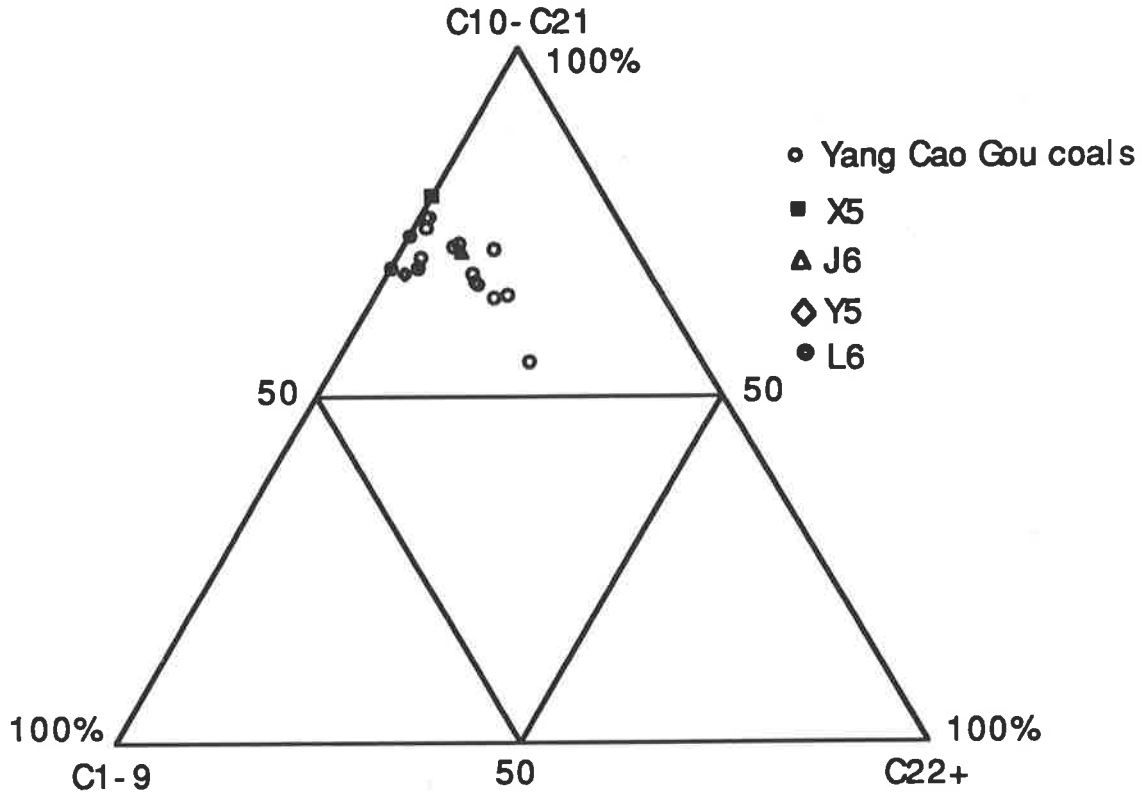

Fig. 6.6. Triangular diagram of n-alkane + n-alkene distribution of the coals from Songliao Basin

6.4.2. EXPECTED HYDROCARBON PRODUCTS

Tables 6.2 and 6.3 clearly indicate that the coals examined have great ability to generate significant quantities of hydrocarbons on the basis of their S1 + S, wax (C_{17}-C_{27} normal hydrocarbons as percent of total normal hydrocarbons), and A/K (sum of C_7 - C_{27} normal hydrocarbons) values. Figure 6.6 is a triangular diagram based on C_1-C_9, C_{10}-C_{21} and C_{22+} carbon number ranges in the pyrolysis-gas chromatography. It can be seen that the C_{22+} heavy hydrocarbons acount for less than 10% of the product, C_1-C_9 for about 10-30%, and C_{10}-C_{21} liquid intermediate hydrocarbons for more than 50%. High wax and low sulfur contents are typical characteristics of

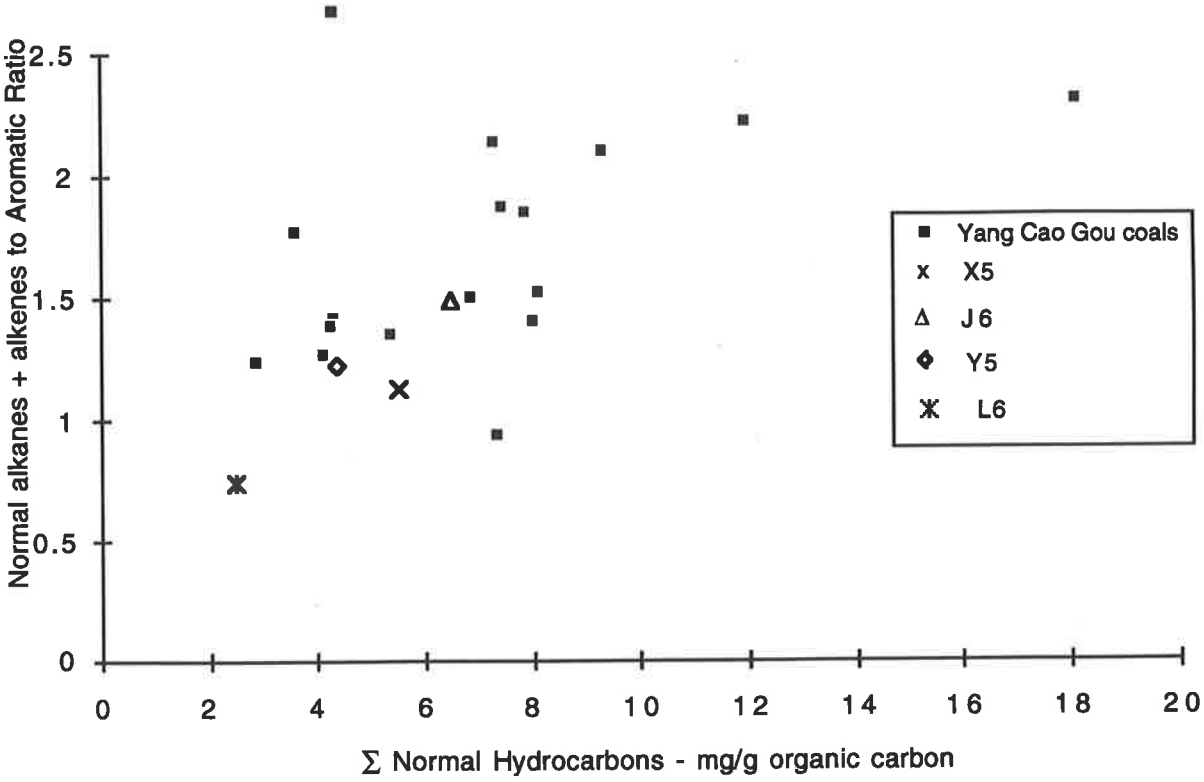

Fig. 6.7 Variation in yield of normal alkanes + alkenes with ratio of normal hydrocarbons to C6-C8 aromatics for pyrolysates of eastern Songliao Basin coals

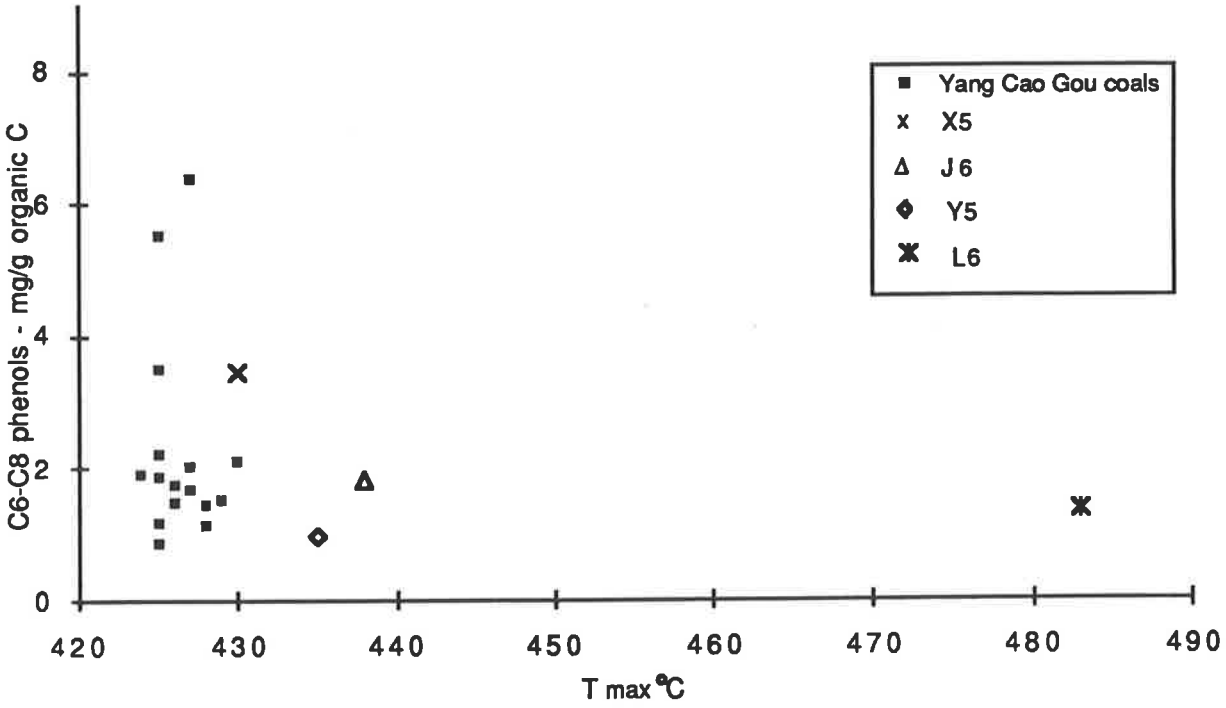

Fig. 6.8. Variation in yield of C_6 - C_8 phenols in pyrolysis-GC with maturation as measured by T max from Rock-Eval analysis for eastern Songliao Basin coals

nonmarine crude oil. The waxy, C_{22}+ n-paraffins and sulfur in the Songliao Basin oils are 15-20% and < 0.2% respectively (Yang et al., 1985).

There is a good correlation between the ratio of normal alkanes + alkenes to light aromatics and hydrocarbon yield; the ratio of normal alkanes + alkenes to light aromatics increases with rising hydrocarbon yield (Fig. 6.7). Figure 6.8 shows that the yield of phenols decreases with increasing rank. The amount of normal alkanes + alkenes obtained in pyrolysis-GC increases with rising liptinite content (Fig. 6.9). Figure 6.9 is good evidence that the liptinite content has an appreciable influence on hydrocarbon potential. There are no significant differences in the yield of normal hydrocarbons and phenolic compounds among different sub-basins near the eastern edge of the Songliao Basin (Figs. 6.8 and 6.9). Figure 6.10 is an adaptation of Larter and Sentfle's (1985) approach in which they used the yield of C_9-C_{30} normal alkanes + alkenes and hydrogen index to refine the classification of kerogen types. It shows that the yield of n-alk-1-enes/n-alkanes for the immature to marginally mature coals on the eastern edge of the Songliao Basin (mainly from Yang Cao Gou) are consistent with Larter and Sentfle's (1985) Type IIIP (phenol /paraffin) classification. These are considered to be a vitrinite-rich terrestrial kerogen that gives a high yield of normal hydrocarbons on flash pyrolysis. On the whole, coals from the Yang Cao Gou Basin yield more normal hydrocarbons upon pyrolysis than do coals from other sub-basins on the eastern edge of the Songliao Basin (Fig. 6.10).

Plots of Production Index and free hydrocarbons (S_1) obtained from Rock-Eval pyrolysis versus vitrinite reflectance (Fig. 6.11a and b) show well defined hydrocarbon generation curves. Based on this set of data, the onset of thermogenic hydrocarbon generation occurs at a PI of about 0.02 and a Rv of about 0.55% corresponding to the first liptinite coalification jump (Teichmüller,1974). In comparison to work by Espitalie et al. (1985), the PI values at maximum hydrocarbon generation are lower for Yang Cao Gou basin coals than expected for Type III kerogens in general. Espitalie et al. (1985) found that the average PI value at maximum hydrocarbon generation is about 0.25. The proportion of waxy components in the normal hydrocarbons range from 13 to 40% (Fig. 6.12). The correlation between

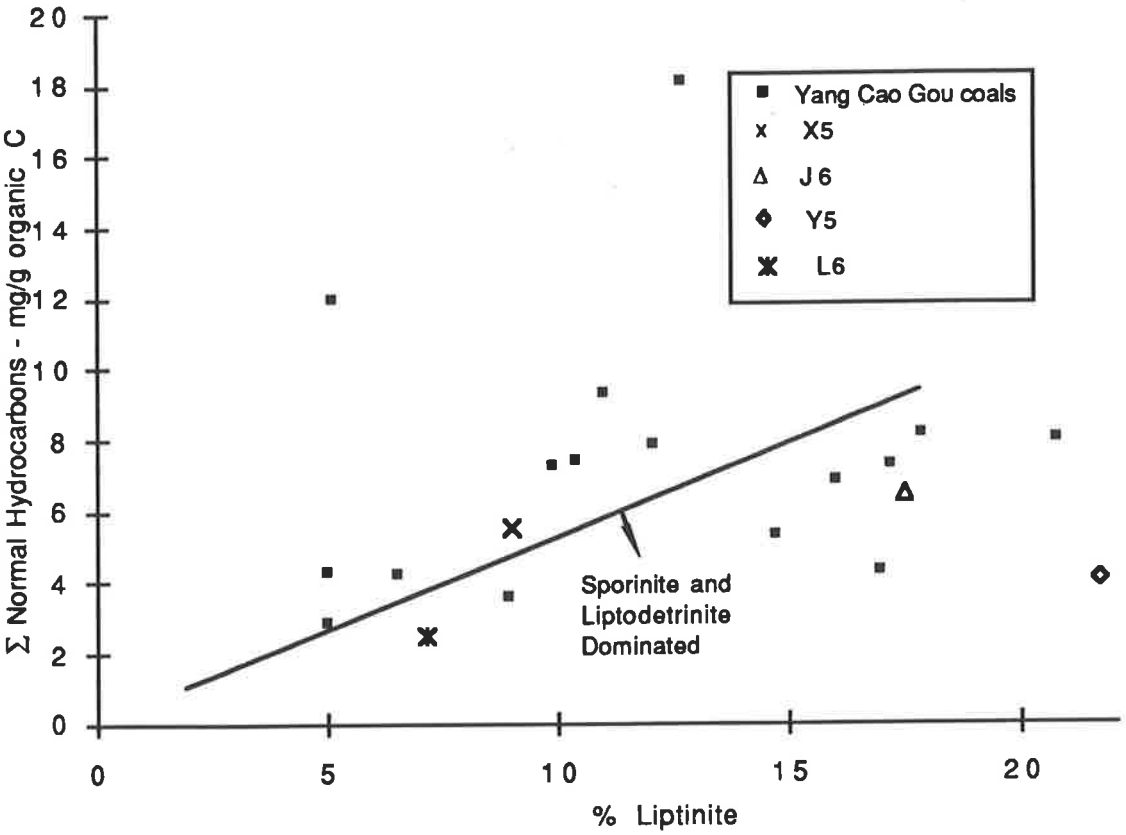

Fig. 6.9. Variation in yield and composition of normal hydrocarbons in pyrolysis-GC with proportion of liptinite for eastern Songliao Basin coals

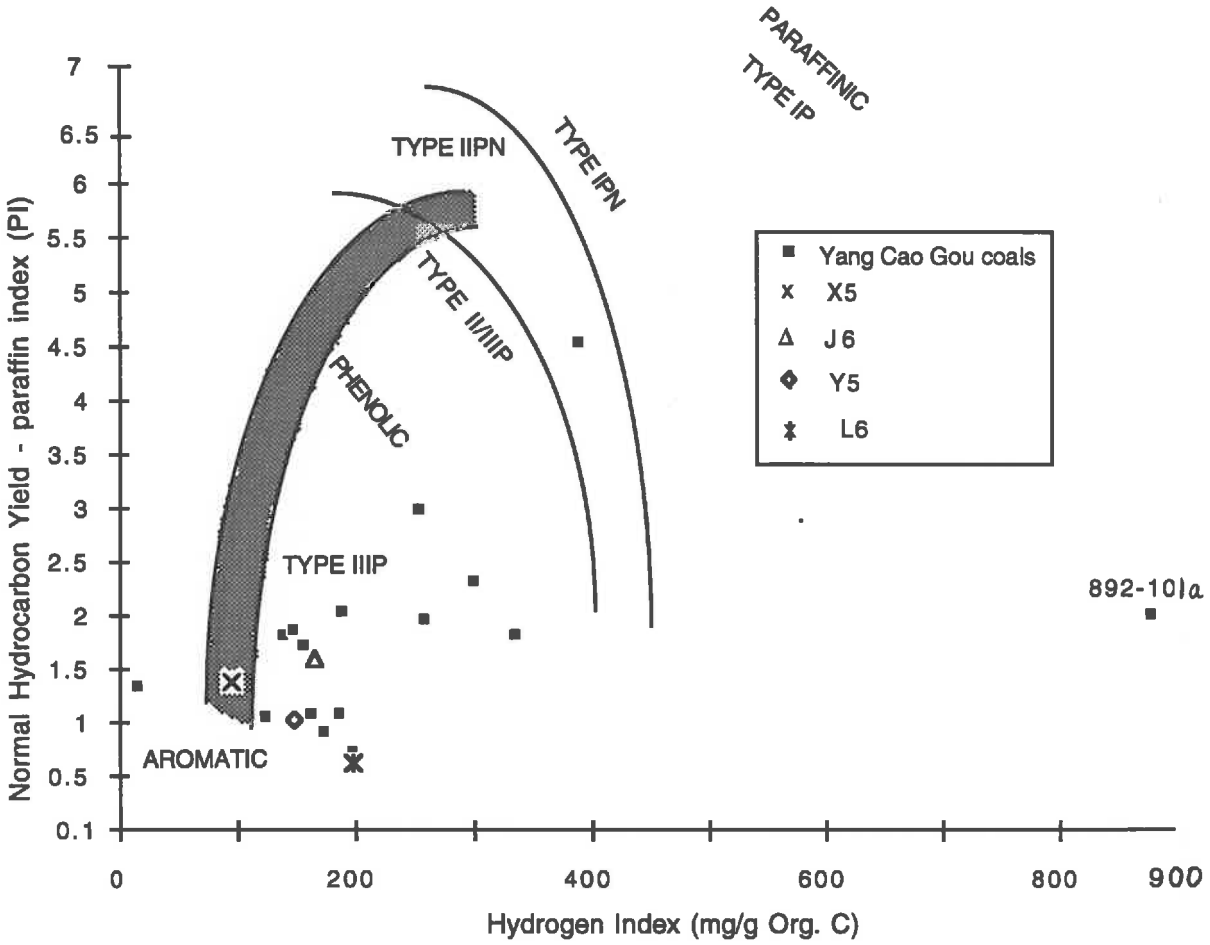

Fig. 6.10. Relationship between Paraffin Index and Hydrogen Index for Songliao Basin coals (after Larter and Sentfle, 1985). Paraffin index = 0.25% xΣ(C_7 - C_{32} n-alkanes + n-alkenes mg/g TOC).

proportion of waxy component and liptinite content is very poor (Fig. 6.12). Figure 6.13 indicates a linear relationship between free hydrocarbons and hydrogen index in the Yang Cao Gou coals and shales.

Figures 6.14, 6.15 and 6.16 show some typical pyrolysis-GC fraces for Yang Cao Gou coals and for coals and carbonaceous shale from Xinlicheng, Liutia and Yingcheng Basins. Fig. 6.15 illustrates the pyrogram for sample 892-101a, a carbonaceous shale which has the highest Hydrogen Index of 879. It shows that the hydrocarbon composition is dominated by aromatic and phenols in the less than nC_{19} portion of the chromatogram. The presence of several large peaks identified as methyl, dimethyl and trimethyl phenols, have been derived from lignins (Chaffee et al., 1986). Figure 6.15 for sample 892-119 of Yang Cao Gou coal indicates that the low molecular weight normal hydrocarbons are dominant. Figure 6.16 for sample 892-Y5 of the Yingcheng coal shows a dominanance of alkane-alkene doublets extending from nC_7 to nC_{27}, and a dominance of low molecular weight aromatics and phenols over normal hydrocarbons. The carbon number distribution of n-alkanes plus n-alkenes in the kerogen pyrolysate can be subdivided into three groups: C_1 - C_8, C_9 - C_{14}, and C_{15+}. Overall the products generated from all samples in this study appear to be dominantly in the less than nC_{15} fraction and the pyrolysates of coals appear to be much richer in aromatic hydrocarbons than the oils believed to be derived. from them. Thomas (1982) stated that most of the oils derived from coal are paraffinic. The major components of the kerogen pyrolysates are C_1 - C_8 light hydrocarbons, reflecting the essential structure of Type III kerogen, because the short chain alkanes were major substituents on the condensed aromatic rings in the kerogen structure.

6.4.3. SUMMARY AND CONCLUSION

There is no doubt that terrestrial plants contribute to the formation of both coal and petroleum, but humic coals in particular probably can not generate oil on a large scale after burial. In most cases, coals which are associated with lacustrine petroleum, were formed in sub-basins at the margin of the basin (coals in the Songliao Basin are a good example). In

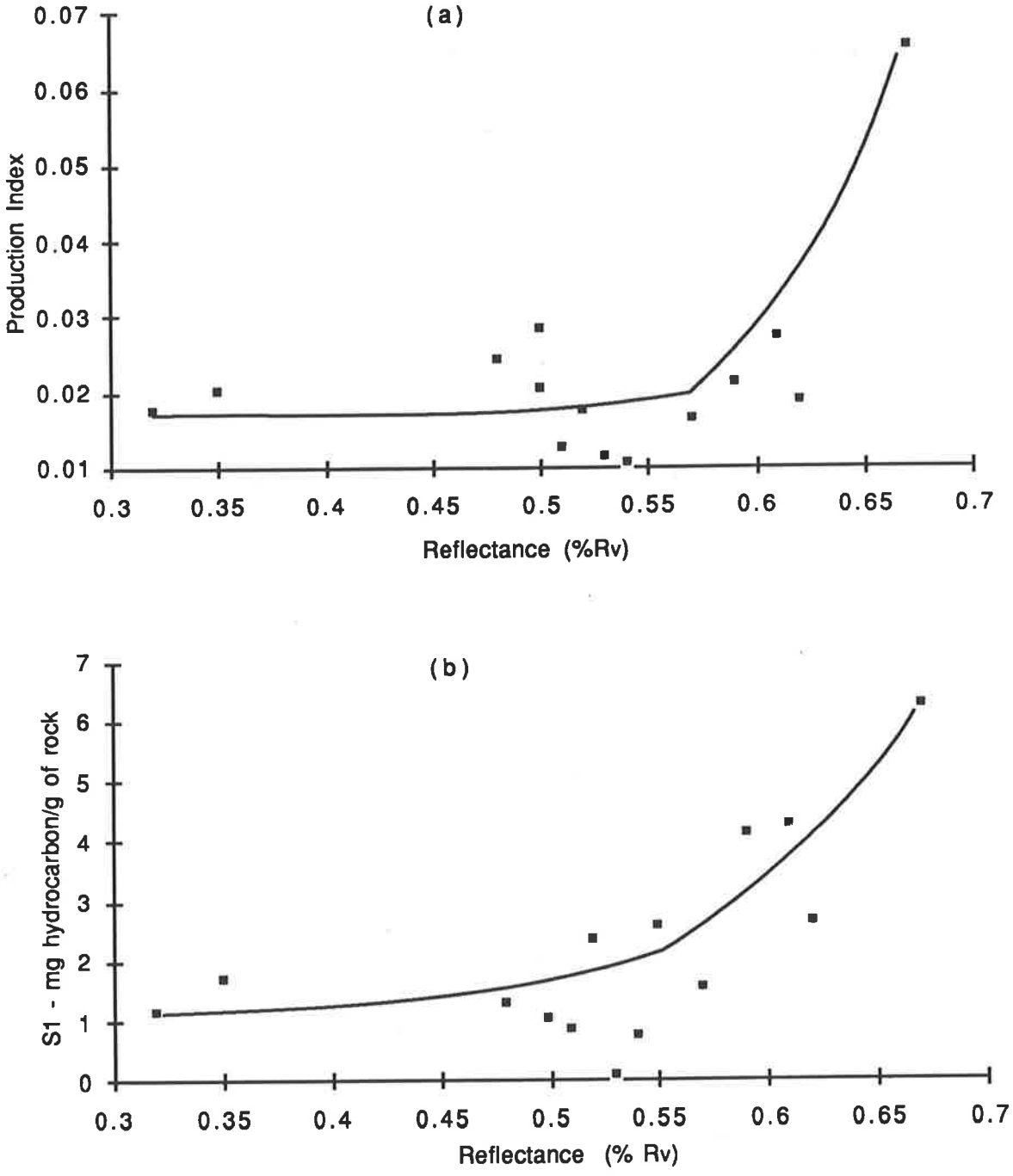

Fig. 6.11. Plot of vitrinite reflectance vs (a) production index; (b) S1 value for the Yang Cao Gou coals

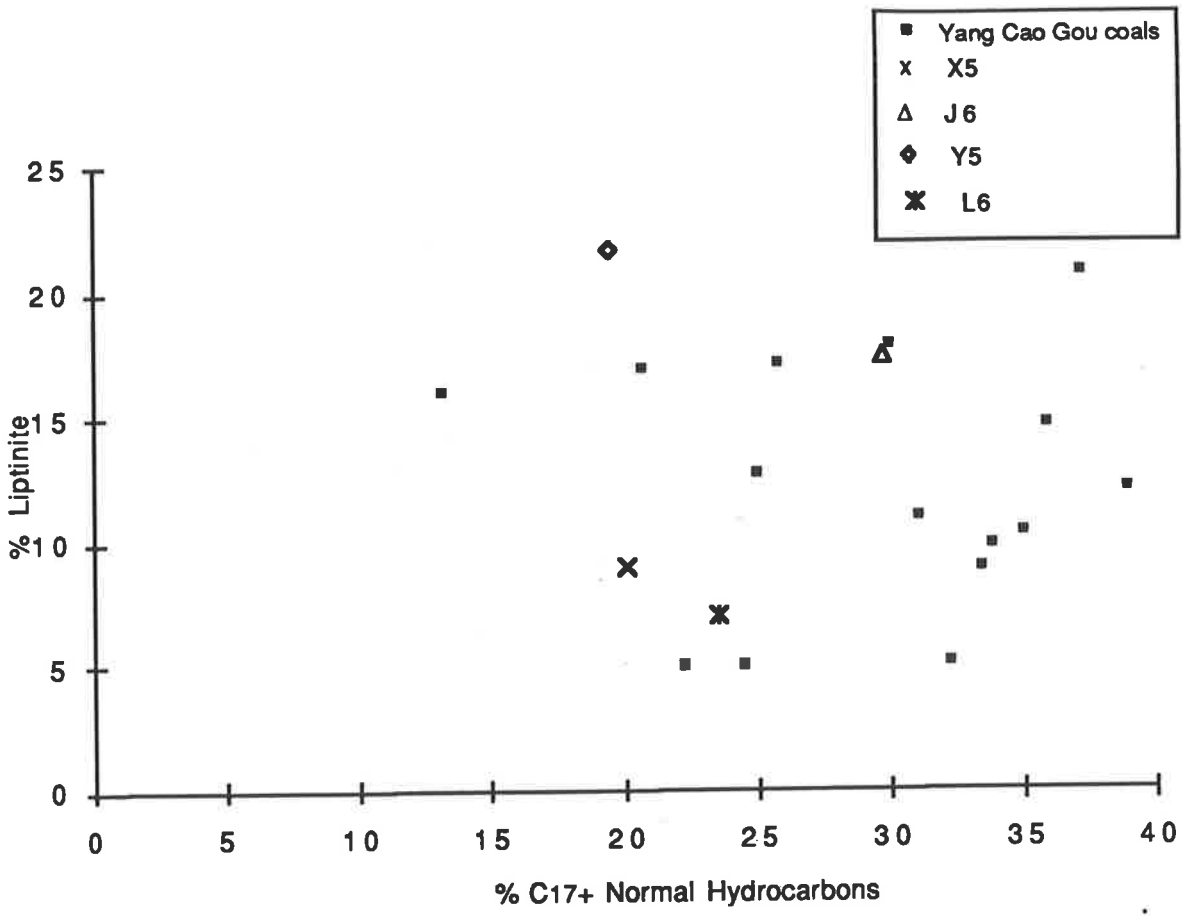

Fig. 6.12. Variation in composition of Normal Hydrocarbons with proportion of Liptinite in Songliao Basin coals

Table 6.3 Petrographic and geochemical data from Songliao basin coals

Sample No.	TOC (%)	Rmax	Petrographic composition(%)			Rock-Eval		Pyrolysis-GC			
			V	L	I	Tmax (ºC)	HI (mg/g)	Alk (mg/g)	Wax (%)	Alk/Arom	ph (mg/g)
892-96a	57.6	0.55	93.4	5	1.4	425	187	4.31	24.73	1.42	1.15
892-71	38	0.53	78.6	14.7	6.7	428	16	5.27	35.22	1.35	1.11
892-184	54	0.62	79.9	12.1	8	424	260	7.73	38.29	1.85	1.89
892-101a	10.8	0.67	78.3	20.8	1.6	430	879	8.01	37.22	1.41	2.08
892-102	58.3	0.59	83.4	9.9	6.7	426	335	7.27	33.8	2.14	1.75
892-107	52.4	0.61	83.7	11	5.3	427	300	9.32	31.12	2.1	2.03
892-112	49.2	0.54	75.9	17.2	6.9	427	141	7.32	25.84	0.94	6.34
892-119	41.7	0.32	83.9	16	0.6	426	157	6.88	13.29	1.5	1.46
892-129a	63	0.57	87.2	10.4	2.4	425	149	7.46	34.92	1.87	1.85
892-157	35.61	0.51	68.6	17.9	13.5	425	189	8.12	29.99	1.52	2.21
892-188	46.2	0.63	87.3	8.9	3.8	429	175	3.62	33.53	1.77	1.5
892-52	52.3	0.52	92.2	5.1	2.9	425	255	11.96	32.27	2.22	3.5
892-59	42.4	0.48	90.7	6.5	2.9	428	124	4.17	39.22	1.38	1.44
892-68	51	0.35	70.2	17	12.8	427	164	4.35	20.68	1.22	1.65
892-44	48.8	0.5	81.2	12.7	4.7	425	389	18.11	25.03	2.31	5.5
892-83	59	0.5	90.9	5	4.1	425	198	2.87	22.35	1.23	0.87
892-L6	49.9	0.61	80	7.1	12.9	483	198	2.5	23.8	0.74	1.34
892-Y5	42.7	0.67	67.4	21.7	10.9	435	148	4.11	19.48	1.27	0.99
892-J6	38.6	0.58	57.1	17.5	25.4	438	166	6.46	29.74	1.49	1.81
892-X5	63.7	0.68	87.6	9	3.4	430	94.47	5.52	20.14	1.13	3.45

TOC=total organic carbon; Rmax=mean maximum vitrinite reflectance; V= vitrinite; L=liptinite; I=inertinite; HI=Hydrogen Index; mg/g=milligrams per gram organic carbon; Alk=sum of C7-C27 normal hydrocarbons; Wax=C17-C27 normal hydrocarbons as a percent of total normal hydrocarbons; Alk/arom=ratio of normal hydrocarbons to C7-C9 aromatics; Ph=C6-C8 phenols

that case, peat swamps were buried while the centre of the basin, the site of source rock deposition, was still covered by water and receiving sediments. That is to say, the major petroleum source beds are geographically separated from the coals. Most humic coals consist mainly of vitrinite, which is unlikely to generate great amounts of oil because of its inapproprate chemical composition. The bulk of the vitrinite, which contains mainly cellulose and lignin, has little capacity to generate oil, although it can yield natural gas. Smyth et al. (1984) and Cook et al. (1985) suggested that the oil generation potential of vitrinite is about one tenth of that liptinite. Tissot (1984) put the figure at three or four times less than liptinite.

Boghead and cannel coals differ from nomal humic coals. In these materials, the coal-like material is better defined as oil shale. 'Boghead/cannel coals', contain mainly Type II kerogens (mostly spores). They are hydrogen-rich and have high concentration of alkanes and fatty acids (Waples, 1981). Bustin (1983) claimed that cannel coal deposits are normally limited in area to less than 50 km^2 and boghead coals are less than 20 km^2, so that amount of petroleum generated from these 'coals' is likely to be quite small.

Accumulations of petroleum are, in many cases, associated with coal. This is because at the time that both coal and petroleum source beds formed, persistently humid climates prevailed. These conditions were favourable for plant growth which contributed to both coal and petroleum source beds. Most petroleum occurrences originated from non-coaly source rocks. However, there are a few notable exceptions where mature organic-rich marine or lacustrine source rocks are lacking, and where coals are considered as the primary source rocks (e.g. Gippsland Basin in Australia; Ardjuna Basin, central Sumatra and Malacca Strait in Indonesia). However, we should not conclude that coals can generate large amounts of petroleum, as it is possible non-coaly source rocks may have been eroded. It is also possible that source rocks may be located in deeper horizons which have not been penetrated. This may be the reason why the biomarker composition of the crude oil from central Sumatra Basin and coal extracts differ (MacGregor & Mackenzie, 1986). Smith et al. (1977) found that the isotopic composition of coal extracts in Gippsland Basin are inconsistent

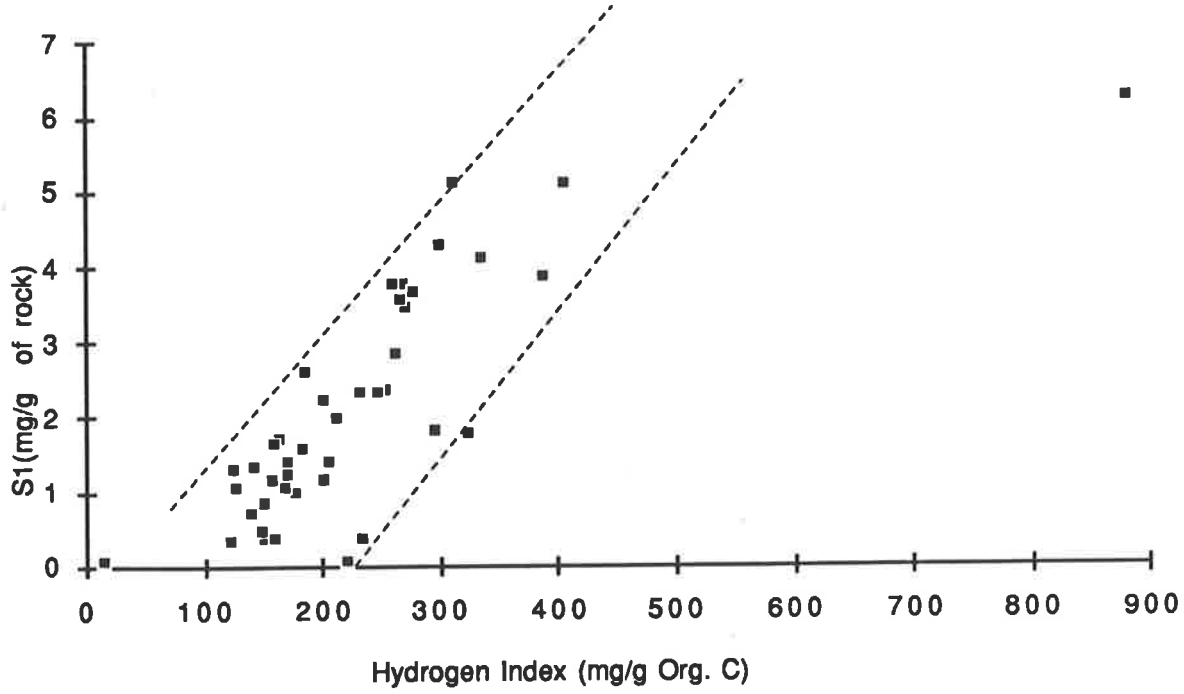

Fig. 6.13. Relationship between free (S1) hydrocarbons and the hydrogen index using conventional Rock-Eval pyrolysis data for eastern edge Songliao Basin coals.

with these coals acting as the source of petroleum, but Brooks (1970) suggested that shales associated with the coals may be the source rocks for the Gippsland Basin oil and gas. If large amounts of petroleum were generated by coal then, between the coal and reservoir rock, traces of petroleum should be found along migration pathways.

At any rate, estimates of the oil-source potential of coal in the Malacca Strait made by Longley et al. (1990), are doubtful because they used S_1+S_2 as one of the assessment parameters. They claimed that " the total generation potentials S_1+S_2 values were all greater than 50mg HC/g rock, reaching maximum values in excess of 600 mg HC/g rock in Australian torbanite." As concluded in chapter 7, most coals have very high (S_1+S_2) and TOC values, and these parameters are not suitable for determining the oil potential of coal. In the Songliao Basin, where large amounts of lacustrine petroleum have been discovered, almost all the coals which surround the Songliao Basin contain Type III kerogen; there is no evidence that coals contributed to petroleum contained in the central basin. The results of the present study support this point. Most of the analysed coal samples have HI values between 93 and 321 mg HC/g C_{org}, vitrinite reflectance below 0.6%, TOC larger than 50% and have high (S_1+S_2) values (Tables 6.2 and 6.3). Clearly, for determination of the oil potential of coal and estimation of oil reserves in basins where coal is the primary source rock, results from the Rock-Eval pyrolysis method are not conclusive.

The vast majority of the crude oils in the Songliao Basin were generated not from the surrounding marginal coal measures, but from the deep water lacustrine black shale beds of Members Nen1, Qin1 and Qin2 (Cheng, 1982; Yang et al., 1980, 1985; Ma, 1985). These contain Type1 and Type II kerogens that are dominated by degraded terrestrial organic matter with a varying contribution from bacterial and algal remains. Although a high wax content is the characteristic feature of most non-marine oils, including Chinese ones (Hedberg, 1968; Powell and McKirdy, 1973), the question remains: whether the wax content is due to land-plant lipids or to a substantial freshwater algal contribution (McKirdy et al., 1986). Waxy oils are commonly believed to be associated with coals or terrestrial material. Based research on the Songliao Basin, Yang et al.(1985) concluded that following conditions were most favorable for non-marine petroleum

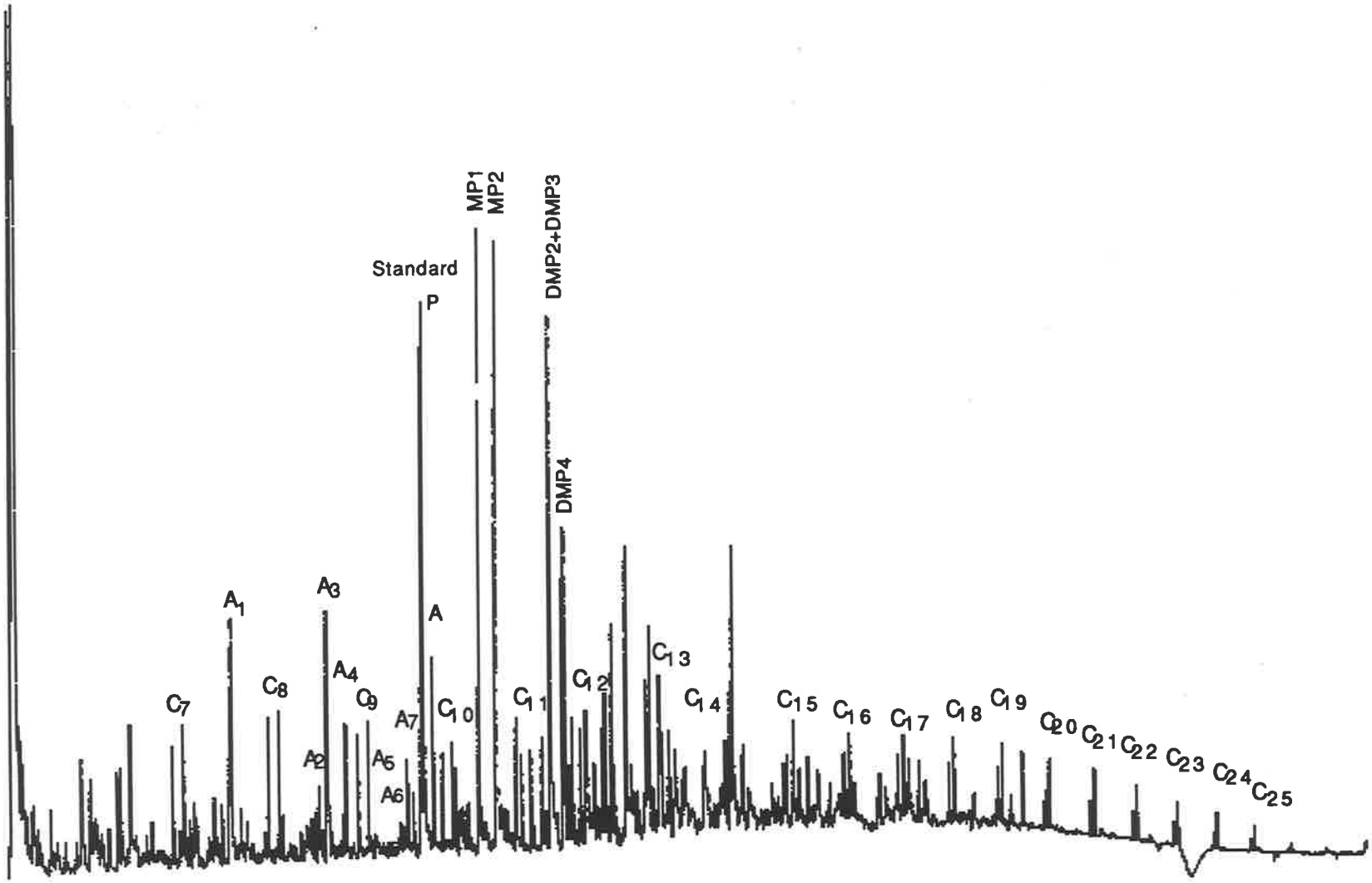

Figure 6.14 Pyrolysis gas chromatogram of sample 892-101A (V=78.3%, L=20.8%, I=1.6%)

Key: A = aromatic hydrocarbon, P = phenol, ; numbers refer to carbon numbers of n-alkene/ n-alkane doublets.
MP1=MPHENOL1, MP2=MPHENOL2, DMP2=DMPHENOL1, DMP3=DMPHENOL3, DMP4=DMPHENOL4.

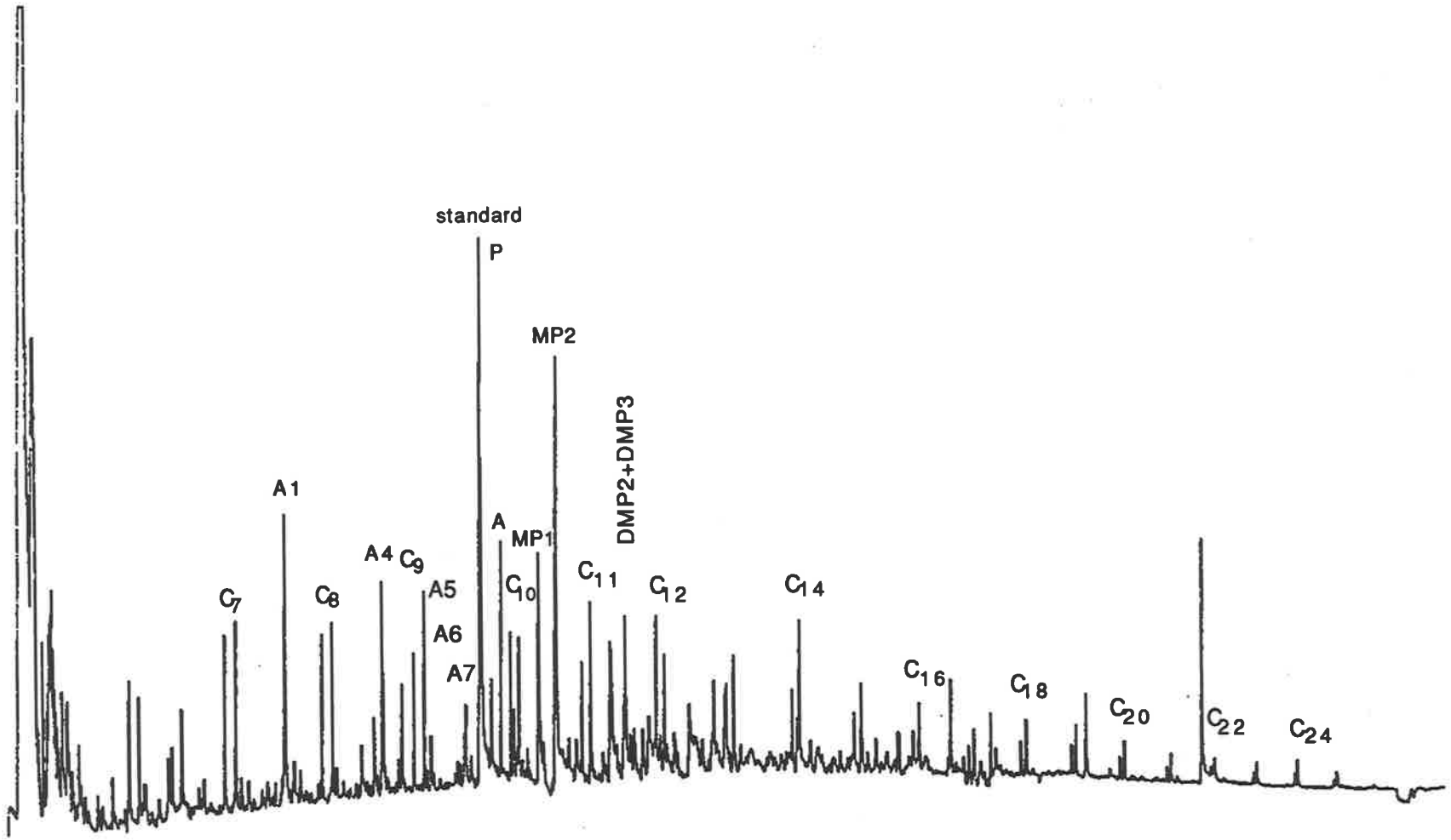

Fig. 6.15 Pyrolysis gas chromatogram of sample 892-119 (V=83.4%, L=16.0%, I=0.6%)

Key: A = aromatic hydrocarbon, P = phenol, ; numbers refer to carbon numbers of n-alkene/ n-alkane doublets.

MP1=MPHENOL1, MP2=MPHENOL2, DMP2=DMPHENOL1, DMP3=DMPHENOL3, DMP4=DMPHENOL4.

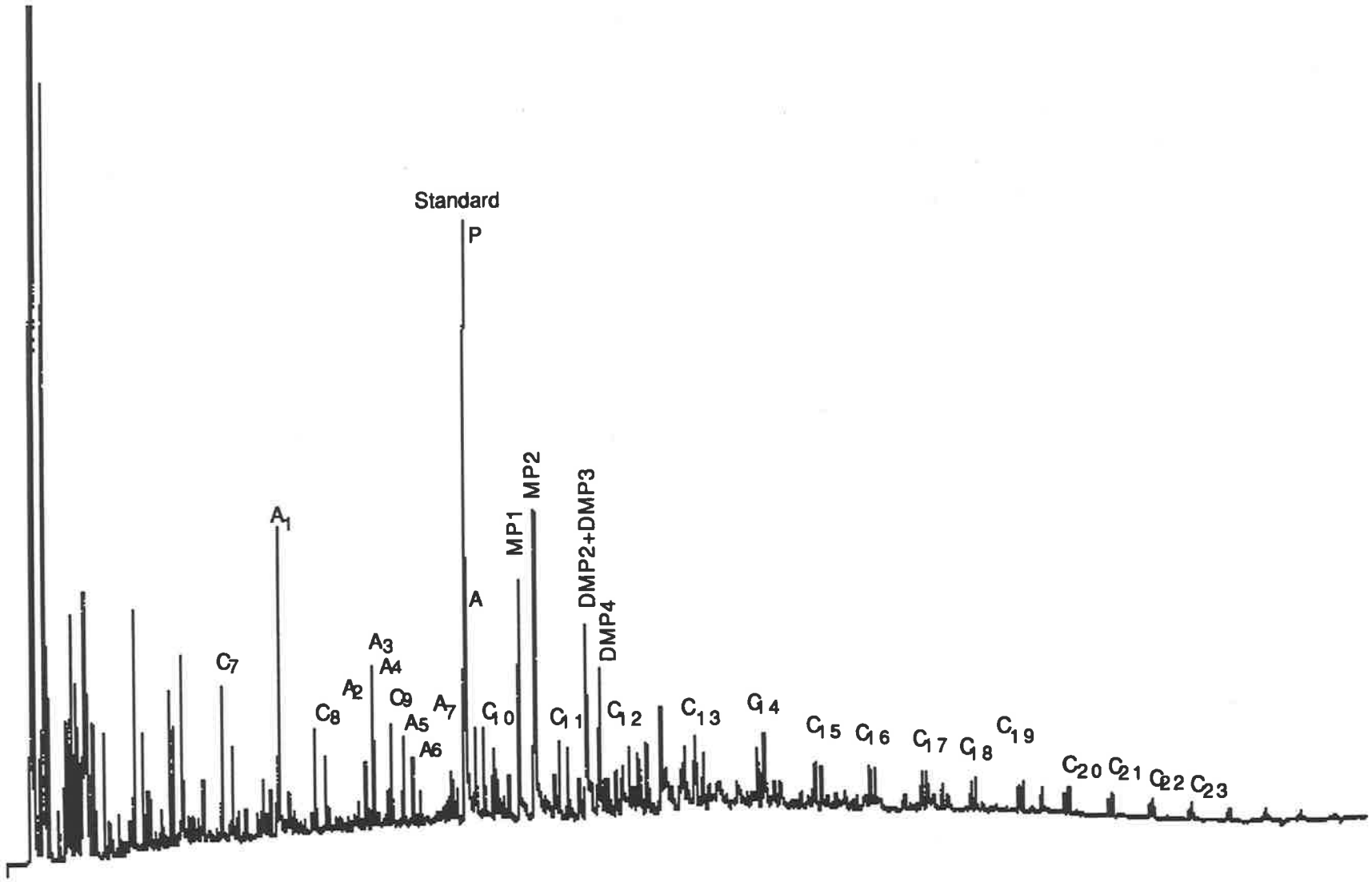

Figure 6.16 Pyrolysis gas chromatogram of sample 892-Y5 (V=67.4%, L=21.7%, I=10.9%)

Key: A = aromatic hydrocarbon, P = phenol, ; numbers refer to carbon numbers of n-alkene/ n-alkane doublets.
MP1=MPHENOL1, MP2=MPHENOL2, DMP2=DMPHENOL1, DMP3=DMPHENOL3, DMP4=DMPHENOL4.

formation: 1. A large deep eutrophic lake; 2. A long-standing structural depression; 3. Rapid lake transgression and starved clastic deposition forming organic-rich source beds with a high transformation ratio and a high potential for petroleum genesis; and 4. The focussing effect of high geothermal flux in bowl-like closed basins. None of the coal measures around Songliao Basin meet the above conditions. The marginal coals have high vitrinite content, and alginite is less concentrated than in the depocentre. Towards the center of the lake, Yang et al. (1985) found that algae were the dominant source of organic input to the sediments.

The Yang Cao Gou Basin coals have lower vitrinite reflectance and lower Tmax than late Jurassic Yingcheng and Xinlicheng coals. The former coals have not undergone sufficient maturation to be effective source beds for petroleum hydrocarbons.

The oil-source potential of coal is best determined by a combination of petrographic, elemental and pyrolysis-GC analysis because the parameters commonly used to define the source rock potential (such as Hydrogen Index, TOC, S_1+S_2 and Tmax) are only partially suitable for coal. Indeed, they are sometimes contradictory. From Rock-Eval pyrolysis analysis, all of the samples have relatively very small S1 and large S2 values. The Yang Cao Gou coals are Type III on the basis of H/C and O/C ratios and immature on the evidence of vitrinite reflectance data. Type III kerogen is considered to be 'gas ' prone and to have low potential for oil. The same coals have very high S_1+S_2 values (some of them > 150) and TOC values (mostly > 45%, Table 6.1). But if S1 + S2 > 6 and TOC > 4%, excellent source rocks are indicated (Table 3.3). These two parameters thus give conflicting results when used to determine oil-source potential of coal. So the parameters for source rock evaluation of coal need reconsideration, and a new method to estimate their oil potential is much needed. The assessment of source rock potential for coals cannot be based just on bulk geochemical techniques or petrographic techniques alone (Powell et al., 1991).

In the Songliao Basin, Yang et al., (1985) found that the Type I kerogen consists mainly of lipids, and has a liptinite content >90% (atomic H/C ratio > 1.4 and O/C < 0.1). Type IIA kerogen with a atomic H/C ratio of 0.8-

1.0 and O/C ratio of 0.15-0.2 has a liptinite content ranging from 50-90%. Type III kerogen with a H/C atomic ratio of less than 0.8 and O/C ratio of larger than 0.2 contains up to 90% vitrinite. Hunt (1991) stated that oil, gas and coal has about same carbon content, around 80%. But the hydrogen content of oil and gas is 2 to 5 times higher than that of coal. So the higher the hydrogen content of a coal, the greater its ability to generate oil and gas. Lewan (1983) has used laboratory experiments to demonstrate the importance of hydrogen content for oil generation. He pyrolyzed 13 coal samples under hydrous conditions and obtained oil yields ranging from 5 to 16 wt% on a mineral-free basis. The yield of high wax oil increased with an increase in the hydrogen content of the coal. The liptinites being hydrogen-rich, were found to be the major control on the potential of a coal to generate liquid hydrocarbons. Cook (1987) concluded that liptinite has up to 12 times the generating potential of inertinite. Type III coals do not respond to pyrolysis in the same way as dispersed Type III OM (Peters, 1986). So the results from Rock-Eval pyrolysis overestimate the liquid-hydrocarbon generative potential of the coals.

CHAPTER 7 CONCLUSIONS

(1) Maceral characteristics

The present study suggests that the coals in the Yang Cao Gou Basin have distinctive petrographic characteristics. Vitrinite is by far the most important maceral throughout the basin. It occurs as bands of telovitrinite and detrovitrinite. Liptinite comprises mainly sporinite, cutinite and liptodetrinite. Inertinite consists of fusinite, semifusinite and inertodetrinite. Macrinite and micrinite are rare.

The coal-bearing sediments of the Yingcheng Formation were deposited in high energy fluvial, and deltaic to low energy lacustrine environments. Group II coals, which account for about 98% of the resources in the basin, were deposited in shallow lake environments, and are characterized by high telovitrinite, moderate liptinite and relatively low inertinite contents.

(2) Coal facies

Coals and shale partings contain the same Type III and Type II/III organic matter. The organic matter is derived from higher plants with significant contributions of bacteria and a minor input of algae. The Group II coals were deposited under stable reducing conditions, whereas the Group I and Lower coals were laid down in a partly oxidising environment.

The Group II coals formed from forest swamp vegetation deposited in a lacustrine environment. The Group I coals formed in woody peat facies of delta environments, whereas the Lower coals were formed in interlobe depressions of alluvial fan environments.

Each facies can be clearly grouped into 3 zones which correspond to variations in depositional environment, or the different water regimes.

On the basis of their petrographic compositions, Group II coals can clearly be divided into 3 zones. Zone 1 represents the low energy, stagnant water, distal lacustrine environment. The most abundant maceral in zone 1 is telocollinite. Coals in zone 1 also contain slightly more inertinite than those in zone 2 and zone 3.

Zone 2, with limited clastic influx, represents a transitional area between stagnant and open water areas. The highest liptinite content occurs in this zone.

Coals in Zone 3 represent the marginal area of the basin with intermittent high energy conditions and the highest detrovitrinite contents.

(3) Origin of the coals

The Group II coals were formed *in situ* (i.g. *autochthonous*). The Group I coals are *hypautochthonous* , whereas the Lower coals are *allochthonous.*

(4) Characteristics of coal accumulation

Coal deposits along the eastern margin of the Songliao Basin occur in three contrasting palaeoenvironments. The areas in front of and between alluvial fans, on fan delta plains and on lake shores are the most favourable areas for coal accumulation.

Lower Coals were deposited in the inter-lobe depressions of alluvial fans under an unstable water regime. They are thin and of limited areal extent. High contents of detrovitrinite and structured vitrinite are petrographic features of this coal.

Group I coals formed on fan delta plains and are relatively persistent. They contain more telovitrinite and liptinite than the Lower coals. After volcanic eruptions, the basin floor subsided rapidly, causing lakes to form within the basin and the development of marginal alluvial fans. These alluvial fan sediments partially infilled the lake to form fan delta deposits. Peat swamps formed on abandoned delta plains.

Group II coals are the most important resource in the basin, and were deposited in lake shore areas. After the Group I coals formed, fluvial and shallow lacustrine sediments were deposited, then the lake shallowed and was infilled. Peat swamps formed and were covered by very thick shallow-lake mudstones. This environment was the site for formation of the major coal deposits in the Yang Cao Gou basin.

Structurally, coal depocentres and thick coal seams are found on palaeo-highs and in basement depressions.

(5) Coal rank

Most of the coal samples are between subbituminous and high volatile bituminous rank.

(6) Organic matter type

Most of the coals and shales in Yang Cao Gou Basin contain Type III kerogen. In some the kerogen is of Type II/III composition.

(7) Hydrocarbon generation potential

Most of the organic matter is of land plant origin and gas-prone (Type III). In places, local concentrations of liptinite or bacterially degraded plant tissue give rise to better quality Type II-III kerogen with enhanced oil source potential. Rock-Eval and elemental analyses both suggest that the Yang Cao Gou coals have the potential to generate liquid hydrocarbons. This may be caused by abundant liptinite macerals. However, the ability of the coals to generate oil is not supported by the amounts of hydrocarbons that can be extracted from the coals. These coals are not mature enough to have generated hydrocarbons. The coals still have most of their hydrocarbon potential remaining, as is evidenced by the high HI values of some samples.

The organic geochemical trends in the Yang Cao Gou coals are controlled primarily by thermal maturity and secondarily by biodegradation effects.

Evidence that maturation controlled effects on the chemistry of the coal are as follows:

(1) hydrogen indices as high as 879, decrease systematically with increasing thermal maturation;

(2) production indices show little change until the onset of hydrocarbon generation at about 0.55% R_v, corresponding to the first coalification jump of liptinite (Teichmüller, 1974).

REFERENCES

Standards Association of Australia, 1981. Australia Standard AS 2486.

Standards Association of Australia, 1984. Australia Standard AS 2646.6

Standards Association of Australia, 1986. Australia Standard AS 2856.

Bertrand, P., 1984. Geochemical and petrographic characterization of humic coals considered as possiple oil source rocks. Organic Geochemistry, 6, 481-488.

Brooks, J. D., 1970. The use of coals as indicators of the occurrence of oil and coal. Aust. Pet. Explor. Assoc. J., 10, 35-40.

Bustin, R. M., 1980. Oxidation characteristics of some sheared coal seams of the Mist Mountain Formation, southeastern Canadian Cordillera. Geol. Surv. of Can., 80, 249-254.

Bustin, R. M., 1983. Heating during thrust faulting in the Rocky Mountains: friction or fiction? Tectonophysics, 95, 309-328.

Brown, H. R., Cook, A. C. and Taylor, G. H., 1964. Variation in the properties of vitrinite in isometamorphic coal. Fuel, 42, 111-124.

Cameron, A. R., 1978. Megascopic description of coal with particular reference to seams in southern Illinois; in Dutcher, R. R., editor, Field Description of Coal; ASTM Special Technical Publication 661, Philadelphia, Pennsylvania, 9-32.

Casagrande, D. J., Siefert, K., Berschinsky, C. and Sutton, N., 1977. Sulphur in peat forming systems of the Okefenokee Swamp and Florida Everglades: origins of sulphur in coal; Geochimica et Cosmochimica Acta, 41, 161-167.

Chaffee, A., Hoover, D. S., Johns, R. B. and Schweighardt, F. K., 1986. Boilogical markers extractable from coal. In: Biological Markers in the sedimentary record (edited by Johns, R. B.), Elsevier, Amsterdam, 311-345.

Chen, J., 1987. A futher study on coal formation model of the late Permian coal measures in South China. The Permo-Carbonifieous stratigraphy and geology of China (in Chinese).

Chen, J. and Li, Y., 1983. Coal formation and algal swamp model of the upper Permian in Guangxi Province (in Chinese).

Coal Geology Section of Wuhan College of Geology, 1979. Coal Geology, 2 (in Chinese). The Geological Publishing House, Beijing, 280pp.

Cohen, A. D. and Spackman, W., 1980. Phytogenic organic sediments and sedimentary environments in the Everglades-mangrove complex of Florida- Part III, The alteration of plant material in peat and origin of coal macerals; Palaeontographica, Abt. B. 172, 125-149.

Cook, A. C., 1979a. Organic petrology of samples from six wells from the Otway Basin. Department of Minerals and Energy, Victoria, Oil and Gas Division, Open File Report (unpubl).

Cook, A. C., 1986. The nature and significance of the organic facies in the Eromanga Basin. Geol. Soc. Aust., Special Publications, 12, 203-219.

Cook, A. C., 1987. Source potencial and maturation of hydrocarbon source rocks in Indonesian sedimentary basins. 6th regional Congress on Geology, Mineral and Hydrocarbon Resources of Southeast Asia, GEOSEA VI, Jakarta, Indonesia, July 1987, 1-42.

Cook, A. C., Hutton, A. C. and Kantsler, A. J., 1980. Oil shales. Scientific Australian, 4, 6-14.

Cook, A. C. (editor), 1982a. The origin and petrology of organic matter in coals, oil shales and petroleum source rocks. Univ. Wollongong, Wollongong, 166pp.

Cook, A. C., 1982b. Organic facies in the Eromanga Basin; in: Moore, P. S. and Mount, T. J. (compilers), Eromanga Basin Symposium, Summary Papers, Geol. Surv. of Aust. and Pet. Explor. Soc. of Aust., Adelaide, 234-257.

Cook, A. C., Smyth, M. and Vos, R. G., 1985. Source potential of upper Triassic fluvio-deltaic systems of the Exmouth Plateau. Aust. Pet. Explor. Assoc. J., 25.

Davis, A. and Spackman, W., 1964. The role of the cellulosic and lignitic components of wood in artificial coalification. Fuel, 43, 215-224.

Diessel, G. F. K., 1965. Correlation of macro- and micro-petrography of some New South Wales coals. in: Woodcock, J. T et al. (editors), Proceedings-general, 6, 8th Commonw. Min. Metall. Congr., Melbourne, 669-677.

Diessel, G. F. K., 1982. An appraisal of facies based on maceral characteristics. Aust. Coal Geolo., 4(2), 474-483.

Diessel, G. F. K., 1986. The correlation between coal facies and depositional environments. Advances in the Study of the Sydney Basin, Proc. 20th Symp., Univ. Newcasle, 19-22.

Durand, B., 1980. Kerogen (insoluble organic matter from sedimentary rocks), in: Durand (editor), Editions Technip, Paria, 113-42.

Durand, B. and Parratte, M., 1983. Oil potential of coals: a geochemical approach. in: Brooks,J. (editor), Pet. Geochem. and Explor. of Europe, Geol. Soc. of London, Special Publication No. 12, Blackwell, 255-266.

Espitalie, J., Madec, M., and Tissot, B., 1980. Role of mineral matrix in kerogen pyrolysis: influence on petroleum generation and migration. Am. Assoc. Pet. Geol. Bull., 64, 59-66.

Espitalie, J., Deroo, G. and Marquis, F., 1985. La Pyrolyse Rock-Eval et set applications. Deuxiéme Rev. Inst. Francais Pétrol., 40, 755-784.

Espitalie, J., Deroo, G. and Marquis, F., 1986. Rock-Eval Pyrolysis and its applications. Institute Francais du Petrole, Publication No. 27299, English Translation.

Fan, P., 1979. Atlas of the palaeogeography of China. Cartographic Publishing House, Beijing.

Fan, P. F., 1979. Geology of Songliao Basin, China - tectonic evolution of a failed rift system. Abstracts with programs, Bull. Am. Assoc. Pet. Geol., 19, 422.

Frakes, L. A., 1979. Climates Throughout Geological Time. Elsevier Scientific Publishing Company, Amsterdam, 310pp.

Geological Survey of Jilin, P. R. China, 1984. Report of the exploration on Yang Cao Gou Basin (in Chinese, unpubl).

Geological Survey of Jilin, P. R. China, 1986. Report of the exploration on Yang Cao Gou Basin (in Chinese, unpubl).

Gong, S., 1986. Shallow deltaic deposition and coal accumulation of the lower Permian in Yuxian coalfield, Henan (in Chinese). J. Coal. Geol. Explor., 6, 14-23.

Goodarzi, F. and Gentzis, T., 1987., Depositional setting, as determined by coal petrology of the Middle-Eocene Hat Creek No. 2 coal deposit, British Columbia. Bull. Can. Pet. Geol., 35, 197-211.

Grand' eury, F. C., 1962. Memoire sur la formation de la houille; Ann. Mines, 1, ser. 8, 106pp.

Guo, T. and Chi, X., 1985. The occurrences of the heavy minerals in the Yingcheng Formation, Yang Cao Gou Basin (in Chinese, unpublished).

Hacquebard, P. A., Birmingham, T. F., and Donaldson, J. R., 1967. Petrography of Canadian coals in relation to environment of deposition; Symposium in the Science and Technilogy of coal, Ottawa, March, 1967, Energy, Mines, and Resources, Ottawa, 84-97.

Hacquebard, P. A. and Donaldson, J. R., 1969. Carboniferous coal deposition associated with flood-plain and limnic environments in Nova Scotia; in Dapples, E. C. and Hopkins, M. E.(editors), Environments of Coal Deposition; Geol. Soc. Am. Special Paper, 114, 143-191.

Hagemann, H. W. and Wolf, M., 1987. New interpretations of the facies of the Rhenish brown coal of West Germany. Int. J. Coal Geol., 7, 335-348.

Han, D. and Yang, Q.(chief editors), 1981. Coal Geology of China, 2 (in Chinese). The Coal Industrial Press, Beijing, 413pp.

Huang, T. D., Wang, J., Fan, C., Shang, H., and Cheng K., 1980. Genisis of oil and gas of continental origin in the Meso-Cenozoic basins in China (in Chinese): Acta Petrolei Sinica, 1, 31-41.

Hutton, A. C., Cook, A. C., Kantsler, A. J. and McKirdy, D. M., 1980. Organic matter in oil shales. Aust. Pet. Explor. Assoc. J., 20, 44-67.

International Handbook of Coal Petrology, 1963. International Commettee for Coal Petrology, Centre National Recherche Scientifique, Paris.

International Handbook of Coal Petrology, 1975. International Commettee for Coal Petrology, Centre National Recherche Scientifique, Paris.

Larter, S. R. and Senftle, J. T., 1985. Improved kerogen typing for petroleum source rock analysis. Nature, 318, 277-280.

Liu, J., 1988. Depositional environment and coal accumulation of the Yingcheng coal measures, Yang Cao Gou Basin (in Chinese, unpublished).

Ma, L., 1985. Subtle oil pools in Xingshugang delta, Songliao Basin. Am. Assoc. Pet. Geol. Bull. 69, 1123-1132.

MacGregor, D. S. and MacKenzie, A. S., 1986. Quantification of oil generation and migration in the Malacca Strait region Central Sumatra. Indonesian Pet. Assoc. Proc. 15 Annual Convention, 1, 305-320.

Marchioni, D. L., 1980. Petrography and depositional environment of the Liddell seam, upper Hunter Valley, New South Wales. Int. J. Coal Geol., 1, 35-61.

McKirdy, D. M. and Kantsler, A. J., 1983. Oil geochemistry and potential source rocks of the Officer Basin, South Australia. APEA J, 1, 68-86.

McKirdy, D. M., 1985a. Coorongite, coastal bitumen and their origins from the lacustrine alga Botryococcus in the western Otaway Basin, Otway 85-Earth resources of the Otway Basin, 7-10th Feb. 1985. Summary Papers and Excursion Guides, South Australian and Victoria Divisions Geol. Soc. Aust., 34-49.

McKirdy, D. M., Cox, R. E. and Morton, J. G. G., 1985b. Biological maker, isotopic and geological studies of lacustrine crude oils in the western Otway Basin South Australia, Lacustrine Petroleum source rocks. Joint Meet IGCP Proj. 219 and Petroleum Group Geol. Soc. 10-1 Sept. 1985, Abstr.

McKirdy, D. M., Cox, R. E., Volkman, J. K. and Howell, V. J., 1986. Botryococcane in a new class of Australian non-marine crude oils. Nature, 320, 57-59.

Monthioux, M. and Landais, P., 1987. Evidence of free but trapped hydrocarbons in coals. Fuel, 66, 1703-1708.

Patteisky, K. and Teichmüller, M., 1960. Inkohlungs-Verlauf, Inkohlungs-Masstable und Klassifikation der Kohlen auf Grund von Vitrit-Analysen. Brennst chemie, 41: 79-84; 97-104; 133-137.

Peters, K. E., 1986. Guidelines for interpreting petroleum source rock using programmed pyrolysis. Bull. Am. Assoc. Pet. Geol. 70, 318-329.

Powell, T. G. and McKirdy, D. M., 1972. The geochemical characterisation of Australian crude oils. Aust. Pet. Explor. Assoc. J. 12, 125-131.

Powell, T. G. and McKirdy, D. M., 1973. Relationship between ratio of pristane to phytane, crude oil composition and geological environment in Australia: Nature(Physical Sci.), 243, 37-39.

Powell, T. G. and McKirdy, D. M., 1975. Geological factors controlling crude oil composition in Australia and Papua New Guinea. Bull. Am. Assoc. Pet. Geol. 59, 1176-1197.

Powell, T. G. and Snowdon, L. R., 1980. Geochemical controls of hydrocarbon generation in Canadian sedimentary basins; in Miall, A. D.(ed), Facts and Principles of World Petroleum Occurrence. Can. Soc. Pet. Geol., mem. 6, 421-446.

Powell, T. G., 1986. Petroleum geochemistry and depositional setting of lacustrine source rocks. Marine and Petroleum Geology, 3, 200-219.

Powell, T. G., Boreham, C. J., Smyth, M., Russell, N. and Cook, A. C., 1991. Petroleum source rock assessment in non-marine sequences: pyrolysis and petrographic analysis of Australian coals and carbonaceous shales. Org. Geochem. 17, 375-394.

Robert, P., 1981. classification of organic matter by means of fluorescence: Application to hydrocarbon source rocks; Int. coal Geol., 1, 101-137.

Saxby, J. D. and Shibaoka, M., 1986. Coal and coal macerals as source rocks for oil and gas. Appl. Geochem. 1, 25-36.

Seyler, C. A., 1929. The microscopical examination of coal; D. S. I. R., Fuel research, Physics and Chemical Survey, National coal Resources, No. 16, H. M. S. O., 67pp.

Seyler, C. A., 1943. Recent progress in the petrology of coal; Journal Institute Fuel, 16, 134-141.

Shanmugam, G., 1985. Significance of coniferous rain forests and related organic matter in generating commercial quantities of oil, Gipsland Basin, Australia. Am. Assoc. Pet. Geol. Bull., 69, 1241-1254.

Smith, W. H., Roux, H. J., and Steyn, J. G. D., 1981. The classification of coal macerals and their relation to certain chemical and phicical parameters of coal; Proceedings of International Conference on Applied Mineralogy in the mineral Industrial, Johannesburg, South Africa.

Smyth, M., 1979. Hydrocarbon generation in the Fly Lake - Brolga area of the Cooper Basin. J. Aust. Pet. Explor. Assoc., 19: 1-7.

Smyth, M., 1984. Coal microlithotypes related to sedimentary environments in the Cooper Basin, Australia. Spec. Publ. Int. Assoc. Sedimentol., 7: 333-347.

Smyth, M., 1988. Organic petrology of the Triassic Snake Member in ATM 145P, Sturat Basin, Queensland. CSIRO unpubl. rep., 18pp.

Stach, E. et al., 1982. The lithotypes of humic and sapropelic coals. in stach, E., Mackowsky, M.-Th, Teichmüller, M., Taylor, G. H., Chandra, D., and Teichmüller, R., editors, Coal Petrology; Gebruder Borntraeger, Berlin-Stuttgart, 171-177.

Stopes, M. C., 1919. On the four visible ingredients in banded bituminous coals. Proceedings of the Royal Society, B, 90, 470-487.

Stopes, M. C., 1935. On the petrology of banded bituminous coals. Fuel, 14, 4-13.

Styan, W. B. and Bustin, R. M., 1983a. Petrography of some Fraser Delta peat: deposits: coal maceral and microlithotype precursors in temperate-climate peats; International . Journal of. Coal Petrology, 2, 321-371.

Styan, W. B. and Bustin, R. M., 1983b. Sedimentology of Fraser River peat: A model analogue for some ancient deltaic coals; International Journal of Coal Petrology, 3, 101-143.

Tasch, K. H., 1960. die Moglichkeiten der Flozleichstellung under Zuhifenahme von Flozbildungsdiagrammen; Bergbau-Rdsch., 12, 153-157.

Teichmüller, M., 1962. Die Genese der Kohle; Compte Rendu 4th Congress Stratigraphy Geology Carboniferous, Heerlen, 1958, 3, 699-722.

Teichmüller, M., 1974. Generation of petroleum-like substances in coal seams as seen under the microscope. In: Tissot, B. and Bienner, F. (editors): Adv. Organic Geochem. 1973, 321-348.

Teichmüller, M., 1982a. Application of coal petrological methods in geology including oil and natural gas prospecting; in Stach, E., Mackowsky, M.-Th., Teichmüller, M., Taylor, G. H., Chandra, D., and Teichmüller, R., editors, Coal Petrology, 3rd Edition; Gebruder Borntraeger, Berlin-Stuttgart, 381-413.

Teichmüller, M., 1982b. Origin of the petrographic constituents of coal; in Stach, E., mackowsky, M.-Th., Teichmüller, M., Taylor, G. H., Chandra, D., and Teichmüller, R., editors, Coal Petrology, 3rd Edition; Gebruder Borntraeger, Berlin-Stittgart, 219-294.

Teichmüller, M. and Durand, B., 1983. Fluorescence microscopical rank studies on liptinites and vitrinites in peat and coals, and comparison with result of the Rock-Eval Pyrolysis. Int. J. Coal Geol. 2, 197-230.

Teichmüller, M., 1989. The genesis of coal from the viewpoint of coal petrology. in: Lyons, P. C. and Alpern, B. (editors), Peat and Coal,1. Origin, Facies and Depositional Models. Int. J. Coal Geol., 12, 1-87.

Thomas, B. M., 1982. Land plant source rocks for oil and their significance in Austrlian Basins. Aust. Pet. Explor. Assoc. J. 22, 164-178.

Thompson, S., Cooper, B., Morley, R. J. and Barnard, P. C., 1985. Oil-generting coals. In Petroleum Geochemistry in Exploration of the Norwegian Shelf (Edited by Thomas, B. M.), 59-73. Graham and Trotman, London.

Thornton, R. C., 1979. Regional stratigraphic analysis of the Gidgealpa Group, Southern Cooper Basin, Australia, Geol. Survey South Australia, Bulletin 49.

Tian, Z., Chang, C., Huang, D. and Wu, C., 1983. Sedimentry facies, oil generation in Meso-Cenozoic continental Basins in China, Oil gas J. 81, 120-126.

Tissot, B. and Welte, D. H., 1978. Petroleum formation and occurrence; Springer-verlag, New York, 538pp.

Tissot, B. and Welte, D. H., 1984. Petroleum formation and occurrence. A new Approach to oil and gas Exploration, 2nd edn. Springer, Berlin.

Wang, H. Z. and Chu, X. (chief editors), 1985. Atlas of the Palaeogeography of China. The Cartographic Publishing House Beijing, 85pp.

Waples, D., 1981. Organic Geochemistry for Exploration Geologists. Burgess Publishing Company.

Yang, C. Z., 1986. Stratigraphic dinision and correlation of the Mesozoic coal-bearing series in the eastern edge of the Songliao Basin (in Chinese). Jilin Geology, 3, 49-58.

Yang, C. Z., Zhou, S. A., Zhang, L., Ma, W., and Xin, L., 1987. Report of the exploration on Tang Cao Gou area (in Chinese). Report to Bureau of Geology of Jilin, report, 178pp (unpubl).

Yang, W., 1985. Daqing oil field, People's Republic of China: A giant field with oil of non-marine origin. AAPG bull. 69, 1101-1111.

Yang, W., Li, Y. and Gao, R., 1985. Formation and evolution of non-marine petroleum in Songliao Basin, China, AAPG Bull. 69, 1112-1122

Zhao, D., 1989. Coal Resources and Coal Geology of eastern edge of the Songliao Basin (in Chinese, unpubl), report, 278pp.

Zhao, D., Yang, C. Z., and Zhou, S., 1987. Yang Cao Gou coal (in Chinese, unpubl), report to bureau of Geology, Jilin.

Key to Symbols

CC= Changchun City' Colliery, Yang Cao Gou
JT= Jiutai Colliery, Yang Cao Gou
ACC= Artillery's Colliery, Yang Cao Gou
R= Rural Colliery, Yang Cao Gouy
ZK3245= Name of the borehole, Yang Cao Gou
ZK3245(1)=Coal sample
Zk3245(G1)=Shale or parting sample

SUMMARY OF SAMPLES

APPENDIX 1

Sample Localities	No. of Samples
A. Collieries	
CC	16
JT	9
ACC	8
R	5
B. Boreholes	
ZK4004	9
ZK4803	11
ZK6401	6
ZK912	4
ZK1721	3
ZK5705	11
ZK806	6
ZK5601	4
ZK3202	8
ZK4804	11
ZK3203	3
ZK2501	5
ZK2502	3
ZK2505	3
ZK1603	7
ZK11202	6
ZK3305	5
ZK3204	2
ZK1717	1
ZK1718	3
ZK807	2
ZK2504	1
ZK2403	1
ZK103	1
ZK4105	1
ZK4901	1
ZK5703	1
ZK8002	6
ZK805	1
ZK106	2
ZK1604	1
ZK5604	3
ZK2401	5
ZK108	8
ZK4001	1

SAMPLE LIBRARY

Borehole or Location	Sample Names	Chinese Well/Sample No	Depth From (m) To
CC	892-1		
CC	892-2		
CC	892-3		
CC	892-4		
CC	892-5		
CC	892-6		
CC	892-7		
CC	892-8		
CC	892-9		
CC	892-10		
CC	892-11		
CC	892-12		
CC	892-13		
CC	892-14		
CC	892-15		
CC	892-16		
JT	892-17		
JT	892-18		
JT	892-19		
JT	892-20		
JT	892-21		
JT	892-22		
JT	892-23		
JT	892-24		
JT	892-25		
ACC	892-26		
ACC	892-27		
ACC	892-28		
ACC	892-29		
ACC	892-30		
ACC	892-31		
ACC	892-32		
ACC	892-33		
R	892-34		
R	892-35		
R	892-36		
R	892-37		
R	892-38		
ZK4004	892-39	ZK4004(1)	980.4 TO 980.8
ZK4004	892-40	ZK4004(2)	986.4 TO 987.5
ZK4004	892-41	ZK4004(3)	987.5 TO 988.8
ZK4004	892-42	ZK4004(4)	988.8 TO 990.6

APPENDIX 1

ZK4004	892-43	ZK4004(5)	995.2 TO 996.7
ZK4004	892-44	ZK4004(6)	996.7 TO 998.4
ZK4004	892-45	ZK4004(7)	998.4 TO 999.6
ZK4004	892-46	ZK4004(8)	999.6 TO 1001.4
ZK4004	892-47	ZK4004(9)	1001.4 TO 1003.1
ZK4803	892-48	ZK4803(1)	841.5 TO 843.3
ZK4803	892-49	ZK4803(2)	843.5 TO 843.9
ZK4803	892-50	ZK4803(3)	849.7 TO 851.3
ZK4803	892-51	ZK4803(4)	851.3 TO 852.3
ZK4803	892-52	ZK4803(5)	852.3 TO 853.3
ZK4803	892-53	ZK4803(6)	853.3 TO 855.4
ZK4803	892-54	ZK4803(7)	855.4 TO 856.2
ZK4803	892-55	ZK4803(8)	856.9 TO 857.1
ZK4803	892-56	ZK4803(9)	857.4 TO 859.4
ZK4803	892-57	ZK4803(10)	860.6 TO 861.0
ZK4803	892-58	ZK4803(G)	844.3 TO 845.2
ZK6401	892-59	ZK6401(3)	372.5 TO 373.7
ZK6401	892-60	ZK6401(5)	375.4 TO 376.0
ZK6401	892-61	ZK6401(6)	376.3 TO 376.8
ZK6401	892-62	ZK6401(8)	387.9 TO 388.2
ZK6401	892-62A	ZK6401(9)	388.2 TO 388.7
ZK6401	892-63	ZK6401(10)	388.7 TO 389.5
ZK6401	892-64	ZK6401(11)	389.5 TO 392.5
ZK912	892-65	ZK912(1)	283.0 TO 285.0
ZK912	892-66	ZK912(2)	285.0 TO 287.0
ZK912	892-67	ZK912(3)	287.0 TO 289.0
ZK912	892-68	ZK912(4)	289.0 TO 291.0
ZK1721	892-69	ZK1721(1)	378.0 TO 378.9
ZK1721	892-70	ZK1721(2)	378.9 TO 380.1
ZK1721	892-71	ZK1721(3)	380.1 TO 380.9
ZK5705	892-72	ZK5705(1)	920.4 TO 920.8
ZK5705	892-73	ZK5705(2)	922.5 TO 923.6
ZK5705	892-74	ZK5705(3)	924.6 TO 925.1
ZK5705	892-75	ZK5705(4)	925.6 TO 927
ZK5705	892-76	ZK5705(5)	932.1 TO 932.8
ZK5705	892-77	ZK5705(6)	932.8 TO 935.1
ZK5705	892-78	ZK5705(7)	935.7 TO 936.2
ZK5705	892-79	ZK5705(8)	942.9 TO 944.3
ZK5705	892-80	ZK5705(9)	947.3 TO 948.0
ZK5705	892-81	ZK5705(10)	948.1 TO 948.8
ZK5705	892-82	ZK5705(G)	921.9 TO 922.5
ZK806	892-83	ZK806(1)	232.9 TO 234.0
ZK806	892-84	ZK806(2)	234 TO 234.4
ZK806	892-85	ZK806(3)	234.4 TO 235.4
ZK806	892-86	ZK806(4)	235.4 TO 237.7

APPENDIX 1

ZK806	892-87	ZK806(6)	238.3 TO 239.8
ZK806	892-88	ZK806(7)	239.8 TO 241.0
ZK5601	892-89	ZK5601(1)	202.1 TO 204.0
ZK5601	892-90	ZK5601(4)	208.0 TO 210.0
ZK5601	892-91	ZK5601(5)	210.0 TO 212.0
ZK5601	892-92	ZK5601(6)	215.1 TO 216.4
ZK3202	892-93	ZK3202(1)	510.4 TO 512.4
ZK3202	892-94	ZK3202(2)	512.5 TO 515.0
ZK3202	892-95	ZK3202(3)	515.0 TO 516.3
ZK3202	892-96	ZK3202(4)	516.3 TO 517.2
ZK3202	892-96a	ZK3202(5)	517.2 TO 518.5
ZK3202	892-96b	ZK3202(7)	519.8 TO 521.3
ZK3202	892-97	ZK3202(8)	521.3 TO 522.9
ZK3202	892-98	ZK3202(9)	522.9 TO 523.7
ZK3202	892-99	ZK3202(10)	523.7 TO 525.3
ZK3202	892-100	ZK3202(11)	525.3 TO 528.2
ZK4804	892-101a	ZK4804(1)	1004.8 TO 1006
ZK4804	892-101	ZK4804(2)	1008.4 TO 1010.4
ZK4804	892-102	ZK4804(3)	1010.4 TO 1012.4
ZK4804	892-103	ZK4804(4)	1012.4 TO 1014.4
ZK4804	892-104	ZK4804(5)	1014.4 TO 1015.8
ZK4804	892-105	ZK4804(6)	1015.8 TO 1017.8
ZK4804	892-106	ZK4804(7)	1017.8 TO 1019.8
ZK4804	892-107	ZK4804(8)	1019.8 TO 1021.8
ZK4804	892-108	ZK4804(9)	1021.8 TO 1022.4
ZK4804	892-109	ZK4804(10)	1022.7 TO 1023.3
ZK4804	892-110	ZK4804(G1)	1004.2 TO 1004.8
ZK4804	892-111	ZK4804(G2)	1006 TO 1006.4
ZK3203	892-112	ZK3202(1)	349.5 TO 351.3
ZK3203	892-113	ZK3202(2)	352.1 TO 353.7
ZK3203	892-114	ZK3202(3)	354.2 TO 355.7
ZK3203	892-114a	ZK3202(6)	359.5 TO 361.5
ZK2501	892-115	ZK2501(1)	276.8 TO 278.0
ZK2501	892-116	ZK2501(3)	280.6 TO 281.9
ZK2501	892-117	ZK2501(4)	281.9 TO 284.2
ZK2501	892-118	ZK2501(5)	286.6 TO 288.5
ZK2501	892-119	ZK2501(8)	315.8 TO 316.4
ZK2502	892-120	ZK2502(2)	402.6 TO 404.4
ZK2502	892-121	ZK2502(3)	416 TO 416.5
ZK2502	892-122	ZK2502(6)	428.4 TO 429.3
ZK2505	892-123	ZK2505(1)	55.6 TO 52.9
ZK2505	892-124	ZK2505(2)	52.9 TO 56.1
ZK2505	892-125	ZK2505(3)	57.2 TO 59

APPENDIX 1

ZK1603	892-126	ZK1603(1)	308 TO 309.1
ZK1603	892-127	ZK1603(2)	309.1 TO 310.5
ZK1603	892-128	ZK1603(3)	310.5 TO 312.3
ZK1603	892-129	ZK1603(4)	312.3 TO 313.8
ZK1603	892-129a	ZK1603(5)	313.8 TO 316.4
ZK1603	892-130	ZK1603(7)	319.1 TO 320.4
ZK1603	892-131	ZK1603(8)	320.4 TO 321.6
ZK1603	892-132	ZK1603(9)	321.6 TO 322.9
ZK11202	892-133	ZK11202(1)	494 TO 494.4
ZK11202	892-134	ZK11202(2)	494.5 TO 495.3
ZK11202	892-135	ZK11202(3)	495.4 TO 495.9
ZK11202	892-136	ZK11202(4)	496.3 TO 497.3
ZK11202	892-137	ZK11202(5)	497.6 TO 499
ZK11202	892-138	ZK11202(7)	521 TO 522
ZK3305	892-139	ZK3305(1)	777.1 TO 778.6
ZK3305	892-140	ZK3305(2)	778.6 TO 780.8
ZK3305	892-141	ZK3305(3)	780.8 TO 782.8
ZK3305	892-142	ZK3305(4)	782.8 TO 785.5
ZK3305	892-143	ZK3305(5)	792.3 TO 793.3
ZK3204	892-144	3204(2)	367.8 TO 368.4
ZK3204	892-145	3204(6)	368.4 TO 369.1
QZ908	892-146	QZ908(1)	40.8 TO 41.5
QZ908	892-147	QZ908(2)	41.5 TO 42.2
QZ908	892-148	QZ908(3)	42.4 TO 43.6
QZ908	892-149	QZ908(G1)	42.4 TO 43.6
QZ6204	892-150	QZ6204(1)	
QZ6204	892-151	QZ6204(2)	
QZ6204	892-152	QZ6204(3)	
QZ7201	892-153	QZ7202(1)	
QZ7201	892-154	QZ7202(2)	
ZK1717	892-155	ZK1717(8)	316.8 TO 317.8
ZK1718	892-156	ZK1718(1)	366.1 TO 366.7
ZK1718	892-157	ZK1718(3)	367.8 TO 368.9
ZK1718	892-158	ZK1718(G2)	396.0 TO 396.5
ZK807	892-159	ZK807(2)	512.5 TO 513.3
ZK807	892-160	ZK807(3)	514.5 TO 515.6
QZ1702	892-161	QZ1702(1)	
QZ2504	892-162	QK2504	
ZK2403	892-163	ZK2403(2)	524.2

ZK103	892-164	ZK103(1)	28 TO 29
ZK4105	892-165	ZK4105(2)	416.5 TO 418.2
ZK4901	892-166	ZK4901(2)	432.5 TO 433.1
ZK5703	892-167	ZK5703(1)	917 TO 920.8
QZ8001	892-168	QZ8001(2)	73.1 TO 73.6
ZK8002	892-169	ZK8002(1)	229.8 TO 231.0
ZK805	892-170	ZK805(4)	328.0 TO 330.0
ZK106	892-171	ZK106(1)	318.6 TO 319.3
ZK106	892-171a	ZK106(2)	3193 TO 322.7
ZK106	892-172	ZK106(1)	322.7 TO 325.7
ZK1604	892-173	ZK1604(1)	364.2 TO 366.6
ZK5604	892-174	ZK5604(1)	258.3 TO 259.5
ZK5604	892-175	ZK5604(3)	262.7 TO 263.8
ZK5604	892-176	ZK5604(4)	263.8 TO 265.5
ZK2401	892-177	ZK2401(1)	279.0 TO 281.0
ZK2401	892-178	ZK2401(2)	281.0 TO 283.3
ZK2401	892-179	ZK2401(3)	283.3 TO 284.7
ZK2401	892-180	ZK2401(4)	284.7 TO 285.5
ZK2401	892-181	ZK2401(5)	285.8 TO 286.7
ZK2401	892-182	ZK2401(G1)	285.5 TO 285.8
ZK108	892-183	ZK108(1)	453.6 TO 454.3
ZK108	892-184	ZK108(2)	454.7 TO 455.6
ZK108	892-185	ZK108(3)	455.6 TO 456.3
ZK108	892-186	ZK108(5)	456.3 TO 457.2
ZK108	892-187	ZK108(6)	457.2 TO 458.1
ZK108	892-188	ZK108(8)	459.3 TO 460.2
ZK108	892-189	ZK108(9)	460.2 TO 460.9
ZK108	892-190	ZK108(10)	460.9TO 461.4

Plate

APPENDEX II PLATES

Plate

Plate 1 Photomicrographs of selected macerals in Yang Cao Gou coals. All photomicrographs are from polished sections of coal, Yang Cao Gou Basin, reflected light, oil immersion, X 500.

a Telocollinite. Photomicrograph of typical field of a vitrite layer from the Group II coal, characterized by the lack of liptinite and inertinite macerals. Sample 892-1

b Eu-ulminite. Sample 892-8

c Bands of vitrinite B (B) associated with bands of vitrinite A (A). Sample 892-36.

d Telinite with uncompressed cell walls; cell cavities filled with resin. Sample 892-9.

e Eu-ulminite (EU), desmocollinite (DC), in association with cutinite (CT), occurring as clarite. Sample 892-57.

f Densinite (D) and inertodetrinite (IN), occurring as vitrinertite (vitrinite-rich). Sample 892-26.

PLATE 1

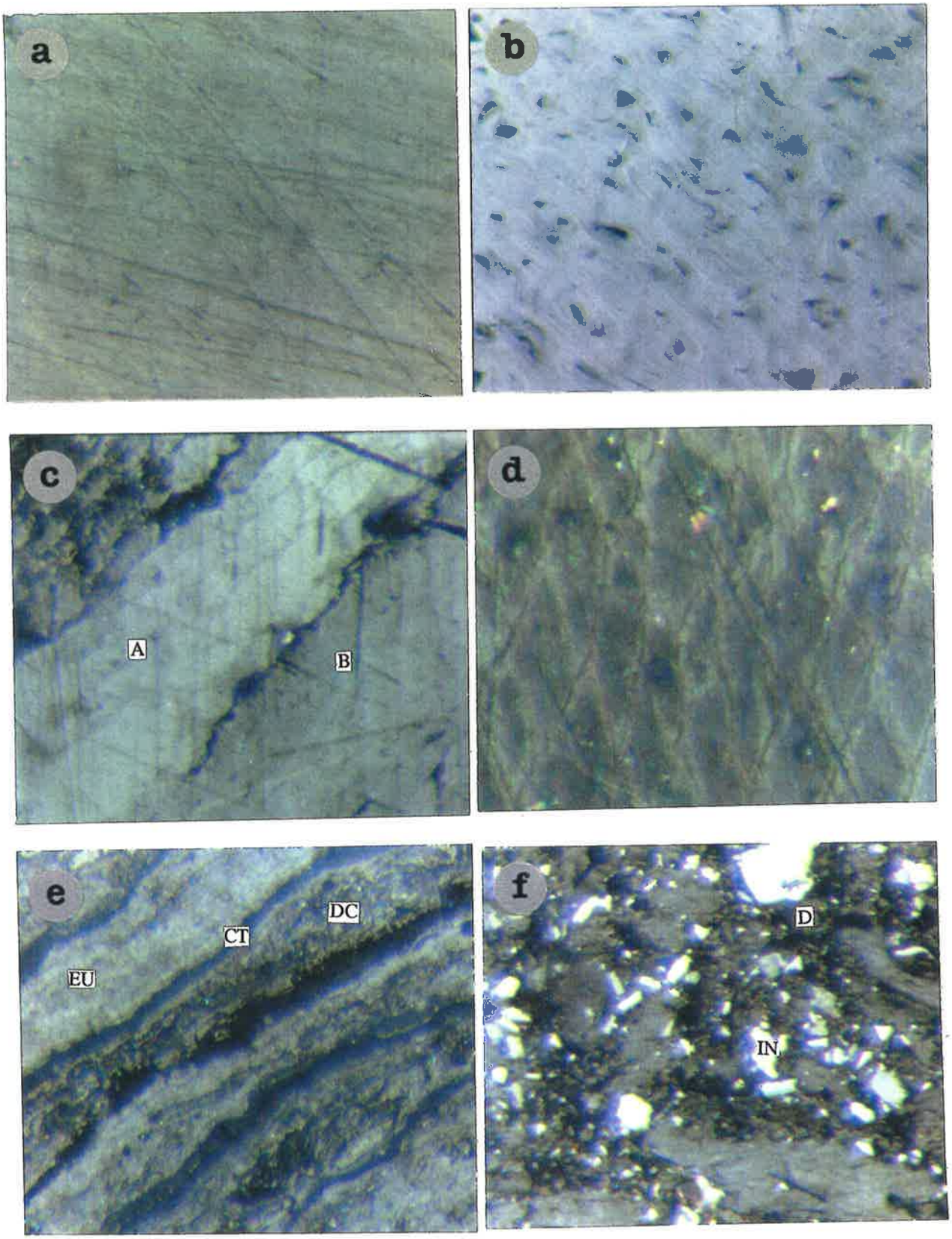

PLATE 2

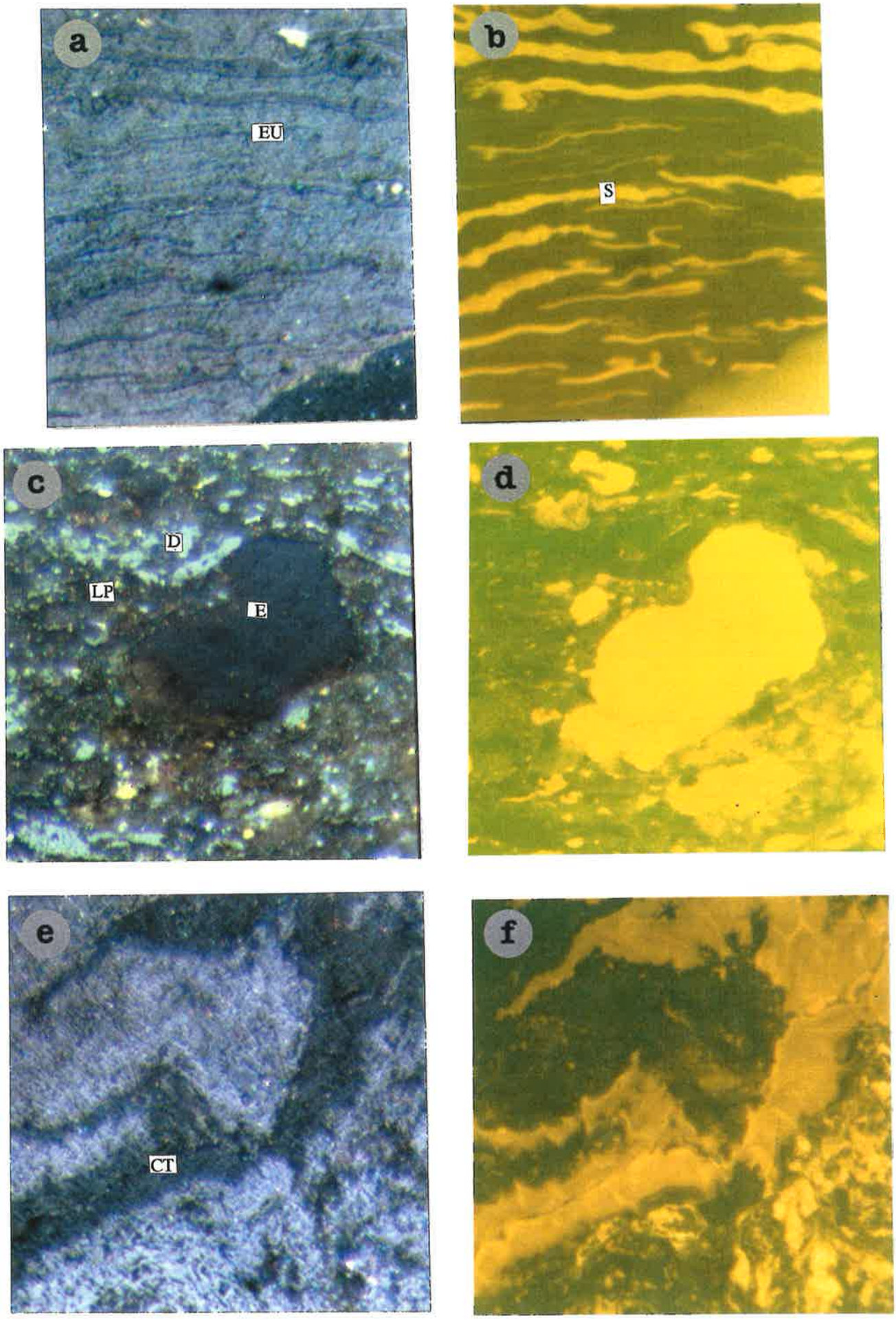

Plate

Plate 2 Macerals of the liptinite and vitrinite groups.(all photomicrographs are from polished sections of coal, Yang Cao Gou Basin, oil immersion, X 500).

a Resinite (S) associated with eu-ulminite (EU) in normal reflected light. Sample 892-9.

b Same field of observation as in Figure a, but now under fluorescence mode.

c Exsudatinite (E) associated with liptodetrinite (LP) and densinite (D) in normal reflected light. Sample 892-98.

d Same section as in Figure c under fluorescence mode.

e Thick-walled cutinite (CT) in desmocollinite (DC) in normal reflected light. Sample 892-59.

f Same section as in Figure e under fluorescence mode.

Plate

Plate 3 Photomicrographs of selected macerals in Yang Cao Gou coals. (all photomicrographs are from polished sections of coal, Yang Cao Gou Basin, oil immersion, X 500).

a Alginite (AG) associated with inertodetrinite (IN), occurring as duroclarite in normal reflected light. Sample 892-110

b Same section as in Figure a under fluorescence mode.

c Carbonate closely adhering to one another. Sample 892-176.

d Same section as in Figure c under fluorescence mode.

e Liptodetrinite (LT) associated with densinite (D) and inertodetrinite (IN), occurring as tri-macerite; normal reflected light. Sample 892-39.

f Same section as in Figure e under fluorescence mode.

PLATE 3

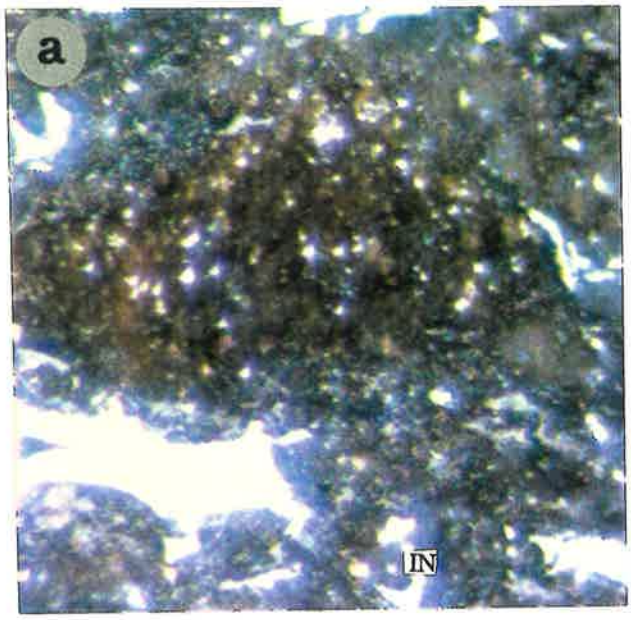

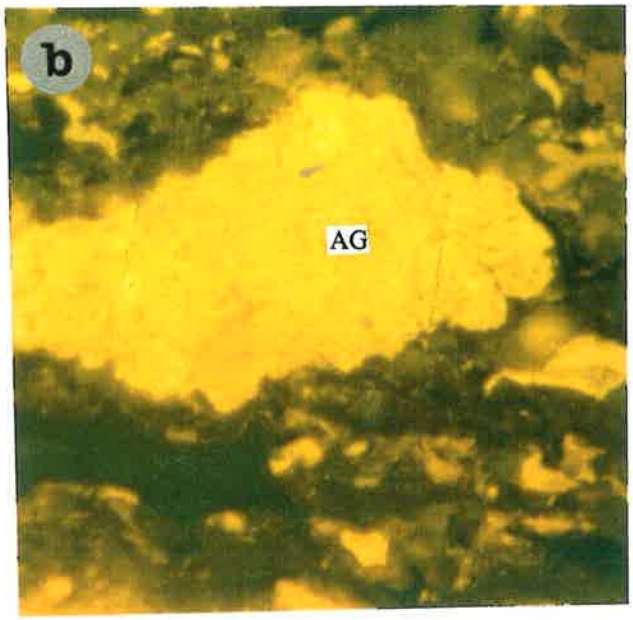

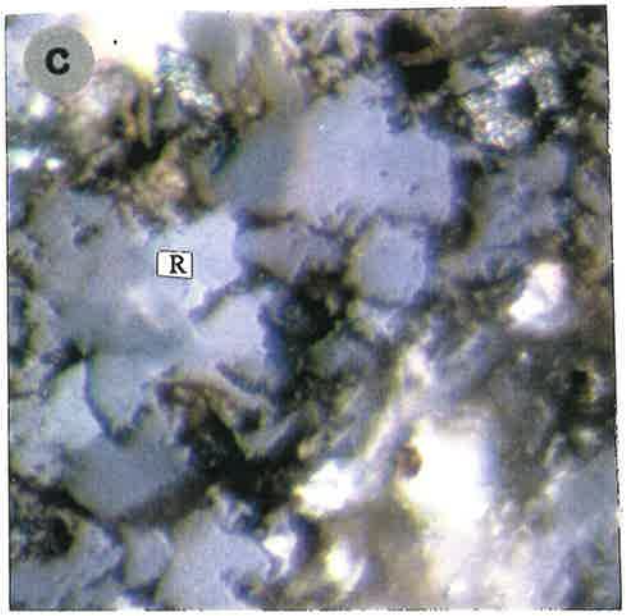

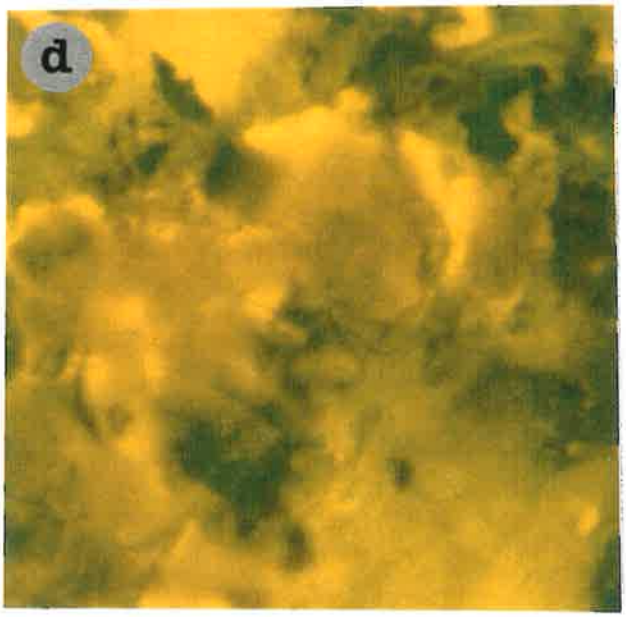

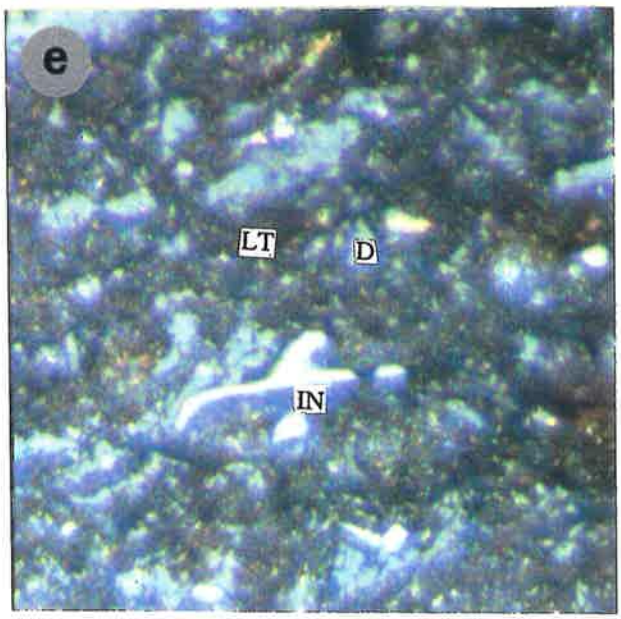

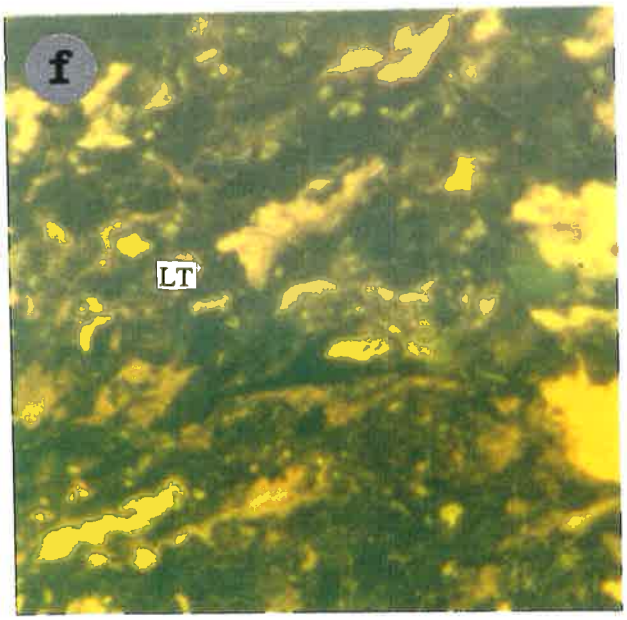

Plate

Plate 4 Macerals of the inertinite group (all phtographs in reflected light, oil immersion, X 500).

a Fusinite with well-preserved cell structure, occuring as inertite. Sample 892-22.

b Fusinite with typical parenchymous tissue with slightly unevenly thickened cell walls. Sample 892-34.

c Fusinite with well preserved bordered pits in longitudinal section. This structure is typical of gymnospermous wood. Sample 892-26.

d Sclerotinite (SC) in vitrinite matrix. Sample 892-16.

e Fusinite, inertodetrinite and densinie, occurring as vitrinertite (inertinite-rich). Sample 892-17.

f Semi-fusinite. Sample 892-33.

PLATE 4

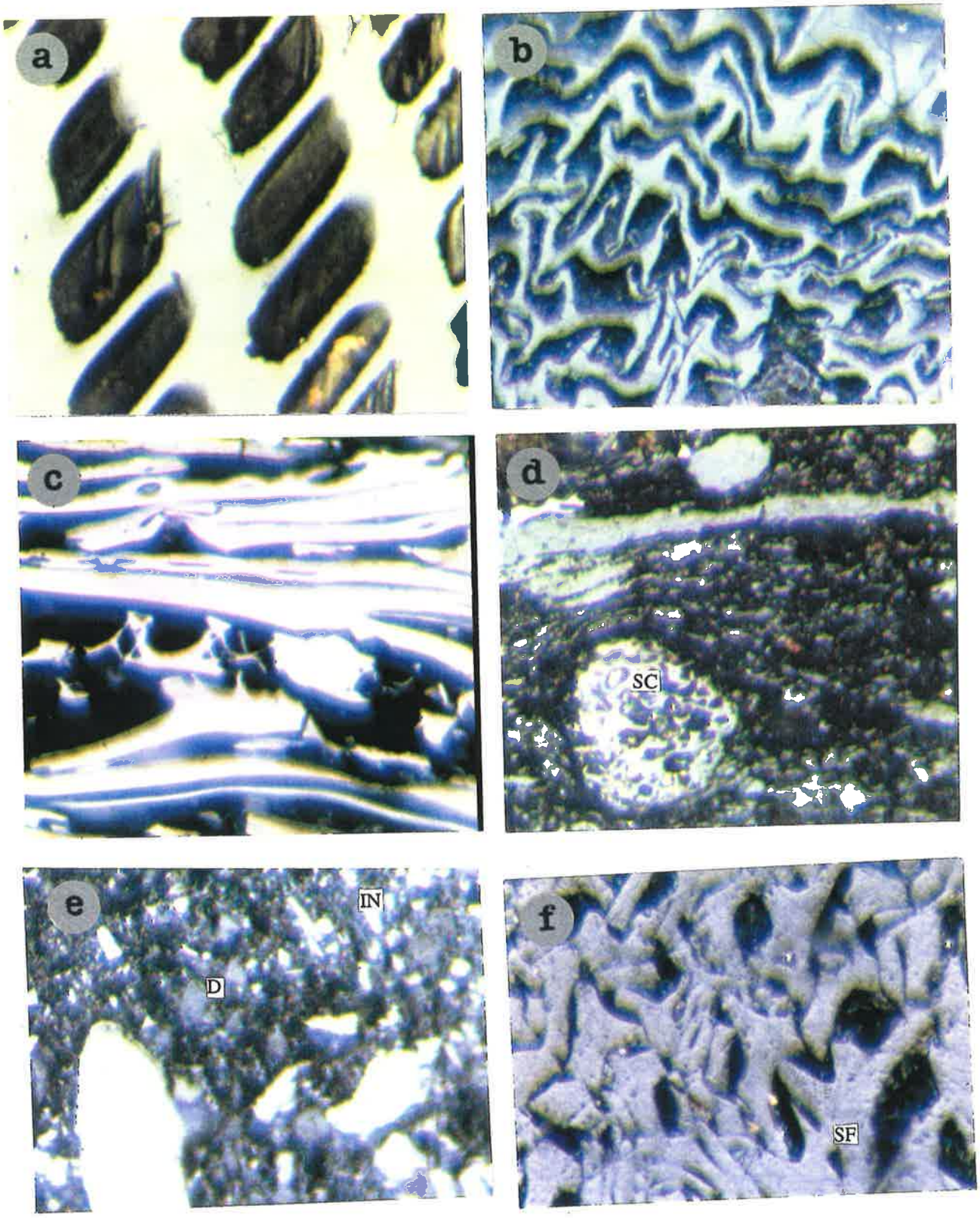

Plate

Plate 5. Pyrite and marcarite in coal
(all photomicrographs are from polished sections of coal, Yang Cao Gou Basin, reflected light, oil immersion, X 500).

a Framboidal pyrite in vitrinite. Group I coal, sample 892-38.

b Massive pyrite framboids, Group II coal, sample 892-101.

c Pyrite filling cleat in vitrinite. Lower Group coal, sample 892-147.

d Cluster of marcasites, Group II coal, sample 892-4.

e Pyrite, Group II coal, sample 892-157.

f Framboidal pyrite associated with vitrinite, Group II coal, sample 892-122..

PLATE 5